Signal Detection and Equalization in Cooperative Communication Systems Having Multiple Carrier Frequency Offsets

TIAN, Feng

A Thesis Submitted in Partial Fulfillment
of the Requirements for the Degree of
Doctor of Philosophy
in
Electronic Engineering

May 2009

Thesis/Assessment Committee

Chair of Committee

Professor CHAN Kam-Tai

Thesis Supervisor

Professor CHING Pak-Chung

Committee Member

Professor MA Wing-Kin

External Examiner

Professor CHI Chong-Yung

To my parents and my wife SUN Jingxin

Acknowledgements

First of all, I would like to express my gratitude to my supervisors, Professor Pak-Chung CHING, The Chinese University of Hong Kong (CUHK), and co-supervisor Professor Xiang-Gen XIA, University of Delaware (UDel), for guiding me throughout the course of my PhD study. They provided me not only insightful technical advices but also many encouragements during these years. I am also much obliged for their support to conducting research in CUHK and UDel and attending oversea academic activities.

I would also like to thank Professor Wing-Kin MA for his advice and suggestions in my research. His serial DSP lab seminars and lectures ELE5481 showed me an insightful view of signal processing and optimization techniques. Prof. MA also helped me a lot to improve my written English. I am very grateful to Professor Tan LEE, who arranged regular activities of DSP lab and helped me to improve my presentation skills.

Many thanks to my friends in DSP and Speech Technology Laboratory, who gave me warmth and courage all these years. Special thanks are given to Dr. ZHANG Wei, Dr. LEE Siu Wa and Dr. ZHENG Nengheng. Dr. ZHANG Wei shared me with a lot of his own experience on both research and life. Dr. Lee Siu Wa is always kind to discuss and help me. Dr. ZHENG Nengheng give me many suggestions on study and life as well. Also I would like to thank all members of Professor XIA's group in Udel for great help they gave to me.

I wish to express my deepest gratitude to my parents for their continuous love throughout my life. Finally, the deepest gratitude and appreciation are given to my wife SUN Jingxin, who has been with me in the whole journey.

Abstract of thesis entitled:

Signal Detection and Equalization in Cooperative Communication Systems Having Multiple Carrier Frequency Offsets

Submitted by **TIAN Feng**

for the degree of **Doctor of Philosophy**

in **Electronic Engineering**

at **The Chinese University of Hong Kong** in

May 2009

Different from multiple-input multiple-output (MIMO) systems, a major challenge for cooperative communications is the problem of synchronization because multiple transmissions undertaken by cooperative systems may not be synchronized in time and/or frequency. With synchronization errors, conventional space-time (ST) codes may not be directly applicable any longer. To tackle the problem of timing synchronization, space-frequency (SF) coded orthogonal frequency division multiplexing (OFDM) cooperative systems have recently been proposed to achieve asynchronous diversity due to their insensitivity to timing errors. However, these systems still need to face the problem of multiple carrier frequency offsets (CFOs). Since each node in a cooperative system is equipped with its own oscillator, the received signals from different relay nodes may have multiple CFOs which cannot be compensated simultaneously at the destination node. For SF coded OFDM cooperative systems, this problem becomes more complicated because CFOs can lead to inter-carrier interference (ICI). To address this challenge, in this thesis we consider the signal detection problem in cooperative systems having multiple CFOs.

First, we investigate the effect of multiple CFOs on two classic ST codes. They are delay diversity and the Alamouti code. For delay diversity, we find that both its achieved diversity order and diversity product are not decreased by multiple CFOs arising from maximum-likelihood (ML) detection. For the Alamouti code, the diversity product may be decreased by multiple CFOs. In the worst case situation, full diversity order 2 cannot be achieved.

Since OFDM systems are robust to timing errors, we turn to an SF coded cooperative communication system with multiple CFOs, where the SF codes are rotational based and can achieve both full cooperative and full multipath diversity orders. We begin with the traditional way of ICI mitigation. To preserve the performance of the SF code, we suggest increasing the SINR of each subcarrier but not equalizing the SF precoding matrix. By exploiting the structure of the SF codes, we propose three signal detection methods to deal with the multiple CFOs problem in SF coded OFDM systems. They are the minimum mean-squared filtering (MMSE-F) method, the two-stage simple frequency shift Q taps (FS-Q-T) method, and the multiple fast Fourier transform (M-FFT) method, all of which offer different tradeoffs between performance and computational complexity. Our simulation results indicate that the proposed detection methods perform well as long as the CFOs between nodes are small.

For deeper insights into the SF coded communication system with multiple CFOs, we then carry out diversity analysis. By treating the CFOs as part of the SF codeword matrix, we show that if all the absolute values of normalized CFOs are less than 0.5, then the full diversity order for the SF codes are not affected by the multiple CFOs in the SF coded OFDM cooperative system. We further prove that this full diversity property can still be preserved if the zero forcing (ZF) method is used to equalize the multiple CFOs. This method, by some reasonable approximations, is actually equivalent to the MMSE-F detection method. To improve the robustness of the SF codes to multiple CFOs, we propose a novel permutation method. With this method, the achieved diversity order of SF codes remains the same even when the absolute values of normalized CFOs are equal to or greater than 0.5. To reduce computational complexity, we further propose two full diversity achievable detection methods, namely the ZF-ML-Zn and ZF-ML-PIC detection methods, which are suitable for the case when the ICI matrix is singular.

In summary, in this study, we demonstrate that with proper design, the SF coded OFDM approach can be made robust to both timing errors and CFOs in a cooperative communication system.

摘要

不同于多輸入多輸出系統 （MIMO），協作通信（Cooperative communications）所面臨的一個主要問題是同步， 包括時間同步和載波頻率同步。 而當存在同步誤差時，傳統的空時碼（STC）在協作通信繫統中通常無法正常工作。 利用正交頻分複用（OFDM）系統對時間同步誤差不敏感的特性，人們提出在協作通信系統中使用空頻（SF）編碼技術來對抗時間同步誤差。 然而，SF 編碼的協作通信系統依然需要克服多個載波偏移（carrier frequency offsets）的問題。由于協作通信系統中的每一個參加協作的終端都有獨立的工作振蕩器， 所以在接收端有可能會存在多個載波頻率偏移使得接收機無法同時補償所有載波頻率偏移。在 SF 编码的 OFDM 系统中，此问题更加复杂，因为载波频率偏移将会导致子载波间干扰（ICI）。 從而嚴重降低系統性能。爲了解决這個問題，本文主要討論了當協作通信繫統中存在多個載波頻率偏移時，如何有效檢測信號的問題.

首先，我們探討了多個載波偏移对两种典型 ST 編碼的影响。它们分别是延时分集（delay diversity）和 Alamouti 碼。在最大似然（Maximum-likelihood）檢測的情況下，我們發現多載波頻率偏移不影響延時分集的分集階數（diversity order）和碼子乘積距離 （diversity product）。 而多載波頻率偏移可能會造成 Alamouti 碼碼子乘積距離的减小，并且在最壞的情況下將使 Alamouti 碼將不能獲得滿分集增益.

因为OFDM系统对時間同步誤差不敏感性，我們接着研究了一種SF編碼的協作通信系統在存在多載波頻率偏移的情況下的信號檢測問題。這裏所研究的SF碼不僅可以獲得滿協作分集增益, 也可以獲得滿多徑分集增益。我們首先從傳統的ICI消除方法入手。利用綫性濾波的方法來增加系統的信擾噪比（SINR）而不是均衡掉預編碼矩陣。通過充分利用SF碼的碼字結構，我們提出了三種具有不同復雜度和性能的檢測方法。他们分别是 MMSE-F，FS-Q-T 和M-FFT檢測方。仿真結果表明，在載波偏移小的情況下， 這三種方法可以取得良好的系統性能。

爲了进一步研究存在多載波頻率偏移的 SF 編碼的協作通信繫統，我們進行了分集增益分析。 通過將 ICI 看成是 SF 碼字的一部分， 我們發現當歸一化載波頻率偏移的絕對值小于 0.5 的時候，SF 碼依然可以取得滿分集增益。我們進一步證明，即使先用迫零（ZF）均衡器消除 ICI，SF 編碼的系統依然可以取得滿分集增益。此方法实际上近似等同于 MMSE-F 方法。爲了更進一步增强 SF 編碼的協作通信系統對多載波頻率偏移的抵禦能力， 我們接著提出了一種交織方法。從而即使歸一化載波頻率偏移的絕對值大于或者等于 0.5，系統依然可以取得滿分集增益。之后为降低计算复杂性，我又提出了兩種次最優的可以獲得滿分集增益的檢測方法。他们分别是 ZF-ML-Zn 和 ZF-ML-PIC 檢測方法。

综上所述，我們的研究結果表明，通過采用適當的檢測方法，SF 編碼的協作通信系統對時間和載波頻率同步錯誤都有較强的抵抗能力。

Contents

List of Tables

List of Figures

Abbreviations

AWGN	Additive white Gaussian noise
BER	Bit-error rate
BPSK	Binary phase shift keying
CDMA	Code-division multiple access
CFO	Carrier frequency offset
CP	Cyclic prefix
CRC	Cyclic redundancy check
DAB	Digital audio broadcasting
DFT	Discrete Fourier transform
DVB	Digital video broadcasting
FFT	Fast Fourier transform
FIR	Finite impulse response
i.i.d.	Independent and identically distributed
ICI	Inter-carrier interference
ISI	Inter-symbol interference
MIMO	Multiple-input multiple-output
MISO	Multiple-input single-output
MMSE	Minimum mean square error
MMSE-DFE	Minimum mean square error decision feedback equalizer
ML	Maximum-likelihood
MRC	Maximal-ratio-combiner
MLSD	Maximum-likelihood sequence detection
MSE	Mean square error

OFDM	Orthogonal frequency division multiplexing
OSTBC	Orthogonal space-time block codes
PAM	Pulse amplitude modulation
PIC	Parallel interference cancellation
PPM	Parts-per-million
PSK	Phase shift keying
QAM	Quadrature amplitude modulation
QPSK	Quadrature phase shift keying
SER	Symbol-error rate
SF	Space-frequency
SFBC	Space-frequency block codes
SIMO	Single-input multiple-output
SINR	Signal-to-interference plus noise ratio
SISO	Single-input single-output
SNR	Signal-to-noise ratio
ST	Space-time
STBC	Space-time block codes
STFC	Space-time-frequency codes
WLAN	Wireless personal area networks
ZF	Zero-forcing

Notations

a	the scalar a
$\mathbf{a}(k)$	the kth entry of vector $\mathbf{a}$
$\mathbf{A}$	the matrix $\mathbf{A}$
$\mathbf{A}(l,k)$	the (l,k)th entry of matrix $\mathbf{A}$
$(\cdot)^*$	the complex conjugate
$(\cdot)^{\mathcal{T}}$	the transpose
$(\cdot)^{\mathcal{H}}$	the conjugate transpose
$\mathbf{A}^\dagger$	Pseudoinverse of non-square matrix $\mathbf{A}$
j	the imaginary unit ($j = \sqrt{-1}$)
$\mathbf{I}_n$	the identity matrix of dimension $n \times n$
$\otimes$	the Kronecker product
$\odot$	the Hadamard product
$\mathrm{E}[x]$	statistical expectation of variable x
$\log(a)$	the natural logarithm of a
$\mathrm{var}(x)$	the variance of a random variable x
$\mathrm{tr}(\mathbf{A})$	the trace of the matrix $\mathbf{A}$
$\mathrm{rank}(\mathbf{A})$	the rank of the matrix $\mathbf{A}$
$\det(\mathbf{A})$	the determinant of the square matrix $\mathbf{A}$
$\| \mathbf{a} \|_F$	Euclidean norm of the vector $\mathbf{a}$
$\| \mathbf{A} \|_F$	Frobenius norm of the matrix $\mathbf{A}$
$\min(\cdot)$	the minimization
$\max(\cdot)$	the maximization
$\lceil a \rceil$	the smallest integer larger than a
$\lfloor a \rfloor$	the largest integer smaller than a

$\text{diag}(d_0, d_1, \cdots, d_{N-1})$	an $N \times N$ diagonal matrix with diagonal scalar entries $d_0, d_1, \cdots, d_{N-1}$
$\text{diag}(D_0, \cdots, D_{N-1})$	an $NM \times NM'$ block diagonal matrix with diagonal $M \times M'$ matrix entries $D_0, \cdots, D_{N-1}$
$\mathbf{0}_N$	the $N \times 1$ all zero vector
$\mathbf{0}_{N \times M}$	the $N \times M$ all zero matrix
$\mathbf{1}_N$	the $N \times 1$ all one vector
$\mathbf{F}_N$	the $N \times N$ normalized FFT matrix
$()_N$	modular operation
$\delta(\cdot)$	dirac delta function
$\lvert\mathcal{A}\rvert$	cardinality of the set $\mathcal{A}$
ϕ	empty set
$\subset$	proper subset symbol
$\cup$	union symbol
$\text{P}\{a\}$	probability of event a

Chapter 1

Introduction

Summary

Orthogonal frequency-division multiplexing (OFDM) and multiple-input multiple-output (MIMO) have been well recognized as two key technologies to meet people's increasing demand for wireless communications. By applying space-time (ST) or space-frequency (SF) codes, MIMO/MIMO-OFDM systems can achieve spatial diversity gain to combat channel fading. However, the nodes in a network may not be able to support multi-antennas. To overcome this problem, cooperative communications is proposed to allow single-antenna transmitters to achieve spatial diversity by cooperation. However, a major problem for cooperative communication systems is synchronization. In the situation that multiple transmission paths are not synchronized, both ST and SF codes may not work properly. Therefore in this thesis we focus on the problem of multiple carrier frequency offsets (CFOs) which is an inherent synchronization problem in cooperative communication systems. This chapter first provides an overview of OFDM, MIMO and cooperative communications which are the background knowledge of this study. Then, the problem of multiple CFOs is highlighted and the motivation for this investigation is deliberated. Finally, the organization of this thesis is outlined.

1.1 Introduction to OFDM and MIMO

The demand for wireless communication service has been growing rapidly in the past decade and it is predicted that it will continue to grow in a more explosive manner in the future. High rate and reliable access to information through wireless communications is becoming an integral part of modern society. Currently, although the existing cellular communication systems have provided the convenience for people to talk to one another regardless of distances, it is still much behind people's needs compared to what wireline technologies can provide, e.g., high-rate internet/data/video [1,2]. Due to multipath propagation of electromagnetic waves, the main challenge for wireless communications is channel fading (including flat fading and frequency-selective fading) which is a fundamental limitation of the performance of wireless systems [3–7]. Orthogonal frequency division multiplexing (OFDM) and multiple-input multiple-output (MIMO) are two key technologies to combat this difficulty [8, 9].

OFDM

In broadband wireless communication systems, the channels may possess a constant-gain and linear phase response over a bandwidth smaller than the bandwidth of the transmitted signal, hence creating *frequency-selective fading*, i.e., the gain is different for different frequency components of the received signal [3, 5, 7]. From the time domain perspective the channel response under these situations will have multipath delay spreads which thus lead to the transmitted signal arriving over multiple symbol times. In this case the channel induces *inter-symbol interference* (ISI) which significantly increases equalization complexity at the receiver. The characteristics of a frequency-selective fading channel are illustrated in Fig.1.1, where the channel is modeled as a linear system with transform function $h(t)$ and $s(t)/r(t)$ is the transmitted/received signal in time domain.

To combat frequency-selective fading, OFDM has been recognized as an effective modulation scheme in broadband wireless communications [10] and has been suc-

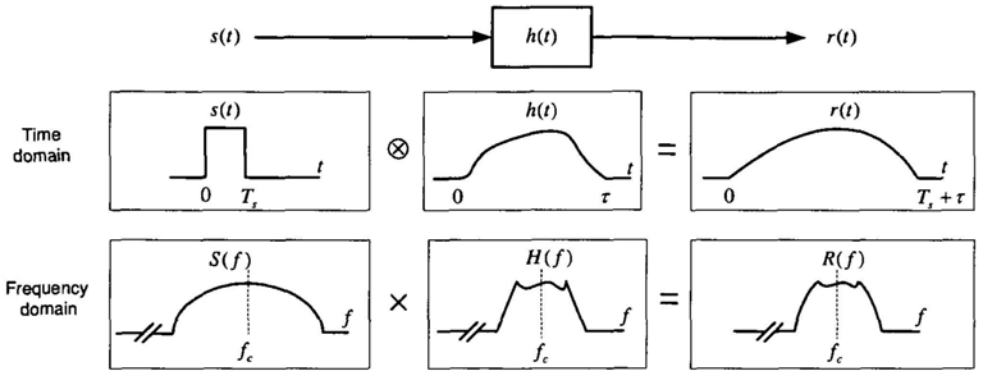

Figure 1.1: Frequency-selective fading channel characteristics.

cessfully applied in digital audio broadcasting (DAB) [11], digital video broadcasting (DVB) [12], the wireless local area networks (WLAN) IEEE 802.11a/.11g [13, 14], IEEE 802.16 family of standards and its associated industry consortium WiMax [15]. Recently, OFDM has also been considered as a potential air interface candidate for the next generation mobile wireless system.

OFDM has been extensively studied in the last few decades since it was first proposed in 1970s [10, 16–18]. Its basic principle is that the channel with ISI can be considered a linear system with non-ideal frequency response while the function of OFDM is to split the whole system into several frequency subchannels (slots) as narrow as having no ISI. In other words, OFDM converts a frequency-selective fading channel into a parallel collection of frequency flat fading subchannels.

The OFDM's major advantages [9] include:

- *High spectral efficiency.* For OFDM systems, the time domain waveforms of the subcarriers are orthogonal, yet the signal spectra corresponding to the different subcarriers overlap in frequency. Hence, OFDM has high bandwidth efficiency.

- *Simple implementation by fast Fourier transform (FFT).* OFDM applies the discrete Fourier transform (DFT) to realize the modulation/demodulation operation [16], which can be more efficiently realized by FFT.

- *Low receiver complexity.* Since OFDM converts a frequency-selective fading

channel into a parallel collection of frequency flat fading subchannels, which only require single-tap equalizers.

The OFDM's disadvantages include:

- *Higher peak-to-average power ratio (PAPR).* Due to inverse fast Fourier transform (IFFT) at the transmitter, the OFDM modulated signal has large PAPR, which requires sophisticated (expensive) radio transmitters with high-power amplifiers operating in a very large linear range [19].
- *Sensitivity to carrier frequency offset (CFO).* OFDM is very sensitive to CFO which often leads to inter-carrier interference (ICI) resulting in severe degradation on the performance of reception [20, 21].

MIMO

The demand for broadband wireless communications with large capacity, e.g. WLAN and cellular systems [1, 2], has grown explosively during recent years. The challenge in designing these broadband wireless systems lies in the availability of a comparable quality of service (QoS) with similar cost as competing wireline technologies [8]. Both in theory and practice, people have commonly recognized that this increasing demand can be achieved by using multiple antennas at both the transmitter and the receiver, widely termed as a MIMO system which can provide both *multiplex gain* (increasing channel capacity) and *diversity gain* (increasing communication reliability) [9, 22].

Channel capacity is the tightest upper bound on the amount of information that can be reliably transmitted over a communication channel. In 1948, Claude Shannon [23] first derived the channel capacity C_{SISO} for single-input single-out (SISO) AWGN channels, given by

$$C_{\text{SISO}} = B\log_2(1 + \text{SNR}) \text{ bps}, \tag{1.1}$$

where SNR is signal-to-noise ratio, B is the bandwidth (in Hz) of channel and bps means bits per second. From (1.1), it is clear that bandwidth B is the most important parameter for increasing channel capacity. However, bandwidth is a very limited

natural resource compared to people's demand. Fortunately, MIMO opens a new dimension, space, in increasing channel capacity [24–27]. In [26] Foschini et. al. show that at high SNR, with M_t/M_r transmit/receive antennas, and independent and identically distributed (i.i.d.) Rayleigh fading between each antenna pair, the capacity of a MIMO channel is given by

$$C_{\text{MIMO}} = \min(M_t, M_r)B \log_2 \text{SNR} \text{ bps}. \tag{1.2}$$

It suggests that for a fixed SNR, channel capacity C_{MIMO} can be enhanced linearly by increasing the number of transmit and receiver antennas in a MIMO system and frequency bandwidth B as well.

The other gain provided by MIMO is *diversity gain* which can be used to improve power efficiency. Diversity is an important technique in combating channel fading. Its basic idea is that if a receiver can get multiple replicas of transmitted signals which are over independent channel realizations through different time slots, frequency bands or antennas, the fading effect can be averaged by using some combing techniques. Generally, if the symbol/bit error rate of a wireless system at high SNR may be expressed as

$$P_{\text{error}}(\text{SNR}) \sim c^{-1} \cdot \text{SNR}^{-d}, \tag{1.3}$$

for some positive constants c and d, we can say that the system achieves *coding gain* c and *diversity gain* (also known as *diversity order*) d [28]. Fig.1.2 highlights the differences between coding gain and diversity gain. From this figure we can see that if the error rate is plotted versus the SNR on a log-log scale, the diversity order can be interpreted as the slope of the so-obtained curve and shows the speed at which the error rate decreases with increasing SNR, whereas the coding gain corresponds to the horizontal shift of the SER curve.

Among all the diversity techniques, spatial diversity techniques are particularly attractive because they provide diversity gain without consuming additional transmission time or bandwidth. An M_t/M_r transmit/receive antennas MIMO system can provide potential spatial diversity gain M_tM_r [29], which can be achieved by applying space-time (ST) codes at the transmitter [30–33].

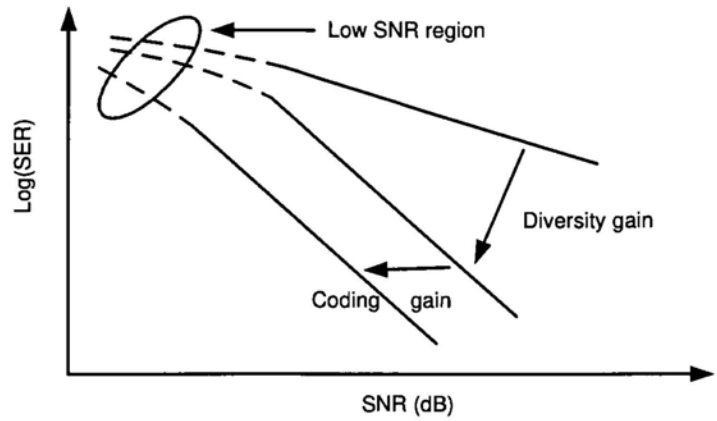

Figure 1.2: Schematic highlighting the difference between coding gain and diversity gain.

As shown in Fig.1.3, for ST coded MIMO systems, each N dimension information symbol vector $\mathbf{s}$ is first mapped into an M_t by T ST code matrix $\mathbf{C}$ with *symbol rate* at N/T information symbols per channel use. Then, $(m-1)$th $(1 \leq m \leq M_t)$ row of $\mathbf{C}$ is transmitted from the mth transmit antenna. If for any two distinct ST code matrices $\mathbf{C}_1$ and $\mathbf{C}_2$, the rank of the difference matrix $\mathbf{C}_1 - \mathbf{C}_2$ is at least equal to d, then diversity order $M_r d$ can be achieved, when maximum-likelihood (ML) detection/decoding is used at the receiver. For carefully designed ST codes such as [31–33], full diversity $M_t M_r$, i.e., the maximum diversity gain provided by MIMO channels, can be achieved.

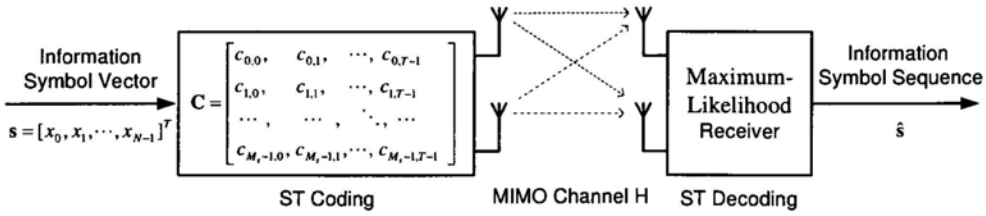

Figure 1.3: Space-time coded MIMO system.

Due to their advantages, the combination of these two powerful techniques, MIMO and OFDM, and consequently referred to as MIMO-OFDM, has become a promising broadband wireless access scheme for next generation high-data-rate wireless systems [8]. In case of frequency-selective fading channels, there is an ad-

ditional source of diversity, which is multipath diversity. Due to the existence of multiple propagation paths between each link, the total achievable diversity order is $M_r \sum_{i=1}^{M_t} L_i$, where L_i is the number of independent paths for the ith link [34,35]. Thus, it is of interest to consider coding schemes for MIMO-OFDM systems to achieve both spatial and multipath diversities. Toward this approach *space-frequency* (SF) codes are proposed in [34,36–39], where the coding is across space (transmit antennas) and frequency (OFDM subcarriers), and *space-time-frequency* (STF) codes are proposed in [40–43], where the coding is likewise across different OFDM symbols.

1.2 Introduction to Cooperative Communication

As introduced in Chapter1.1, the advantages of MIMO systems have been widely acknowledged, to the extent that certain transmit diversity methods (e.g., Alamouti codes [33]) have been incorporated into wireless standards (e.g., 802.16 [15]). Although transmit diversity is clearly advantageous on a cellular base station, it may not be practical for other scenarios. Specifically, due to size, cost, or hardware limitations, a wireless agent may not be able to support multiple transmit antennas. Examples include most handsets (size, power) or the nodes in a mobile cellular network, wireless sensor networks, home networks (e.g., HomeRF), device networks (e.g., Bluetooth). and Ad Hoc networks [44].

To tackle this problem, a new class of methods called cooperative communication has been proposed [45–49]. Its basic idea is that by sharing the single antennas of single transmitters in a network, several single-antenna transmitters can form a virtual multi-antenna transmitter to achieve transmit diversity through cooperation. The concept of cooperative communications is based on two properties of wireless communications. First, it is in the nature of wireless communications to broadcast. This means that transmitted signals can be received by some other nodes apart from the destination node at the same time. Second, spatially distributed nodes have different propagation conditions indicating that the fading of each link between nodes is independent from one another. Thus, it is possible that the destination node can collect multiple independently faded replicas of the transmitted signal. Therefore,

cooperative communications generate spatial diversity in a new and interesting way.

Fig.1.4 illustrates a typical two phase cooperative protocol. In phase one, the source node broadcasts information to all potential relay nodes. In phase two, since all the R relay nodes have the same information transmitted from the source node, they can assist in communicating with the destination node to achieve spatial diversity by forming a virtual multi-antenna transmitter. For example, each relay node just works as one transmit antenna of a multi-antenna transmitter and transmits one row of an ST/SF code matrix [47, 49, 50]. Generally, according to the transmission schemes applied by relay nodes, cooperative protocols are classified into two types: the amplifying-and-forwarding (AF) cooperative protocol and the decoding-and-forwarding (DF) cooperative protocol [48,51]. For the DF cooperative protocol, before retransmission all relay nodes need to decode or detect the received information symbols. In a case for DF cooperative protocol as shown in [47], the relay node will join the cooperative transmission only if in phase two the received symbols are decoded correctly. On the other hand, in the AF cooperative protocol, there is no need to detect or decode the received information symbols at relay nodes. For example, in the cooperative protocol proposed in [50], without decoding, each of the R relay nodes uses a noise version of the received information symbols to generate a row of linear dispersion ST code matrices. Although the noise is amplified during the transmission in phase two, the destination node will still achieve diversity gain.

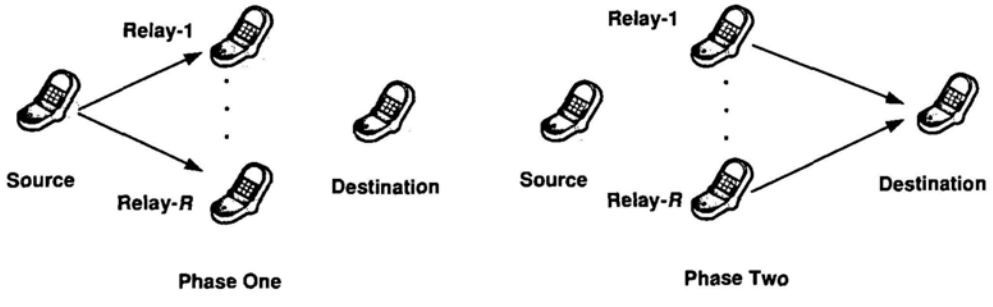

Figure 1.4: A two phase cooperative protocol.

From the above description, it is clear that the most attractive advantage of cooperative communications compared to traditional (non-cooperative) communications is that it enables single-antenna transmitters to achieve spatial diversity. By

using appropriate cooperative protocols, a full diversity achieving ST or SF code for MIMO or MIMO-OFDM systems may be directly applied to a cooperative system [47,49,50,52]. However, from a practical point of view and due to its distributed property, a major disadvantage of cooperative communication is that it is difficult to realize accurate *synchronization* in either time or carrier frequency [53].

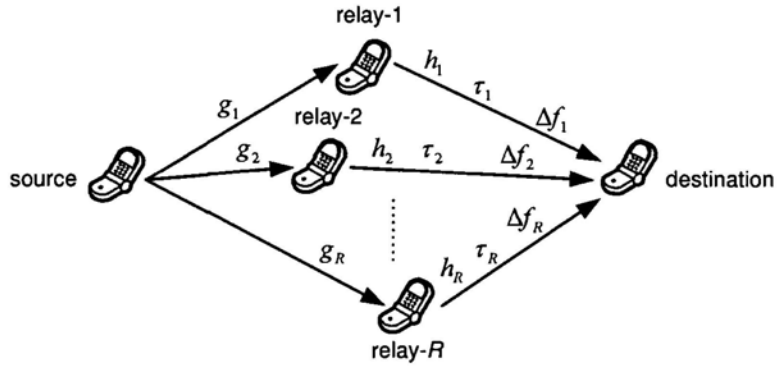

Figure 1.5: A cooperative system with synchronization errors.

Fig.1.5 illustrates a cooperative system with synchronization errors, where g_i ($1 \leq i \leq R$) is the channel coefficient for the link from the source node to ith relay node and h_k, τ_k and Δf_k ($1 \leq k \leq R$) are the channel coefficient, time delay and carrier frequency offset (CFO) for the link from kth relay node to the destination node, respectively. From this figure, we can observe the following two points. First, since relay nodes are located at different places, the time delay from each relay node to the destination node τ_k may be very different compared to that of MIMO systems. Second, since each node in a cooperative system is equipped with its own oscillator, at the destination node, multiple CFOs may exist, which are difficult to be compensated simultaneously.

Without the assumption of synchronization, the advantages of cooperative communications would not hold much. In the presence of different time delays in the received signal, the destination node may not sample at the optimal sampling time of all the components which are transmitted from different relay nodes. According to the Nyquist ISI criterion, for the non-optimally sampled components, each symbol will contribute ISI to its neighbors leading to degraded performance of the system [3,5]. In the case that all different time delays are multiples of an information

symbol duration, although at the destination node all the components of the received signal can be optimally sampled, the equivalent ST code matrix would be a row-wise shifted version of $\mathbf{C}$ due to different time delays. As such, the row-wise shifted ST codes may not be able to preserve their original good properties such as fast decoding or full diversity achievement. For example, the orthogonal ST block codes (STBC) [32, 33] would lose their fast decoding property. For some delay profile, the well-known Alamouti code [33] and delay diversity cannot achieve full diversity any longer. On the other hand, multiple CFOs can degrade the performance of cooperative communication systems, as well. Generally, CFOs cause channels to change with time. If time-varying channels are not compensated, e.g., by equalization, in detection, the communication system will suffer from ISI [5, 54, 55]. However, we cannot be sure whether the equalization based detection methods can still achieve full diversity gain. Furthermore, if we incorporate the effect of CFOs as a part of an ST code matrix, each entry of the ST code matrix will be rotated by CFOs. Once the structure of the ST code matrix is changed, the ST codes may not hold their good properties. In chapter 3, we will see that in the presence of multiple CFOs, Alamouti code not only loses fast decoding property but also in the worst case scenario cannot achieve full diversity order 2. For SF coded cooperative communication systems, multiple CFOs become more stringent because OFDM's sensitivity to it can lead to ICI and result in severe degradation of system performance.

1.3 Motivation of This Study

As discussed in great detail in Chapter1.2, a major problem of cooperative communication systems is synchronization. Currently, most of the distributed ST coding strategies only consider the synchronous scenario [47, 49, 50, 52, 56–59], i.e., all the nodes in the cooperative system are perfectly synchronized in both time and carrier frequency. However, without the assumption of synchronization, the good properties of these strategies may not hold any longer.

To avoid synchronization, some works have already been performed (see for examples [60–66]). In [60], the time reversal ST block codes [67–69] are used, where

although the requirement for time synchronization is relaxed, the rate of the constructed code is low. In [61], a delay diversity [30] based asynchronous cooperative communication strategy is proposed, where at the destination node, the minimum mean square error (MMSE) estimator is used to achieve some diversity gain. However, full diversity is not guaranteed for any delay profile. In [63], delay-tolerant distributed threaded algebraic ST block codes are proposed. However, their symbol rate is low. In [64, 65], a family of ST trellis codes, which can achieve the full diversity property under any delay profile, is proposed. Due to the fact that OFDM are robust to timing errors, in [62] Alamouti ST coded OFDM is proposed to achieve full asynchronous diversity, where the paths from relay nodes to destination node are treated as multipaths. Based on this idea, the SF coded OFDM system is proposed in cooperative communication systems [66], where the applied SF codes can achieve both full cooperative and full multipath diversities when a channel from a relay node to the destination node is, by itself, frequency-selective.

However, all the above works do not consider the multiple CFO problem, which may exist in cooperative communication systems. Since at the destination node multiple CFOs cannot be compensated simultaneously via mixing with a sinusoid [70], the problem is more different and complex than non-cooperative systems, where only one CFO exists. Because OFDM is very sensitive to CFO which often leads to ICI, combating multiple CFOs has been an urgent issue for OFDM based cooperative communication systems [62, 66, 71]. Without ICI mitigation, OFDM systems will quickly suffer from an error floor. On the other hand, even single-carrier systems are not as sensitive as OFDM systems to CFO, multiple CFOs may not be ignored for single-carrier cooperative communication systems as well. First, current or future communication systems are almost certainly to be located well above the 2 GHz band used by the third generation (3G) cellular communication system. Since a good oscillator only guarantees a frequency reference with an error of the order of parts-per-million (PPM), a CFO of dozens of KHz is possible. With multiple CFOs, the channels become time-varying, and can lead to ISI [54, 55, 72, 72, 73]. Second, for long block transmission schemes (see for example [61,64]), the phase rotation caused by CFO is accumulated with the increment of the symbol index in a transmission

block. Therefore for the last few information symbols in a transmission block, the phase rotation may not be be ignored.

Recently, the multiple CFO problem has been considered in [74, 75]. In [74], a subcarrier-wise Alamouti coded OFDM system is considered and a simplified zero-forcing (ZF) equalizer is applied to suppress ICI, where the equalization matrix inverses need to be retaken for every OFDM symbol even in a channel coherent time. In [75], delay diversity is considered and an MMSE decision feedback equalizer (DFE) is employed by the destination node, where multiple CFOs are compensated at each symbol index. However, the process by which multiple CFOs affect the delay diversity from the view of ST codes design is not analyzed.

In this thesis, we study the multiple CFO problem in cooperative communication systems. The goal of this research is to design effective and efficient signal detection methods to combat ISI/ICI caused by multiple CFOs in cooperative communication systems. Additionally, we also try to answer the following questions:

- How do multiple CFOs affect the diversity order or coding gain achieved by ST or SF codes?

- How much diversity gain can our proposed detection methods achieve?

In this study, we consider three kinds of typical ST or SF codes. The first is delay diversity [30] which may be the simplest ST code and one which has been used in [61] to achieve asynchronous cooperative diversity. On the other hand, for delay diversity, compensating multiple CFOs during the decoding procedure does not increase the computational complexity much, because for the ML sequence detection (MLSD), compensation of CFOs in the computing branch metric nearly add on additional computation burden. The second is the well-known Alamouti code [33] which not only can achieve full diversity order 2, but also has full rate one. More importantly, it possesses only linear decoding complexity. Due to these good properties, the Alamouti code has been adopted in many cooperative strategies such as [49, 52, 60, 76]. The third is a family of rotation-based SF codes [36, 37, 39]. Compared with codes used in [61] and [74], these SF codes are powerful in the sense that they can achieve both full cooperative and full multipath diversity orders, and their

rate is always equal to one regardless of the number of transmit antennas. In [66,77], these SF codes have been realized in a distributed fashion in either AF or DF protocols to obtain both full cooperative diversity and full multipath diversity orders. Since OFDM systems are not sensitive to timing errors, these SF codes may be well applied in broadband cooperative communications.

Throughout this study, full channel knowledge including CFOs at the destination node is assumed. In practical systems, the channel knowledge with acceptable quality can be obtained by using training based methods [78,79]. Furthermore, how estimation errors affect SF codes may be a research direction in the future.

1.4 Contributions of This Thesis

The major contributions of this thesis are highlighted as follows:

- We analyze the effect of multiple CFOs on delay diversity and Alamouti code. For delay diversity, we find that multiple CFOs do not affect its achieved diversity order and diversity product. For Alamouti code we find that its achieved diversity product may be decreased by multiple CFOs, and that in the worst case scenario it cannot achieve full diversity order 2.

- We consider the signal detection problem in an SF coded cooperative communication system with multiple CFOs, where the SF codes proposed in [36,37,39] are applied. By fully exploiting the structure of the SF codes, we propose three signal detection methods to deal with the multiple CFO problem. They are the minimum mean-squared error filtering (MMSE-F) method, the two-stage simple frequency shift Q taps (FS-Q-T) method , and the multiple fast Fourier transform (M-FFT) method, all of which offer different tradeoffs between performance and computational complexity. Our simulation results indicate that our proposed detection methods work well as long as CFOs are small.

- We further conduct diversity analysis for the considered SF coded cooperative communication system. We show that the full diversity property still holds for

this family of SF codes [36, 37, 39] when there are multiple CFOs from relay nodes under the condition that the absolute values of normalized CFOs are less than 0.5. We also prove that this full diversity property is still preserved if we seek to reduce the receiver complexity by using a ZF method to equalize the multiple CFOs, before applying ML decoding. In addition, to further improve the robustness of this family of SF codes to multiple CFOs, we also propose a novel permutation (interleaving) method , by using which the SF codes can still achieve full diversity, even when the absolute values of normalized CFOs are larger than or equal to 0.5. For the case that the inter-carrier interference (ICI) matrix is singular, to avoid jointly considering all the subcarriers, two suboptimal full diversity achievable detection methods are proposed as well. Since OFDM system is robust to timing errors, we can conclude that this SF coded OFDM system is robust to both timing errors and CFOs.

Part of the results in this thesis have appeared or will appear in major competitive conferences in the area of wireless communications [80–84]. Moreover, the work regarding signal detection in an SF coded cooperative communication system with multiple CFOs has recently accepted as a full paper in IEEE transactions on vehicular technology [85].

1.5 Organization of This Thesis

The rest of this thesis is organized as follows:

Chapter 2 provides a brief review of ST and SF codes. The ST and SF codes design criteria are described. Furthermore, the structures of some typical ST and SF codes, i.e., delay diversity, orthogonal ST block codes (OSTBC) and a family of rotation-based SF codes, are introduced.

Chapter 3 gives an introduction to cooperative communication, e.g., motivation and some typical cooperative protocols. Then, the problems of time and carrier frequency synchronization in ST and SF coded cooperative communication systems are discussed. Finally, the effect of multiple CFOs on delay diversity and the Alamouti code is analyzed in great detail.

In Chapter 4, we consider the signal detection problem in an SF coded cooperative communication system, where the applied SF codes are rotation-based and can achieve both full spatial and multipath diversities in a multi-antenna system. By exploiting the structure of SF codes, we propose three effective and efficient signal detection methods for the SF coded cooperative system with multiple CFOs.

In Chapter 5, following the work in Chapter 4, we conduct an extensive investigation on the effect of multiple CFOs in the SF coded cooperative communication system. We find that under the condition that the absolute values of normalized CFOs are less than 0.5, these SF codes can still achieve full diversities. After that, we further introduce a novel permutation (interleaving) method to improve the robustness of SF codes to multiple CFOs. To reduce computational complexity, we also propose three full diversity achievable two-stage detection methods applicable to different cases of multiple CFOs.

Chapter 6 summarizes this thesis and presents our perspectives for future work.

□ End of chapter.

Chapter 2

Spatial Diversity Techniques (Multi-Antenna Coding)

Summary

For wireless communications, it has been well recognized that diversity is an effective way to combat channel fading. Among all the diversity techniques, spatial (antenna) diversity is popularly attractive, which can be achieved by applying multi-antenna coding, e.g., space-time (ST) coding and space-frequency (SF) coding at the transmitter without consuming additional time and frequency resources. In this chapter, we begin with an overview of channel fading and diversity techniques. After that we focus on multi-antenna coding. We shall introduce ST codes design criteria for MIMO flat fading channels. As examples, two typical full diversity achievable ST codes are reviewed. After that, we shall discuss SF codes design techniques for MIMO frequency-selective fading channels, where there is an additional source of diversity, namely multipath diversity. A family of rotation-based SF codes will also be reviewed. These codes can achieve both full spatial and full multipath diversity orders.

2.1 Challenge of Wireless Communications

Although wireless communications have been growing rapidly in the past decade, it is apparent that we are still at the early stage of a full development of the wireless world. Today, high demands for fast and reliable transmission over wireless channels motivate the unprecedented development of communication systems towards the high date-rate, low error probability and low complexity implementation. To satisfy all these demands, channel fading is the major challenge to be overcome.

2.1.1 Fading

Due to multipath propagation, channel fading places fundamental limitations on the performance of wireless communications [3–7]. For wireless channels, the emitted electromagnetic waves often do not reach the receive antenna directly due to obstacles blocking the line-of-sight path. In fact, the received waves are often a superposition of waves coming from all directions due to reflection, diffraction, and scattering caused by buildings, trees, and other obstacles. This effect is know as *multipath propagation* [3, 5, 6]. Fig.2.1 illustrates an example of multipath propagation in a terrestrial environment.

Since the received signal consists of an infinite sum of attenuated, delayed, and phase-shifted replicas of the transmitted signal, depending on the phase of each partial wave, the superposition can be either constructive or destructive. Therefore, the strength of the received signal may be increased or decreased, amplified or attenuated. This is the phenomenon of multipath fading [3, 5, 6]. Thus fading is the distortion that a carrier-modulated telecommunication signal experience over certain propagation media. Fundamentally, fading causes poor performance in traditional wireless communication systems because the quality of the communication link depends on a single path or channel, and due to fading there is a significant probability that the channel will experience a deep fade, i.e., the received signal-to-noise ratio (SNR) is seriously degraded. In this case the receiver often suffers from *burst errors* [3, 6], i.e., errors with strong statistical correlations to each other.

Further defining *coherence bandwidth* as the minimum separation of frequencies

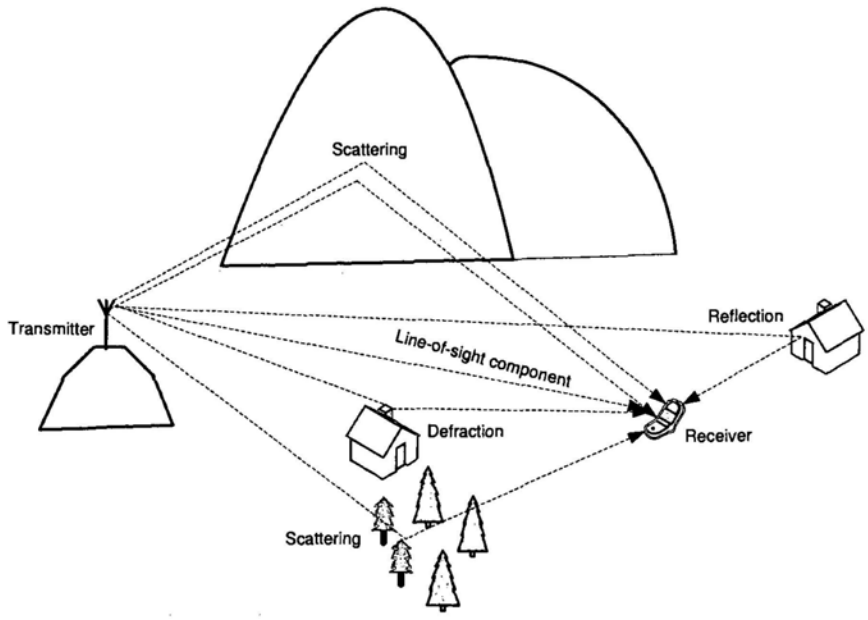

Figure 2.1: Typical wireless radio scenario illustrating multipath propagation in a terrestrial environment.

over which the channel can be considered flat (i.e., a channel which passes all spectral components with approximately equal gain and linear phase) [5], fading channels are generally classified into *flat fading* channel and *frequency-selective fading* channel [3]. An example of frequency-selective fading channel is shown in Fig.1.1.

For the flat fading channel, the coherence bandwidth of the channel is larger than the bandwidth of the transmitted signal. Therefore, all frequency components of the signal will experience the same magnitude of fading. Generally, the flat fading channel is modeled as

$$y = hs + w, \tag{2.1}$$

where y is the output of channel, s is the transmitted information symbol. w is the noise term which is modeled as white Gaussian random variable with zero mean and variance σ^2. Such noise is called additive white Gaussian noise. Here, h is the channel gain and is modeled as a complex Gaussian random variable with zero mean. This model is made for the fading effect induced by local scattering in the absence of a line-of-sight component [3–5, 7].

For the frequency-selective fading channel, the coherence bandwidth of the chan-

nel is smaller than the bandwidth of the transmitted signal [3, 7]. Different frequency components of the received signal therefore experience different magnitude of fading. In the time domain, frequency-selective fading often leads to inter-symbol interference (ISI) which significantly increases equalization complexity at the receiver [3]. The frequency-selective fading channel is generally modeled as a finite impulse response (FIR) filter with impulse response h as

$$h(\tau) = \sum_{l=0}^{L-1} \alpha_l \delta(\tau - \tau_l), \tag{2.2}$$

where L is the number of resolvable paths (multipath). The delay and channel gain for the lth multipath are τ_l and α_l, respectively, where α_l is modeled as a zero mean complex Gaussian variable.

2.1.2 Diversity

For wireless systems, the reliable communication depends on the strength of the channel gain between the transmitter and the receiver. Generally, there is a fairly high probability that the channel will be in deep fading, e.g., for the signal model (2.1). When the channel is in deep fading, any communication scheme will likely suffer from errors. A natural solution to improve the performance is to ensure that the information symbols pass through multiple channels, each of which fades independently, making sure that reliable communication is possible as long as one of the channels is strong enough. This technique is called *diversity* [7].

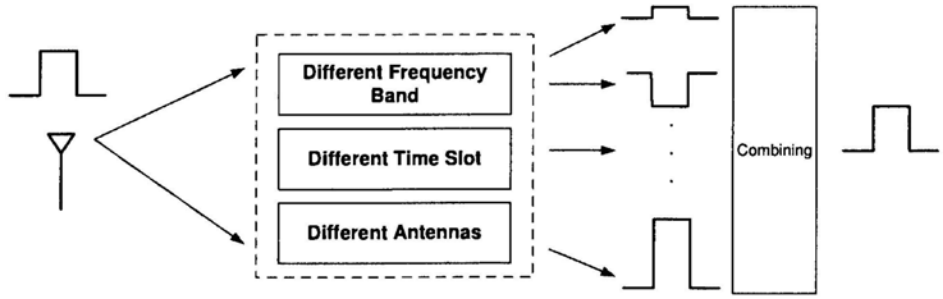

Figure 2.2: The illustration of diversity technique.

Diversity is a powerful technique to improve the performance of wireless com-

munication systems over fading channels. Fig.2.2 shows an example of diversity techniques. If a receiver can get multiple replicas of the signal that are transmitted over essentially independent channels through different time slot, frequency band or antenna, then the fading effect can be averaged by using some combining techniques [3, 7]. Two measures to evaluate diversity techniques are *diversity gain* and *coding gain* which have been introduced in Chapter 1.1.

For deeper insights into the diversity technique, here we give a simple example - *repetition coding* [7], which can clearly show the essence of diversity techniques.

Without repetition, the signal model is given by

$$y = \sqrt{\rho} h s + w, \tag{2.3}$$

where ρ is the transmitting power, s is transmitted information symbol with unit power, channel coefficient h is modeled as zero-mean complex Gaussian random variable with unit variance and w denotes the additive complex Gaussian noise with zero mean and unit variance. Therefore, ρ is the average received SNR and for a given channel h, the instantaneous received SNR is $\rho|h|^2$ denoted by SNR_1.

For repetition coding, the same information symbol s is transmitted L times through independent fading channels, e.g., different time slot, frequency band or receive antenna. Then, we have the signal model

$$\mathbf{y} = \sqrt{\frac{\rho}{L}} \mathbf{h} s + \mathbf{w}, \tag{2.4}$$

where $\mathbf{y} = [y_1, y_2, \cdots, y_L]^{\mathcal{T}}$, $\mathbf{h} = [h_1, h_2, \cdots, h_L]^{\mathcal{T}}$, and $\mathbf{w} = [w_1, w_2, \cdots, w_L]^{\mathcal{T}}$. The elements of $\mathbf{h}$ and $\mathbf{w}$ are i.i.d zero mean unit variance complex Gaussian random variables. Note that due to the scalar $\sqrt{1/L}$, repetition coding does not increase transmitting power. For the maximal ratio combining (MRC) detection method [3], timing $\mathbf{y}$ by $\mathbf{h}^{\mathcal{H}}/\|\mathbf{h}\|_2$, we have the single-input single-output (SISO) model

$$\frac{\mathbf{h}^{\mathcal{H}}}{\|\mathbf{h}\|_2} \mathbf{y} = \sqrt{\frac{\rho}{L}} \|\mathbf{h}\|_2 s + \frac{\mathbf{h}^{\mathcal{H}}}{\|\mathbf{h}\|_2} \mathbf{w}. \tag{2.5}$$

For the equivalent signal model (2.5), the instantaneous received SNR is $\rho\|\mathbf{h}\|_2^2/L$, denoted by SNR_L. Since the elements of $\mathbf{h}$ are i.i.d. complex Gaussian random variables, the term in SNR_L $\|\mathbf{h}\|_2^2 = \sum_{i=1}^{L} |h_i|^2$ is Chi-square distributed with $2L$ degrees of freedom [86]. Furthermore, due to the law of large numbers, $\|\mathbf{h}\|_2^2/L$ converges

to $\mathrm{E}(\sum_{i=1}^{L} |h_i|^2)/L = 1$ with increasing L. Fig.2.3 plots the distribution of $\|\mathbf{h}\|_2^2/L$ for different values of L. It is clear that the larger the L is, the lighter the tail of the distribution near zero is. This means that without increasing the transmitting power, the probability of the overall channel gain being small is drastically decreased with increasing L.

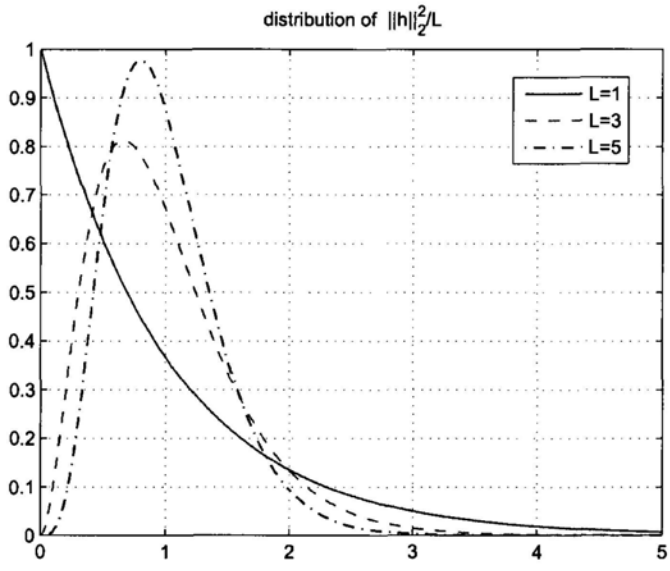

Figure 2.3: The probability density function of $\|\mathbf{h}\|_2^2/L$ for different values of L.

It has been derived in [5, 7] that at high SNR, the symbol/bit error rate of the repetition coded system has the following form as

$$P_{error}(\rho) \approx \alpha \rho^{-L}, \tag{2.6}$$

where the constant α depends on the value of L and modulation methods. From (2.6), diversity order L is clearly achieved by repetition coding. Fig.2.4 shows the SER performance of a binary phase shift keying (BPSK) modulated repetition coding scheme for different values of L. We can see that increasing L drastically improve the SER performance since the SER decreases as the Lth power of SNR, which corresponds to a slop of $-L$ in the SER curve (in dB scale).

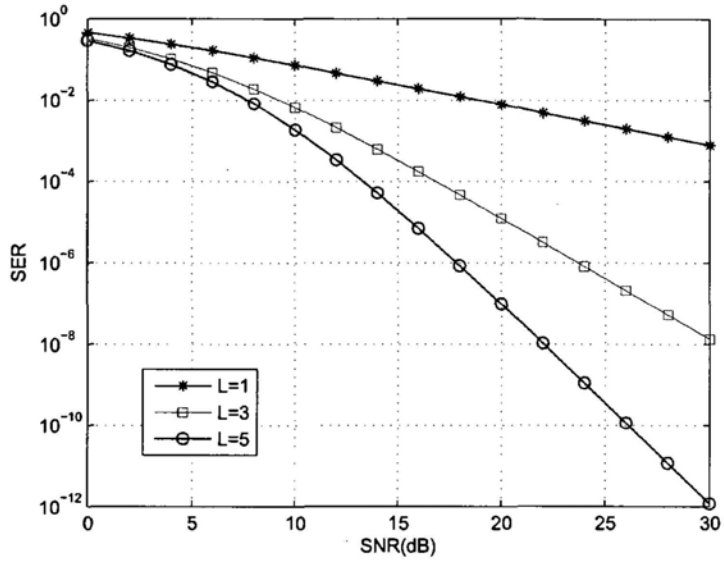

Figure 2.4: The SER performance of a BPSK modulated repetition coding scheme for different values of L.

2.1.3 Multi-Antenna Coding

From the previous introduction, it is clear that diversity is a powerful technique for combating fading in wireless communication systems. Among all of the diversity techniques, spatial diversity, or antenna diversity techniques, are particularly attractive in that they provide diversity gain without consuming additional transmission time or bandwidth. Spatial diversity can be obtained by placing multiple antennas at the transmitter and/or the receiver. If the antennas are placed sufficiently far apart, the channel gains between different antenna pairs fade more or less independently, and independent signal paths are created [7].

There are two ways of exploiting spatial diversity, i.e., *receive diversity* and *transmit diversity* [7,29]. For receive diversity, multiple antennas are only equipped at the receiver to form a single-input multiple-output (SIMO) system. Hence, at the receiver independently faded multiple replicas of the transmitted signal can be obtained. Thus by combining these signals from the multiple receive antennas, e.g., MRC, spatial diversity can be achieved. Actually, many established cellular communication systems today use receive diversity at the base station. For example, a base station in the

Global System for Mobile communications (GSM) [87] typically equips two receive antennas. However, deploying multiple antennas at the receiver is often not feasible due to cost or space limitations. Instead, for transmit diversity, spatial diversity can also be achieved by deploying multiple antennas at the transmitter in combination with multi-antenna coding techniques. [30–33, 88–90].

In the rest of this chapter, first we briefly review the space-time (ST) coding techniques for MIMO flat fading channels. Then, we focus on the space-frequency (SF) coding techniques for MIMO frequency-selective fading channels. Especially, the typical ST and SF codes are also introduced.

2.2 Space-Time Codes for Flat Fading

In this section, we briefly review the techniques of ST codes including design criteria and typical ST codes [29, 32, 33].

2.2.1 Design Criteria of ST Codes

As shown in Fig.1.3, we consider an ST coded MIMO system with M_t transmit antennas and M_r receive antennas. For ST coding, an $N \times 1$ information symbol vector $\mathbf{s} = [s_1, s_2, \cdots, s_N]^{\mathcal{T}}$, whose elements are selected from a signal constellation such as phase shift keying (PSK) or quadrature amplitude modulation (QAM), is encoded into an $M_t \times T$ ST code matrix $\mathbf{C}$ by some coding strategies as follows:

$$\mathbf{C} = \begin{bmatrix} c_{1,1} & c_{1,2} & \cdots & c_{1,T} \\ c_{2,1} & c_{2,2} & \cdots & c_{2,T} \\ \cdots & \cdots & \ddots & \cdots \\ c_{M_t,1} & c_{M_t,2} & \cdots & c_{M_t,T} \end{bmatrix}, \tag{2.7}$$

where $c_{i,k}$ $(1 \le i \le M_t,\ 1 \le k \le T)$ denotes the (i,k)th element of $\mathbf{C}$. Then the ith row of $\mathbf{C}$ is transmitted from the ith transmit antenna and for each channel use one column of $\mathbf{C}$ is transmitted from M_t transmit antennas. Hence the rate of an ST codes is defined as the number of information symbols transmitted per channel use and is given by

$$\mathcal{R} = \frac{N}{T}. \tag{2.8}$$

Assuming the channel between each transmit/receive antenna pair is under quasi-static flat fading, i.e., the channel does not change over T channel uses, we can express the MIMO channel matrix $\mathbf{H}$ as

$$\mathbf{H} = \begin{bmatrix} h_{1,1} & h_{1,2} & \cdots & h_{1,M_t} \\ h_{2,1} & h_{2,2} & \cdots & h_{2,M_t} \\ \vdots & \vdots & \ddots & \vdots \\ h_{M_r,1} & h_{M_r,2} & \cdots & h_{M_r,M_t} \end{bmatrix}, \tag{2.9}$$

where $h_{i,m}$ is the channel gain between the mth transmit antenna and ith receive antenna for $1 \leq i \leq M_r$ and $1 \leq m \leq M_t$. All of the $M_r M_t$ channel gains are modeled as i.i.d. complex Gaussian variables with zero mean and unit variance.

At the receiver, the received $M_r \times T$ signal matrix $\mathbf{Y}$ is given by

$$\mathbf{Y} = \sqrt{\frac{\rho}{M_t}}\mathbf{HC} + \mathbf{W}, \tag{2.10}$$

where $\mathbf{W}$ is the $M_r \times T$ additive complex Gaussian noise matrix whose elements are i.i.d. complex Gaussian variables with zero mean and unit variance. The factor $\sqrt{\rho/M_t}$ ensures that ρ is the average SNR at each receive antenna, independent of the number of transmit antennas.

Assume that the channel is perfectly known to the receiver, the maximum-likelihood (ML) detector is given by

$$\hat{\mathbf{C}} = \arg\min_{\mathbf{C}\in C} \left\| \mathbf{Y} - \sqrt{\frac{\rho}{M_t}}\mathbf{HC} \right\|_F^2, \tag{2.11}$$

where $\| \mathbf{A} \|_F$ strands for Frobenius norm of the matrix $\mathbf{A}$ and the minimization is performed over C, the set of all ST code matrices [29,32].

Let $\mathbf{C}$ and $\tilde{\mathbf{C}}$ be two distinct ST code matrices encoded from two distinct information symbol vectors $\mathbf{s}$ and $\tilde{\mathbf{s}}$. Then an upper bound of pair-wise error probability, i.e., the probability that the ML detection mistakes the transmitted code matrix $\mathbf{C}$ by $\tilde{\mathbf{C}}$, can be shown to be [31,32]:

$$P(\mathbf{C} \to \tilde{\mathbf{C}}) \leq \left(\Pi_{i=1}^{\gamma} \lambda_i\right)^{-M_r} \left(\frac{\rho}{4M_t}\right)^{-\gamma M_r}, \tag{2.12}$$

where γ is the rank of the matrix $\mathbf{C}-\tilde{\mathbf{C}}$ and $\lambda_1, \lambda_2, \cdots, \lambda_\gamma$ are the nonzero eigenvalues of the matrix $(\mathbf{C}-\tilde{\mathbf{C}})^{\mathcal{H}}(\mathbf{C}-\tilde{\mathbf{C}})$. Based on the above pair-wise probability upper bound, the design criteria of the ST codes can be stated as follows:

- *Diversity (Rank) criterion:* The minimum rank of the matrix $\mathbf{C} - \tilde{\mathbf{C}}$ over all pairs of distinct code matrices $\mathbf{C}$ and $\tilde{\mathbf{C}}$ in the ST code matrix set should be as large as possible.

- *Product criterion:* The minimum value of the product $\Pi_{i=1}^{\gamma} \lambda_i$ over all pairs of distinct code matrices in the ST code matrix set should be as large as possible.

The other two major considerations on ST design are the rate defined in (2.8) and the decoding complexity. In the remainder of this section, we will briefly review two kinds of ST codes with different tradeoff among the diversity, rate and decoding complexity.

2.2.2 Delay Diversity

Delay diversity is the simplest ST codes to achieve transmit diversity and is proposed in [30, 88]. For delay diversity (see Fig.2.5), the first transmit antenna directly transmits the N dimension information symbol stream/vector $\mathbf{s} = [s_1, s_2, \cdots, s_N]$ while the mth $(2 \leq m \leq M_t)$ transmit antenna transmits the same stream $\mathbf{s}$ delayed by $m-1$ symbol intervals. Actually, if the symbol delay applied by each transmit antenna is different from one another, full diversity gain can be achieved.

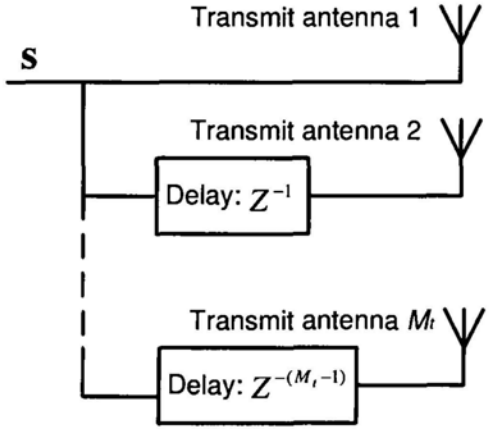

Figure 2.5: Delay diversity.

Delay diversity is a kind of ST trellis codes [31]. In a certain case, it can be also regarded as ST block codes [32], since we can stack the stream transmitted by each

transmit antenna to a wide ST code matrix as

$$\mathbf{C} = \begin{bmatrix} s_1 & s_2 & \cdots & s_{M_t} & \cdots & s_N & 0 & \cdots & 0 \\ 0 & s_1 & \cdots & s_{M_t-1} & \cdots & s_{N-1} & s_N & \cdots & 0 \\ \vdots & \vdots & \ddots & \vdots & \ddots & \vdots & \vdots & \ddots & 0 \\ 0 & 0 & \cdots & s_1 & \cdots & s_{N-M_t+1} & s_{N-M_t+2} & \cdots & s_N \end{bmatrix}. \tag{2.13}$$

In principle, same as the ST trellis codes, the detection of the delay diversity code requires an ML sequence detection (MLSD) algorithm, which is commonly implemented via the Viterbi algorithm. Thus the major drawback of delay diversity is its high decoding complexity which grows exponentially with the number of transmit antennas. Fortunately, because of the linearity of delay diversity code, delay diversity code can be decoded by zero-forcing (ZF), minimum mean square error (MMSE) and minimum mean square error decision feedback equalizer (MMSE-DFE) linear receivers. It can be shown that delay diversity code can also achieve full diversity gain when using these linear receivers as indicated in some recent results in [91, 92].

2.2.3 Orthogonal STBC

Orthogonal space-time block codes (OSTBC) may be the most important subclass of linear space-time block codes (STBC), because OSTBC not only achieves full diversity order $M_t M_r$, but also guarantees to decouple the vector $\mathbf{s}$ ML detection problem into simple scalar s_i detection problems for $1 \leq i \leq N$. OSTBC has the following unitary property:

$$\mathbf{C}\mathbf{C}^{\mathcal{H}} = \left(\sum_{i=1}^{N} |s_i|^2 \right) \mathbf{I}_{M_t}, \tag{2.14}$$

where $\mathbf{I}_{M_t}$ is the $M_t \times M_t$ identity matrix. This property is the major reason which leads to the low decoding complexity of OSTBC [32, 33].

The first OSTBC is the Alamouti code proposed in [33], which is a rate-one OSTBC designed for two transmit antennas. It has the following code matrix

$$\mathbf{C}_2 = \begin{bmatrix} s_1 & -s_2^* \\ s_2 & s_1^* \end{bmatrix}, \tag{2.15}$$

and it is easy to verify that $\mathbf{C}_2\mathbf{C}_2^{\mathcal{H}} = \left(|s_1|^2 + |s_2|^2\right)\mathbf{I}_2$. Later a systemic design of OSTBC for any number of transmit antennas is proposed in [32]. For an arbitrary complex constellation such as PSK and QAM the proposed OSTBC cannot achieve a symbol rate greater than $1/2$ for any number of transmit antennas. Only for three and four transmit antennas, a rate $3/4$ OSTBC exists. Since then OSTBC design for more than four transmit antennas has greatly attracted people's research interest [93–97]. A rate $(\lceil M_t/2 \rceil + 1)/(2\lceil M_t/2 \rceil)$ general OSTBC design is proposed in [96] for $M_t \leq 18$. In [95], it is shown that the symbol rate of OSTBC with fast ML decoding cannot be greater than $3/4$ for more than two transmit antennas.

2.2.4 Illustration of Performance of ST Codes

In order to investigate the SER performance of delay diversity and OSTBC, in this subsection, we simulate a system with two transmit antennas and one receive antenna. The channels are under flat fading and quadrature phase shift keying (QPSK) modulation is employed.

Fig.2.6 shows simulation results. From them we can see that both delay diversity with either the MLSD or MMSE-DFE receiver and the Alamouti code significantly outperform the non-coded SISO system, since these two codes can achieve diversity order 2. Alamouti code has the best performance. Delay diversity with the MLSD receiver has a better SER performance than that of the delay diversity with the MMSE-DFE receiver, since MLSD is the optimal detection method. For the MMSE-DFE receiver, the length of feedforward and feedback filter is 8 and 1, respectively, and the detection delay is 7.

2.3 Space-Frequency Codes for Frequency-Selective Fading

In Section 2.1.3, the ST codes design criteria for MIMO flat fading channels are reviewed and two ST codes are briefly introduced. For broadband wireless communications, the MIMO channels may be under frequency-selective fading which often

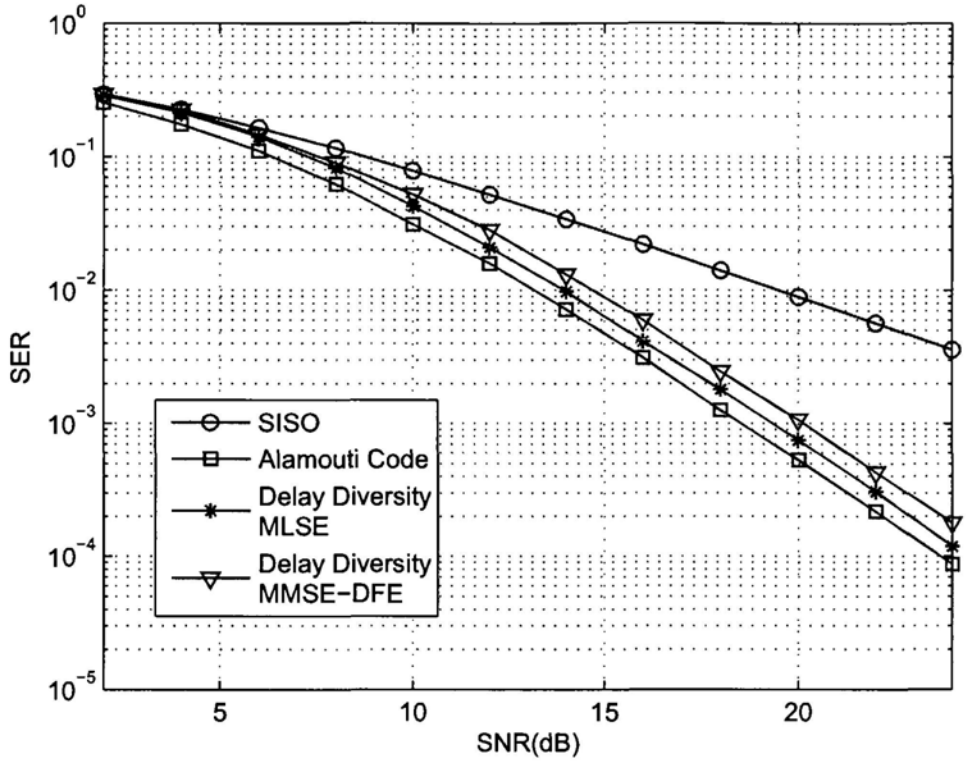

Figure 2.6: SER performance of delay diversity and Alamouti code with QPSK modulation.

leads to ISI. Thus those ST codes designed for flat fading channels may not work any longer. Since OFDM technique can convert the frequency-selective fading channel into a parallel collection of frequency flat fading subchannels, it is a natural idea to combine OFDM with MIMO, referred as MIMO-OFDM, to tackle the problem of ISI [8,9].

For MIMO-OFDM systems, ST codes can be directly applied at each subchannel to achieve diversity order $M_t M_r$. However, in case of frequency-selective fading channels, there is an additional source of diversity, multipath diversity, which cannot be achieved by subcarrier-wise ST coded MIMO-OFDM systems. Due to the existence of multiple propagation paths in each link, the total achievable diversity order is LM_tM_r, where L is the number of independent paths for each link [34,35]. Thus it is of interest to consider coding strategies for MIMO-OFDM systems to achieve both

spatial diversity and multipath diversity. Toward this approach different SF codes are proposed in [34, 36–39], where the coding is across not only space (transmit antennas) but also frequency (subcarriers).

In this section, we first give the design criteria of SF codes derived for MIMO-OFDM systems under frequency-selective fading and then review a family of full rate rotation based SF codes [36, 37, 39].

2.3.1 Design Criteria for SF Codes

Channel Model

We consider a MIMO-OFDM system with M_t transmit antennas and M_r receive antennas [39, 98]. The number of OFDM subcarriers is equal to N. The channel between each transmit/receive antenna pair is under frequency-selective fading with L independent paths. Moreover we also assume that MIMO channels are quasi-static over each code matrix, i.e., the channel gains keep constant for one OFDM symbol interval. The channel impulse response from the mth ($1 \leq m \leq M_t$) transmit antenna and ith ($1 \leq i \leq M_r$) receive antenna is denoted as

$$h_{i,m} = \sum_{l=0}^{L-1} \alpha_{i,m}(l)\delta(\tau - \tau_l), \tag{2.16}$$

where τ_l is the lth delay and $\alpha_{i,m}(l)$ denotes the channel gain of lth multipath between mth transmit antenna and ith receive antenna. All $\alpha_{i,m}(l)$ for $1 \leq m \leq M_t$, $1 \leq i \leq M_r$ and $0 \leq l \leq L-1$ are independent zero-mean complex Gaussian random variables. We assume that the link between each transmit/receive antenna pair has the same normalized power delay profile. Thus we have $\mathrm{E}(|\alpha_{i,m}(l)|^2) = \sigma_l^2$ and $\sum_{l=0}^{L-1} \sigma_l^2 = 1$. Note that for cooperative communications, this assumption may not be appropriate, since the channel profiles from different relay nodes to the destination node may be much different compared to that of MIMO systems. In Chapter 5, we will consider the general case where the channel profiles are not the same for all channels. We further assume that all the delays are rounded to the sampling position, i.e., τ_l is an integer multiple of $1/F_s$, where F_s is the sampling frequency. Then the frequency response of the channel (2.16), $\mathrm{H}_{i,m} = [H_{i,m}(0), H_{i,m}(1), \cdots, H_{i,m}(N-1)]^T$, can be

given by

$$\mathrm{H}_{i,m} = \hat{\mathbf{F}}\mathbf{h}_{i,m}, \tag{2.17}$$

where $\mathbf{h}_{i,m} = [\alpha_{i,m}(0), \alpha_{i,m}(1), \cdots, \alpha_{i,m}(L-1)]^{\mathcal{T}}$ and $\hat{\mathbf{F}} = [\mathbf{f}^{\tau_0}, \mathbf{f}^{\tau_1}, \cdots, \mathbf{f}^{\tau_{L-1}}]$. The column vector $\mathbf{f}^{\tau_l} = [1, \zeta^{\tau_l}, \cdots, \zeta^{(N-1)\tau_l}]^{\mathcal{T}}$, where $\zeta = \exp(-j\frac{2\pi}{T_S})$ and T_S is the OFDM symbol duration.

Signal Model

Each SF code matrix $\mathbf{C}$ is an $N \times M_t$ matrix and is encoded from an $\hat{N} \times 1$ information symbol vector $\mathbf{s}$ whose elements are from QAM or PSK constellation set with normalized unit power [39,98]. The symbol rate per channel use is defined as

$$\mathcal{R} = \frac{\hat{N}}{N}. \tag{2.18}$$

We write the SF code matrix $\mathbf{C}$ as

$$\begin{aligned} \mathbf{C} &= \begin{bmatrix} \mathbf{c}_1 & \mathbf{c}_2 & \cdots & \mathbf{c}_{M_t} \end{bmatrix} \\ &= \begin{bmatrix} c_{1,1} & c_{1,2} & \cdots & c_{1,M_t} \\ c_{2,1} & c_{2,2} & \cdots & c_{2,M_t} \\ \vdots & \vdots & \ddots & \vdots \\ c_{N,1} & c_{N,2} & \cdots & c_{N,M_t} \end{bmatrix}, \end{aligned} \tag{2.19}$$

where mth ($1 \le m \le M_t$) column of $\mathbf{C}$ denoted by $\mathbf{c}_m$ is transmitted from mth transmit antenna by standard OFDM technologies.

Under the assumption of perfect timing and carrier frequency synchronization, at the receiver after removing cyclic prefix (CP) and FFT operation, the received $N \times 1$ signal vector at the ith ($1 \le i \le M_r$) receive antenna can be given by

$$\mathbf{z}_i = \sqrt{\frac{\rho}{M_t}} \sum_{m=1}^{M_t} \mathrm{diag}(\mathbf{c}_m)\mathrm{H}_{i,m} + \mathbf{w}_i, \tag{2.20}$$

where $\mathbf{w}_i$ is an $N \times 1$ noise vector with each entry an independent zero mean unit variance complex Gaussian random variable and ρ stands for the SNR at the receive antenna.

Let $\mathbf{J}_l = \mathrm{diag}(\mathbf{f}^{\tau_l})$, we have

$$\mathbf{J}_l\mathbf{c}_m = \mathrm{diag}(\mathbf{c}_m)\mathbf{f}^{\tau_l}. \tag{2.21}$$

Substituting (2.17) into (2.20) and using (2.21), we get

$$\mathbf{z}_i = \sqrt{\frac{\rho}{M_t}} \sum_{m=1}^{M_t} [\mathbf{J}_0\mathbf{c}_m \ \mathbf{J}_1\mathbf{c}_m \ \cdots \ \mathbf{J}_{L-1}\mathbf{c}_m]\, \mathbf{h}_{i,m} + \mathbf{w}_i. \tag{2.22}$$

Let $\hat{\mathbf{h}}_{i,l} = [\alpha_{i,1}(l), \alpha_{i,2}(l), \cdots, \alpha_{i,M_t}(l)]^{\mathcal{T}}$, for $0 \le l \le L-1$. Following (2.22) we can rewrite $\mathbf{z}_i$ as

$$\begin{aligned} \mathbf{z}_i &= \sqrt{\frac{\rho}{M_t}} \sum_{l=0}^{L-1} [\mathbf{J}_l\mathbf{c}_1 \ \mathbf{J}_l\mathbf{c}_2 \ \cdots \ \mathbf{J}_l\mathbf{c}_{M_t}]\, \hat{\mathbf{h}}_{i,l} + \mathbf{w}_i \\ &= \sqrt{\frac{\rho}{M_t}} \sum_{l=0}^{L-1} \mathbf{J}_l\mathbf{C}\hat{\mathbf{h}}_{i,l} + \mathbf{w}_i. \end{aligned} \tag{2.23}$$

Let $\mathbf{X} = [\mathbf{J}_0\mathbf{C}, \mathbf{J}_1\mathbf{C}, \cdots, \mathbf{J}_{L-1}\mathbf{C}]$ and $\mathbf{h}_i = [\hat{\mathbf{h}}_{i,0}^{\mathcal{T}}, \hat{\mathbf{h}}_{i,1}^{\mathcal{T}}, \cdots, \hat{\mathbf{h}}_{i,L-1}^{\mathcal{T}}]^{\mathcal{T}}$. Then from (2.23), we have

$$\mathbf{z}_i = \mathbf{X}\mathbf{h}_i + \mathbf{w}_i. \tag{2.24}$$

Further defining $\mathbf{z} = [\mathbf{z}_1^{\mathcal{T}}, \mathbf{z}_2^{\mathcal{T}}, \cdots, \mathbf{z}_{M_r}^{\mathcal{T}}]^{\mathcal{T}}$, $\mathbf{w} = [\mathbf{w}_1^{\mathcal{T}}, \mathbf{w}_2^{\mathcal{T}}, \cdots, \mathbf{w}_{M_r}^{\mathcal{T}}]^{\mathcal{T}}$, $\mathbf{h} = [\mathbf{h}_1^{\mathcal{T}}, \mathbf{h}_2^{\mathcal{T}}, \cdots, \mathbf{h}_{M_r}^{\mathcal{T}}]^{\mathcal{T}}$, and $\bar{\mathbf{X}} = \mathbf{I}_{M_r} \otimes \mathbf{X}$, we have the signal model

$$\mathbf{Y} = \sqrt{\frac{\rho}{M_t}}\bar{\mathbf{X}}\mathbf{h} + \mathbf{w}. \tag{2.25}$$

Design Criteria of SF Codes

Assume that the channel is perfectly known to the receiver, the ML detector is given by

$$\hat{\mathbf{C}} = \arg\min_{\mathbf{C}\in C} \left\| \mathbf{Y} - \sqrt{\frac{\rho}{M_t}}\bar{\mathbf{X}}\mathbf{h} \right\|_F^2, \tag{2.26}$$

where the minimization is performed over C, the SF code matrix set. Let $\mathbf{C}$ and $\tilde{\mathbf{C}}$ are two distinct $N \times M_t$ SF code matrices encoded from two distinct information symbol vector $\mathbf{s}$ and $\tilde{\mathbf{s}}$, an upper bound of the pairwise error probability is given by [99–101]

$$P(\mathbf{C} \to \tilde{\mathbf{C}}) \le \binom{2\gamma - 1}{\gamma} \left(\prod_{i=1}^{\gamma} \lambda_i \right)^{-1} \left(\frac{\rho}{M_t} \right)^{-\gamma}, \tag{2.27}$$

where γ is the rank of the matrix $(\bar{\mathbf{X}} - \tilde{\bar{\mathbf{X}}})\Lambda(\bar{\mathbf{X}} - \tilde{\bar{\mathbf{X}}})^{\mathcal{H}}$, $\lambda_1, \lambda_2, \cdots, \lambda_\gamma$ are the nonzero eigenvalues of $(\bar{\mathbf{X}} - \tilde{\bar{\mathbf{X}}})\Lambda(\bar{\mathbf{X}} - \tilde{\bar{\mathbf{X}}})^{\mathcal{H}}$ and $\Lambda = \mathrm{E}(\mathbf{h}\mathbf{h}^{\mathcal{H}})$.

Further from the definition of $\mathbf{h}$, it is easy to get

$$\Lambda = \mathrm{E}(\mathbf{h}\mathbf{h}^{\mathcal{H}}) = \mathbf{I}_{M_r} \otimes \mathbf{Q}, \tag{2.28}$$

where $\mathbf{Q} = \text{diag}(\sigma_0^2, \sigma_1^2, \cdots, \sigma_{L-1}^2) \otimes \mathbf{I}_{M_t}$. By using the property of Kronecker product [102], after some matrix operations, we can get

$$(\bar{\mathbf{X}} - \tilde{\bar{\mathbf{X}}})\Lambda(\bar{\mathbf{X}} - \tilde{\bar{\mathbf{X}}})^{\mathcal{H}} = \mathbf{I}_{M_r} \otimes \left((\mathbf{X} - \tilde{\mathbf{X}})\mathbf{Q}(\mathbf{X} - \tilde{\mathbf{X}})^{\mathcal{H}}\right). \tag{2.29}$$

So we have

$$\begin{aligned} \text{rank}\left((\bar{\mathbf{X}} - \tilde{\bar{\mathbf{X}}})\Lambda(\bar{\mathbf{X}} - \tilde{\bar{\mathbf{X}}})^{\mathcal{H}}\right) &= \text{rank}\left(\mathbf{I}_{M_r} \otimes \left((\mathbf{X} - \tilde{\mathbf{X}})\mathbf{Q}(\mathbf{X} - \tilde{\mathbf{X}})^{\mathcal{H}}\right)\right) \\ &= M_r \text{rank}\left((\mathbf{X} - \tilde{\mathbf{X}})\mathbf{Q}(\mathbf{X} - \tilde{\mathbf{X}})^{\mathcal{H}}\right), \end{aligned} \tag{2.30}$$

and

$$\prod_{i=1}^{\gamma} \lambda_i = \left(\prod_{i=1}^{\hat{\gamma}} \hat{\lambda}_i\right)^{M_r}, \tag{2.31}$$

where $\hat{\gamma}$ is the rank of $(\mathbf{X} - \tilde{\mathbf{X}})\mathbf{Q}(\mathbf{X} - \tilde{\mathbf{X}})^{\mathcal{H}}$, and $\hat{\lambda}_1, \hat{\lambda}_2, \cdots, \hat{\lambda}_{\hat{\gamma}}$ are nonzero eigenvalues of $(\mathbf{X} - \tilde{\mathbf{X}})\mathbf{Q}(\mathbf{X} - \tilde{\mathbf{X}})^{\mathcal{H}}$. Therefore, the design criteria of SF codes can be stated as follows:

- *Diversity (Rank) criterion:* The minimum rank of the matrix $(\mathbf{X} - \tilde{\mathbf{X}})\mathbf{Q}(\mathbf{X} - \tilde{\mathbf{X}})^{\mathcal{H}}$ over all pairs of distinct code matrices $\mathbf{C}$ and $\tilde{\mathbf{C}}$ in the SF code matrix set should be as large as possible.

- *Product criterion:* The minimum value of the produce $\prod_{i=1}^{\hat{\gamma}} \hat{\lambda}_i$ over all pairs of distinct code matrices $\mathbf{C}$ and $\tilde{\mathbf{C}}$ in the SF code matrix set should be as large as possible.

2.3.2 Rate One Rotation Based SF Codes

In this subsection, we briefly review a family of rotation based SF codes, which are proposed in [36, 37, 39, 66]. These SF codes have the following two advantages:

- They can achieve both full spatial diversity and full multipath diversity.

- Their rate is always equal to one regardless of the number of transmit antennas.

Here we adopt the code structure proposed in [39].

Each SF code $\mathbf{C}$ is an $N \times M_t$ matrix and is mapped from an $\hat{N} \times 1$ information symbol vector $\mathbf{s}$. Here N is equal to the number of subcarriers in one OFDM symbol, M_t is equal to the number of transmit antennas, and $\hat{N} \leq N$.

For the coding strategy proposed in [39], each SF codeword $\mathbf{C}$ is a concatenation of some $M_t\Gamma \times M_t$ matrices $\mathbf{G}_p$

$$\mathbf{C} = \left[\mathbf{G}_1^{\mathcal{T}} \quad \mathbf{G}_2^{\mathcal{T}} \quad \cdots \quad \mathbf{G}_P^{\mathcal{T}} \quad \mathbf{0}_{(N-\hat{N})\times M_t}^{\mathcal{T}}\right]^{\mathcal{T}}, \tag{2.32}$$

where $P = \lfloor N/(\Gamma M_t) \rfloor$, $\hat{N} = P\Gamma M_t$, each matrix $\mathbf{G}_p$, for $p = 1, 2, \cdots, P$, is of size ΓM_t by M_t and Γ is a coding parameter. The zero padding matrix $\mathbf{0}_{(N-\hat{N})\times M_t}$ is an $(N - \hat{N}) \times M_t$ all zero matrix which is used if the number of subcarriers N is not an integer multiple of ΓM_t. In the remainder of this thesis, unless otherwise specified, we always assume that N is an integer multiple of ΓM_t. Each matrix $\mathbf{G}_p$, $1 \leq p \leq P$, has the same structure given by

$$\mathbf{G}_p = \sqrt{M_t}\begin{bmatrix} \mathbf{x}_1^p & \mathbf{0}_\Gamma & \cdots & \mathbf{0}_\Gamma \\ \mathbf{0}_\Gamma & \mathbf{x}_2^p & \cdots & \mathbf{0}_\Gamma \\ \vdots & \vdots & \ddots & \vdots \\ \mathbf{0}_\Gamma & \mathbf{0}_\Gamma & \cdots & \mathbf{x}_{M_t}^p \end{bmatrix}, \tag{2.33}$$

where $\mathbf{x}_m^P = [x_{(m-1)\Gamma+1}^p x_{(m-1)\Gamma+2}^p \cdots x_{m\Gamma}^p]^{\mathcal{T}}$, $m = 1, 2, \cdots, M_t$, and all x_k^p, $k = 1, 2, \cdots, \Gamma M_t$, are complex symbols and are mapped from an information subvector $\mathbf{s}_p = [s_1^p, s_2^p, \cdots, s_{\Gamma M_t}^p]^{\mathcal{T}}$ by a rotation operation

$$\mathbf{x}^p = [\mathbf{x}_1^{p\mathcal{T}}, \mathbf{x}_2^{p\mathcal{T}}, \cdots, \mathbf{x}_{M_t}^{p\ \mathcal{T}}]^{\mathcal{T}} = \mathbf{\Theta}\mathbf{s}_p, \tag{2.34}$$

where s_l^p is $((p-1)\Gamma M_t + l - 1)$th entry of $\mathbf{s}$ for $1 \leq l \leq \Gamma M_t$ and $\mathbf{\Theta}$ is an $M_t\Gamma \times M_t\Gamma$ rotation matrix. The effect of the constellations rotation will be briefly explained in the following paragraphs. The energy constraint is $\mathrm{E}\left[\sum_{k=1}^{\Gamma M_t} |x_k|^2\right] = \Gamma M_t$. For a certain p, the symbols in $\mathbf{G}_p$ are designed jointly, but the design of $\mathbf{G}_{p_1}$ and $\mathbf{G}_{p_2}$, $p_1 \neq p_2$, is independent of each other. At the destination node, each SF submatrix $\mathbf{G}_p$ is decoded by ML or sphere decoding [103–105] independently.

The idea of rotated constellation was first proposed in [106]. Rotations were proposed based on the fact that given a constellation Q with dimension n, i.e., each element of Q is an n-dimensional vector, if any given vector $\mathbf{s} \in Q$ has its components $s_1, \cdots, s_n$ different from all the other components of the vectors in Q, then affecting $(s_1, s_2, \cdots, s_n)$ by independent fadings $\rightarrow (\alpha_1 s_1, \alpha_2 s_2, \cdots, \alpha_n s_n)$, allows the receiver to recover $(s_1, s_2, \cdots, s_n)$ unless all the components fall in deep fading, i.e., $|\alpha_i| \ll 1$,

$\forall i$ [107]. The latter property is called full modulation diversity of the constellation Q, and it can be measured by the minimum product distance of Q [106], which is defined as

$$d_{\min} \triangleq \min_{\Delta \mathbf{s}=\mathbf{s}-\tilde{\mathbf{s}},\mathbf{s}\neq\tilde{\mathbf{s}}\in Q} \prod_{i=1}^{n} |\Delta s_i|. \tag{2.35}$$

It is clear that if the elements of $\mathbf{s}$ are independently selected from a signal constellation, e.g., QAM and pulse amplitude modulation (PAM), the constellation Q with dimension n has not full modulation diversity and its minimum product distance is equal to 0. To achieve full modulation diversity, it is proposed to rotate the elements of Q so that $\boldsymbol{\Theta}\mathbf{s} - \boldsymbol{\Theta}\tilde{\mathbf{s}}$ has no zero entries for $\mathbf{s}$ and $\tilde{\mathbf{s}}$ are two distinct elements of Q. Here $\boldsymbol{\Theta}$ is the $n \times n$ rotation matrix and the optimal rotations are those that have full modulation diversity and maximize the minimum product distance. Some optimal rotation matrices $\boldsymbol{\Theta}$ have been found when the elements of $\mathbf{s}$ are from a signal constellation of QAM or PAM [108]. For example, if $n = 2^k$ ($k \geq 1$), the optimum $\boldsymbol{\Theta}$ is given by

$$\boldsymbol{\Theta} = \sqrt{\frac{1}{n}} \begin{bmatrix} 1 & \theta_1 & \cdots & \theta_1^{n-1} \\ 1 & \theta_2 & \cdots & \theta_2^{n-1} \\ \vdots & \vdots & \ddots & \vdots \\ 1 & \theta_n & \cdots & \theta_n^{n-1} \end{bmatrix}, \tag{2.36}$$

where $\theta_i = e^{j\frac{4i-3}{2n}\pi}$ for $1 \leq i \leq M_t\Gamma$. The details regarding the construction of $\boldsymbol{\Theta}$ can be found in [39] and the references therein.

Then, let us look at the achieved diversity order by this family SF codes. For two distinct SF code matrices $\mathbf{C}$ and $\tilde{\mathbf{C}}$, there is at least one index p_0 ($1 \leq p_0 \leq P$) such that $\mathbf{s}_{p_0} \neq \tilde{\mathbf{s}}_{p_0}$. Assume information symbols are selected from QAM or PAM constellations. Then, due to rotations, the vector $\Delta\mathbf{x}^{p_0} = \mathbf{x}^{p_0} - \tilde{\mathbf{x}}^{p_0}$ has no zero entries for distinct rotated symbol vectors $\mathbf{x}^{p_0}$ and $\tilde{\mathbf{x}}^{p_0}$. By using this property, we will see that the SF code can achieve full diversity. On the other hand, it is shown in [39] that increasing the minimum product distance of rotated symbol vector $\mathbf{x}$ can increase the diversity product of the SF code.

We may further assume that $\mathbf{s}_p = \tilde{\mathbf{s}}_p$ for any $p \neq p_0$ since the rank of $\mathbf{X} - \tilde{\mathbf{X}}$ does not decrease if $\mathbf{s}_p \neq \tilde{\mathbf{s}}_p$ for some $p \neq p_0$. To simplify notation, in the remainder of this subsection we just omit the scalar $\sqrt{M_t}$ in $\mathbf{G}_p$ (2.33), since it does not affect

the diversity analysis. Consequently, from the structure of $\mathbf{G}_p$ and the definition of $\mathbf{X}$ (2.24), the $(p_0 - 1)$th $M_t\Gamma \times M_tL$ submatrix of $\mathbf{X} - \tilde{\mathbf{X}}$ is given by $\Delta\mathbf{X}_{p0} = [\Delta\mathbf{X}^0_{p0}, \Delta\mathbf{X}^1_{p0}, \cdots, \Delta\mathbf{X}^{L-1}_{p0}]$. The $M_t\Gamma \times M_t$ matrix $\Delta\mathbf{X}^l_{p0}$ $(0 \le l \le L-1)$ has the form as

$$\Delta\mathbf{X}^l_{p0} = \begin{bmatrix} \mathrm{diag}(\Delta\mathbf{x}^{p_0}_1)\mathbf{f}^{\tau_l}_{p_0,1} & \mathbf{0}_\Gamma & \cdots & \mathbf{0}_\Gamma \\ \mathbf{0}_\Gamma & \mathrm{diag}(\Delta\mathbf{x}^{p_0}_2)\mathbf{f}^{\tau_l}_{p_0,2} & \cdots & \mathbf{0}_\Gamma \\ \vdots & \vdots & \ddots & \vdots \\ \mathbf{0}_\Gamma & \mathbf{0}_\Gamma & \cdots & \mathrm{diag}(\Delta\mathbf{x}^{p_0}_{M_t})\mathbf{f}^{\tau_l}_{p_0,M_t} \end{bmatrix}, \quad (2.37)$$

where $\Delta\mathbf{x}^{p_0}_m = \mathbf{x}^{p_0}_m - \tilde{\mathbf{x}}^{p_0}_m$ for $1 \le m \le M_t$ and $\mathbf{f}^{\tau_l}_{p_0,m}$ is the $((p_0 - 1)M_t + m - 1)$th $\Gamma \times 1$ subvector of $\mathbf{f}^{\tau_l}$ for $1 \le m \le M_t$ and $0 \le l \le L-1$. By collecting all the L nonzero $\Gamma \times 1$ vectors from $((m-1)\Gamma))$th row to $(m\Gamma - 1)$th row of $\Delta\mathbf{X}_{p0}$, we construct the $\Gamma \times L$ matrix $\mathbf{B}^{p_0}_m$ for $1 \le l \le M_t$ with the form

$$\mathbf{B}^{P_0}_m = [\mathrm{diag}(\Delta\mathbf{x}^{p_0}_m)\mathbf{f}^{\tau_0}_{p_0,m}, \mathrm{diag}(\Delta\mathbf{x}^{p_0}_m)\mathbf{f}^{\tau_1}_{p_0,m}, \cdots, \mathrm{diag}(\Delta\mathbf{x}^{p_0}_m)\mathbf{f}^{\tau_{L-1}}_{p_0,m}]. \quad (2.38)$$

Since $\Delta\mathbf{X}^l_{p0}$ $(0 \le l \le L-1)$ is a block diagonal matrix, it is not hard to see that the rank of $\Delta\mathbf{X}_{p_0}$ is equal to $\sum_{m=1}^{M_t} \mathrm{rank}(\mathbf{B}^{p_0}_m)$.

Considering the definition of $\mathbf{f}^{\tau_l}$, we can further rewrite $\mathbf{B}^{p_0}_m$ by

$$\mathbf{B}^{P_0}_m = \mathrm{diag}(\Delta\mathbf{x}^{p_0}_m)\mathbf{B}\mathbf{A}^{p_0}_m, \quad (2.39)$$

where $\mathbf{A}^{p_0}_m = \mathrm{diag}(\exp(-j2\pi\frac{((p_0-1)M_t\Gamma+(m-1)\Gamma)\tau_0}{T_s}), \cdots, \exp(-j2\pi\frac{((p_0-1)M_t\Gamma+(m-1)\Gamma)\tau_{L-1}}{T_s}))$ and the $\Gamma \times L$ matrix $\mathbf{B}$ is given by

$$\mathbf{B} = \begin{bmatrix} 1 & 1 & \cdots & 1 \\ \exp(-j2\pi\frac{\tau_0}{T_s}) & \exp(-j2\pi\frac{\tau_1}{T_s}) & \cdots & \exp(-j2\pi\frac{\tau_{L-1}}{T_s}) \\ \exp(-j2\pi\frac{2\tau_0}{T_s}) & \exp(-j2\pi\frac{2\tau_1}{T_s}) & \cdots & \exp(-j2\pi\frac{2\tau_{L-1}}{T_s}) \\ \vdots & \vdots & \ddots & \vdots \\ \exp(-j2\pi\frac{(\Gamma-1)\tau_0}{T_s}) & \exp(-j2\pi\frac{(\Gamma-1)\tau_1}{T_s}) & \cdots & \exp(-j2\pi\frac{(\Gamma-1)\tau_{L-1}}{T_s}) \end{bmatrix}. \quad (2.40)$$

As $\Delta\mathbf{x}^{p_0}_m$ $(1 \le m \le M_t)$ has no zero entries, both $\mathrm{diag}(\Delta\mathbf{x}^{p_0}_m)$ and $\mathbf{A}^{p_0}_m$ are nonsingular diagonal matrices. So, we can obtain that

$$\mathrm{rank}(\mathbf{B}^{P_0}_m) = \mathrm{rank}(\mathbf{B}). \quad (2.41)$$

Observing (2.40), we can see that $\mathbf{B}$ is a $\Gamma \times L$ Vandermonde matrix. Due to the fact that $\tau_0 < \tau_1 < \cdots < \tau_L < T_s$, it is clear that $\exp(-j2\pi\frac{\tau_l}{T_s})$ $(0 \le l \le L-1)$ are distinct

from one another. Therefore, matrix $\mathbf{B}$ has full rank $\min(\Gamma, L)$. Consequently, we have

$$\text{rank}(\mathbf{X} - \tilde{\mathbf{X}}) = \text{rank}(\Delta\mathbf{X}_{p_0}) = \sum_{m=1}^{M_t} \text{rank}(\mathbf{B}_m^{p_0}) = \sum_{m=1}^{M_t} \text{rank}(\mathbf{B}) = M_t \min(\Gamma, L). \quad (2.42)$$

From the fact that $\mathbf{Q}$ (2.28) is a diagonal matrix with positive diagonal entries, we obtain

$$\text{rank}((\mathbf{X} - \tilde{\mathbf{X}})\mathbf{Q}(\mathbf{X} - \tilde{\mathbf{X}})^{\mathcal{H}}) = \text{rank}((\mathbf{X} - \tilde{\mathbf{X}})\mathbf{Q}^{\frac{1}{2}}) = \text{rank}(\Delta\mathbf{X}_{p_0}) = M_t \min(\Gamma, L). \quad (2.43)$$

So, according to the *rank criterion* of SF codes design, from (2.43) we can conclude that this family of SF codes can achieve diversity order $M_t \min(\Gamma, L)$. If Γ is chosen not to be smaller than L, both full spatial and full multipath diversity orders $M_t L$ can be achieved.

2.3.3 Illustration of Performance of SF Codes

In order to investigate the performance of SF codes introduced in Section 2.3.2, we have conducted many experiments. Here, we show some of the simulation results. The simulated MIMO-OFDM system has two transmit antennas, one receive antennas and 64 subcarriers, i.e., $M_t = 2$, $M_r = 1$ and $N = 64$. The bandwidth is 20 MHz and the cyclic prefix of the OFDM is fixed to $N/4 = 16$. The channels from transmit antennas to the receive antennas are all frequency-selective with two equal power rays $[\tau_0, \tau_1] = [0, 0.5]\mu s$ for $1 \leq m \leq M_t$. The SF code proposed in [39] is applied. To achieve both full cooperative diversity and multipath diversity, the parameter Γ is set to 2.

To evaluate the SER performance of SF codes, we also simulate the Alamouti code which is applied at each subcarrier of the MIMO-OFDM system. As we have discussed, it can only achieve diversity order 2. From Fig.2.7, we can see that at the low and medium SNR, Alamouti code has a better SER performance than that of the SF codes. However, when SNR is larger than 14dB, SF codes quickly outperform the Alamouti code, since SF codes can achieve diversity order 4.

□ End of chapter.

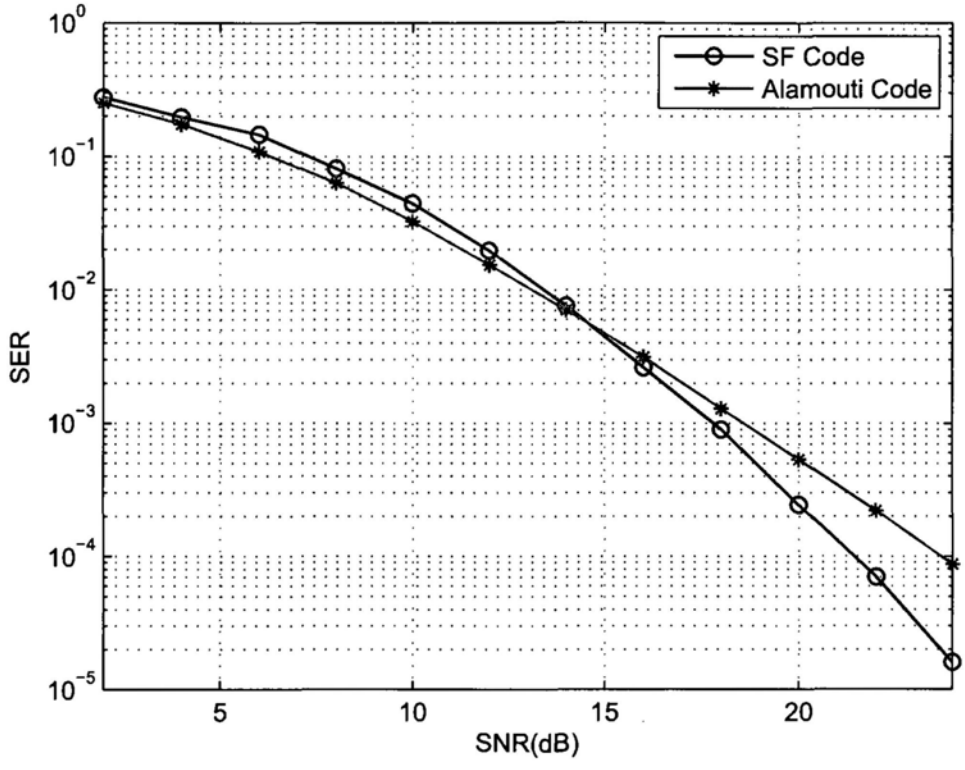

Figure 2.7: SER performance of SF codes with QPSK modulation.

Chapter 3

Cooperative Communications

Summary

Although transmit diversity has been widely acknowledged, due to hardware constraints, equipment with multiple transmit antennas in the terminal nodes in wireless networks may not be practical. To tackle this problem, a state of the art technology has been proposed and this is general referred as cooperative communication. Its principle is to build a *virtual multi-antenna* transmitter to achieve transmit diversity, as widely called *cooperative diversity*, by using a collection of distributed antennas in different terminals. However, a major challenge for practice of cooperative communications is synchronization. As terminals, located at different places, are operated with their own oscillators, the destination node may suffer from both multiple delays and multiple carrier frequency offsets (CFOs). This chapter begins with an introduction of cooperative communications, in which typical cooperative protocols are reviewed. Then it focuses on the synchronization problems in cooperative communication systems. Finally, the effect of multiple CFOs on delay diversity and Alamouti code is analyzed detailedly.

3.1 Motivation of Cooperative Communications

As introduced in Chapter 2, if multiple antennas are placed at the transmitter, transmit diversity can be achieved by applying space-time (ST) or space-frequency (SF) coding techniques. The advantages of transmit diversity have been well recognized, to the extent that the Alamouti code [33] has been incorporated into wireless 802.16 standards [15]. Although transmit diversity is clearly advantageous on a cellular base station, its application may not be practical for other scenarios. Specifically, due to size, cost, or hardware limitations, a wireless agent may not be able to support multiple transmit antennas. Examples include most handsets (size, power) or the nodes in a mobile cellular network, wireless sensor network, home networks (e.g., HomeRF), device networks (e.g., Bluetooth) and Ad Hoc networks [44].

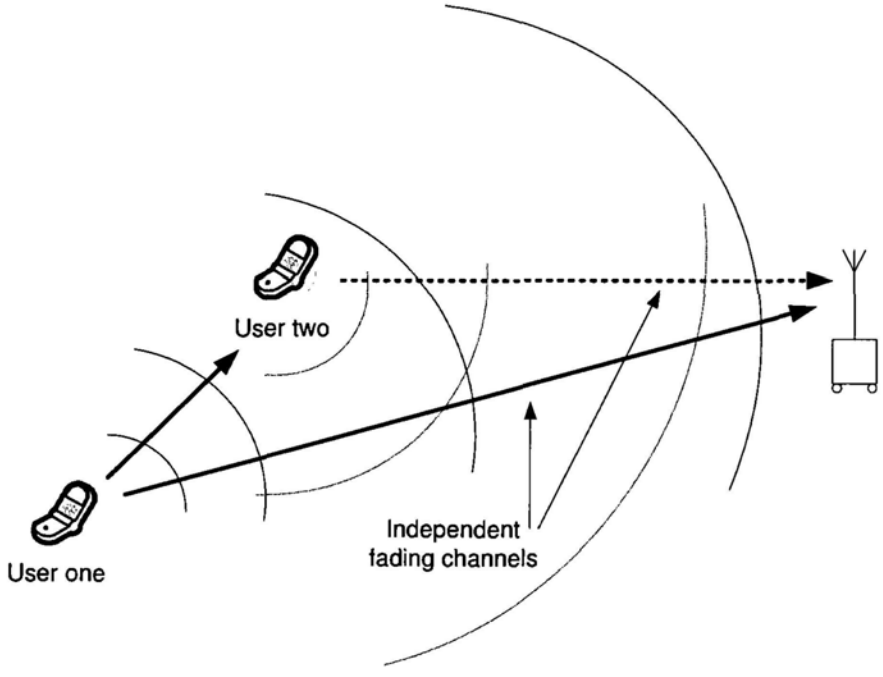

Figure 3.1: Cooperative communication.

To solve this problem, researchers have proposed a new class of method called cooperative communication [45–49], which is built on the classical relay channel model [109]. Their basic idea is to generate a virtual multi-antenna transmitter to achieve transmit diversity by cooperation of single-antenna transmitters in a net-

work. The fundamentals behind cooperative communications are based on two inherent properties of wireless communications. The first one is the nature of wireless communications to broadcast, in which transmitted signals can be received and processed simultaneously by the nodes other than the destination node. The second one is different propagation conditions among spatially distributed nodes, which make the fading of each link among nodes independent from one another.

For example, as shown in Fig.3.1, user 1 intends to communicate with the destination node. Since each user has only one transmit antenna, user 1 cannot generate transmit diversity by itself. However, user 2 may possibly receive user 1, and forward some version of the data transmitted by user 1 to the destination node. Then, statistical independence of the fading channels for these two users can create transmit diversity. Therefore, cooperative communications can produce transmit diversity in a novel and interesting way.

3.2 Cooperative Protocols

By applying some cooperative protocols, multiple users (nodes) equipped with single-antenna in a network can cooperate to form a virtual antenna array realizing transmit diversity in a distributed fashion. This section will briefly review some cooperative protocols which are frequently employed by different cooperative strategies.

Half-duplex transmission:

Half-duplex transmission, in which the wireless agent cannot simultaneously receive and transmit, is generally assumed in cooperative communications because it can be implemented with lower complexity by using either time or frequency division [47–49]. However, *full-duplex*, in which wireless agents receive and transmit simultaneously, is generally a microwave design challenge, due to the large difference in the transmitting and receiving signal power levels [110]. This thesis will adopt the assumption of *half-duplex* transmission as well.

Classification of cooperative protocols:

Broadly speaking, all the cooperative protocols can be classified into two types, namely, *amplify-and-forward (AF)* protocol and *decode-and-forward (DF)* protocol [48, 51]. In AF protocols, relay nodes simply amplify and retransmit the received signals from the source node without demodulation or decoding. Although the noise is amplified along with the signal in this technique, spatial diversity can still be achieved by signal transmission over spatially independent channels. In DF protocols, relay nodes need to demodulate or decode the received signals from the source node before retransmission. In practice, the AF protocols require significantly lower implementation complexity at relay nodes than that of DF protocols.

Multihop (Multinode) cooperative protocol:

Multihop (Multinode) cooperative protocol [47–49, 111, 112] is a kind of cooperative protocols based on repetition transmission. Its major characteristic is that all the transmitters incorporated into cooperation (including the source node and all the relay nodes) have orthogonal channels which may be achieved through some combination of time, frequency, and code-division multiple access (CDMA) as part of an overall channel and resource allocation scheme.

Fig.3.2 shows an example of multihop cooperative protocol which includes one source node, one destination node and R relay nodes. The cooperative protocol consists of $R+1$ phases. In phase one, the source node broadcasts the information signal to all relay nodes and the destination node. In phase $k+1$ ($1 \leq k \leq R$), the kth relay node combines (e.g, using maximal-ratio-combiner (MRC) [5]) the signals received from the previous m ($0 \leq m \leq R-1$) relay nodes along with that from the source node. Here the relay nodes can work on either AF transmission or DF transmission. For AF transmission, the kth relay node directly amplifies and forwards the combined signal to other nodes. For DF transmission, after combination and decoding, the kth relay node judges whether the received symbols are decoded correctly or not (e.g., by checking cyclic redundancy check (CRC) code [5] or comparing the received SNR to a threshold) and only forwards the signal if decoded correctly. Otherwise, it remains

idle. Finally, in phase $R + 1$, the destination node combines all of the received $R + 1$ signals and then decodes. As totally $R + 1$ spatially independent channels exist from the source and relay nodes to the destination node, this multihop cooperative protocol can achieve diversity order $R + 1$.

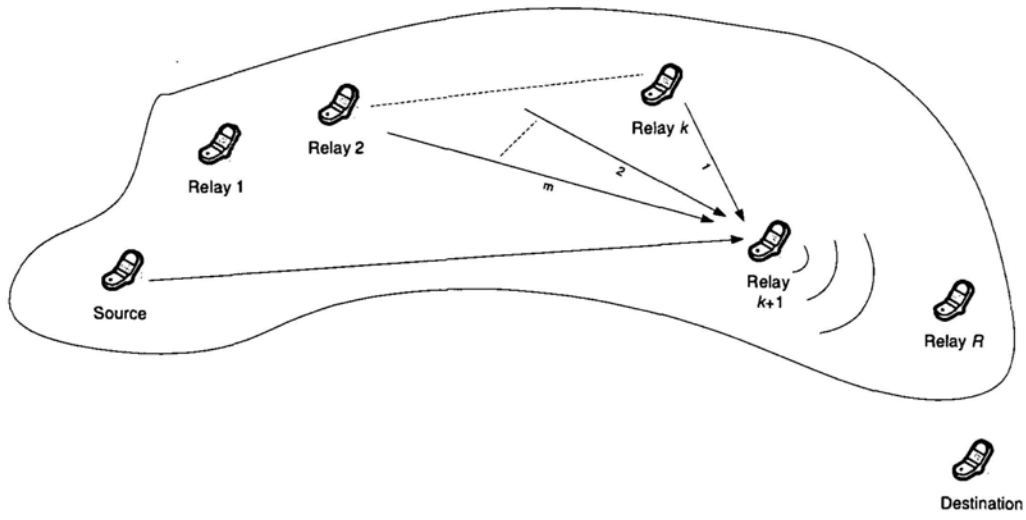

Figure 3.2: Multihop cooperative protocol.

A simple case of this protocol for $m = 0$ and $R = 1$ is elaborated in [48] and [49], where the kth relay node only *amplify-and-forward* or *decode-and-forward* its received signal from the source node to the destination node in phase $k + 1$. The case is extended to $m = 0$ and $R \geq 1$ in [47]. Then in [111], the case for $R \geq 1$ and $m = R - 1$ is considered , where each relay node combines the signals received from all of the previous transmissions. Furthermore, a general case for $R \geq 1$ and $1 \leq m \leq R - 1$ is analyzed in [112], where DF transmission is applied. A major advantage of this protocol is the low computational complexity of relay nodes, as each relay node only need retransmit its received signal to the destination node. However, a price of this advantage is the decrease of bandwidth efficiency with the number of cooperating relays, in that all the relay nodes and the source node should have their own orthogonal channels.

Space-time coded cooperative protocol:

To increase the bandwidth efficiency of cooperative communications, ST coded cooperative protocols have been proposed based on either AF or DF transmission [47, 49, 50, 52, 56–58, 64, 66, 76, 113, 114], since ST coding has higher bandwidth efficiency than that of repetition based transmission schemes.

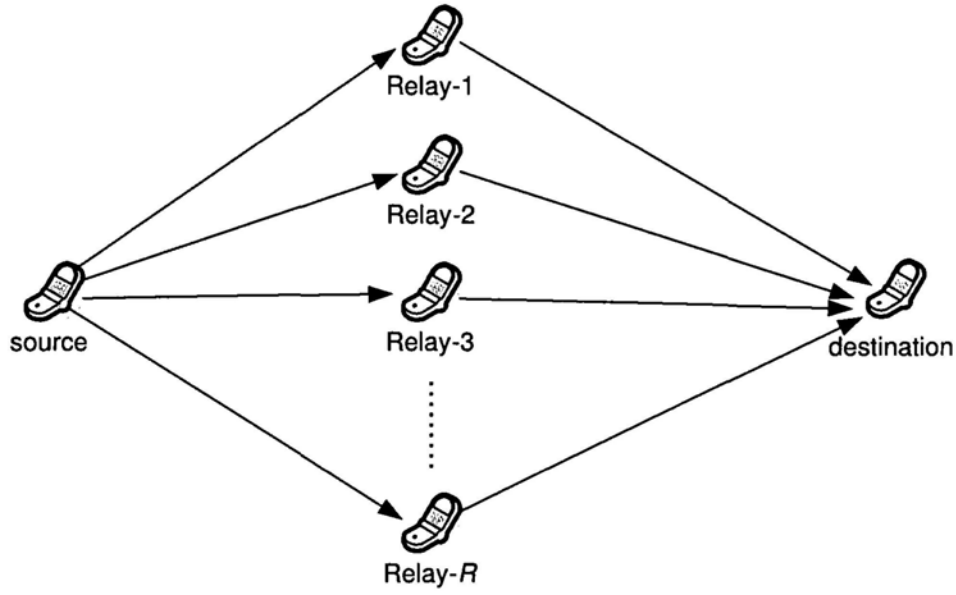

Figure 3.3: ST coded cooperative protocol based on AF transmission.

Fig.3.3 shows a typical two phase ST coded cooperative protocol based on AF transmission which has been adopted in many cooperative strategies, e.g., in [48–50, 52, 56, 114]. The whole system includes one source node, one destination node and R relay nodes. In phase one, the source node broadcasts the information signal to all the R relay nodes. In phase two, the kth ($1 \leq k \leq R$) relay node transmits the $(k-1)$th row of the ST or distributive space-time (DST) code matrix which is generated from the received signal by certain coding strategies. Thus the ST or DST codes are realized in a distributed fashion and at high SNR diversity order R can be achieved. If the link between the source node and the destination node exist, diversity order $R+1$ can be achieved by combining the received signal from the direct link at the destination node. It is noted that the relay nodes here do not need to detect or decode the received signal. This cooperative protocol is initially mentioned in [48].

The case for $R = 2$ is described in [49] and [52], where the Alamouti code is applied. Then a general discussion on distributed orthogonal and quasi-orthogonal codes design is given in [56]. A distributed linear dispersion coding [115] scheme is proposed in [50]. Furthermore, this protocol is extended to broadband cooperative communications. In [114], a distributed space-frequency (SF) coding scheme is proposed for this protocol. The proposed strategy can achieve diversity gain of $\min(RL_1, RL_2)$, where L_1 and L_2 are the number of taps of the frequency selective fading channels from the source node to the relay nodes and from the relay nodes to the destination nodes, respectively.

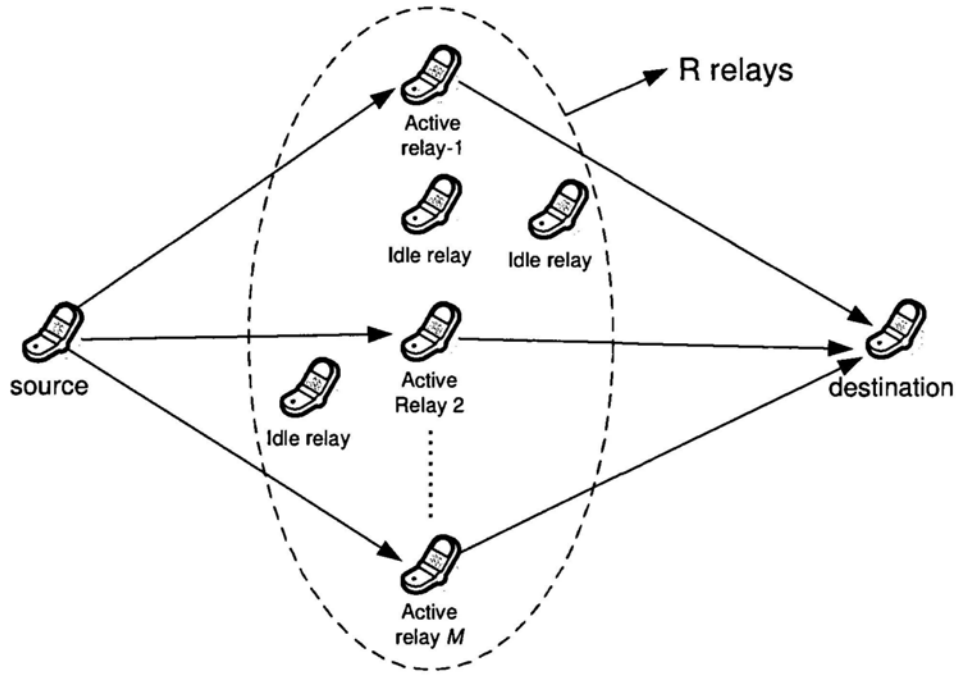

Figure 3.4: ST coded cooperative protocol based on DF transmission.

Fig.3.4 shows a typical two phase ST coded cooperative protocol based on DF transmission, which includes one source node, R relay nodes and one destination node. In phase one, the source node broadcasts the information signal to the destination node and all R relay nodes. In phase two, each relay node decodes or detects the received signal and judge whether the received symbols are decoded correctly or not (e.g., by checking CRC code or comparing the received SNR to a threshold). Only if the received symbols are decoded correctly, the relay node will assist the source

node to transmit. Otherwise, it remains idle. Assume that M ($M \leq R$) relay nodes are active in the second phase. Then, the mth ($1 \leq m \leq M$) relay node transmits the $(m-1)$th row of a ST or SF code matrix, which is generated from decoded information symbols by some coding strategies. Therefore, R relay nodes just work as a transmitter with R transmit antennas. Although not all the relay nodes transmit signals in each cooperative transmission, this protocol has been shown to achieve diversity order $R+1$ when the destination node also use the received signal from the source node to decode [48] . From the above description, we can see that actually any ST codes can be directly applied to this protocol. This protocol is proposed and analyzed in great detail in [48]. The case for $R = 1$ is also discussed in [48, 49]. In [64], based on this particular protocol, a family of ST trellis codes are suggested to achieve the full spatial diversity even in the absence of time synchronization of all the relay nodes. The broadband cooperative communications is considered in [77], where the SF code proposed in [36, 37, 39] is applied.

3.3 Problems of Cooperative Communications

It is apparent that cooperative communication enables single-antenna transmitters to achieve transmit diversity through cooperation. However, from a practical point of view, a major challenge for cooperative communication is the synchronization problem because multiple transmissions in cooperative systems may not be synchronized in either time or frequency domains [62, 74, 75]. Fig.3.5 shows a cooperative system with synchronization errors, where τ_k and Δf_k for $1 \leq k \leq R$ are the time delay and carrier frequency offset (CFO), respectively, for the link from the kth relay node to the destination node.

3.3.1 Time Synchronization

Since the relay nodes of a cooperative system are located at different places, the time delay from each relay node to the destination node τ_r may be much more different than that of MIMO systems as shown in Fig.3.5. Therefore, it is difficult for the destination node to synchronize all the relay nodes at the same time. Even if syn-

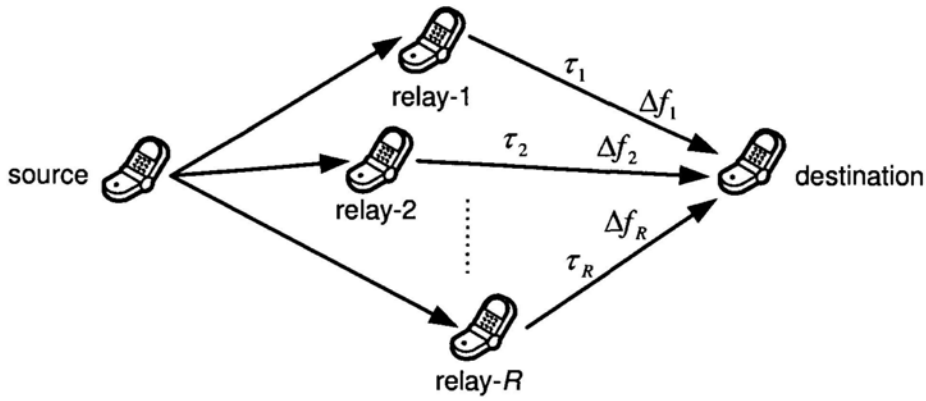

Figure 3.5: An cooperative system with synchronization errors.

chronization can be achieved, it will introduce significant overhead to cooperative systems.

When there is a timing error among the relay nodes, the destination node receives a superposition of multiple transmitted signals from all the relay nodes, and these received signals are not aligned (synchronized) with one another. The case that delays between the relay nodes are not multiples of an information symbol duration is studied in [116, 117]. In this case the destination node cannot sample all the components in the received signal at the optimal sampling time. According to the Nyquist inter-symbol interference (ISI) criterion for the non-optimally sampled components, ISI from neighboring symbols will be brought to the system leading to degraded performance [5]. Fig.3.6 illustrates an example of this case, where the transmitted information symbols are pulse-shaped by a raised cosine function [5]. It is clear that the received signals from two relay nodes cannot be optimally sampled simultaneously. Thus, at the sampling time, the received signal from the relay node two suffers from ISI. The simulation results in [116, 117] show that when the synchronization errors are much smaller than a symbol interval, the performance of the cooperative system deteriorates gracefully.

When the timing errors are multiples of an information symbol duration, all the components of the received signal from the relay nodes can be optimally sampled. Therefore, ISI no longer exists. However, in this case the equivalent ST code matrix $\mathbf{C}'$ will be a row-wise shifted version of the original ST code matrix $\mathbf{C}$ as shown in

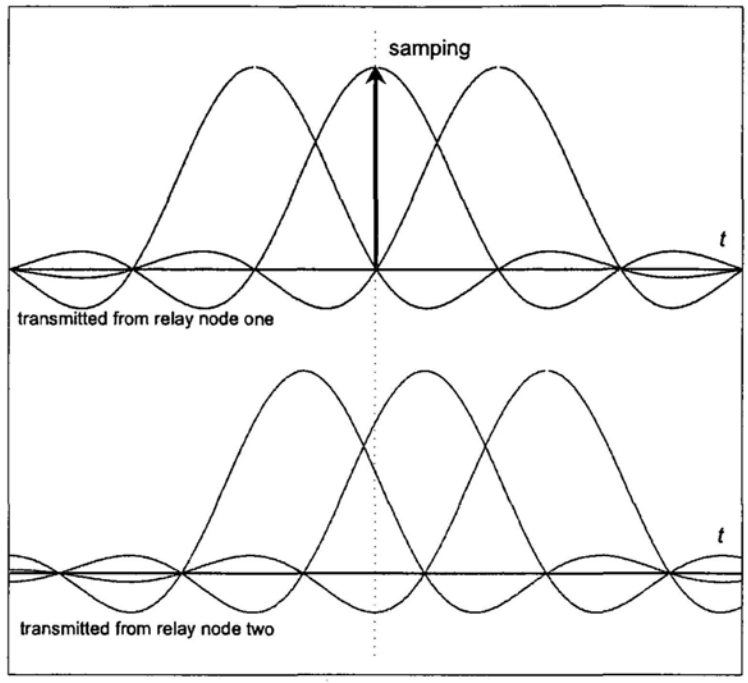

Figure 3.6: Two baseband signals transmitted from two relay nodes with a timing error.

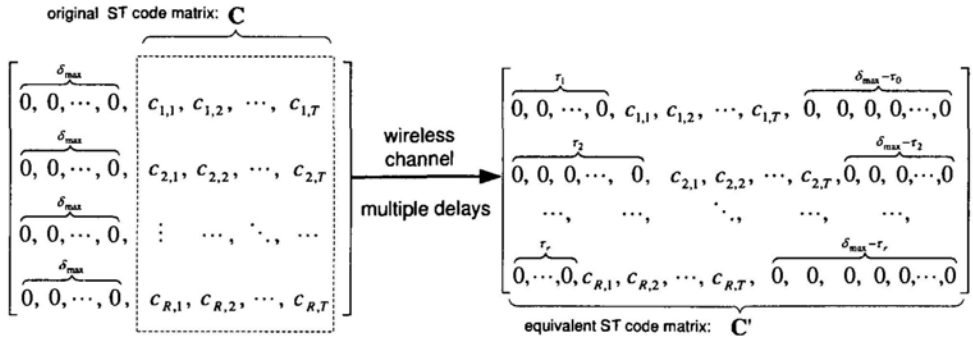

Figure 3.7: ST code matrix under timing errors, which are multiples of an information symbol duration.

Fig.3.7, where τ_k $(1 \leq k \leq R)$ is the delay of the link from the kth relay node to the destination node. To avoid inter-frame interference, a zero guard interval, with

a length $\delta_{\max}$ equal to or greater than the maximum delay, is inserted between two consecutive frames. So in the asynchronous case, the equivalent ST code matrix $\mathbf{C}'$ may not be able to achieve full diversity any longer. For example, in the Alamouti code [33], without delays, the difference code matrix $\Delta\mathbf{C}$ between two distinct code matrix $\mathbf{C}$ and $\hat{\mathbf{C}}$ has the following structure:

$$\Delta\mathbf{C} = \begin{bmatrix} \Delta s_1 & -\Delta s_2^* \\ \Delta s_2 & \Delta s_1^* \end{bmatrix}, \tag{3.1}$$

where $\Delta s_k = s_k - \hat{s}_k$ for $k = 1, 2$. It is easy to see that as long as either Δs_1 or Δs_2 is not zero, the rank of $\Delta\mathbf{C}$ is always equal to two. If the second row of $\Delta\mathbf{C}$ is right shifted by one element due to delay, the sifted difference code matrix $\Delta\mathbf{C}'$ will be

$$\Delta\mathbf{C}' = \begin{bmatrix} \Delta s_1 & -\Delta s_2^* & 0 \\ 0 & \Delta s_2 & \Delta s_1^* \end{bmatrix}. \tag{3.2}$$

From the expression of $\Delta\mathbf{C}'$, we can see that when $\Delta s_1 = 0$ and $\Delta s_2 \neq 0$, the rank of $\Delta\mathbf{C}$ is only equal to one. As a consequence, in this case the Alamouti code cannot achieve full diversity order 2.

To avoid synchronization, many studies have been conducted by researchers, see for examples [60–66]. In [60], the time reversal ST block codes [67–69] are used. Although the requirement for the time synchronization is relaxed, the rate of the constructed code is low. In [61], a delay diversity codes [30] based asynchronous cooperative communication strategy is proposed, where the minimum mean square error (MMSE) estimator at the destination node is used to achieve some diversity gain. In [63], delay-tolerant distributed threaded algebraic ST block codes are proposed, but with low symbol rate. In [64, 65], a family of ST trellis codes is proposed with achievement of full diversity under any delay profile.

OFDM's low sensitivity to time synchronization errors has been especially utilized to combat timing errors in cooperative communication systems. Its underlying fundamental is obvious if recalling the channel impulse response (2.2). For the channel from one relay node to the destination node, timing errors may only increase all the multipath delays τ_l $(0 \leq l \leq L-1)$ of this channel in a constant manner. As long as the increased maximum multipath delay τ_{L-1} is shorter than the guard interval which is inserted between OFDM symbols to avoid ISI, the OFDM systems can

still work well. By reason of this property, in [62] Alamouti ST coded OFDM is proposed to achieve full asynchronous diversity, where the paths from relay nodes to the destination node are treated as multipaths. Then, an SF coded OFDM system is proposed in cooperative systems [66], where the applied SF codes can achieve both full cooperative and full multipath diversities when a channel from a relay node to the destination node is, by itself frequency-selective.

3.3.2 Carrier Frequency Synchronization

Apart from the time synchronization, carrier frequency synchronization is another challenge for cooperative communications [74, 75]. As shown in Fig.3.5, each relay node in a cooperative communication system is equipped with its own oscillator. Therefore multiple carrier frequency offsets (CFOs) Δf_k $(1 \leq k \leq R)$ may exist at the destination node. Since the received signal is a superposition of transmitted signals from the relay nodes with different CFOs, the destination node cannot compensate these multiple CFOs at the same time via mixing with a sinusoid. The problem is more different and complex than non-cooperative systems, where only one CFO exists.

For OFDM based cooperative communication systems [62, 66, 71], the problem of multiple CFOs becomes very critical because OFDM's sensitivity to CFO often leads to inter-carrier interference (ICI). If ICI is not mitigated, OFDM systems will quickly suffer from an error floor. In Chapter 4, more details of this issue will be discussed

On the other hand, although single-carrier systems are not as sensitive as OFDM systems to CFO, multiple CFOs in them may not be ignored either. Firstly, current or future communication systems are almost certainly to be located well above the 2 GHz band used by the third generation (3G) cellular communication system. As a good oscillator only guarantees a frequency reference with an error of the order of parts-per-million (PPM), a CFO of dozens of KHz is possible. With multiple CFOs, the channels becomes time-varying leading to ISI [54, 55, 72, 73]. We can also regard channels as time-invariant and incorporate the effect of CFOs into ST code matrices. By this approach, the entries of ST code matrices will be rotated by CFOs. Therefore,

the ST codes may no longer work well. In Section 3.4, the effect of multiple CFOs on delay diversity and the Alamouti code will be investigated in great detail. Secondly, for long block transmission schemes, see for example [61, 64], the phase rotation caused by CFO is accumulated with the increment of the symbol index in a data block. Therefore, the phase rotation may not be ignored for the last few information symbols in a data block.

The multiple CFO problem has been noted in [74, 75]. In [74], a subcarrier-wise Alamouti coded OFDM system is considered and a simplified zero-forcing (ZF) equalizer is applied to suppress ICI, where the equalization matrix inverses need to be retaken for every OFDM symbol even in a channel coherent time. In [75], delay diversity codes is considered and an MMSE decision feedback equalizer (DFE) is employed by the destination node, in which multiple CFOs are compensated at each symbol index. But, how multiple CFOs affect the diversity order achieved by delay diversity codes is not analyzed. In [80–85] a family of rotation-based SF codes proposed in [36,37,39] is considered. Compared with codes used in [74,75], these SF codes are more powerful in the sense that they can achieve both the full cooperative diversity and the full multipath diversity, with a constant rate equal to one regardless of the number of transmit antennas. The details will be shown in Chapter 4 and Chapter 5.

3.4 Effect of Multiple CFOs on ST Codes

In this section we focus on the effect of multiple CFOs on delay diversity [30,88] and Alamouti code [33], both of which have been widely applied in different cooperative communication systems, see examples in [49, 52, 61, 75, 76, 118]. Here, to simplify analysis all relay nodes incorporated in cooperation are assumed to be synchronized in time but not in CFO, i.e., multiple CFOs exist at the destination node. The ST coded DF cooperative protocol mentioned in 3.2 is adopted. Thus the receive signal model is equivalent to that of a multiple-input and single-output (MISO) system with M_t transmit antennas, where M_t is the number of the relay nodes which can correctly decode/detect the received signal transmitted from the source node.

3.4.1 Effect of Multiple CFOs on the Delay Diversity

In this subsection, we look at the effect of multiple CFOs on delay diversity.

Receive Signal Model

According to the coding strategy of delay diversity, the 1st relay node directly transmits the N dimension information symbol vector $\mathbf{s} = [s_1, s_2, \cdots, s_N]$ while the mth ($2 \leq m \leq M_t$) relay node transmit the same information symbol vector $\mathbf{s}$ delayed by $m-1$ symbol intervals. So at the destination node the bth, $b = 1, 2, \cdots, N + M_t - 1$, received symbol y_b is given by

$$y_b = \sqrt{\frac{\rho}{M_t}} \sum_{m=1}^{M_t} e^{j\theta_{\varepsilon_m}^b} h_m s_{b+1-m} + w_b, \tag{3.3}$$

where $s_k = 0$ if $k < 1$ or $k > N$, h_m is the channel coefficient of the link from the mth relay node to the destination node and w_b is the noise sample. Both the channel coefficients and noise samples are modeled as independent zero-mean complex Gaussian random variables with unit variance. Information symbol s_k ($1 \leq k \leq N$) obeys the energy constraint $\mathrm{E}(s_k) = 1$. Thus the average transmitting power ρ also stands for the signal-to-noise ratio (SNR) at the destination node. Let Δf_m be the CFO between the mth relay node and the destination node. Then $\varepsilon_m = \Delta f_m T$ is its normalized value by symbol duration T. In (3.3), $\theta_{\varepsilon_m}^b = 2\pi\varepsilon_m(b-1) + \theta_{0,m}$, where $2\pi\varepsilon_m(b-1)$ is the phase rotation of the bth received symbol transmitted from mth relay node induced by CFO Δf during the time of $b-1$ information symbols, and $\theta_{0,m}$ is the phase rotation between the phase of the destination node local oscillator and the carrier phase of the mth relay node at the start of the received signal.

Diversity Analysis in the Presence of Multiple CFOs

Let us now look at the achieved diversity order of delay diversity in the presence of multiple CFOs. Toward our approach, we regard delay diversity as a kind of space-time block codes (STBC) with a wide ST code matrix [29]. As a consequence, we rewrite (3.3) as

$$\mathbf{y} = \sqrt{\frac{\rho}{M_t}}\mathbf{h}\mathbf{C} + \mathbf{w}, \tag{3.4}$$

where $\mathbf{y} = [y_1, y_2, \cdots, y_{N+M_t-1}]$, $\mathbf{h} = [h_1, h_2, \cdots, h_{M_t}]$, $\mathbf{w} = [w_1, w_2, \cdots, w_{N+M_t-1}]$ and the $M_t \times (N + M_t - 1)$ ST code matrix $\mathbf{C}$ is given by

$$\mathbf{C} = \begin{bmatrix} e^{j\theta_{\varepsilon_1}^1} s_1 & e^{j\theta_{\varepsilon_1}^2} s_2 & \cdots & e^{j\theta_{\varepsilon_1}^{M_t}} s_{M_t} & \cdots & e^{j\theta_{\varepsilon_1}^{N}} s_N & \cdots & 0 \\ 0 & e^{j\theta_{\varepsilon_2}^2} s_1 & \cdots & e^{j\theta_{\varepsilon_2}^{M_t}} s_{M_t-1} & \cdots & e^{j\theta_{\varepsilon_2}^{N}} s_{N-1} & \cdots & 0 \\ \vdots & \vdots & \ddots & \vdots & \ddots & \vdots & \ddots & \vdots \\ 0 & 0 & \cdots & e^{j\theta_{\varepsilon_{M_t}}^{M_t}} s_1 & \cdots & e^{j\theta_{\varepsilon_{M_t}}^{N}} s_{N-M_t+1} & \cdots & e^{j\theta_{\varepsilon_{M_t}}^{N+M_t-1}} s_N \end{bmatrix}. \quad (3.5)$$

According to the *rank* criterion introduced in Chapter 2.2.1, the achieved diversity order of delay diversity with multiple CFOs is equal to the minimum rank of the difference matrix $\Delta\mathbf{C} = \mathbf{C} - \tilde{\mathbf{C}}$, where $\mathbf{C}$ and $\tilde{\mathbf{C}}$ are two distinct ST code matrices and are encoded from two distinct information symbol vectors $\mathbf{s} = [s_1, s_2, \cdots, s_N]^{\mathcal{T}}$ and $\tilde{\mathbf{s}} = [\tilde{s}_1, \tilde{s}_2, \cdots, \tilde{s}_N]^{\mathcal{T}}$, respectively.

By observing the structure of the ST code matrix in the presence of multiple CFOs (3.5), we propose the following theorem.

Theorem 1 *In the presence of multiple CFOs, delay diversity can still achieve full diversity order M_t, where M_t is the number of equivalent transmit antennas.*

Proof 1 *Since $\Delta\mathbf{C}$ is the difference matrix of two distinct ST code matrices, we can always find an integer k' so that $\Delta s_{k'} \neq 0$ and $\Delta s_k = 0$ for $k = 1, 2, \cdots, k' - 1$ if $k' > 1$, where $\Delta s_k = s_k - \tilde{s}_k$. Then the $M_t \times M_t$ submatrix of $\Delta\mathbf{C}$ (denoted by $\Delta\hat{\mathbf{C}}$), whose kth $(0 \leq k \leq M_t - 1)$ column is the $(k' + k)$th column of $\Delta\mathbf{C}$, is given by*

$$\Delta\hat{\mathbf{C}} = \begin{bmatrix} e^{j\theta_{\varepsilon_1}^{k'}} \Delta s_{k'} & e^{j\theta_{\varepsilon_1}^{k'+1}} \Delta s_{k'+1} & \cdots & e^{j\theta_{\varepsilon_1}^{k'+M_t-1}} \Delta s_{k'+M_t-1} \\ 0 & e^{j\theta_{\varepsilon_2}^{k'+1}} \Delta s_{k'} & \cdots & e^{j\theta_{\varepsilon_2}^{k'+M_t-1}} \Delta s_{k'+M_t-2} \\ \vdots & \vdots & \ddots & \vdots \\ 0 & 0 & \cdots & e^{j\theta_{\varepsilon_{M_t}}^{k'+M_t-1}} \Delta s_{k'} \end{bmatrix}. \quad (3.6)$$

Since $\Delta\hat{\mathbf{C}}$ is an upper triangular matrix and $\Delta s_{k'} \neq 0$, we have

$$\det(\Delta\hat{\mathbf{C}}) = \prod_{m=1}^{M_t} e^{j\theta_{\varepsilon_m}^{k'+m-1}} \Delta s_{k'} \neq 0.$$

Thus we immediately get that $\operatorname{rank}(\Delta\hat{\mathbf{C}}) = M_t$. *Further, because $\Delta\hat{\mathbf{C}}$ is a submatrix of $\Delta\mathbf{C}$, we have*

$$\operatorname{rank}(\Delta\hat{\mathbf{C}}) \leq \operatorname{rank}(\Delta\mathbf{C}) \leq \min(M_t, N + M_t - 1).$$

Finally, considering $\text{rank}(\Delta\hat{\mathbf{C}}) = M_t$ *and* $\min(M_t, N + M_t - 1) = M_t$*, we can conclude that* $\text{rank}(\Delta\mathbf{C}) = M_t$*. This means that in the presence of multiple CFOs, the achieved diversity order of delay diversity is still equal to* M_t*.*

Diversity Product Analysis in the Presence of Multiple CFOs

Apart from achieving full diversity order M_t, according to the *product* criterion of ST codes design introduced in Chapter 2.2.1, the minimum value of the product $\prod_{m=1}^{M_t} \lambda_m$ over all pairs of distinct code matrices $\mathbf{C}$ and $\tilde{\mathbf{C}}$ should also be as large as possible, where λ_k $(1 \leq k \leq M_t)$ is the kth nonzero eigenvalue of the matrix $\Delta\mathbf{C}^{\mathcal{H}}\Delta\mathbf{C}$. In this subsection, we will see that multiple CFOs do not affect the value of $\min_{\mathbf{C}\neq\tilde{\mathbf{C}}} \prod_{m=1}^{M_t} \lambda_m$.

Since $\mathbf{s}$ and $\tilde{\mathbf{s}}$ are two distinct information symbol vectors, we can always find an integer k' $(1 \leq k' \leq N)$ so that $\Delta s_{k'} = s_{k'} - \tilde{s}_{k'} \neq 0$ and $\Delta s_k = 0$ $(1 \leq k < k')$ if $k' > 1$. Thus an $M_t \times M_t$ submatrix of $\Delta\mathbf{C}$ (denoted by $\Delta\hat{\mathbf{C}}$) has the form shown by (3.6), where the kth $(0 \leq k \leq M_t - 1)$ column is the $(k + k')th$ column of $\Delta\mathbf{C}$. Then from the fact that $\Delta\mathbf{C}$ has full row rank, we have

$$\begin{aligned}
\prod_{m=1}^{M_t} \lambda_m &= \det(\Delta\mathbf{C}\Delta\mathbf{C}^{\mathcal{H}}) \\
&\geq \det(\Delta\hat{\mathbf{C}}\Delta\hat{\mathbf{C}}^{\mathcal{H}}) \qquad (3.7) \\
&= \left| \prod_{m=1}^{M_t} e^{j\theta_{\varepsilon_m}^{k'+m-1}} \Delta s_{k'} \right|^2 \\
&= |\Delta s_{k'}|^{2M_t}, \qquad (3.8)
\end{aligned}$$

where the second inequality follows from the fact that the mth $(1 \leq m \leq M_t)$ ordered singular value of $\Delta\mathbf{C}$ is always larger than or equal to that of $\Delta\hat{\mathbf{C}}$ for $\Delta\hat{\mathbf{C}}$ can be obtained by deleting some columns of $\Delta\mathbf{C}$ [102]. Furthermore, it is easy to see that the equality of (3.7) can hold if $\Delta s_{k'} \neq 0$ and $\Delta s_k = 0$ for $k \neq k'$. So, we have

$$\begin{aligned}
\min_{\mathbf{C}\neq\tilde{\mathbf{C}}} \prod_{m=1}^{M_t} \lambda_m &= \min_{\mathbf{C}\neq\tilde{\mathbf{C}}} \det(\Delta\hat{\mathbf{C}}\Delta\hat{\mathbf{C}}^{\mathcal{H}}) \\
&= \min_{\Delta s_{k'}\neq 0} \left| \prod_{m=1}^{M_t} e^{j\theta_{\varepsilon_m}^{k'+m-1}} \Delta s_{k'} \right|^2 \\
&= \min_{\Delta s_{k'}\neq 0} |\Delta s_{k'}|^{2M_t} \\
&= d^{2M_t}, \qquad (3.9)
\end{aligned}$$

where d is the minimum Euclidean distance of the signal constellation. Clearly, the minimum value of $\prod_{m=1}^{M_t} \lambda_m$ does not depend on multiple CFOs. This leads to the derivation of Theorem 2

Theorem 2 *For delay diversity, multiple CFOs do not affect the minimum value of the product* $\prod_{m=1}^{M_t} \lambda_m$ *over all pairs of distinct code matrices* $\mathbf{C}$ *and* $\tilde{\mathbf{C}}$*, where* λ_m *is the mth nonzero eigenvalue of the matrix* $\Delta\mathbf{C}^{\mathcal{H}}\Delta\mathbf{C}$ *and* $\Delta\mathbf{C} = \mathbf{C} - \tilde{\mathbf{C}}$.

Proof 2 *The proof directly follows from the above discussion.*

Simulation Results

In this subsection, some simulation results are presented to verify the above analysis. Systems with two and three active relay nodes with Quadrature amplitude modulation (QPSK) modulation are simulated, respectively. The channel between the relay node and the destination node is quasi-static Rayleigh flat fading and perfect time synchronization is assumed. For each channel realization, each ε_m for $(1 \leq m \leq M_t)$ is uniformly selected from $[-\varepsilon_{Max}, \varepsilon_{Max}]$. Here we set ε_{Max} as 0.5. The length of the symbol sequence N is equal to 20. Additionally, two special cases of $M_t = 2$, $\varepsilon_1 = 0.4$, $\varepsilon_2 = -0.4$ and $M_t = 3$, $\varepsilon_1 = -0.3$, $\varepsilon_2 = 0.2$, $\varepsilon_3 = -0.5$ are also simulated. Here full channel knowledge including CFOs at the destination node is assumed. At the destination node the maximum-likelihood sequence detection (MLSD) is employed to maximum-likelihood (ML) detect the received signals. Note when $\varepsilon_{Max} > 0$, multiple CFOs are compensated in computing the branch metric between trellis states, which adds hardly any additional computation burden.

Fig.3.8 shows our simulation results. From them we can see that for all the simulated values of M_t and CFOs, the symbol-error rate (SER) curves of the cases with CFOs nearly overlap the curves of the cases without CFOs. This result is consistent with previous analysis, i.e., multiple CFOs do not affect the achieved diversity order and the minimum value of $\prod_{m=1}^{M_t} \lambda_m$ of delay diversity.

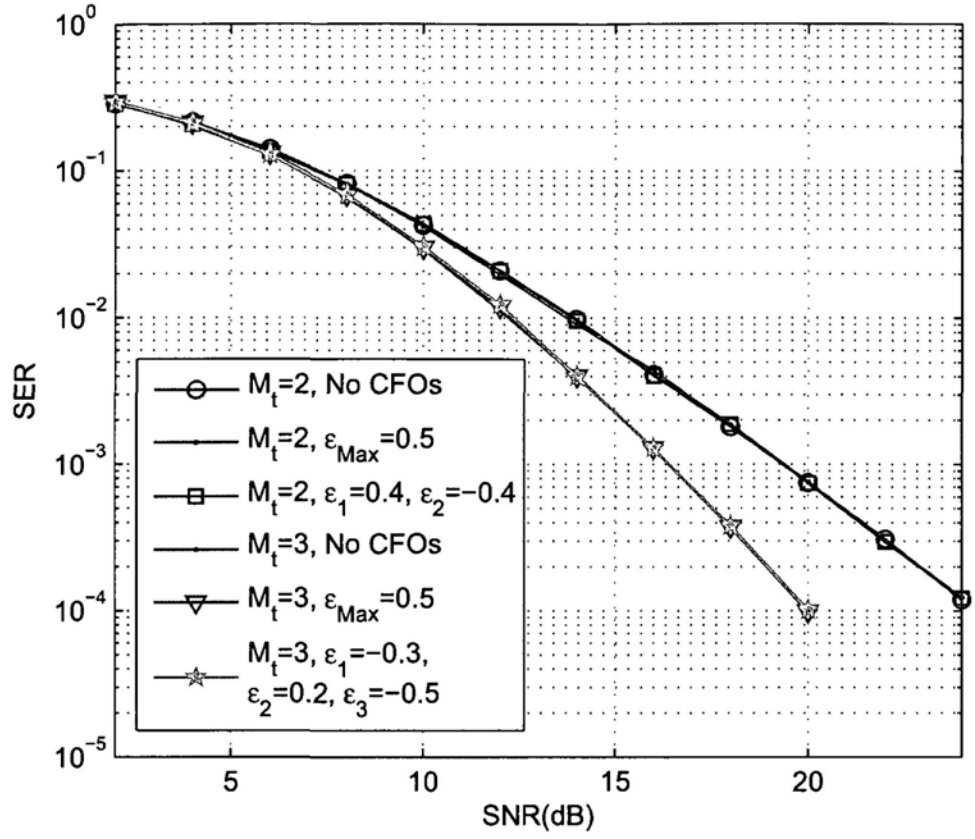

Figure 3.8: SER performance of delay diversity in the presence of multiple CFOs.

3.4.2 Effect of Multiple CFOs on the Alamouti Code

In this subsection, we focus on the effect of multiple CFOs on the Alamouti code, which has been adopted by some cooperative systems, e.g., in [49,52,76]. We will see that in the presence of multiple CFOs, the minimum value of the product $\lambda_1\lambda_2$ may degrade. In the worst case situation, full diversity order 2 cannot even be achieved.

Receive Signal Model

According to the coding strategy of the Alamouti code, during the bth ($b = 1,3,5,\cdots$) symbol period, information symbols s_1 and s_2 are transmitted from the relay node one and the relay node two, respectively. Then, during the $(b+1)$th symbol period $-s_2^*$ and s_1^* are transmitted from the relay node one and the relay node two,

respectively. The destination node with one receive antenna, and a flat fading channel model are assumed. So that the receiver observations y_b and y_{b+1} corresponding to the two information symbol periods are given by

$$\begin{aligned} y_b &= \sqrt{\frac{\rho}{2}} e^{j\theta^b_{\varepsilon_1}} h_1 s_1 + \sqrt{\frac{\rho}{2}} e^{j\theta^b_{\varepsilon_2}} h_2 s_2 + w_b, \\ y_{b+1} &= -\sqrt{\frac{\rho}{2}} e^{j\theta^{b+1}_{\varepsilon_1}} h_1 s_2^* + \sqrt{\frac{\rho}{2}} e^{j\theta^{b+1}_{\varepsilon_2}} h_2 s_1^* + w_{b+1}, \end{aligned} \tag{3.10}$$

where h_1 and h_2 are channel coefficients of the links from the relay node one and the relay node two to the destination node, respectively and w_b and w_{b+1} are the noise samples. Both the channel coefficients and noise samples are modeled as independent zero-mean complex Gaussian random variables with unit variance. Information symbols obey the energy constraint $\mathrm{E}(|s|^2) = 1$. Thus, ρ stands for the average SNR at the destination node. Let Δf_m be the CFO between the mth ($1 \leq m \leq 2$) relay node and the destination node. Then $\varepsilon_m = \Delta f_m T$ is its normalized value by symbol duration T. In (3.10), $\theta^b_{\varepsilon_m} = 2\pi\varepsilon_m(b-1) + \theta_{0,m}$, where $2\pi\varepsilon_m(b-1)$ is the phase rotation of the bth received symbol transmitted from mth relay node induced by CFO Δf during the time of $b-1$ information symbol periods, and $\theta_{0,m}$ is the phase rotation between the phase of the destination node local oscillator and the carrier phase of the mth relay node at the start of the received signal. Since the realizations of $\theta_{0,1}$ and $\theta_{0,2}$ are independent of each other and $e^{j\theta_{0,m}} h_m$ has the same distribution as h_m, the value of $\theta_{0,m}$ does not affect the following analysis. Thus to simplify notation, we just set $\theta_{0,m}$ as zero for $m = 1, 2$.

The Conventional Detection Method

In a standard approach [29,33], we can construct the received signal vector $[y_b, y^*_{b+1}]^T$ as

$$\begin{bmatrix} y_b \\ y^*_{b+1} \end{bmatrix} = \sqrt{\frac{\rho}{2}} \begin{bmatrix} e^{j\theta^b_{\varepsilon_1}} h_1 & e^{j\theta^b_{\varepsilon_2}} h_2 \\ e^{-j\theta^{b+1}_{\varepsilon_2}} h_2^* & -e^{-j\theta^{b+1}_{\varepsilon_1}} h_1^* \end{bmatrix} \begin{bmatrix} s_1 \\ s_2 \end{bmatrix} + \begin{bmatrix} w_b \\ w^*_{b+1} \end{bmatrix}, \tag{3.11}$$

or with obvious notation

$$\mathbf{y}_b = \sqrt{\frac{\rho}{2}} \mathbf{H}_b \mathbf{s} + \mathbf{w}_b. \tag{3.12}$$

Following the way of the conventional detection (CD) method, we multiply $\mathbf{y}_b$ by $\mathbf{H}_b^{\mathcal{H}}$ and get $\mathbf{y}'_b = \mathbf{H}_b^{\mathcal{H}}\mathbf{y}_b$ as

$$\mathbf{y}'_b = \sqrt{\frac{\rho}{2}}\mathbf{H}'_b\mathbf{s} + \mathbf{w}'_b, \tag{3.13}$$

where $\mathbf{H}'_b = \mathbf{H}_b^{\mathcal{H}}\mathbf{H}_b$ and $\mathbf{w}'_b = \mathbf{H}_b^{\mathcal{H}}\mathbf{w}_b$. Defining $\Delta\varepsilon = \varepsilon_2 - \varepsilon_1$, we get the expression of $\mathbf{H}'_b$ as

$$\mathbf{H}'_b = \begin{bmatrix} |h_1|^2 + |h_2|^2 & h_1^* h_2(e^{j2\pi\Delta\varepsilon b} - e^{j2\pi\Delta\varepsilon(b+1)}) \\ h_1 h_2^*(e^{-j2\pi\Delta\varepsilon b} - e^{-j2\pi\Delta\varepsilon(b+1)}) & |h_1|^2 + |h_2|^2 \end{bmatrix}. \tag{3.14}$$

In the signal model (3.13) by observing the expression of the equivalent channel matrix $\mathbf{H}'_b$, we can see that when no CFOs exist or $\varepsilon_1 = \varepsilon_2$, $\mathbf{H}'_b$ turns to a diagonal matrix. Then the detection of s_1 and s_2 are decoupled and diversity order 2 can be achieved. However, when $\varepsilon_1 \neq \varepsilon_2$, the non-diagonal elements in $\mathbf{H}'_b$ exist and lead to inter-symbol interference (ISI). So in this case if we still apply the conventional detection (CD) method and just ignore the ISI terms, the system will suffer from an error floor as SNR increases. To remove the error floor of the CD method for the signal model (3.13), a popular detection method to suppress ISI is the minimum mean square error (MMSE) detection method. However, it is not confirmed whether the MMSE detection method can still achieve full diversity, since the Alamouti code is not designed based on the MMSE criterion.

The ML Detection Method

Due to orthogonal design, it is well-known that for the Alamouti code when no CFOs exist or $\Delta\varepsilon = 0$, the CD method is equivalent to the maximum-likelihood (ML) detection method. Unfortunately, when $\Delta\varepsilon \neq 0$, Alamouti code does not hold this good property any longer. Thus in the presence of multiple CFOs, for the ML detection method, we need to consider two information symbols jointly. This can be efficiently realized by the sphere decoding algorithm [103–105]. In the remainder of this subsection, we will see how the multiple CFOs affect the diversity product and diversity order of the Alamouti code under the condition of ML detection.

To our purpose, we reconstruct the received signal vector $\hat{\mathbf{y}}_b = [y_b, y_{b+1}]^{\mathcal{T}}$ as

$$\begin{aligned}\hat{\mathbf{y}}_b &= \sqrt{\frac{\rho}{2}}\begin{bmatrix} e^{j2\pi\varepsilon_1 b}s_1 & e^{j2\pi\varepsilon_2 b}s_2 \\ -e^{j2\pi\varepsilon_1(b+1)}s_2^* & e^{j2\pi\varepsilon_2(b+1)}s_1^* \end{bmatrix}\begin{bmatrix} h_1 \\ h_2 \end{bmatrix} + \begin{bmatrix} w_b \\ w_{b+1} \end{bmatrix} \\ &= \sqrt{\frac{\rho}{2}}\begin{bmatrix} s_1 & s_2 \\ -e^{j2\pi\varepsilon_1}s_2^* & e^{j2\pi\varepsilon_2}s_1^* \end{bmatrix}\begin{bmatrix} e^{j2\pi\varepsilon_1 b}h_1 \\ e^{j2\pi\varepsilon_2 b}h_2 \end{bmatrix} + \begin{bmatrix} w_b \\ w_{b+1} \end{bmatrix} \\ &= \sqrt{\frac{\rho}{2}}\mathbf{C}\mathbf{h}_b + \hat{\mathbf{w}}_b \end{aligned} \tag{3.15}$$

where

$$\mathbf{C} = \begin{bmatrix} s_1 & s_2 \\ -e^{j2\pi\varepsilon_1}s_2^* & e^{j2\pi\varepsilon_2}s_1^* \end{bmatrix},$$

$\mathbf{h}_b = [e^{j2\pi\varepsilon_1 b}h_1, e^{j2\pi\varepsilon_2 b}h_2]^{\mathcal{T}}$ and $\hat{\mathbf{w}}_b = [w_b, w_{b+1}]^{\mathcal{T}}$. Since the channel coefficient vector $\mathbf{h} = [h_1, h_2]^{\mathcal{T}}$ is a circular symmetric complex random vector, $\mathbf{h}_b$ has the same statistic property as that of $\mathbf{h}$. So we can see that (3.15) is a standard ST coded MISO receive signal model and $\mathbf{C}$ is the equivalent Alamouti code matrix in the presence of multiple CFOs.

According to the *rank* criterion of ST codes design introduced in Chapter 2.2.1, the achieved diversity order of the Alamouti code in the presence of multiple CFOs is equal to the minimum rank of the difference matrix $\Delta\mathbf{C} = \mathbf{C} - \tilde{\mathbf{C}}$ over all pairs of distinct code matrices $\mathbf{C}$ and $\tilde{\mathbf{C}}$, which are mapped from $[s_1, s_2]^{\mathcal{T}}$ and $[\tilde{s}_1, \tilde{s}_2]^{\mathcal{T}}$, respectively. Then the determinant of the difference matrix $\Delta\mathbf{C}$ can be calculated as

$$\det(\Delta\mathbf{C}) = |\Delta s_1|^2 e^{j2\pi\varepsilon_2} + |\Delta s_2|^2 e^{j2\pi\varepsilon_1}, \tag{3.16}$$

where $\Delta s_k = s_k - \tilde{s}_k$ for $k = 1, 2$. Clearly, if $|\Delta s_1| \neq |\Delta s_2|$, $\det(\Delta\mathbf{C})$ cannot be equal to zero and full diversity order 2 can be achieved. However, for general signal constellations such as quadrature amplitude modulation (QAM) , pulse amplitude modulation (PAM), it is possible that $\Delta s_1 = \Delta s_2 = \Delta s \neq 0$. In this case, we have

$$\det(\Delta\mathbf{C}) = |\Delta s|^2(1 + e^{j2\pi\Delta\varepsilon})e^{j2\pi\varepsilon_1}, \tag{3.17}$$

where $\Delta\varepsilon = \varepsilon_2 - \varepsilon_1$. By observing (3.17), we can see that if $(\Delta\varepsilon)_1 = 0.5$ the value of $\det(\Delta\mathbf{C})$ is equal to zero, where $(\Delta\varepsilon)_a$ stands for $\Delta\varepsilon$ modulo a. This implies that in the presence of multiple CFOs, for the worst case of $(\Delta\varepsilon)_1 = 0.5$, the Alamouti code cannot achieve full diversity order 2.

Besides full diversity, according to the *product* criterion of ST codes design introduced in Chapter 2.2.1, the minimum value of the product $\lambda_1\lambda_2$ over all pairs of distinct code matrices $\mathbf{C}$ and $\tilde{\mathbf{C}}$ should also be as large as possible, where λ_k $(k = 1, 2)$ is the nonzero eigenvalue of the matrix $\Delta\mathbf{C}^{\mathcal{H}}\Delta\mathbf{C}$. In the case of $(\Delta\varepsilon)_1 \neq 0.5$, which means that $\det(\Delta\varepsilon) \neq 0$, the minimum value of the product $\lambda_1\lambda_2$ can be calculated as

$$\begin{aligned}
\min(\lambda_1\lambda_2) &= \min_{\mathbf{C}\neq\tilde{\mathbf{C}}} \det(\Delta\mathbf{C}^{\mathcal{H}}\Delta\mathbf{C}) \\
&= \min_{\mathbf{C}\neq\tilde{\mathbf{C}}} |\det(\Delta\mathbf{C})|^2 \\
&= \min_{|\Delta s_1|+|\Delta s_2|\neq 0} \left||\Delta s_1|^2 e^{j2\pi\Delta\varepsilon} + |\Delta s_2|^2\right|^2 \\
&\leq \min_{|\Delta s_1|+|\Delta s_2|\neq 0} \left(|\Delta s_1|^2 + |\Delta s_2|^2\right)^2 \\
&= \min_{\Delta s_1\neq 0} |\Delta s_1|^4 \\
&= d^4, \qquad (3.18)
\end{aligned}$$

where d is the minimum Euclidean distance of the signal constellation. Note that in (3.18), the upper bound of $\min(\lambda_1\lambda_2)$ is achieved when $\Delta\varepsilon = 0$. So that d^4 is just the value of $\min(\lambda_1\lambda_2)$ when no CFOs exist. Therefore, in the presence of multiple CFOs, $\min(\lambda_1\lambda_2)$ of the Alamouti code is always equal to or less than that of the case without CFOs.

Consequently, when $\Delta s_1 \cdot \Delta s_2 \neq 0$, we have

$$\begin{aligned}
&\min_{\Delta s_1\cdot\Delta s_2\neq 0} (\lambda_1\lambda_2) \\
&= \min_{\Delta s_1\cdot\Delta s_2\neq 0} \left||\Delta s_1|^2 e^{j2\pi\Delta\varepsilon} + |\Delta s_2|^2\right|^2 \\
&= \min_{\Delta s_1\cdot\Delta s_2\neq 0} |\Delta s_1|^4 + |\Delta s_2|^4 + |\Delta s_1|^2|\Delta s_2|^2(e^{j2\pi\Delta\varepsilon} + e^{-j2\pi\Delta\varepsilon}) \\
&= \min_{\Delta s_1\cdot\Delta s_2\neq 0} |\Delta s_1|^4 + |\Delta s_2|^4 + 2|\Delta s_1|^2|\Delta s_2|^2\cos(2\pi\Delta\varepsilon) \\
&= \min_{\Delta s_1\cdot\Delta s_2\neq 0} (|\Delta s_1|^2 - |\Delta s_2|^2)^2 + 2|\Delta s_1|^2|\Delta s_2|^2(1 + \cos(2\pi\Delta\varepsilon)) \\
&= 2d^4(1 + \cos(2\pi\Delta\varepsilon)) \qquad (3.19)
\end{aligned}$$

Combining(3.18) and (3.19), we can express $\min(\lambda_1\lambda_2)$ for the case of $|\Delta s_1|+|\Delta s_2| \neq 0$ as

$$\begin{aligned}
\min_{|\Delta s_1|+|\Delta s_2|\neq 0} (\lambda_1\lambda_2) &= \min\left(\min_{\Delta s_1\cdot\Delta s_2=0,\, |\Delta s_1|+|\Delta s_2|\neq 0} (\lambda_1\lambda_2), \min_{\Delta s_1\cdot\Delta s_2\neq 0} (\lambda_1\lambda_2)\right) \\
&= \min\left(d^4, 2d^4(1 + \cos(2\pi\Delta\varepsilon))\right). \qquad (3.20)
\end{aligned}$$

From (3.20), we see that the value of $\min(\lambda_1\lambda_2)$ also depends on $\Delta\varepsilon$. On the other hand, since cosine is a periodic function with period 2π, we only need to consider all the possible values of $(\Delta\varepsilon)_1$. Following this idea, we further simplify (3.20) as

$$\min_{|\Delta s_1|+|\Delta s_2|\neq 0}(\lambda_1\lambda_2) = \begin{cases} 2d^4(1+\cos(2\pi\Delta\varepsilon)) < d^4 & \text{if } \frac{1}{3} < (\Delta\varepsilon)_1 < \frac{2}{3} \\ d^4 & \text{elsewise} \end{cases}, \tag{3.21}$$

where without loss of generality we release λ_k ($k = 1, 2$) from the *nonzero* eigenvalue to the eigenvalue of the matrix $\Delta\mathbf{C}^{\mathcal{H}}\Delta\mathbf{C}$. Since without CFOs $\min(\lambda_1\lambda_2) = d^4$, from (3.21), we can clearly see that when $\frac{1}{3} < (\Delta\varepsilon)_1 < \frac{2}{3}$, the minimum value of the product $\lambda_1\lambda_2$ will be decreased by multiple CFOs.

The effect of multiple CFOs on the Alamouti code can be concluded as

- When $(\Delta\varepsilon)_1 = 0.5$, full diversity order 2 cannot be achieved.
- When $\frac{1}{3} < (\Delta\varepsilon)_1 < \frac{2}{3}$, the minimum value of the product $\lambda_1\lambda_2$ is smaller than that of the case without CFOs.

Simulation Results

In order to investigate the performance of Alamouti code with CD, MMSE and ML detection methods in the presence of multiple CFOs, we have conducted many experiments and studied the simulation results thoroughly. Here the constellation we used is QPSK. The channels between two relay nodes and the destination node are all quasi-static Rayleigh flat fading. Perfect time synchronization is assumed. Full channel knowledge including CFOs at the destination node is assumed. For each channel realization, each ε_m for $1 \leq m \leq 2$ is uniformly selected from $[-\varepsilon_{Max}, \varepsilon_{Max}]$. Moreover, for a comparison, a single-input single-output (SISO) system with QPSK modulation is also simulated.

Fig.3.9 shows the SER performance of the CD method in the presence of multiple CFOs, where the ISI terms (the non-diagonal elements of $\mathbf{H}_b'$ in signal model (3.14)) are simply ignored. Due to the existence of ISI, it is not surprising that the higher the value of ε_{Max}, the more SER performance degradation for the CD method is. When $\varepsilon_{Max} = 0.1$, the performance loss is about 1.7dB in the simulated SNR range. As ε_{Max} increases, the SER performance is quickly decreased. For example, when

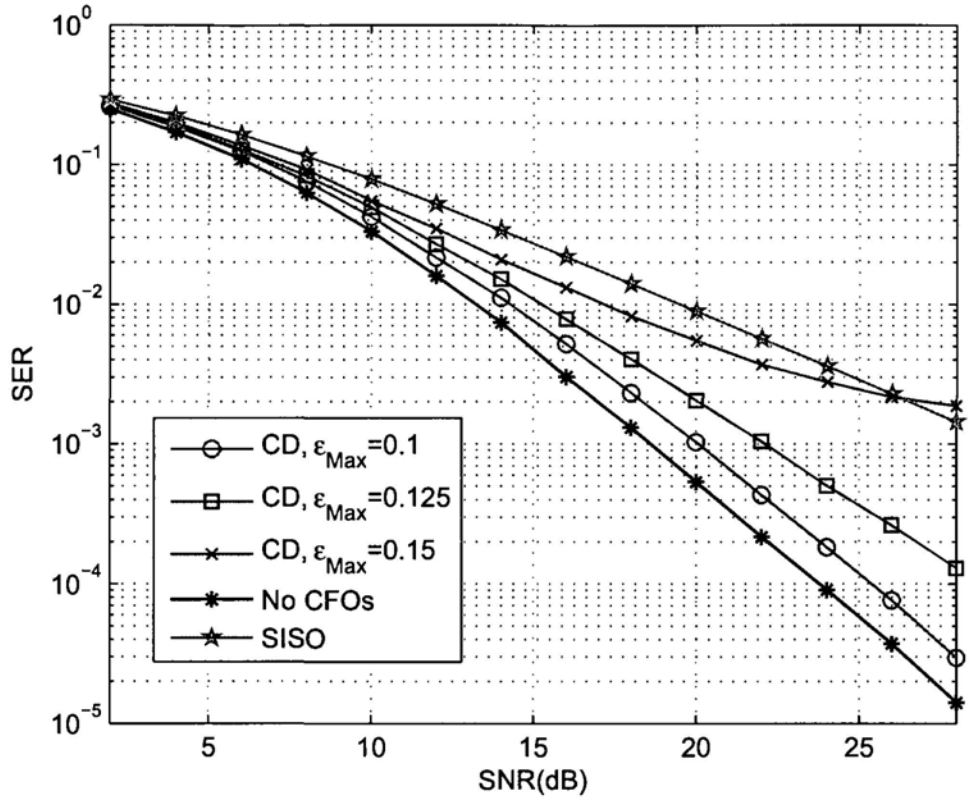

Figure 3.9: SER performance of the CD method in the presence of multiple CFOs.

ε_{Max} = 0.15, an error floor is observed in the simulated SNR range and its SER performance is even worse than that of the SISO system when SNR > 26dB.

Fig.3.10 shows the SER performance of the MMSE detection method in the presence of multiple CFOs. Comparing Fig.3.10 with Fig.3.9, we can see that the MMSE detection method significantly outperforms the CD method with a little additional computations. When ε_{Max} = 0.15, the performance loss of the MMSE detection method is smaller than 0.5dB compared with that of the case without CFOs. When ε_{Max} is increased to 0.5, nearly no diversity gain is observed. However, its performance is still better than that of the SISO system with about 2dB gain.

Fig.3.11 shows the SER performance of the ML detection method. We can see that when ε_{Max} = 0.15, the ML detection method nearly achieves the same performance as that of the case without CFOs, because not only full diversity order 2 can still be achieved, but also the minimum value of $\lambda_1\lambda_2$ is preserved. However, when

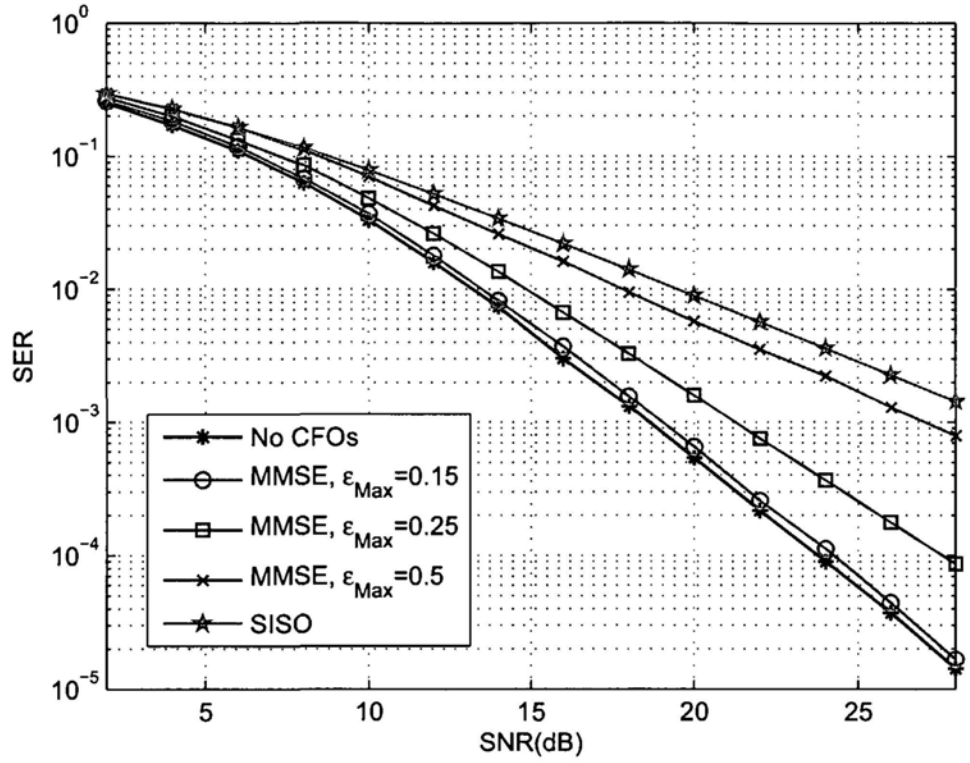

Figure 3.10: SER performance of the MMSE detection method in the presence of multiple CFOs.

$\varepsilon_{Max} = 0.25$ and 0.5, the slop is no longer parallel with the curve without CFOs at the high SNR range, since when $\varepsilon_{Max} \geq 0.25$ full diversity can not always be achieved for each realization of CFOs. Finally, we simulated a special case, i.e., $\varepsilon_1 = -0.25$ and $\varepsilon_2 = 0.25$. Combined with the previous analysis, we see that full diversity order 2 can not be achieved for this special case. The simulation result conforms with our analysis. In Fig.3.11, the slop of its SER curve is nearly the same as that of the SISO system, whose diversity order is only equal to one.

□ End of chapter.

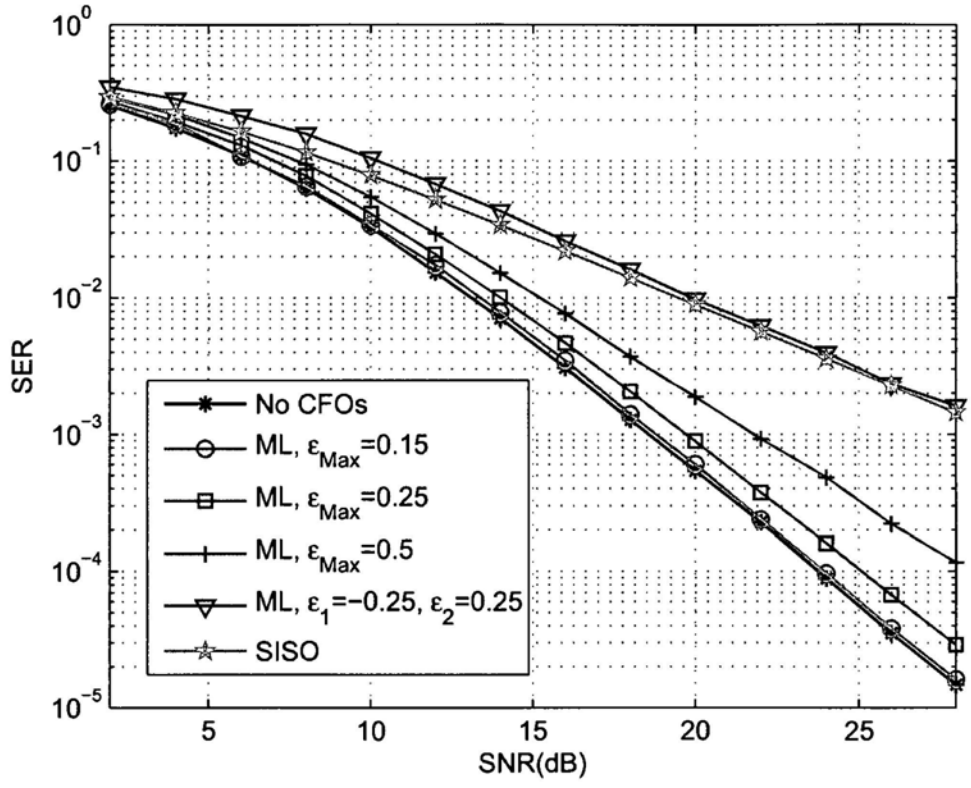

Figure 3.11: SER performance of the ML detection method in the presence of multiple CFOs.

Chapter 4

Signal Detection in an SF Coded Cooperative Communication System with Multiple CFOs

Summary

In SF coded communications, multiple carrier frequency offsets (CFOs) may drastically degrade the system performance. In this chapter, we consider the signal detection problem in an SF coded cooperative communication system with multiple CFOs. The SF codes here are rotational based and can achieve both full spatial and full multipath diversity orders in a multi-antenna system. By fully exploiting the structure of the SF codes, we propose three signal detection methods to deal with the multiple CFO problem. They are the minimum mean-squared error filtering (MMSE-F) method, the two-stage simple frequency shift Q taps (FS-Q-T) method , and the multiple fast Fourier transform (M-FFT) method, all of which offer different tradeoffs between performance and computational complexity. Our simulation results indicate that our proposed detection methods perform well as long as the carrier frequency offsets are small.

4.1 Introduction

It has been introduced in previous chapters that different from MIMO systems, one difficulty for most cooperative systems is the synchronization problem including both timing errors of multiple carrier frequency offsets (CFOs). Recently, this problem has been discussed in various literature [60–62, 64, 65, 71, 113, 119]. One of the approaches being investigated is based on OFDM due to the fact that OFDM is not sensitive to timing errors [62, 71, 113]. In [62] space-time coded OFDM is used to reduce the timing error effects. Subsequently, in [113], a distributive high-rate full-diversity space-frequency (SF) coding is proposed. Under the situation that a channel from a relay node to the destination node is frequency selective, this distributive coding strategy can achieve both full cooperative diversity and full multipath diversity for asynchronous communications.

It is well-known that OFDM is sensitive to carrier frequency offset (CFO) which often leads to inter-carrier interference (ICI). For the conventional OFDM or MIMO-OFDM systems, only one CFO between transmitter and receiver exists. Thus if the CFO is accurately estimated, it can be easily compensated. However, in a cooperative communication system, since SF codes are transmitted from various distributed nodes, there may exist multiple CFOs at the destination node. It is difficult for the destination node to synchronize the signals from multiple relay nodes at the same time. Therefore, ICI exists and ICI mitigation is needed to improve performance.

The problem of multiple CFOs in cooperative communication systems has recently been studied in [74] and [75]. In [74], a subcarrier-wise Alamouti coded OFDM system is considered and a simplified zero-forcing (ZF) equalizer is applied to suppress the ICI. In [75], delay diversity is considered and a minimum mean square error (MMSE) decision feedback equalizer (DFE) is employed by the destination node, where the DFE filter coefficient calculation requires a matrix inversion per information symbol.

In this chapter, we consider the signal detection problem in an SF coded cooperative communication system in the presence of multiple CFOs, where rotation-based

SF codes [36,37,39,113] are considered. Compared with codes used in [74] and [75], these SF codes are powerful in the sense that they can achieve both full cooperative diversity as well as full multipath diversity, and their rate is always equal to one regardless of the number of transmit antennas.

Judging from the fact that the SF codes are designed based on maximum-likelihood (ML) criterion, we consider appropriately increasing signal-to-interference plus noise ratio (SINR) or mitigating ICI before ML decoding of the SF codes. By fully exploiting the structure of SF codes, we find that for the considered multiple-input single-output (MISO) signal model, a single-input single-out (SISO) MMSE equalizer can be used to maximize the SINR and thus the computational complexity can be significantly reduced. Similar to [75], we also consider channel changing caused by CFO and find that due to the structure of the SF codes, the updating of the filter coefficients is easier than that of [75] in the sense that the MMSE filter matrix inverse is independent of the OFDM symbol (or block) index for a channel realization.

It is well-known that the Q taps (Q-T) method is a common method to reduce computational complexity, e.g., [120] and [121]. In this chapter we will use the Q taps method as a benchmark and compare it with our proposed simplified methods. Our simulation results will show that for the same symbol error rate (SER) performance, our proposed methods require less operations than the Q-T method. Following the idea in [120], we also derive a two-stage Q taps method to enhance the performance of the Q-T method. Because the channel changing is caused by CFO, we can pre-process a received signal by the simple frequency shift (FS) operation.

We then introduce a novel multiple FFT (M-FFT) method which can be realized by simply re-arranging the SF code with little loss in system performance. As a matter of fact, not only is its performance comparable with the Q-T method, but M-FFT can also be used as preprocessing of the Q-T method. Our analysis shows that if the coherence time of the channel is not very long, the M-FFT based methods have a lower computational complexity than that of the Q-T method.

This chapter is organized as follows. In Section 4.2, the system and the signal models are introduced and in Section 4.3, the structure of the SF codes described

in [39] is reviewed. The fundamentals as well as the implementation topologies of the three new detection methods for tackling the multiple CFO problem are explained in great detail in Section 4.4. In Section 4.5 the computational complexity of our proposed detection methods are analyzed and simulation results are shown in Section 4.6. Throughout this chapter, full channel knowledge including CFOs at the destination node is assumed.

4.2 System Model

4.2.1 Cooperative Protocol

Fig.4.1 shows the structure of cooperative communication system in this study, which includes one source node, one destination node, and a number of relay nodes. In the first phase, the source node S broadcasts the information while the relay nodes receive the same information. In the second phase, the M_t relay nodes, which have detected the received information symbols correctly, will help the source to transmit. The detected symbols are parsed into blocks of size N and the bth block, $b = 0, 1, \cdots$, is encoded to an SF codeword matrix $\mathbf{C}^b$ in a distributed fashion [66]. Here we assume that before the transmission in the second phase, by exchanging some information with the source node, the mth ($1 \leq m \leq M_t$) relay node is assigned the number m. Thus, each relay node knows which column of the SF code matrix it should transmit. So, the mth relay node transmits the $(m-1)$th column of the codeword matrix, denoted as $\mathbf{c}_m^b$, by the standard OFDM technology. Another way is to pre-assign the column indices to all the potential relay nodes in case there are not too many potential relay nodes. In this case no information exchange may be needed among the relay nodes. Then, at the destination node, the received OFDM symbols are used to decode the SF code. Here, the *decode-and-forward* protocol is adopted. We also assume that each node has only one transmit/receive antenna, and that there is no direct link between the source node and the destination node. Although in a cooperative communication system, each column of an SF code corresponds to one relay node, to be consistent with the notation used in the SF coding literature, we will use the term *antenna* instead of *relay node* in this chapter.

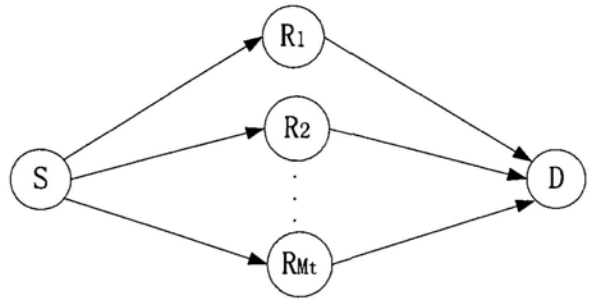

Figure 4.1: System structure.

4.2.2 Receive Signal Model

At the destination node, after matched filtering, and removing the cyclic prefix of length L_{cp} and applying FFT for each channel realization, the bth received OFDM symbol $\mathbf{z}^b$ in the frequency domain is given by

$$\mathbf{z}^b = \sqrt{\frac{\rho}{M_t}} \sum_{m=1}^{M_t} e^{j\theta^b_{\varepsilon_m}} \mathbf{U}_{\varepsilon_m} \mathbf{H}_m \mathbf{c}^b_m + \mathbf{w}^b, \tag{4.1}$$

where $\mathbf{H}_m$ is an $N \times N$ diagonal matrix whose diagonal elements are the channel frequency response from mth relay node to the destination node, $\mathbf{w}^b$ is an $N \times 1$ vector with each entry being a zero mean unit variance complex Gaussian random variable and ρ stands for the signal-to-noise ratio (SNR) at the destination node. Let Δf_m be the CFO between the mth relay node and the destination node. Then $\varepsilon_m = \Delta f_m T$ is its normalized value by OFDM symbol duration T. In (4.1), $\theta^b_{\varepsilon_m} = 2\pi\varepsilon_m(bN + bL_{cp} + L_{cp})/N + \theta_{0,m}$, where $2\pi\varepsilon_m(bN + bL_{cp} + L_{cp})/N$ is the phase rotation of the bth OFDM symbol transmitted from the mth relay node induced by CFO Δf_m during the time of b OFDM symbols and $b + 1$ CPs, and $\theta_{0,m}$ is the phase rotation between the phase of the destination node local oscillator and the carrier phase of the mth relay node at the start of the received signal. $\mathbf{U}_{\varepsilon_m}$ is the ICI matrix induced by ε_m and is given by

$$\mathbf{U}_{\varepsilon_m} = \mathbf{F}_N \mathbf{\Omega}_{\varepsilon_m} \mathbf{F}_N^{\mathcal{H}}, \tag{4.2}$$

where $\mathbf{\Omega}_{\varepsilon_m} = \text{diag}(1, e^{j2\pi\varepsilon_m/N}, \cdots, e^{j2\pi\varepsilon_m(N-1)/N})$. From the definition of $\mathbf{U}_{\varepsilon_m}$, clearly $\mathbf{U}_{\varepsilon_m}$ is a unitary matrix and the element at its lth row and kth column is

$$\mathbf{U}_{\varepsilon_m}(l,k) = u_{\varepsilon_m,(k-l)_N} = \frac{\sin[\pi((k-l)_N + \varepsilon_m)]e^{j\pi((k-l)_N+\varepsilon_m)(N-1)/N}}{N\sin[\pi((k-l)_N + \varepsilon_m)/N]}, \tag{4.3}$$

where $0 \leq l, k \leq N-1$.

From (4.2) and (4.3) we can see that if $\varepsilon_m \neq 0$, $m = 1, 2, \cdots, M_t$, the matrix $\mathbf{U}_{\varepsilon_m}$ is no longer diagonal and (4.3) shows the effect of CFO. The amplitude of the concerned subcarrier is attenuated and its phase is rotated due to $u_{\varepsilon_m,0}$. At the same time, the desired subcarrier is also interfered in by the ICI power coming from other subcarriers. Furthermore, if more than one CFO exists, which is possible in a cooperative communication system, it is difficult for the destination node to compensate all the CFOs at the same time.

4.3 Structure of Space-Frequency Codes

The SF code for the cooperative communication system under investigation is based on the code in [39], [66], [37]. In this section, we will briefly review the structure of this SF code and some of the properties to be utilized in consequent sections. Here we adopt the code structure proposed in [39].

Each SF code $\mathbf{C}$ is an $N \times M_t$ matrix and is mapped from an $N' \times 1$ information symbol vector $\mathbf{s}$. Here N is equal to the number of subcarriers in one OFDM symbol, M_t is equal to the number of transmit antennas, and $N' \leq N$.

For the coding strategy proposed in [39], each SF codeword $\mathbf{C}$ is a concatenation of some matrices $\mathbf{G}_p$

$$\mathbf{C} = \begin{bmatrix} \mathbf{G}_1^{\mathcal{T}} & \mathbf{G}_2^{\mathcal{T}} & \cdots & \mathbf{G}_P^{\mathcal{T}} & \mathbf{0}_{(N-N')\times M_t}^{\mathcal{T}} \end{bmatrix}^{\mathcal{T}}, \tag{4.4}$$

where $P = \lfloor N/(\Gamma M_t) \rfloor$, $N' = P\Gamma M_t$ and each matrix $\mathbf{G}_p$ is of size ΓM_t by M_t for $p = 1, 2, \cdots, P$. The zero padding matrix $\mathbf{0}_{(N-N')\times M_t}$ is an $(N-N') \times M_t$ all zero matrix which is used if the number of subcarriers N is not an integer multiple of ΓM_t. In the remainder of this chapter, unless otherwise specified, we always assume that N is an integer multiple of ΓM_t. Each matrix $\mathbf{G}_p$, $1 \leq p \leq P$, has the same structure given by

$$\mathbf{G}_p = \sqrt{M_t} \begin{bmatrix} \mathbf{x}_1^p & \mathbf{0}_\Gamma & \cdots & \mathbf{0}_\Gamma \\ \mathbf{0}_\Gamma & \mathbf{x}_2^p & \cdots & \mathbf{0}_\Gamma \\ \vdots & \vdots & \ddots & \vdots \\ \mathbf{0}_\Gamma & \mathbf{0}_\Gamma & \cdots & \mathbf{x}_{M_t}^p \end{bmatrix}, \tag{4.5}$$

where $\mathbf{x}_m^p = [x_{(m-1)\Gamma+1}^p x_{(m-1)\Gamma+2}^p \cdots x_{m\Gamma}^p]^\mathcal{T}$, $m = 1, 2, \cdots, M_t$, and all x_k^p, $k = 1, 2, \cdots, \Gamma M_t$, are complex symbols and are mapped from an information subvector $\mathbf{s}_p = [s_1^p, s_2^p, \cdots, s_{\Gamma M_t}^p]^\mathcal{T}$ by a rotation operation

$$[\mathbf{x}_1^{p\mathcal{T}}, \mathbf{x}_2^{p\mathcal{T}}, \cdots, \mathbf{x}_{M_t}^{p\ \mathcal{T}}]^\mathcal{T} = \mathbf{\Theta}\mathbf{s}_p, \tag{4.6}$$

where s_l^p is $((p-1)\Gamma M_t + l - 1)$th entry of $\mathbf{s}$ for $1 \leq l \leq \Gamma M_t$ and $\mathbf{\Theta}$ is an $M_t\Gamma \times M_t\Gamma$ rotation matrix. If the signal constellations are QAM and PAM, it can be shown that the optimum rotation matrix $\mathbf{\Theta}$ is a unitary matrix [39]. More introduction to $\mathbf{\Theta}$ has been given in Chapter 2.3.2. The details regarding the construction of $\mathbf{\Theta}$ can be found in [39] and the references therein. The energy constraint is $\mathrm{E}\left[\sum_{k=1}^{\Gamma M_t} |x_k|^2\right] = \Gamma M_t$. For a certain p, the symbols in $\mathbf{G}_p$ are designed jointly, but the design of $\mathbf{G}_{p_1}$ and $\mathbf{G}_{p_2}$, $p_1 \neq p_2$, is independent of each other. At the destination node, each SF submatrix $\mathbf{G}_p$ is decoded by ML or sphere decoding independently. We can see that through rotation and allocation to different subcarriers and antennas, the information of each entry in $\mathbf{s}$ disperses in Γ subcarriers of each antenna. Thus the maximum diversity order achieved by this kind of SF codes is equal to $\Gamma M_t M_r$ where M_r is the number of receive antennas. Here, by realizing the SF code in a distributed fashion, for each cooperative transmission, the achieved diversity order is equal to $\sum_{m=1}^{M_t} L_m$, if $\max(L_m) \leq \Gamma$ for $m = 1, 2, \cdots, M_t$, where M_t is the number of relay nodes incorporated in this cooperative transmission, and L_m is the number of multipaths for the link from mth relay node to the destination node [66].

4.4 Signal Detection with Multiple CFOs

By modeling ICI as additional Gaussian noise, it is shown in [122] that the design criterion for SF codes without CFO is still valid in the presence of CFO. This means that CFO may not decrease diversity order and the performance degradation can be regarded as that due to the loss of equivalent SNR, i.e., signal-to-interference-plus-noise ratio (SINR). Thus, if SINR is increased, the performance loss can be diminished. Based on this observation, we propose to deal with ICI mitigation due to multiple CFOs by first increasing the SINR using linear filtering or other methods, and then decoding the SF code by the commonly used ML or sphere decoding method.

4.4.1 MMSE Filtering Method (MMSE-F)

In this subsection, we consider using a linear filtering $N \times N$ matrix $\mathbf{V}^b$ to maximize the SINR of each subcarrier based on the MMSE criterion, where b is the index of OFDM symbols. Each row of $\mathbf{V}^b$, denoted by $\mathbf{v}_k^b$, is a $1 \times N$ filter coefficient vector corresponding to the kth subcarrier, $0 \leq k \leq N-1$, with the constraint $\mathbf{v}_k^b \mathbf{v}_k^{b\mathcal{H}} = 1$. Let $\tilde{\mathbf{z}}^b = \mathbf{V}^b \mathbf{z}^b$ and $\mathbf{D}_m = \mathbf{U}_{\varepsilon_m} \mathbf{H}_m$. Then subsequent to the filtering process, we obtain

$$\tilde{\mathbf{z}}^b = \sqrt{\frac{\rho}{M_t}} \sum_{m=1}^{M_t} e^{j\theta_{\varepsilon_m}^b} \mathbf{V}^b \mathbf{D}_m \mathbf{c}_m^b + \mathbf{V}^b \mathbf{w}^b. \tag{4.7}$$

The filtered signal of the kth subcarrier can be written as

$$\tilde{\mathbf{z}}^b(k) = \sqrt{\frac{\rho}{M_t}} \sum_{m=1}^{M_t} e^{j\theta_{\varepsilon_m}^b} \mathbf{v}_k^b [\mathbf{D}_{m,0}, \mathbf{D}_{m,1}, \cdots, \mathbf{D}_{m,N-1}] \mathbf{c}_m^b + \mathbf{v}_k^b \mathbf{w}^b, \tag{4.8}$$

where $\mathbf{D}_{m,i}$, $0 \leq i \leq N-1$, is the ith column of $\mathbf{D}_m$.

From (4.8), we can express the SINR at the kth subcarrier as follows:

$$\mathrm{SINR}^b(k) = \frac{\mathrm{E}\left[|\gamma_d^b(k)|^2\right]}{\mathrm{E}\left[|\gamma_r^b(k) - \gamma_d^b(k)|^2\right]}, \tag{4.9}$$

where the expectation is taken over Gaussian noise and elements of SF code $\mathbf{C}^b$.

In (4.9), $\gamma_d^b(k)$ is the desired signal of the kth subcarrier after filtering. It can be expressed as

$$\gamma_d^b(k) = \sum_{m=1}^{M_t} \sqrt{\frac{\rho}{M_t}} e^{j\theta_{\varepsilon_m}^b} \mathbf{v}_k^b \mathbf{D}_{m,k} \mathbf{c}_m^b(k). \tag{4.10}$$

Similarly, $\gamma_r^b(k)$ is the total received signal of the kth subcarrier and is given by

$$\gamma_r^b(k) = \sum_{m=1}^{M_t} \sum_{l=0}^{N-1} \sqrt{\frac{\rho}{M_t}} e^{j\theta_{\varepsilon_m}^b} \mathbf{v}_k^b \mathbf{D}_{m,l} \mathbf{c}_m^b(l) + \mathbf{v}_k^b \mathbf{w}^b. \tag{4.11}$$

Thus $\gamma_r^b(k) - \gamma_d^b(k)$ is the total signal of the filtered Gaussian noise and ICI terms coming from other subcarriers.

The calculation of vector $\mathbf{v}_k^b$ that maximizes $\mathrm{SINR}^b(k)$ is a standard generalized eigenvalue problem [123]. For each subcarrier, its calculation requires one Cholesky factorization and the computation of the dominant eigenvector, each of which requires $O(N^3)$ operations when a general MISO equalizer is applied [80]. However, if

the structure of the SF code is carefully exploited, the computational complexity of $\mathbf{v}_k^b$ can be reduced to $O(N^2)$.

One property of the SF code is that each subcarrier is only used by one transmit antenna. From (4.5), we can write $\mathbf{c}_m^b$ as

$$\mathbf{c}_m^b = \sqrt{M_t}\mathbf{P}_m(\mathbf{I}_P \otimes \mathbf{\Theta})\mathbf{s}^b = \sqrt{M_t}\mathbf{P}_m\mathbf{x}^\mathbf{b}, \tag{4.12}$$

where $\mathbf{x}^\mathbf{b} = (\mathbf{I}_P \otimes \mathbf{\Theta})\mathbf{s}^b$ and $\mathbf{P}_m$ is a diagonal matrix corresponding to the $(m-1)$th column of $\mathbf{c}^b$. For the SF code in [39], $\mathbf{P}_m$ has the following form

$$\mathbf{P}_m(l,l') = \begin{cases} 1, & \text{if } l = l' = (t-1)\Gamma M_t + (m-1)\Gamma + i \\ 0, & \text{otherwise} \end{cases}, \tag{4.13}$$

where $0 \le i \le \Gamma - 1$ and $1 \le t \le P$. Based on (4.13) we have

$$\mathbf{P}_m\mathbf{P}_{m'} = \begin{cases} \mathbf{P}_m, & \text{if } m = m' \\ \mathbf{0}_{N\times N}, & \text{otherwise} \end{cases}, \tag{4.14}$$

where $\mathbf{0}_{N\times N}$ is $N \times N$ all zeros matrix.

Furthermore, because the rotation matrix $\mathbf{\Theta}$ is a unitary matrix, it is not difficult to verify that

$$\mathrm{E}[\mathbf{c}_m(l)^*\mathbf{c}_{m'}(l')] = \begin{cases} M_t, & \text{if } l = l',\ m = m' \text{ and } \mathbf{c}_m(l) \neq 0 \\ 0, & \text{otherwise} \end{cases}, \tag{4.15}$$

for $0 \le l, l' \le N-1$ and $1 \le m, m' \le M_t$, which leads to

$$\mathrm{E}[\mathbf{x}(l)^*\mathbf{x}(l')] = \begin{cases} 1, & \text{if } l = l' \\ 0, & \text{otherwise} \end{cases}. \tag{4.16}$$

Assuming that the lth subcarrier is used by the m_lth antenna, equations (4.10) and (4.11) can be written as

$$\gamma_d^b(k) = \sqrt{\frac{\rho}{M_t}}e^{j\theta_{\varepsilon_{m_k}}^b}\mathbf{v}_k^b\mathbf{D}_{m_k,k}\mathbf{c}_{m_k}^b(k), \tag{4.17}$$

and

$$\gamma_r^b(k) = \sum_{l=0}^{N-1}\sqrt{\frac{\rho}{M_t}}e^{j\theta_{\varepsilon_{m_l}}^b}\mathbf{v}_k^b\mathbf{D}_{m_l,l}\mathbf{c}_{m_l}^b(l) + \mathbf{v}_k^b\mathbf{w}^b, \tag{4.18}$$

respectively. By considering (4.15), we have

$$\mathrm{E}\left[|\gamma_d^b(k)|^2\right] = \rho\mathbf{v}_k^b\mathbf{D}_{m_k,k}\mathbf{D}_{m_k,k}^{\mathcal{H}}\mathbf{v}_k^{b\mathcal{H}}, \tag{4.19}$$

and

$$\mathrm{E}\left[|\gamma_r^b(k) - \gamma_d^b(k)|^2\right] = 1 + \sum_{l=0, l\neq k}^{N-1} \rho \mathbf{v}_k^b \mathbf{D}_{m_l,l} \mathbf{D}_{m_l,l}^{\mathcal{H}} \mathbf{v}_k^{b\mathcal{H}}. \tag{4.20}$$

Substituting (4.19) and (4.20) into (4.9) and using the constraint $\mathbf{v}_k^b \mathbf{v}_k^{b\mathcal{H}} = 1$, we get

$$\mathrm{SINR}^b(k) = \frac{\mathbf{v}_k^b \mathbf{D}_{m_k,k} \mathbf{D}_{m_k,k}^{\mathcal{H}} \mathbf{v}_k^{b\mathcal{H}}}{\mathbf{v}_k^b \left(\frac{1}{\rho}\mathbf{I}_N + \sum_{l=0}^{N-1} \mathbf{D}_{m_l,l} \mathbf{D}_{m_l,l}^{\mathcal{H}} - \mathbf{D}_{m_k,k} \mathbf{D}_{m_k,k}^{\mathcal{H}}\right) \mathbf{v}_k^{b\mathcal{H}}}. \tag{4.21}$$

By comparing (4.21) with [124, Equation (20)], we can see that the above SINR for our signal model in (4.1) is the same as that for the following SISO-OFDM signal model:

$$\mathbf{z}^b = \sqrt{\rho}\mathbf{D}^b \mathbf{x}^b + \mathbf{w}^b, \tag{4.22}$$

where $\mathbf{D}^b = \sum_{m=1}^{M_t} e^{j\theta_{\varepsilon m}^b} \mathbf{D}_m \mathbf{P}_m$ and the elements of $\mathbf{x}^b$ are uncorrelated from each other. To calculate $\mathbf{V}^b$ that maximizes SINR based on the SISO model in (4.22), we utilize (4.14) to rewrite (4.22) as follows:

$$\begin{aligned} \mathbf{z}^b &= \sqrt{\rho}\left(\sum_{m=1}^{M_t} e^{j\theta_{\varepsilon m}^b} \mathbf{D}_m \mathbf{P}_m\right) \mathbf{x}^b + \mathbf{w}^b \\ &= \sqrt{\rho}\mathbf{D}\mathbf{P}^b \mathbf{x}^b + \mathbf{w}^b, \end{aligned} \tag{4.23}$$

where $\mathbf{D} = \sum_{m=1}^{M_t} \mathbf{D}_m \mathbf{P}_m$ and $\mathbf{P}^b = \sum_{m=1}^{M_t} e^{j\theta_{\varepsilon m}^b} \mathbf{P}_m$. It is easy to verify that $\mathbf{P}_m \mathbf{P}^b = e^{j\theta_{\varepsilon m}^b} \mathbf{P}_m$ and that $\mathbf{P}^b$ is a unitary matrix.

For the signal model (4.23) or (4.22), the linear MMSE filter maximizes the output SINR for any value of SNR [7]. Thus, the optimal filtering matrix $\mathbf{V}^b$ can be calculated as follows:

1. if $b = 0$ then

   - Compute the MMSE equalization matrix $\hat{\mathbf{V}}$ for (4.23)

$$\hat{\mathbf{V}} = \left(\left(\mathbf{D}\mathbf{P}^0\right)^{\mathcal{H}} \left(\mathbf{D}\mathbf{P}^0\right) + \frac{1}{\rho}\mathbf{I}_N\right)^{-1} \left(\mathbf{D}\mathbf{P}^0\right)^{\mathcal{H}} = \mathbf{P}^{0\mathcal{H}} \Upsilon, \tag{4.24}$$

     where $\Upsilon = \left(\mathbf{D}^{\mathcal{H}}\mathbf{D} + \frac{1}{\rho}\mathbf{I}_N\right)^{-1} \mathbf{D}^{\mathcal{H}}$.

   - Normalize each row of Υ and denote it by $\hat{\Upsilon}$.

   - We have $\mathbf{V}^0 = \mathbf{P}^{0\mathcal{H}} \hat{\Upsilon}$.

2. if $b \geq 1$ then $\mathbf{V}^b = \mathbf{P}^{b\mathcal{H}}\hat{\Upsilon}$ or $\mathbf{V}^b = \mathbf{P}^{\mathcal{H}}\mathbf{V}^{b-1}$ where $\mathbf{P} = \sum_{m=1}^{M_t} e^{j2\pi\epsilon_m(1+L_{cp}/N)}\mathbf{P_m}$ since $\mathbf{P}^b = \mathbf{P}^{b-1}\mathbf{P}$.

Based on the calculation of $\mathbf{V}^b$, the MMSE-F detection method can be summarized as follows

1. Compute the filter matrix $\mathbf{V}^b$.

2. Use $\mathbf{V}^b$ to filter the received signal vector $\mathbf{z}^b$ (4.23). Then, we obtain

$$\begin{aligned} \tilde{\mathbf{z}}^b &= \sqrt{\rho}\mathbf{V}^b\mathbf{D}\mathbf{P}^{\mathbf{b}}\mathbf{x}^b + \mathbf{V}^b\mathbf{w}^b \\ &= \sqrt{\rho}\mathbf{P}^{b\mathcal{H}}\hat{\Upsilon}\mathbf{D}\mathbf{P}^b\mathbf{x}^b + \tilde{\mathbf{w}}^b \\ &= \sqrt{\rho}\mathbf{H}\mathbf{x}^b + \sqrt{\rho}\left(\tilde{\mathbf{D}}^b - \mathbf{H}\right)\mathbf{x}^b + \tilde{\mathbf{w}}^b \end{aligned} \tag{4.25}$$

   where $\tilde{\mathbf{D}}^b = \mathbf{P}^{b\mathcal{H}}\hat{\Upsilon}\mathbf{D}\mathbf{P}^b$ is the filtered channel matrix, $\mathbf{H} = \mathbf{I}_N \odot \tilde{\mathbf{D}}^b$, and $\tilde{\mathbf{w}}^b = \mathbf{V}^b\mathbf{w}^b$ is the filtered noise vector. It is easy to verify that $\mathbf{H}(l,l) = \hat{\Upsilon}_l\mathbf{D}_l$, $0 \leq l \leq N-1$, where $\hat{\Upsilon}_l$ is the lth row of $\hat{\Upsilon}$ and $\mathbf{D}_l$ is the lth column of $\mathbf{D}$. $\sqrt{\rho}\left(\tilde{\mathbf{D}}^b - \mathbf{H}\right)\mathbf{x}^b + \tilde{\mathbf{w}}^b$ expresses the effect of both ICI and filtered Gaussian noise.

3. Ignore both the off-diagonal terms in the covariance matrix of $\tilde{\mathbf{w}}^b$, i.e., $\mathbf{V}^b\mathbf{V}^{b\mathcal{H}}$, and ICI terms. Then decode SF codes vector $\mathbf{x}^b$ by ML or sphere decoding.

For this MMSE-F method, we have the following observations:

- Comparing with the case of delay diversity coding in [75], the filter matrix is easier to update. Here, for each channel realization, the operation of matrix inversion is required only once in (4.24) for different OFDM symbols.

- Different from the blind detection schemes in [125, 126], and the conventional non Space-Time (ST) or non SF coded cases in [120, 127], where after equalization the estimation of the information symbols are directly obtained (we call this method the *complete equalization* (CE) method), here after the equalization, instead of the direct information symbols, the estimation of $\sqrt{\rho}\mathbf{x}^b$ is obtained. Since the SF code is designed based on the ML criterion rather than the MMSE criterion, if we apply CE, we cannot achieve the full diversity gain,

although the CE method requires less computations than the MMSE-F method. To preserve the performance of the SF code, the precoding matrix $\boldsymbol{\Theta}$ should not be equalized. This also implies that after the filtering process, it is still necessary to decode the SF code by ML decoding such as sphere decoding method to achieve the full diversity.

- To avoid the necessity of jointly considering all N subcarriers, two approximations have been adopted when decoding the SF codes through (4.25) in Step 3 above and in our simulations to be described later on. First, the filtered Gaussian noise vector $\tilde{\mathbf{w}}^b$ is considered to be white. Second, the ICI terms $\sqrt{\rho}\left(\tilde{\mathbf{D}}^b - \mathbf{H}\right)\mathbf{x}^b$ are ignored or simply regarded as additional Gaussian noise.

The major drawback of the MMSE-F method is its computational complexity which is of the order of $O(N^3)$. Although this cost can be averaged by the number of OFDM symbols in one channel realization, it could still be a burden when N is large. To mitigate this deficiency, in the remainder of this section we propose several simple detection methods at the cost of some performance loss.

4.4.2 Frequency Shift Q Taps (FS-Q-T) Method

As already studied in the literature, e.g., in [120, 121], for a particular subcarrier, most of the ICI power comes from a few adjacent subcarriers and most of the leaking power appears in its neighboring subcarriers. Although in this study, the change of the channel is caused by CFO and not by the Doppler frequency shift, a similar result can be easily obtained by observing the ICI matrix $\mathbf{U}_{\varepsilon_m}$. Based on this property, the Q taps method is a common way to reduce computational complexity for OFDM system, e.g., [120] and [121], where for the concerned subcarrier only its L circular left and right subcarriers are considered. That means we use Q (Q = $2L+1$) taps filter instead of the full N-taps filter. Roughly speaking, if $N\text{Q}^3 \leq N^3$, the computational complexity can be reduced in the expense of a certain performance loss.

To mitigate this performance loss, in [120], a two-stage equalizer is proposed. Its main idea is that at the receiver before FFT, a time domain windowing is used to decrease the neglected ICI. However, the calculation of the windowing vector requires

the solution of a generalized eigenvalue problem whose computational complexity can exceed the one for computing the N taps MMSE filter for our considered problem.

In this subsection we propose a simple two-stage FS-Q-T method suitable for system with two relay nodes. Its main idea is that before FFT we can shift all CFOs by a certain frequency $\hat{\varepsilon}$. Although this operation cannot completely compensate multiple CFOs, we still hope that frequency shift (FS) can increase the average SINR of each subcarrier (denoted by $\overline{\text{SINR}}(k)$, $0 \leq k \leq N-1$) or in other words decrease the level of the error floor. If this is possible, the performance of the Q-T method can be improved. Here, average SINR means SINR is averaged over the channel realizations. Therefore $\overline{\text{SINR}}(k)$ does not depend on any particular channel.

To express $\overline{\text{SINR}}(k)$, we rewrite $\mathbf{z}^b(k)$ as

$$\mathbf{z}^b(k) = \sqrt{\rho} e^{j\theta^b_{\varepsilon_{m_k}}} u_{\varepsilon_{m_k},0} \mathbf{H}_{m_k}(k,k)\mathbf{x}^b(k) + \mathrm{I}^b(k) + \mathbf{w}^b(k), \tag{4.26}$$

where m_l is the lth subcarrier used by the m_lth antenna. The first term of (4.26) is the desired signal and

$$\mathrm{I}^b(k) = \sum_{l=0, l\neq k}^{N-1} \sqrt{\rho} e^{j\theta^b_{\varepsilon_{m_l}}} u_{\varepsilon_{m_l},(l-k)_N} \mathbf{H}_{m_l}(l,l)\mathbf{x}^b(l) \tag{4.27}$$

is the ICI term for the kth subcarrier.

As discussed in [122], the ICI term $\mathrm{I}^b(k)$ can be modeled as an additional Gaussian noise. Assuming that information symbols have zero-mean such as PAM, PSK, and QAM signal constellations, we have $\mathrm{E}\left[\mathrm{I}^b(k)\right] = 0$. Then, by using (4.16) and the fact that

$$\mathrm{E}\left[|\mathbf{H}_m(l,l)|^2\right] = 1 \text{ and } \mathrm{E}[\mathbf{x}^b(l)] = 0,$$

we can calculate the variance $\sigma^2_{\mathrm{I}^b(k)}$ of ICI term $\mathrm{I}^b(k)$ as

$$\sigma^2_{\mathrm{I}^b(k)} = \mathrm{E}\left[|\mathrm{I}^b(k)|^2\right] = \rho \sum_{l=0, l\neq k}^{N-1} |u_{\varepsilon_{m_l},(l-k)_N}|^2. \tag{4.28}$$

Hence, we have

$$\overline{\text{SINR}}(k) = \frac{\rho |u_{\varepsilon_{m_k},0}|^2}{\rho \sum_{l=0, l\neq k}^{N-1} |u_{\varepsilon_{m_l},(l-k)_N}|^2 + 1}, \tag{4.29}$$

where the index b is dropped since both the desired signal and ICI powers do not depend on b.

From the expression of $\overline{\text{SINR}}(k)$, we can see that for each realization of ε_m, $\overline{\text{SINR}}(k)$ depends on k. On the other hand, according to the SF code structure, it is not difficult to show that the kth and the $(k + pM_t\Gamma)_N$th subcarriers have the same value of $\overline{\text{SINR}}$ for $1 \leq p \leq P-1$. To remove the dependence of the subcarrier index k, we can consider the total $\overline{\text{SINR}}$ of a group of M_t subcarriers which are used by different antennas in one SF submatrix $\mathbf{G}_p$. This is reasonable since at the receiver all subcarriers in one submatrix are jointly decoded. We denote this group $\overline{\text{SINR}}$ by $\overline{\text{SINR}}_g$. Assume the kth subcarrier is used by the 1st antenna, according to (4.5), the $(k + i\Gamma)$th subcarrier is used by the $(i + 1)$th antenna for $0 \leq i \leq M_t - 1$. Then, the total average SINR of these M_t subcarriers can be expressed as

$$\begin{aligned}
\overline{\text{SINR}}_g &= \frac{\rho \sum_{i=0}^{M_t-1} |u_{\varepsilon_{i+1},0}|^2}{\rho \sum_{i=0}^{M_t-1} \sum_{l=0,l\neq k+i\Gamma}^{N-1} |u_{\varepsilon_{m_l},(l-(k+i\Gamma))_N}|^2 + M_t} \\
&= \frac{\rho \sum_{i=0}^{M_t-1} |u_{\varepsilon_{i+1},0}|^2}{\rho \sum_{i=0}^{M_t-1} \sum_{l=1}^{N-1} |u_{\varepsilon_{i+1},l}|^2 + M_t} \\
&= \frac{\rho \sum_{i=1}^{M_t} |u_{\varepsilon_i,0}|^2}{\rho \left(M_t - \sum_{i=1}^{M_t} |u_{\varepsilon_i,0}|^2\right) + M_t}.
\end{aligned} \tag{4.30}$$

It is clear that $\overline{\text{SINR}}_g$ does not depend on the subcarrier index. Then, define function $f(\hat{\varepsilon})$ as

$$f(\hat{\varepsilon}) = \frac{\rho \sum_{i=1}^{M_t} |u_{\varepsilon_i+\hat{\varepsilon},0}|^2}{\rho \left(M_t - \sum_{i=1}^{M_t} |u_{\varepsilon_i+\hat{\varepsilon},0}|^2\right) + M_t}. \tag{4.31}$$

which is the value of $\overline{\text{SINR}}_g$ after the frequency shift by amount $\hat{\varepsilon}$. Thus, we need to calculate $\hat{\varepsilon}$ that increases $f(\hat{\varepsilon})$. When $M_t = 2$, we can show that $\hat{\varepsilon}_* = -\left(\sum_{m=1}^{M_t} \varepsilon_m\right)/M_t$ is the optimal value to maximize $\overline{\text{SINR}}_g$ by considering the fact that $\nabla f(\hat{\varepsilon}_*) = 0$ where ∇f means the gradient of function f. However, when $M_t > 2$, we cannot get a closed solution to maximize $f(\hat{\varepsilon})$.

Finally, it should be noted that any two-stage strategy cannot outperform the MMSE-F method regardless of the value of Q because the MMSE-F method is an optimal linear processing approach in maximizing the SINR of each subcarrier.

4.4.3 Multiple FFT (M-FFT) Method

For the FS-Q-T method, when $M_t > 2$, we cannot get a closed solution to maximize $f(\hat{\varepsilon})$. To partially tackle this problem, we try another approach the multiple FFT (M-

FFT) method, i.e., multiple FS and FFT operations instead of only one FS operation. Since ICI power cannot be easily canceled by only one FS operation due to the effect of multiple CFO, we want to cancel more ICI power through multiple FS and FFT operations and we call this approach the multiple FFT (M-FFT) method.

Intuitively, if we shift the frequency of the received signal by $-\varepsilon_m$ for $1 \le m \le M_t$, the ICI power coming from the mth relay node can be completely canceled. However, the ICI power from other relay nodes may be increased at the same time. To alleviate this problem, we need to utilize the properties of both the SF code and ICI coefficients $u_{\varepsilon_m,l}$.

At the transmitter, we re-arrange the SF code $\mathbf{C}$ in (4.4)-(4.5) by some row permutations and denote this row-wisely permuted SF code by $\mathbf{C}'$, which is written by

$$\mathbf{C}' = \sqrt{M_t}\begin{bmatrix} \mathbf{x}_1^1 & \mathbf{0}_\Gamma & \cdots & \mathbf{0}_\Gamma \\ \vdots & \vdots & \vdots & \vdots \\ \mathbf{x}_1^P & \mathbf{0}_\Gamma & \cdots & \mathbf{0}_\Gamma \\ \mathbf{0}_\Gamma & \mathbf{x}_2^1 & \cdots & \mathbf{0}_\Gamma \\ \vdots & \vdots & \vdots & \vdots \\ \mathbf{0}_\Gamma & \mathbf{x}_2^P & \cdots & \mathbf{0}_\Gamma \\ \vdots & \vdots & \vdots & \vdots \\ \mathbf{0}_\Gamma & \mathbf{0}_\Gamma & \cdots & \mathbf{x}_{M_t}^1 \\ \vdots & \vdots & \vdots & \vdots \\ \mathbf{0}_\Gamma & \mathbf{0}_\Gamma & \cdots & \mathbf{x}_{M_t}^P \end{bmatrix}, \tag{4.32}$$

where $\mathbf{x}_m^p$ is defined in (4.5). From the above expression of $\mathbf{C}'$ we can see that after row permutations, the nonzero entries of the $(m-1)$th column of $\mathbf{C}$ are grouped. Note that the subcarriers from $P\Gamma(m-1)$ to $P\Gamma m - 1$ are used by the mth transmit antenna. We call these subcarriers the mth group.

Assume that the $((m-1)\Gamma + i)$th row, $0 \le i \le \Gamma - 1$, of $\mathbf{G}_p$ is located at the $n^p_{(m-1)\Gamma+i}$th row, $0 \le n^p_{(m-1)\Gamma+i} \le N-1$, of $\mathbf{C}'$, i.e., $x_{(m-1)\Gamma+i+1}$ of $\mathbf{G}_p$ will be transmitted at the $n^p_{(m-1)\Gamma+i}$th subcarrier by the mth transmit antenna. Then, for (4.32) we have $n^p_{(m-1)\Gamma+i} = (m-1)\Gamma P + (p-1)\Gamma + i$.

In [39], it has been shown that the diversity order and coding advantage of this kind of SF codes only depends on the relative positions of the permuted rows cor-

responding to the entries of $\mathbf{x}_m^p$ with respect to the position $n_{(m-1)\Gamma}^p$. Since we do not change the relative positions for the entries of $\mathbf{x}_m^p$, i.e., $n_{(m-1)\Gamma+i}^p - n_{(m-1)\Gamma}^p = i$, for each pair of m and p, $\mathbf{C}'$ should have the same diversity order and coding advantage as that of $\mathbf{C}$. When we use $\mathbf{C}'$, we can get the following frequency domain SISO-OFDM model from (4.22) as

$$\mathbf{z}'^b = \sqrt{\rho}\mathbf{D}'^b\mathbf{x}'^b + \mathbf{w}^b, \tag{4.33}$$

where $\mathbf{x}'^b = \mathbf{T}\mathbf{x}^b$ and $\mathbf{T}$ is a permutation matrix whose element in $\left(n_{(m-1)\Gamma+i}^p\right)$th row and $((p-1)M_t\Gamma + (m-1)\Gamma + i)$th row is equal to 1. Similar to the definition of $\mathbf{D}^b$ in (4.22), $\mathbf{D}'^b = \sum_{m=1}^{M_t} e^{j\theta_{\varepsilon_m}^b}\mathbf{D}_m\mathbf{P}'_m$ and $\mathbf{P}'_m$ is defined as

$$\mathbf{P}'_m(l,l') = \begin{cases} 1, & \text{if } l = l' \text{ and } (m-1)P\Gamma \le l \le mP\Gamma - 1 \\ 0, & \text{else} \end{cases}. \tag{4.34}$$

At the destination node in the time domain we apply FS and FFT operations M_t times. Each time CFO ε_l, $1 \le l \le M_t$, is completely compensated by the FS. Then, after the FFT operation we can get signal vector $\mathbf{z}'^b_l$ in the frequency domain as

$$\mathbf{z}'^b_l = \sqrt{\rho}\mathbf{D}'^b_l\mathbf{x}'^b + \mathbf{w}^b_l, \tag{4.35}$$

where $\mathbf{D}'^b_l = \sum_{m=1}^{M_t} e^{j(\theta_{\varepsilon_m}^b - \theta_{\varepsilon_l}^b)}\mathbf{D}_{m,l}\mathbf{P}'_m$, $\mathbf{D}_{m,l} = \mathbf{U}_{\varepsilon_{m,l}}\mathbf{H}_m$ and $\varepsilon_{m,l} = \varepsilon_m - \varepsilon_l$.

Since ε_l is compensated, we have $\mathbf{D}'^b_l\mathbf{P}'_l = \mathbf{H}_l\mathbf{P}'_l$. This means that the subcarriers of the lth group do not leak their power to all other subcarriers whether they are in the same group or not.

Unfortunately, due to the effect of multiple CFOs, the ICI power arriving from other groups may be increased by this FS operation. However, it is also highly probable that the SINR of the subcarriers in the lth group can be significantly increased.

From (4.2)-(4.3) for the ICI coefficients, one can see that for the desired kth subcarrier in the lth group, most of the ICI power comes from a few of its neighbors and most of which are in the same group. Considering another subcarrier, say the ith subcarrier, as the distance $|k-i|$ increases, the ICI power coming from the ith subcarrier drastically decreases. Therefore, although the ICI power arriving from other groups may be increased by this FS, its effect is insignificant compared with the canceled ICI power of the same group. In other words, the subcarriers in the lth group can

regard each other as separation or guard subcarriers against the ICI power from other groups. Furthermore, the subcarriers in the middle of the lth group should suffer from smaller ICI power than those subcarriers do which are at the boundaries of lth group. Because both sides of the middle subcarrier are separated from other groups and as the position of subcarrier shifts from the middle to left or right boundary, the ICI power coming from $((l-2)_{M_t}+1)$th or $((l)_{M_t}+1)$th group will rapidly increase.

Therefore, after the lth FS and FFT operation, we may only want to preserve the signals of the lth group denoted by $\mathbf{r}_l^b$ which is a $P\Gamma \times 1$ vector. Finally, we collect all of $\mathbf{r}_l^b$ for $1 \leq l \leq M_t$ and construct an equivalent received signal vector $\bar{\mathbf{z}}'^b = \left[\mathbf{r}_1^{b\mathcal{T}}, \mathbf{r}_2^{b\mathcal{T}}, \cdots, \mathbf{r}_{M_t}^{b\mathcal{T}}\right]^{\mathcal{T}}$. It is easy to show that shifting the frequency of the received signal in the time domain by $-\varepsilon_l$ is equivalent to multiply $\mathbf{z}'^b$ by $\left(e^{j\theta_{\varepsilon_l}^b}\mathbf{U}_{\varepsilon_l}\right)^{\mathcal{H}}$. Let $\mathbf{U}^b = \left(\sum_{l=1}^{M_t} e^{j\theta_{\varepsilon_l}^b}\mathbf{U}_{\varepsilon_l}\mathbf{P}'_l\right)$. Then, $\bar{\mathbf{z}}'^b$ can be expressed as

$$\begin{aligned}
\bar{\mathbf{z}}'^b &= \sqrt{\rho}\mathbf{U}^{b\mathcal{H}}\mathbf{D}'^b\mathbf{x}'^b + \mathbf{U}^{b\mathcal{H}}\mathbf{w}^b \\
&= \sqrt{\rho}\mathbf{U}^{b\mathcal{H}}\left(\sum_{m=1}^{M_t} e^{j\theta_{\varepsilon_m}^b}\mathbf{U}_{\varepsilon_m}\mathbf{P}'_m\right)\left(\sum_{l=1}^{M_t}\mathbf{P}'_l\mathbf{H}_l\right)\mathbf{x}'^b + \bar{\mathbf{w}}'^b \\
&= \sqrt{\rho}\mathbf{U}^{b\mathcal{H}}\mathbf{U}^b\mathbf{D}'\mathbf{x}'^b + \bar{\mathbf{w}}'^b, \qquad (4.36)
\end{aligned}$$

where $\mathbf{D}' = \left(\sum_{l=1}^{M_t}\mathbf{P}'_l\mathbf{H}_l\right)$, $\bar{\mathbf{w}}'^b = \mathbf{U}^{b\mathcal{H}}\mathbf{w}^b$, and the second equality follows from the fact that $\mathbf{P}'_m$ has the same property as that of $\mathbf{P}_m$ described in (4.13).

Because $\mathbf{D}'$ is a diagonal matrix, we can see that $\bar{\mathbf{z}}'^b$ is actually the matched filter output of $\mathbf{z}'^b$. Furthermore, $\mathbf{U}^b$ can also be rewritten as

$$\mathbf{U}^b = \left(\sum_{m=1}^{M_t}\mathbf{U}_{\varepsilon_m}\mathbf{P}'_m\right)\left(\sum_{l=1}^{M_t} e^{j\theta_{\varepsilon_l}^b}\mathbf{P}'_l\right) = \mathbf{U}\mathbf{P}'^b, \qquad (4.37)$$

where $\mathbf{U} = \sum_{m=1}^{M_t}\mathbf{U}_{\varepsilon_m}\mathbf{P}'_m$, and $\mathbf{P}'^b = \sum_{l=1}^{M_t} e^{j\theta_{\varepsilon_l}^b}\mathbf{P}'_l$ and it can be verified that $\mathbf{P}'^b$ is a unitary matrix. Substituting (4.37) into (4.36), we get the SISO-OFDM model as

$$\begin{aligned}
\bar{\mathbf{z}}'^b &= \sqrt{\rho}\left(\mathbf{P}'^{b\mathcal{H}}\mathbf{U}^{\mathcal{H}}\mathbf{U}\mathbf{D}'\mathbf{P}'^b\right)\mathbf{x}'^b + \bar{\mathbf{w}}'^b \\
&= \sqrt{\rho}\bar{\mathbf{H}}^b\mathbf{x}'^b + \bar{\mathbf{w}}'^b, \qquad (4.38)
\end{aligned}$$

where $\bar{\mathbf{H}}^b = \left(\mathbf{P}'^{b\mathcal{H}}\mathbf{U}^{\mathcal{H}}\mathbf{U}\mathbf{D}'\mathbf{P}'^b\right)$. As we have discussed that the SINR of a subcarrier can be increased by the M-FFT, we can ignore the ICI terms (non-diagonal elements) of $\bar{\mathbf{H}}^b$ and directly decode $\mathbf{x}'^b$ by ML or sphere decoding method.

Furthermore, for the M-FFT method, we have the following options

- The MMSE filter matrix of $\bar{\mathbf{H}}^b$, denoted by $\bar{\mathbf{V}}^b$, can be computed from

$$\bar{\mathbf{V}}^b = \mathbf{P}'^{b\mathcal{H}} \left(\mathbf{D}'^{\mathcal{H}} \mathbf{U}^{\mathcal{H}} \mathbf{U} \mathbf{U}^{\mathcal{H}} \mathbf{U} \mathbf{D}' + \frac{1}{\rho} \mathbf{I}_N \right)^{-1} \mathbf{D}'^{\mathcal{H}} \mathbf{U}^{\mathcal{H}} \mathbf{U} \mathbf{P}'^{b}, \tag{4.39}$$

  where the matrix inverse is independent of b. Note that we still assume $\bar{\mathbf{w}}^b$ to be white. Therefore, if M-FFT is used as the preprocessing of the Q-T to improve the performance, the filter coefficients of the Q-T can still be updated easily. Since after M-FFT, the ICI power comes from the same group is canceled, for the concerned subcarrier, we need only to consider its nearest $Q-1$ subcarriers which are in its circular left or right neighboring group. We denote this combined scheme as M-FFT-Q-T.

- Since after each FFT operation, only N/M_t outputs are used, the computational complexity of FFT may be further reduced compared with the full length FFT using the algorithm as proposed in [128, 129]. However, considering the fact that the computational saving is obvious only when M_t is large, so in the next section we continue to apply the full length FFT to evaluate the computational complexity of the M-FFT method.

- If we combine M-FFT with *successive interference cancellation* (SIC), the decoding order of $\mathbf{G}_p$, $1 \le p \le P$, should depend on the subcarriers where $\mathbf{G}_p$ are located. For example, considering the structure of $\mathbf{C}'$, $\mathbf{G}_{\lfloor P/2 \rfloor}$ or $\mathbf{G}_{\lceil P/2 \rceil}$ should first be decoded. Although this is not the optimal decoding order, no additional operations are needed to decide the decoding order.

- Since the boundary subcarriers of each group have the worst quality/SINR, we may not use them to improve the SER performance at the cost of even small efficiency loss. On the other hand, if zero padding exists, we can use them to separate groups. We denote this method as M-FFT-Zn, where n is the number of unused subcarriers.

- In [39], the authors also devised an interleaving method to maximize the coding advantage when the power-delay profile is known at transmitter. If the *separation factor* μ [39] is a factor of P, by row permutations the subcarriers used by the same antenna can still be grouped together and at the same time

adjacent subcarriers in each $\mathbf{x}_m^p$ is separated by μ subcarriers. If $\mu > P$, to satisfy this separation factor μ, we cannot permutate the subcarriers used by the same antenna to one group. However, we can still group the subcarriers used by one antenna into multiple groups each of which contains the same number of subcarriers.

4.5 Computational Complexity Comparison

We now compare the computational complexity of each detection method. Here multiplications, divisions, and additions all refer to complex operations. We also assume that multiplication and division have the same complexity and the channel keeps constant during the time period of K OFDM symbols. In counting the number of operations, some results in [130] are used. For the inverse square root operation, we assume the algorithm introduced in [131] is applied.

Complexity of MMSE-F Method

The computational complexity of the MMSE-F method can be evaluated as follows.

1. When $b = 0$

   - As mentioned in [130], inverting matrix $\left(\mathbf{DP}^{\mathbf{b}}\right)^{\mathcal{H}}\left(\mathbf{DP}^{b}\right) + \frac{1}{\rho}\mathbf{I}_N$ via singular value decomposition (SVD) requires $13N^3 + N^2$ multiplications and $13N^3 - N^2$ additions.
   - Multiplying $\left(\left(\mathbf{DP}^{\mathbf{b}}\right)^{\mathcal{H}}\left(\mathbf{DP}^{b}\right) + \frac{1}{\rho}\mathbf{I}_N\right)^{-1}$ by $\left(\mathbf{DP}^{\mathbf{b}}\right)^{\mathcal{H}}$ needs N^3 multiplications and $N^3 - N^2$ additions.
   - Normalizing each row of Υ requires the calculation of the square of the Frobenious norm which requires N multiplications and $N - 1$ additions for each row. The algorithm to compute the inverse square root is generally based on Newton's root finding method. A fast inverse square root algorithm can be found in [131]. With only one Newton iteration, it can provide the solution with acceptable precision. It roughly requires 4 mul-

tiplications and 2 additions. So a total of $N(2N + 4)$ multiplications and $N(N + 1)$ additions are required.

- Calculating the filtered channel frequency response $\mathbf{H}$ requires N^2 multiplications and $N^2 - N$ additions.
- Filtering the received signal vector $\mathbf{Z}^0$ by $\mathbf{P}^{0^{\mathcal{H}}}\hat{\Upsilon}$ requires $N^2 + N$ multiplications and $N^2 - N$ additions.

In total, we need at least $14N^3 + 5N^2 + 5N$ multiplications and $14N^3 + N^2 - N$ additions when $b = 0$

2. When $0 < b < K$

   - Calculating $\mathbf{P}^b = \mathbf{P}^{b-1}\mathbf{P}$ and filtering the received signal vector $\mathbf{Z}^b$ by $\mathbf{P}^{b^{\mathcal{H}}}\hat{\Upsilon}$ requires a total of $N^2 + 2N$ multiplications and $N^2 - N$ additions by considering $\mathbf{P}$ as a diagonal matrix.

Complexity of Q-T Based Method

Following the similar analysis steps as the MMSE-F method, the complexity of the Q-T method can be summarized as

1. When $b = 0$, we roughly need $N(13Q^3 + 2Q^2 + 4Q + 5)$ multiplications and $N(13Q^3 + 2Q - 1)$ additions.
2. When $0 < b < K$, we need $N(Q + 2)$ multiplications and $N(Q - 1)$ additions.
3. For FS-Q-T method, additional N multiplications are required for each OFDM symbol.

Complexity of M-FFT Method

For each OFDM symbol, we need M_t FS operations and $M_t - 1$ additional FFT operation. Each FFT needs $\frac{N}{2}\log_2 N$ multiplications and $N\log_2 N$ additions. Here the Cooley-Tukey radix-2 FFT algorithm is considered [132]. So in total, we need $M_tN+(M_t-1)\frac{N}{2}\log_2 N$ multiplications and $(M_t-1)N\log_2 N$ additions for each OFDM symbol.

Method	Number of multiplications when $b = 0$	Number of multiplications when $0 < b < K$
MMSE-F	$14N^3 + 5N^2 + 5N$	$N^2 + 2N$
Q-T	$N(13Q^3 + 2Q^2 + 4Q + 5)$	$N(Q + 2)$
M-FFT	$M_t N + (M_t - 1)\frac{N}{2}\log_2 N$	$M_t N + (M_t - 1)\frac{N}{2}\log_2 N$

Table 4.1: Number of multiplications of each method.

Method	Number of additions when $b = 0$	Number of additions when $0 < b < K$
MMSE-F	$14N^3 + N^2 - N$	$N^2 - N$
Q-T	$N(13Q^3 + 2Q - 1)$	$N(Q - 1)$
M-FFT	$(M_t - 1)N\log_2 N$	$(M_t - 1)N\log_2 N$

Table 4.2: Number of additions of each method.

The number of multiplications and additions of each method is summarized in Table 4.1 and Table 4.2, respectively. Compared with the Q-T method, for the FS-Q-T method, additional N multiplications are required for each OFDM symbol. From these two tables, we can see that when Q is much smaller than N, the Q-T method has a lower computational complexity than the MMSE-F method. For MMSE-F and Q-T methods, the calculations of initial filter coefficients ($b = 0$) account for most of the computation. However, since the filter coefficients are easy to update for each channel realization, the computation of each OFDM symbol can be averaged as channel coherence time increases. For the M-FFT method, the computational load of each OFDM symbol is always of the order $O(N\log_2 N)$ no matter what the value of K is. Thus if channel coherence time is not very long, the M-FFT method has the least computational complexity.

4.6 Simulation Results

In this section, we present numerical examples to demonstrate the effectiveness and performance of our proposed detection methods for the SF coded cooperative system having multiple CFOs.

First, we consider a system with two relay nodes. The simulated OFDM system has 64 subcarriers, i.e., $N = 64$. The bandwidth is 20 MHz and the cyclic prefix of the OFDM is fixed to $N/4 = 16$. The channels from relay nodes to the destination node are all frequency-selective with two equal power rays $[\tau_m(0), \tau_m(1)] = [0, 0.5]\mu s$ for $1 \leq m \leq 2$. The data symbols are quadrature phase shift keying (QPSK) modulated. We also assume that the destination node only has one receive antenna. For each channel realization, each ε_m is uniformly selected from $[-\varepsilon_{Max}, \varepsilon_{Max}]$. The SF code proposed in [39] is applied. The separation factor μ is equal to 1. To achieve both full cooperative diversity and multipath diversity, the parameter Γ is set to be 2.

Fig.4.2 shows the performance of the MMSE-F method. From the simulation results we can see that as SNR increases, the OFDM system will quickly suffer from an error floor if we directly decode (referred to as DD) the SF code without increasing SINR. In comparison, the MMSE-F method works well. In the simulated SNR range, the performance loss is small when $\varepsilon_{Max} = 0.1$ and 0.2. To make a comparison, we also plot the curve of the CE method when $\varepsilon_{Max} = 0.1$. Its performance is worse than directly decoding since the SF code is not designed for the MMSE criterion. In this figure we also plot the SER curve of a subcarrier-wise delay diversity coded scheme whose parameters are the same as those used in [75]. We can see that even the SF code with $\varepsilon_{Max} = 0.1$ outperforms the delay diversity coded scheme without CFO because the delay diversity coded scheme has at most diversity order 2 while the SF coded scheme has diversity order 4. A subcarrier-wise Alamouti coded OFDM system without CFOs, considered in [74], is also simulated. We can see that its performance is even worse than the SF code with CFOs when the MMSE-F method is applied since the subcarrier-wise Alamouti coded OFDM system can only achieve diversity order 2. We also simulate the method proposed in [74] when $\varepsilon_{Max} = 0.15$. Although the length of ZF filter Q has been set to its maximum value $2N$, the SNR loss is still larger than 3dB when SER = 10^{-3}.

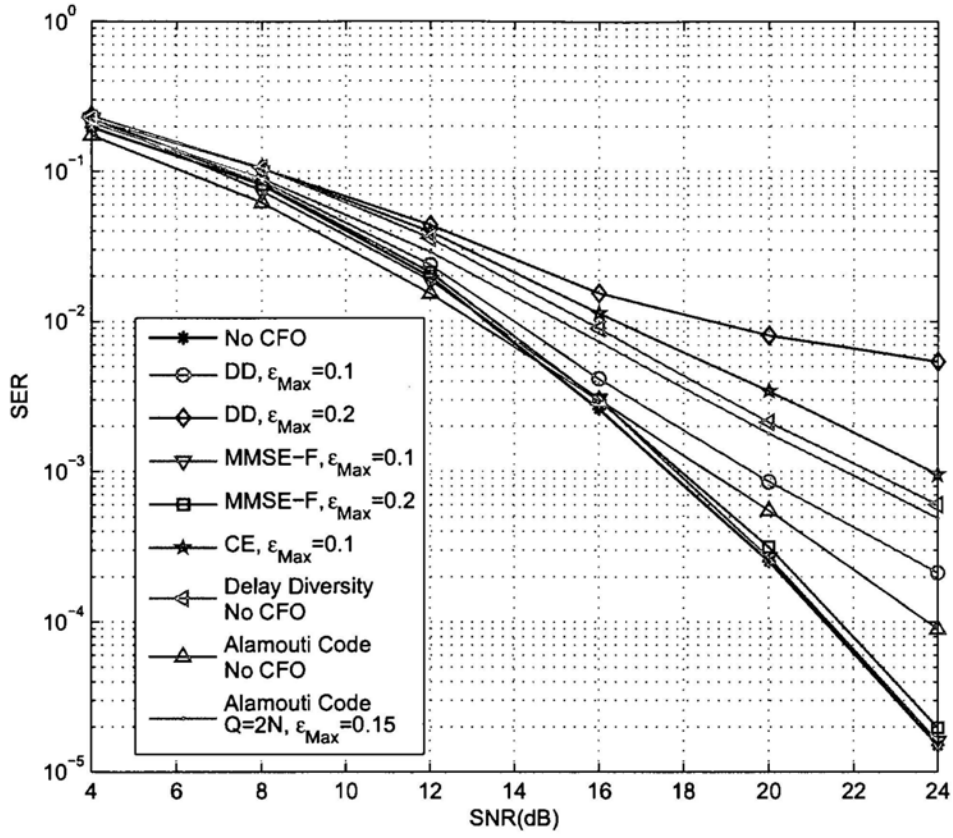

Figure 4.2: Performance of the MMSE-F method with multiple CFOs.

Fig.4.3 shows the performance of the Q-T method with different values of Q. We can observe that as the value of Q increases, the performance loss of the Q-T method decreases compared to that of the MMSE-F method. We also plot the SER curve of the FS method, where before directly decoding the SF code the optimal frequency shift is used to increase average SINR. Same as before, the FS method has a lower error floor than that of directly decoding. Although the FS method gives poor performance on its own, FS can be used as the preprocessing of the Q-T method as FS-Q-T. In Fig.4.3, we can see that the performance of the FS-Q-T method with $Q = 3$ and $Q = 5$ is comparable with that of the Q-T method with $Q = 5$ and $Q = 7$, respectively.

Fig.4.4 compares the output SINR of the directly decoding, FS and M-FFT meth-

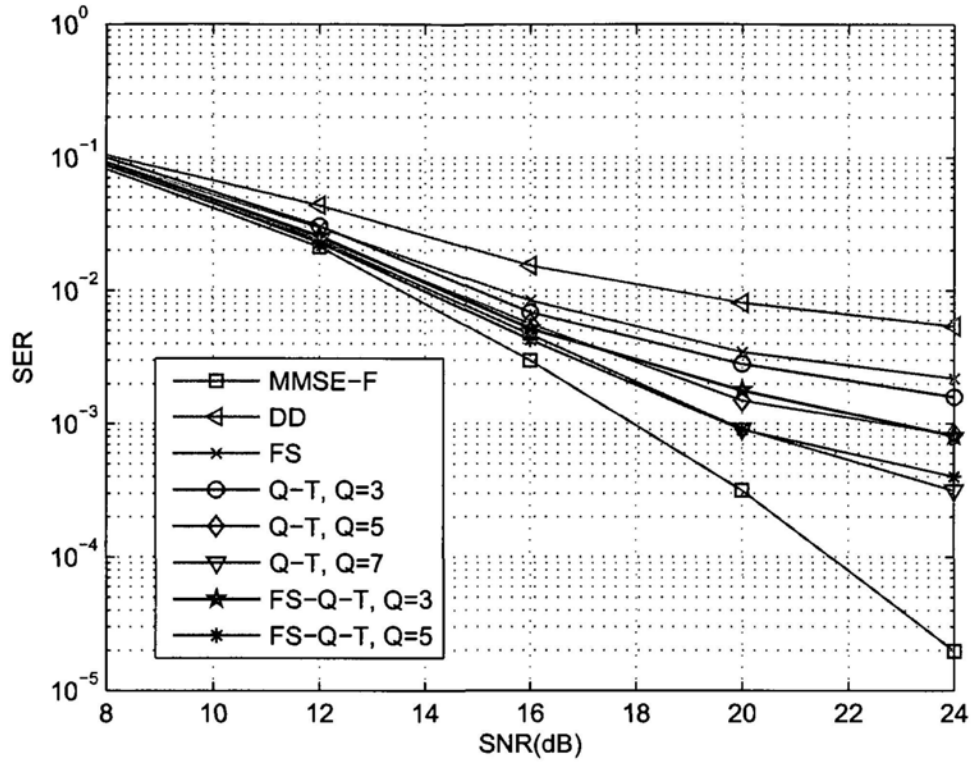

Figure 4.3: Performance of the Q-T method when $\varepsilon_{Max} = 0.2$.

ods. For the directly decoding and FS method, we only draw their average SINR over all subcarriers since each subcarrier has the same value of the average SINR. For the M-FFT method , the subcarriers in the same group have different quality/SINR. The SINR of the 0th, 1st, and 15th subcarriers in the 1st group are also depicted as examples. From the simulation results we can see that the average SINR of the FS method is higher than that of directly decoding. This is consistent with our previous analysis. We can also see that for the M-FFT method, the SINR of the 15th subcarrier which is located in the middle of the 1st group is much higher than that of the 0th and 1st subcarriers. Even the SINR of the 0th subcarrier is still a little higher than that of the directly decoding. As the index shifts from 0 to 1, SINR drastically increases and is higher than that of the FS method.

Fig.4.5 shows the performance of the M-FFT method when $\varepsilon_{Max} = 0.2$. To demonstrate that the grouping operation of subcarriers plays an important role in

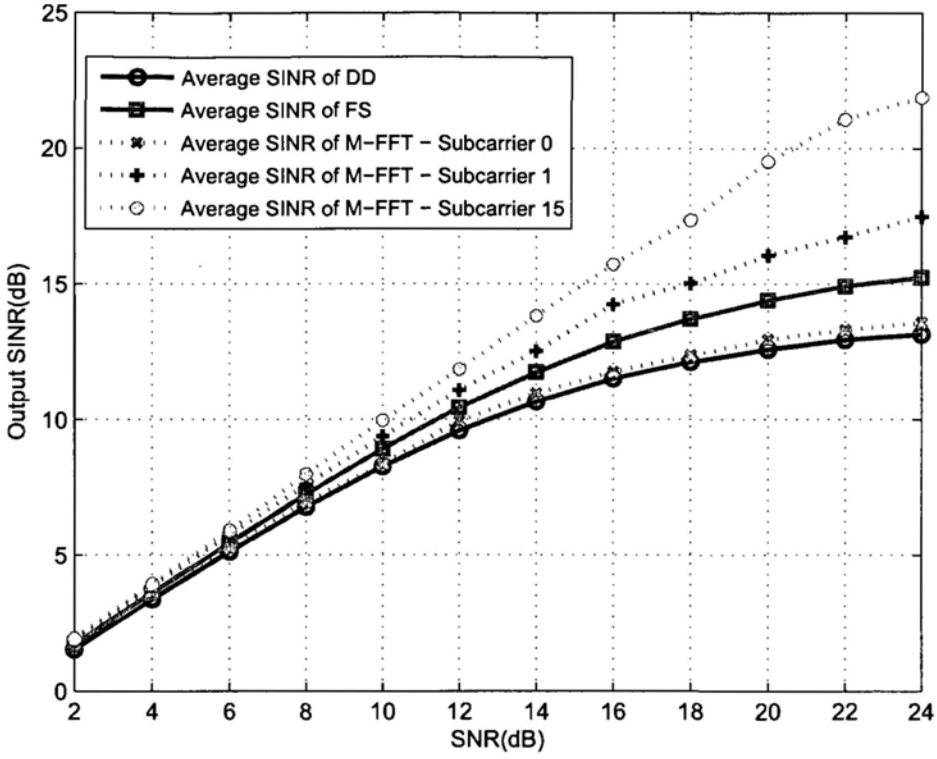

Figure 4.4: Output SINR of different methods when $\varepsilon_{Max} = 0.2$.

the M-FFT method, we also simulate a scheme that we directly apply multiple FS and FFT operations without the grouping operation and it is denoted by M-FFT-WG in the figure. From the simulation results we can see that the performance of the M-FFT-WG method is worse than that of the directly decoding. This is because without the grouping step, in the FS operation, the increased ICI power from other antennas can even exceed the canceled ICI power. Comparing Fig.4.5 with Fig.4.3, the M-FFT method outperforms the Q-T method with $Q = 5$.

Fig.4.6 shows some extensions of the M-FFT method. For M-FFT-Z4, the 0th to 29th subcarriers are used by the first transmit antenna, the 32nd to 61st subcarriers are used by the second transmit antenna and all the other subcarriers are not used. From the simulation results we can see that the performance of the M-FFT method is greatly increased and outperforms that of the Q-T method with $Q = 13$ or the FS-Q-T method with $Q = 9$. The cost is that the frequency efficiency is decreased by

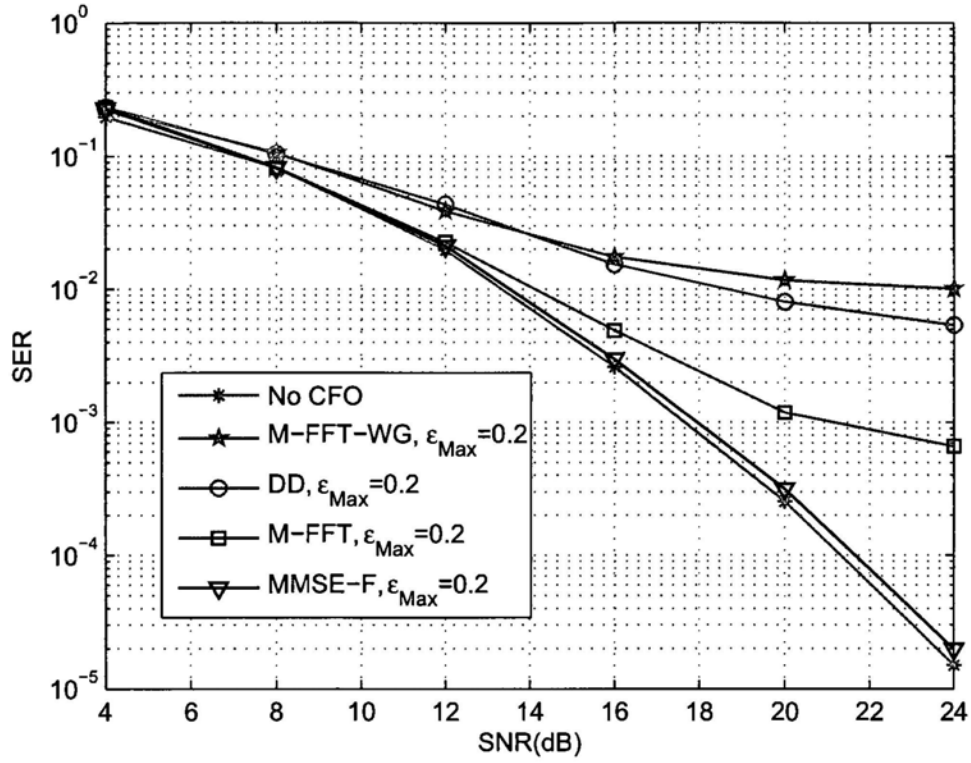

Figure 4.5: SER performance of the M-FFT method.

6.25%. The effect of zero padding can be explained as follows. Since no signals are transmitted at these four subcarriers, no power leaks from them. More importantly, for each group, a large part of the ICI power from the other groups falls on these 4 unused subcarriers. Note that for the Q-T method, zero padding can also increase SER performance. But the improvement is small, because only the subcarriers near these zero pads can significantly benefit from them. For the M-FFT-Q-T method, when $Q = 4$, its performance outperforms that of the M-FFT-Z4 method. Finally, we combine the M-FFT-Z4 method with SIC. For our simulated system, the decoding order is $\mathbf{G}_8, \mathbf{G}_9, \mathbf{G}_7, \mathbf{G}_{10}, \cdots, \mathbf{G}_{15}, \mathbf{G}_1$ according to the average SINR of subcarriers. To contrast their results, we also plot the curves of other two comparable schemes. They are the M-FFT-Q-T method with $Q = 7$ and the FS-QT method with $Q = 15$. For a fair comparison, 4 zero paddings are used at the same subcarriers as that of the M-FFT-Z4 method. Therefore, they are denoted by M-FFT-Q-T-Z4 and FS-Q-T-

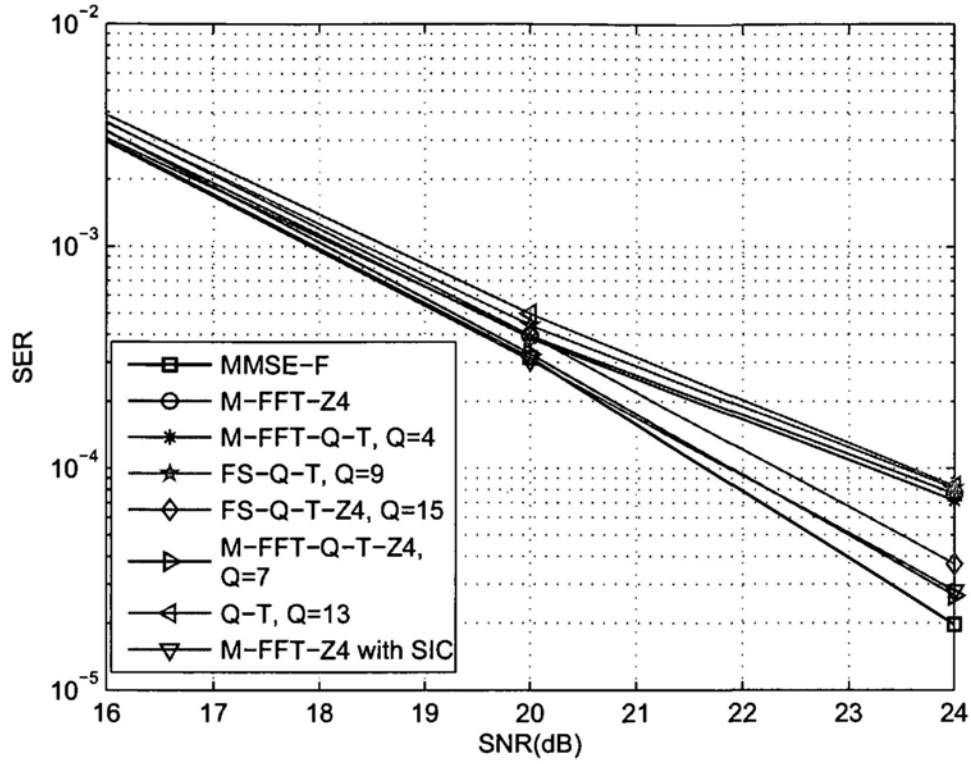

Figure 4.6: Extensions of the M-FFT method when $\varepsilon_{Max} = 0.2$.

Z4, respectively. We can see that among the four methods, i.e., FS-Q-T-Z4 method with $Q = 15$, M-FFT-Z4 method with SIC, M-FFT-Q-T-Z4 method with $Q = 7$, and the MMSE-F method, the FS-Q-T-Z4 method with $Q = 15$ achieves the worst SER performance and other three methods have a comparable performance. Note that for the FS-Q-T method, 15 is the maximum value of Q when $N = 64$ since if $Q > 15$, the FS-Q-T and Q-T methods would lose their computational efficiency compared with the MMSE-F method.

Fig.4.7 illustrates the computational complexity of the different detection schemes. These schemes are divided into two groups each of which can achieve similar SER performance as shown in Fig.4.6. Since one complex multiplication takes 6 floating-point operations and 1 complex addition only needs 2 flops, we only count the average complex multiplications per OFDM symbol. In this figure, symbol K stands for the number of OFDM symbols in one channel realization. It can

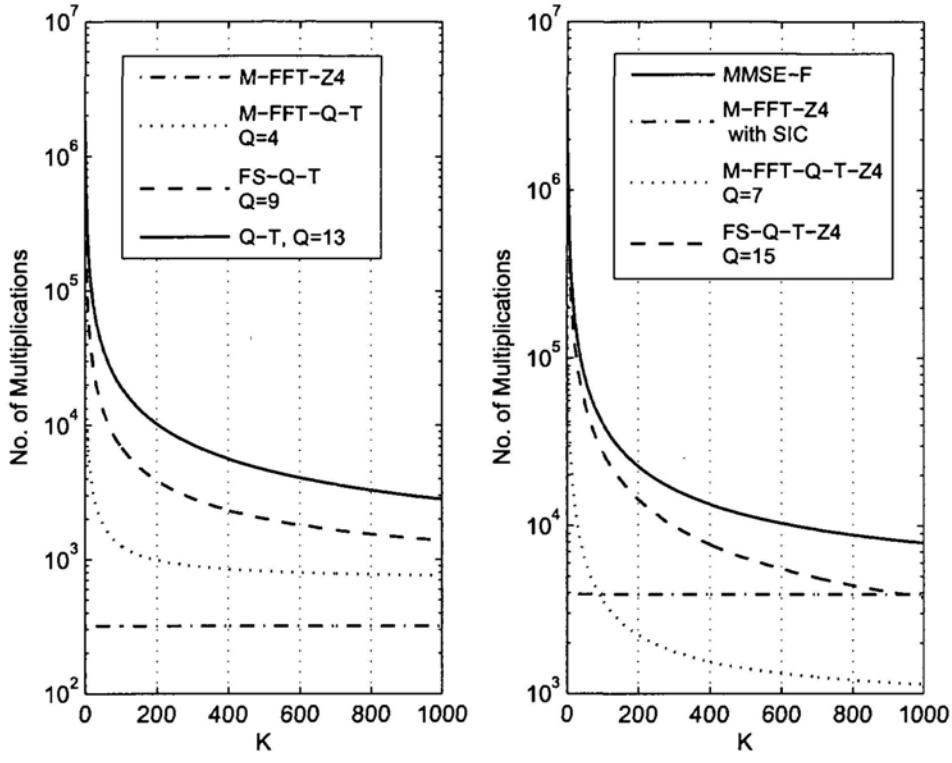

Figure 4.7: Comparison of computational complexities of different detection schemes for various data frame lengths K.

be clearly seen that in each group the M-FFT based methods require less multiplications. In the left sub-figure, the M-FFT-Z4 method always has the least number of multiplications. The M-FFT-Q-T method with $Q = 4$ is still more efficient than the FS-Q-T method with $Q = 9$ and the Q-T method with $Q = 13$ especially when K is not very large. In the right sub-figure, when $K \leq 90$, the M-FFT-Z4 method with SIC has the least number of multiplication since it does not need calculate filter coefficient. When $K > 90$ the M-FFT-Q-T-Z4 method with $Q = 7$ becomes the most efficient scheme as the cost of computing filter coefficients is averaged over K.

To further investigate the SER performance of different schemes, we also consider a system having 4 relay nodes $M_t = 4$. The bandwidth of OFDM system is 20 MHz and $N = 128$. The channels from relay nodes to the destination node are all frequency-selective fading with two equal power rays and $[\tau_m(0), \tau_m(1)] =$

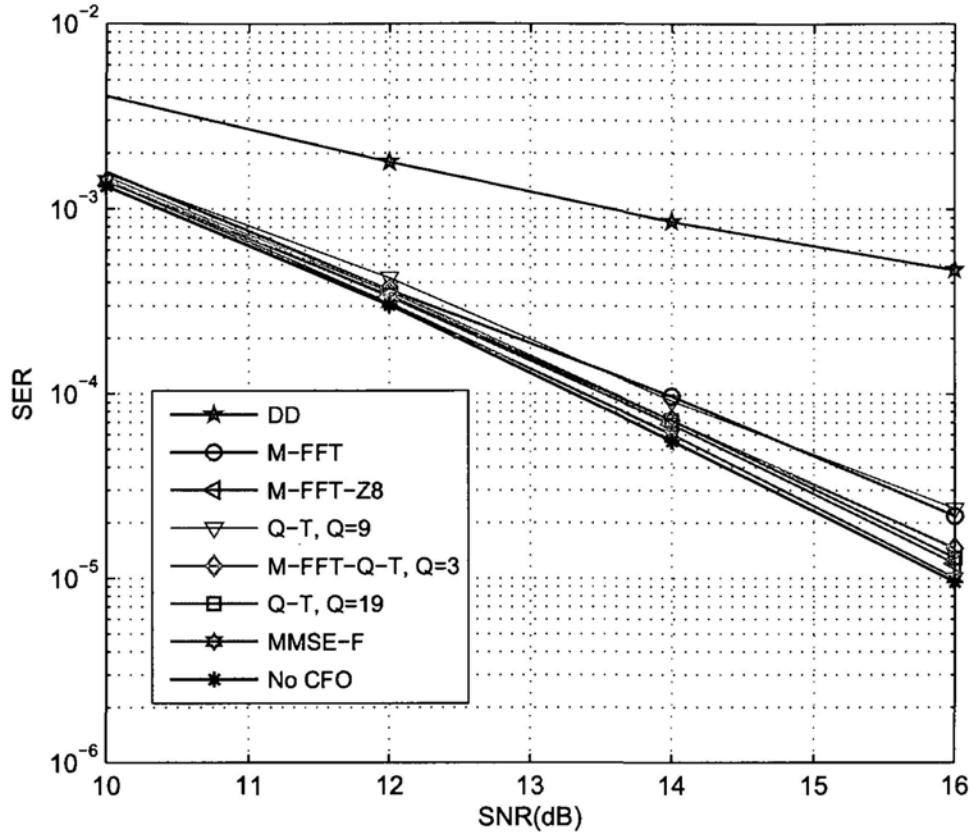

Figure 4.8: Performance of different methods when M_t=4 and $\varepsilon_{Max} = 0.2$.

$[0, 0.45]\mu s$ for $1 \leq m \leq M_t$. The data symbol is binary phase shift keying (BPSK) modulated. μ is set as 1. To achieve full diversity order 8 we set Γ as 2. From Fig.4.8, we can see similar simulation results as that of the case of the two relay nodes. Directly decoding will quickly suffer from an error floor. The MMSE-F method has the best SER performance. The M-FFT method is comparable with the Q-T method with $Q = 9$. The M-FFT-Z8 method, M-FFT-Q-T method with $Q = 3$ and Q-T method with $Q = 19$ can achieve similar performance. By analyzing their computational complexity, we still find that the M-FFT based methods require the least operations.

4.7 Conclusions

In this chapter, we propose several signal detection methods for the multiple CFO problems in an SF coded cooperative communication system. To preserve the performance of an SF code, we suggest increasing the SINR of each subcarrier but not equalizing the SF precoding matrix. Due to the structure of the SF code, where both spatial and multipath diversities can be achieved, increasing each subcarrier's SINR of an MISO-OFDM system is equivalent to that of an SISO-OFDM system. Thus, a classical MMSE filter can be used to maximize the SINR of each subcarrier. Furthermore, we find that due to the structure of the SF codes, the MMSE filter coefficients are easy to update for each realization of channel, where the matrix inverse is independent of the OFDM symbol index. The Q-T method is a popular approximating method for computing the MMSE filter coefficient in OFDM system which can be directly applied to solve the problem. To improve performance, we consider a simple two-stage FS-Q-T method where a frequency shift operation is done before the Q-T method. By exploiting the structure of the SF codes again, we propose an M-FFT method. For this method, at the transmitter we only need to re-arrange the SF codes in a simple way but without performance loss. Then, at the destination node, the SINR can be effectively increased by multiple FS and FFT operations. Based on its properties, the M-FFT method can be easily combined with other methods to improve its performance further, e.g., M-FFT-Q-T, M-FFT-Zn and M-FFT with SIC methods. Simulation results have been presented to illustrate the effectiveness of the methods and show that, for the same SER level, the M-FFT based methods require the least operations.

□ End of chapter.

Chapter 5

On the Full Diversity Property of An SF Code Family with Multiple CFOs

Summary

In this chapter, we first show that the full diversity property of the family of space-frequency (SF) codes (considered in the last chapter) can still hold when there are multiple carrier frequency offsets (CFOs) from relay nodes under the condition that the absolute values of normalized CFOs are less than 0.5. We then prove that this full diversity property is still preserved if we seek to reduce the receiver complexity by using a zero forcing (ZF) method to equalize the multiple CFOs, before applying maximum likelihood (ML) decoding. In addition, to further improve the robustness of this family of SF codes to multiple CFOs, we propose a novel permutation (interleaving) method, which enables the SF codes to achieve full diversity, even when the absolute values of normalized CFOs are larger than or equal to 0.5. In the case that the inter-carrier interference (ICI) matrix is singular, to avoid jointly considering all the subcarriers, two suboptimal full diversity achievable detection methods are proposed. All these imply that the SF coded OFDM system is robust to both timing errors and CFOs.

In chapter 4, we consider the signal detection problem in a space-frequency (SF) coded cooperative communication system in the presence of multiple carrier frequency offsets(CFOs), which applies the family of rotation based SF codes [36, 37, 39, 113]. By modeling inter-carrier interference (ICI) as additional Gaussian noise [122], we propose to deal with ICI mitigation due to multiple CFOs by firstly increasing the signal-to-interference-plus-noise ratio (SINR) using linear filtering or other methods, and then decoding the SF code by the commonly used maximum-likelihood (ML) method. Simulation results indicate that the proposed detection methods perform well as long as CFOs are small. Especially, for the MMSE-F detection method, only very small performance loss is observed. However, from the code design viewpoint, it is not known whether the proposed detection methods can guarantee the achievement of full diversity, i.e., both full cooperative and full multipath diversities.

In this chapter, we shall describe our insight into the full diversity property of this SF code family with multiple CFOs. The key idea for the analysis is to treat the CFO originated ICI terms as a part of an SF code matrix. It turns out that as long as the original SF code achieves the full diversity (both spatial and multipath diversities) and the absolute values of normalized CFOs are less than 0.5, the new (virtual) code after absorbing the CFOs/ICI into the original SF code maintains the full diversity property. The above full diversity property is based on the ML decoding across all the subcarriers of the OFDM system, which may have a high complexity. To overcome this difficulty, we further study an SF coded OFDM system where the ICI, caused by the multiple CFOs, is firstly equalized by a zero forcing (ZF) method, followed by ML decoding for the SF codes (we call this method the ZF-ML method). The complexity of this ZF-ML detection method is much reduced compared to the complete ML method described above, and we prove that the ZF-ML detection method still achieves the same diversity order as that of the case without CFOs. We also show that by some reasonable approximations, the MMSE-F method proposed in chapter 4 is just equivalent to the ZF-ML detection method. This is the primary reason behind the effectiveness of the proposed detection methods in chapter 5.

More importantly, to further improve the robustness of this family of SF codes to multiple CFOs, we propose a novel permutation (interleaving) method, by which the permuted SF codes can still achieve full diversity, even when the absolute values of normalized CFOs are equal to or larger than 0.5. This full diversity property is still based on joint consideration of all the subcarriers of the OFDM system. However, when the ICI matrix is singular, the ZF-ML detection method cannot be directly used to reduce decoding complexity. To tackle this problem, we propose two suboptimal full diversity achievable detection methods with different tradeoff between efficiency and complexity by utilizing the properties of the ICI matrix. They are the ZF-ML-Zn detection method and the ZF-ML-PIC detection method.

The remaining of this chapter is organized as follows. In Section 5.1, the system model is described. In Section 5.2, the structure of the SF codes in [39] is reviewed. In Section 5.3, the effect of multiple CFOs on the SF codes is analyzed. In Section 5.4, we propose a permutation method to enhance the full diversity property of the SF codes. In Section 5.5, some simulations are presented to verify the theoretical results.

5.1 System Model

5.1.1 Cooperative Protocol

The same cooperative protocol used in Section 4.2.1 is applied in this chapter. It includes one source node, one destination node, and a number of relay nodes in the middle. In phase one, the source node S broadcasts the information while the relay nodes receive the same information. In phase two, the M_t relay nodes, which have detected the received information symbols correctly, will help the source to transmit. The detected symbols are parsed into blocks of size N which is also the number of subcarriers in one OFDM symbol. Then, the bth block, $b = 0, 1, \cdots$, is encoded to an SF code matrix $\mathbf{C}$ in a distributed fashion [66]. Finally, the mth ($1 \leq m \leq M_t$) relay transmits the $(m-1)$th column of the code matrix, denoted as $\mathbf{c}_m$, by the standard OFDM technology. Hence, this is a *decode-and-forward* protocol. We assume that each node has only one transmit/receive antenna.

5.1.2 Channel Model

The channel impulse response from the mth relay node to the destination node is denoted as $h_m(\tau) = \sum_{l=0}^{L_m-1} \alpha_m(l)\delta(\tau - \tau_m(l))$, where L_m is the number of multipaths of the link from the mth relay to the destination node. The complex amplitude and delay for the lth multipath of the mth relay are $\alpha_m(l)$ and $\tau_m(l)$, respectively. Here $\alpha_m(l)$ is a zero mean complex Gaussian variable with power $\mathrm{E}[|\alpha_m(l)|^2] = \sigma_m^2(l)$. The powers of each link is normalized so that $\sum_{l=0}^{L_m-1} \sigma_m^2(l) = 1$ for $m = 1, 2, \cdots, M_t$. We further assume that the delays for the relays are rounded to the sampling position, i.e., $\tau_m(l)$ is an integer multiple of $1/F_s$, where F_s is the sampling frequency. The channel taps $\alpha_m(l)$ are assumed to be independent from each other for different m and l. The frequency response of the link between the mth relay node and the destination node, $\mathrm{H}_m = [H_m(0), H_m(1), \cdots, H_m(N-1)]^{\mathcal{T}}$, can be given by

$$\mathrm{H}_m = \hat{\mathbf{F}}_m \mathbf{h}_m, \tag{5.1}$$

where $\mathbf{h}_m = [\alpha_m(0), \cdots, \alpha_m(L_m - 1)]^{\mathcal{T}}$ and $\hat{\mathbf{F}}_m = [\mathbf{f}^{\tau_m(0)}, \cdots, \mathbf{f}^{\tau_m(L_m-1)}]$. The column vector $\mathbf{f} = [1, \zeta, \cdots, \zeta^{N-1}]^{\mathcal{T}}$, where $\zeta = \exp(-j\frac{2\pi}{T})$ and T is the duration of an OFDM symbol. Then, we have $\mathbf{f}^{\tau_m(l)} = [1, \zeta^{\tau_m(l)}, \cdots, \zeta^{(N-1)\tau_m(l)}]^{\mathcal{T}}$.

5.2 Structure of Space-Frequency Codes

In this section we briefly review the structure and properties of SF codes family [36, 37, 39, 113] which are utilized in the following sections. We adopt the code structure proposed in [39].

Each SF code $\mathbf{C}$ is an $N \times M_t$ matrix and is mapped from an $N' \times 1$ information symbol vector $\mathbf{s}$, where M_t is the number of transmit antennas and $N' \leq N$. For the coding strategy proposed in [39], each SF code matrix $\mathbf{C}$ is a concatenation of some matrices $\mathbf{G}_p$

$$\mathbf{C} = \left[\mathbf{G}_1^{\mathcal{T}} \quad \mathbf{G}_2^{\mathcal{T}} \quad \cdots \quad \mathbf{G}_P^{\mathcal{T}} \quad \mathbf{0}_{(N-N')\times M_t}^{\mathcal{T}}\right]^{\mathcal{T}}, \tag{5.2}$$

where $P = \lfloor N/(\Gamma M_t) \rfloor$, $N' = P\Gamma M_t$, each matrix $\mathbf{G}_p$ $(1 \leq p \leq P)$ is of size ΓM_t by M_t, and Γ is a coding parameter related to the achievable diversity order for the code. The zero padding matrix $\mathbf{0}_{(N-N')\times M_t}$ is used if the number of subcarriers N is not an integer

multiple of ΓM_t. In the remainder of this chapter, without loss of generality, N is assumed as an integer multiple of ΓM_t, i.e., $N = P\Gamma M_t$. Each matrix $\mathbf{G}_p$ $(1 \le p \le P)$ has the same structure given by

$$\mathbf{G}_p = \sqrt{M_t}\begin{bmatrix} \mathbf{x}_1^p & \mathbf{0}_\Gamma & \cdots & \mathbf{0}_\Gamma \\ \mathbf{0}_\Gamma & \mathbf{x}_2^p & \cdots & \mathbf{0}_\Gamma \\ \vdots & \vdots & \ddots & \vdots \\ \mathbf{0}_\Gamma & \mathbf{0}_\Gamma & \cdots & \mathbf{x}_{M_t}^p \end{bmatrix}, \tag{5.3}$$

where $\mathbf{x}_m^P = [x_{(m-1)\Gamma+1}^p x_{(m-1)\Gamma+2}^p \cdots x_{m\Gamma}^p]^\mathcal{T}$ for $1 \le m \le M_t$, and all x_k^p $(1 \le k \le M_t\Gamma)$ are complex symbols which are mapped from an information subvector $\mathbf{s}^p = [s_1^p, s_2^p, \cdots, s_{\Gamma M_t}^p]^\mathcal{T}$ by a linear transform $[\mathbf{x}_1^{p\mathcal{T}}, \mathbf{x}_2^{p\mathcal{T}}, \cdots, \mathbf{x}_{M_t}^{p\ \mathcal{T}}]^\mathcal{T} = \mathbf{\Theta}\mathbf{s}^p$, where s_l^p is $((p-1)\Gamma M_t + l - 1)$th entry of $\mathbf{s}$ for $1 \le l \le \Gamma M_t$ and $\mathbf{\Theta}$ is the $N \times N$ linear transformation matrix. The energy constraint is $\mathrm{E}\left[\sum_{k=1}^{\Gamma M_t} |x_k|^2\right] = \Gamma M_t$. By appropriately designing of the linear transformation matrix $\mathbf{\Theta}$, the maximum diversity order achieved by these SF codes is $\sum_{m=1}^{M_t} \min(\Gamma, L_m)$ [39,113]. Therefore, if $\Gamma \ge L_m$ for $1 \le m \le M_t$, the achieved diversity order is $\sum_{m=1}^{M_t} L_m$, which is the maximum diversity order provided by multipath channel.

One property of the above SF codes is that each subcarrier is only used by one transmit antenna. From (5.3), the $(m-1)$th column of $\mathbf{C}$, denoted as $\mathbf{c}_m$, can be written as

$$\mathbf{c}_m = \sqrt{M_t}\mathbf{P}_m(\mathbf{I}_P \otimes \mathbf{\Theta})\mathbf{s} = \sqrt{M_t}\mathbf{P}_m\mathbf{x}, \tag{5.4}$$

where $\mathbf{x} = (\mathbf{I}_P \otimes \mathbf{\Theta})\mathbf{s}$ and $\mathbf{P}_m$ is an $N \times N$ diagonal matrix corresponding to the mth column of $\mathbf{C}$ with the following form

$$\mathbf{P}_m(l, l') = \begin{cases} 1, & \text{if } l = l' = (t-1)\Gamma M_t + (m-1)\Gamma + i \\ 0, & \text{else} \end{cases}, \tag{5.5}$$

where $0 \le i \le \Gamma - 1$ and $1 \le t \le P$. Based on (5.5) we also have

$$\mathbf{P}_m\mathbf{P}_{m'} = \begin{cases} \mathbf{P}_m, & \text{if } m = m' \\ \mathbf{0}_{N\times N}, & \text{otherwise} \end{cases}. \tag{5.6}$$

From (5.4) and (5.6), we can further get

$$\mathbf{c}_m = \mathbf{P}_m\mathbf{c}_m. \tag{5.7}$$

5.3 Effect of Multiple CFOs on the SF Codes

We next analyze the effect of the multiple CFOs to the SF codes described above.

5.3.1 Receive Signal Model

Let b, $b = 0, 1, 2, \cdots$, denote the OFDM symbol index. Then at the destination node, after some standard steps, the bth received OFDM symbol $\mathbf{z}^b$ in the frequency domain is given by

$$\mathbf{z}^b = \sqrt{\frac{\rho}{M_t}} \sum_{m=1}^{M_t} e^{j\theta^b_{\varepsilon_m}} \mathbf{U}_{\varepsilon_m} \mathrm{diag}(\mathrm{H}_m)\mathbf{c}_m + \mathbf{w}, \tag{5.8}$$

where $\mathbf{w}$ is an $N \times 1$ noise vector with each entry being a zero mean unit variance complex Gaussian random variable and ρ stands for the signal-to-noise ratio (SNR) at the destination node. Let Δf_m be the CFO between the mth relay node and the destination node. Then $\varepsilon_m = \Delta f_m T$ is its normalized value by OFDM symbol duration T. In (5.8), $\theta^b_{\varepsilon_m} = 2\pi\varepsilon_m(bN + bL_{cp} + L_{cp})/N + \theta_{0,m}$ where L_{cp} is the length of cyclic prefix, $2\pi\varepsilon_m(bN + bL_{cp} + L_{cp})/N$ is the phase rotation of the bth OFDM symbol transmitted from the mth relay node induced by CFO Δf_m and $\theta_{0,m}$ is the phase rotation between the phase of the destination node local oscillator and the carrier phase of the mth relay at the start of the received signal. $\mathbf{U}_{\varepsilon_m}$ is the $N \times N$ ICI matrix induced by ε_m and is given by

$$\mathbf{U}_{\varepsilon_m} = \mathbf{F}_N \mathbf{\Omega}_{\varepsilon_m} \mathbf{F}_N^{\mathcal{H}}, \tag{5.9}$$

where $\mathbf{\Omega}_{\varepsilon_m} = \mathrm{diag}(1, e^{j2\pi\varepsilon_m/N}, \cdots, e^{j2\pi\varepsilon_m(N-1)/N})$. From the definition of $\mathbf{U}_{\varepsilon_m}$, $\mathbf{U}_{\varepsilon_m}$ is a unitary matrix claerly.

Substituting (5.7) into (5.8), we have

$$\begin{aligned} \mathbf{z}^b &= \sqrt{\frac{\rho}{M_t}} \sum_{m=1}^{M_t} e^{j\theta^b_{\varepsilon_m}} \mathbf{U}_{\varepsilon_m} \mathrm{diag}(\mathrm{H}_m)\mathbf{P}_m\mathbf{c}_m + \mathbf{w} \\ &= \sqrt{\frac{\rho}{M_t}} \sum_{m=1}^{M_t} e^{j\theta^b_{\varepsilon_m}} \mathbf{U}_{\varepsilon_m} \mathbf{P}_m \mathrm{diag}(\mathrm{H}_m)\mathbf{c}_m + \mathbf{w}, \end{aligned} \tag{5.10}$$

where the second equality follows from the equation that $\mathrm{diag}(\mathrm{H}_m)\mathbf{P}_m = \mathbf{P}_m\mathrm{diag}(\mathrm{H}_m)$ in that both of $\mathrm{diag}(\mathrm{H}_m)$ and $\mathbf{P}_m$ are diagonal matrices. Based on (5.6), $\mathbf{P}_m\mathrm{diag}(\mathrm{H}_m)\mathbf{c}_m$

can be expressed by

$$\mathbf{P}_m \text{diag}(\mathrm{H}_m)\mathbf{c}_m = \mathbf{P}_m \sum_{m'=1}^{M_t} \mathbf{P}_{m'} \text{diag}(\mathrm{H}_{m'})\mathbf{c}_{m'}. \tag{5.11}$$

Then, by substituting (5.11) into (5.10), we get

$$\begin{aligned}
\mathbf{z}^b &= \sqrt{\frac{\rho}{M_t}} \sum_{m=1}^{M_t} e^{j\theta^b_{\varepsilon_m}} \mathbf{U}_{\varepsilon_m} \left(\mathbf{P}_m \sum_{m'=1}^{M_t} \mathbf{P}_{m'} \text{diag}(\mathrm{H}_{m'})\mathbf{c}_{m'} \right) + \mathbf{w} \\
&= \sqrt{\frac{\rho}{M_t}} \left(\sum_{m=1}^{M_t} e^{j\theta^b_{\varepsilon_m}} \mathbf{U}_{\varepsilon_m} \mathbf{P}_m \right) \left(\sum_{m'=1}^{M_t} \text{diag}(\mathrm{H}_{m'}) \mathbf{P}_{m'} \mathbf{c}_{m'} \right) + \mathbf{w} \\
&= \sqrt{\frac{\rho}{M_t}} \mathbf{U}^b \sum_{m=1}^{M_t} \text{diag}(\mathrm{H}_m)\mathbf{c}_m + \mathbf{w},
\end{aligned} \tag{5.12}$$

where

$$\mathbf{U}^b = \sum_{m=1}^{M_t} e^{j\theta^b_{\varepsilon_m}} \mathbf{U}_{\varepsilon_m} \mathbf{P}_m. \tag{5.13}$$

From (5.12) and (5.13), we can see that due to the property of the SF codes, i.e., each subcarrier is only used by one transmit antenna, the effect of M_t ICI matrix $\mathbf{U}_{\varepsilon_m}$ $(1 \le m \le M_t)$ is incorporated into the matrix $\mathbf{U}^b$ whose $((p-1)M_t\Gamma + (m-1)\Gamma + l)$th column is the $((p-1)M_t\Gamma + (m-1)\Gamma + l)$th column of $\mathbf{U}_{\varepsilon_m}$ weighted by $e^{j\theta^b_{\varepsilon_m}}$ for $0 \le l \le \Gamma - 1$, $1 \le m \le M_t$ and $1 \le p \le P$.

Substituting (5.1) into (5.12), we further obtain

$$\begin{aligned}
\mathbf{z}^b &= \sqrt{\frac{\rho}{M_t}} \mathbf{U}^b \sum_{m=1}^{M_t} \text{diag}(\hat{\mathbf{F}}_m \mathbf{h}_m)\mathbf{c}_m + \mathbf{w} \\
&= \sqrt{\frac{\rho}{M_t}} \mathbf{U}^b \sum_{m=1}^{M_t} [\mathbf{c}_m \odot \mathbf{f}^{\tau_m(0)}, \cdots, \mathbf{c}_m \odot \mathbf{f}^{\tau_m(L_m-1)}]\mathbf{h}_m + \mathbf{w}.
\end{aligned} \tag{5.14}$$

Assuming that $L = \max_m(L_m)$, we define $N \times M_t$ matrix $\mathbf{J}_l$ as

$$\mathbf{J}_l \triangleq [\mathbf{f}^{\tau_1(l)}, \mathbf{f}^{\tau_2(l)}, \cdots, \mathbf{f}^{\tau_{M_t}(l)}] \tag{5.15}$$

for $0 \le l \le L-1$, and $M_tL \times 1$ vector $\mathbf{h}$ as

$$\mathbf{h} \triangleq [\alpha_1(0), \cdots, \alpha_{M_t}(0), \cdots, \alpha_1(L-1), \cdots, \alpha_{M_t}(L-1)]^{\mathcal{T}}, \tag{5.16}$$

where, $\alpha_m(l) = 0$ and $\tau_m(l) = 0$, if $l \ge L_m$ for $1 \le m \le M_t$. Further define $N \times M_tL$ matrix $\mathbf{X}$ as

$$\mathbf{X} = [\mathbf{J}_0 \odot \mathbf{C}, \mathbf{J}_1 \odot \mathbf{C}, \cdots, \mathbf{J}_{L-1} \odot \mathbf{C}]. \tag{5.17}$$

Then the received signal, $\mathbf{z}^b$ can be written as:

$$\begin{aligned}\mathbf{z}^b &= \sqrt{\frac{\rho}{M_t}}\mathbf{U}^b\mathbf{X}\mathbf{h} + \mathbf{w} \\ &= \sqrt{\frac{\rho}{M_t}}\bar{\mathbf{X}}^b\mathbf{h} + \mathbf{w}, \end{aligned} \tag{5.18}$$

where $\bar{\mathbf{X}}^b = \mathbf{U}^b\mathbf{X}$.

5.3.2 Diversity Analysis of SF Codes in the Presence of Multiple CFOs

It is not hard to see that (5.18) is a standard SF coded MIMO-OFDM receive signal model. According to the *Diversity (Rank) criterion* of SF codes design introduced in Section 2.3.1, clearly in the presence of multiple CFOs, the achieved diversity order of the SF codes is equal to the minimum rank of the matrix $\mathbf{U}^b(\mathbf{X}-\hat{\mathbf{X}})\mathbf{\Lambda}(\mathbf{X}-\hat{\mathbf{X}})^{\mathcal{H}}\mathbf{U}^{b\mathcal{H}}$ for any distinct SF code matrices $\mathbf{C}$ and $\hat{\mathbf{C}}$, where $\mathbf{\Lambda} = \mathrm{E}[\mathbf{h}\mathbf{h}^{\mathcal{H}}]$. On the other hand, we have the inequality

$$\mathrm{rank}\left(\mathbf{U}^b(\mathbf{X}-\hat{\mathbf{X}})\mathbf{\Lambda}(\mathbf{X}-\hat{\mathbf{X}})^{\mathcal{H}}\mathbf{U}^{b\mathcal{H}}\right) \leq \mathrm{rank}\left((\mathbf{X}-\hat{\mathbf{X}})\mathbf{\Lambda}(\mathbf{X}-\hat{\mathbf{X}})^{\mathcal{H}}\right). \tag{5.19}$$

Considering (5.19), we can conclude that in the presence of multiple CFOs, the achieved diversity order by the SF codes can only be less than or equal to their achieved diversity order in the case without CFOs. Furthermore, we have the following observation:

- If $\mathbf{U}^b$ is nonsingular, i.e., $\mathrm{rank}(\mathbf{U}^b) = N$, the equality in (5.19) holds. In this case, the achieved diversity order is not decreased by the multiple CFOs.

Since multiple CFOs affect the SF codes through the matrix $\mathbf{U}^b$, let us investigate it in detail. Substituting (5.9) into (5.13), we have

$$\begin{aligned}\mathbf{U}^b &= \sum_{m=1}^{M_t} e^{j\theta^b_{\varepsilon_m}}\mathbf{F}_N\mathbf{\Omega}_{\varepsilon_m}\mathbf{F}_N^{\mathcal{H}}\mathbf{P}_m \\ &= \mathbf{F}_N\sum_{m=1}^{M_t}\mathbf{\Omega}_{\varepsilon_m}\mathbf{F}_N^{\mathcal{H}}\mathbf{P}_m\left(\sum_{i=1}^{M_t} e^{j\theta^b_{\varepsilon_i}}\mathbf{P}_i\right) \\ &= N^{-\frac{1}{2}}\mathbf{F}_N\mathbf{V}\mathbf{P}^b, \end{aligned} \tag{5.20}$$

where $\mathbf{V} = N^{\frac{1}{2}} \sum_{m=1}^{M_t} \mathbf{\Omega}_{\varepsilon_m} \mathbf{F}_N^{\mathcal{H}} \mathbf{P}_m$, $\mathbf{P}^b = \sum_{i=1}^{M_t} e^{j\theta_{\varepsilon_i}^b} \mathbf{P}_i$, and the second equality follows from (5.6). Here it is easy to verify that $\mathbf{P}^b$ is a diagonal and unitary matrix. Considering the fact that both $\mathbf{F}_N$ and $\mathbf{P}^b$ are unitary matrices, we have the fact that $\text{rank}(\mathbf{U}^b) = \text{rank}(N^{-\frac{1}{2}} \mathbf{F}_N \mathbf{V} \mathbf{P}^b) = \text{rank}(\mathbf{V})$.

For the SF code matrix $\mathbf{C}$, assuming that the kth subcarrier is used by m_kth transmit antenna for $0 \leq k \leq N-1$ and $1 \leq m_k \leq M_t$, and considering the expression of $\mathbf{\Omega}_{\varepsilon_m}$, we have the form of the kth column of $\mathbf{V}$, denoted by $\mathbf{v}_k$, as

$$\mathbf{v}_k = [1, e^{j2\pi(\varepsilon_{m_k}+k)/N}, e^{j2\pi(\varepsilon_{m_k}+k)2/N}, \cdots, e^{j2\pi(\varepsilon_{m_k}+k)(N-1)/N}]^{\mathcal{T}}. \tag{5.21}$$

From (5.21), it is clear that $\mathbf{V}$ is a Vandermonde matrix. Thus the determinant of $\mathbf{V}$ is calculated by

$$\begin{aligned} \det(\mathbf{V}) &= \prod_{0 \leq i < l \leq N-1} \left(e^{j2\pi(\varepsilon_{m_l}+l)/N} - e^{j2\pi(\varepsilon_{m_i}+i)/N} \right) \\ &= \prod_{0 \leq i < l \leq N-1} e^{j2\pi(\varepsilon_{m_i}+i)/N} \left(e^{j2\pi(l-i+\varepsilon_{m_l}-\varepsilon_{m_i})/N} - 1 \right). \end{aligned} \tag{5.22}$$

From (5.22), it is easy to see that $\det(\mathbf{V}) = 0$ if and only if we can find a pair of integers i and l so that $e^{j2\pi(l-i+\varepsilon_{m_l}-\varepsilon_{m_i})/N} - 1 = 0$ for $0 \leq i < l \leq N-1$. Since $2\pi(l-i+\varepsilon_{m_l}-\varepsilon_{m_i})/N = 2t\pi \Leftrightarrow \varepsilon_{m_l} - \varepsilon_{m_i} = tN + i - l$ for t is an integer, finally we have

$$\det(\mathbf{V}) = 0 \Leftrightarrow \varepsilon_{m_l} - \varepsilon_{m_i} = tN + i - l, \tag{5.23}$$

where $0 \leq i < l \leq N-1$ and all of t, i and l are integers.

We now have the following theorem.

Theorem 3 *If the absolute values of normalized CFOs ε_m, $1 \leq m \leq M_t$, are all less than 0.5, then the diversity order of the SF codes is not decreased by the multiple CFOs, where the SF code is that described in Section 5.2.*

Proof 3 *If $|\varepsilon_m| < 0.5$ for all m, we can get $-1 < \varepsilon_{m_l} - \varepsilon_{m_i} < 1$. On the other hand, from $0 \leq i < l \leq N-1$, we have $1 - N \leq i - l \leq -1$. Thus, for (5.23) it is easy to obtain that $\varepsilon_{m_l} - \varepsilon_{m_i}$ can be only integers except the points which are integer multiple of N. So if $\varepsilon_m < 0.5$ for all m, condition (5.23) cannot be satisfied and then the $\det(\mathbf{V}) \neq 0$, which implies that equality in (5.19) holds. This further means that the achieved diversity is not affected by CFOs.*

On the other hand, if $\varepsilon_{Max} \geq 0.5$, the maximum achieved diversity order of the SF codes may be less than $M_t\Gamma$, although $L_m \geq \Gamma$ for $1 \leq m \leq M_t$. Here ε_{Max} is the maximum value of $|\varepsilon_m|$ for $1 \leq m \leq M_t$, which means that $-\varepsilon_{Max} \leq \varepsilon_m \leq \varepsilon_{Max}$. The following is a counterexample corresponding to the case $\varepsilon_{m_l} - \varepsilon_{m_i} = -1$ which is possible if $\varepsilon_{Max} \geq 0.5$.

Before showing this counterexample, we define some additional notations. We denote the $\mathbf{X}_p$ $(1 \leq l \leq P)$ as an $M_t\Gamma \times M_tL$ submatrix of $\mathbf{X}$ which contains all the rows of $\mathbf{X}$ related to $\mathbf{G}_p$. Actually, according to the structure of $\mathbf{X}$ (5.17), $\mathbf{X}_p$ is just the $(p-1)$th $M_t\Gamma \times M_tL$ submatrix of $\mathbf{X}$. According to the rows of $\mathbf{X}$ contained by $\mathbf{X}_p$, we further define $\bar{\mathbf{V}}_p$ $(1 \leq l \leq P)$ as the $(p-1)$th $N \times M_t\Gamma$ submatrix of $\mathbf{V}$ and $\bar{\mathbf{P}}_1^b$ $(1 \leq l \leq P)$ as the $(p-1)$th main diagonal $M_t\Gamma \times M_t\Gamma$ matrix of $\mathbf{P}^b$, respectively. Therefore, according to block matrix multiplication, we have

$$\mathbf{V}\mathbf{P}^b\mathbf{X} = \sum_{p=1}^{P} \bar{\mathbf{V}}_p \bar{\mathbf{P}}_1^b \mathbf{X}_p. \tag{5.24}$$

Suppose that $\mathbf{C}$ and $\hat{\mathbf{C}}$ are distinct SF code matrices which are constructed from $\mathbf{G}_1, \mathbf{G}_2, \cdots, \mathbf{G}_P$ and $\hat{\mathbf{G}}_1, \hat{\mathbf{G}}_2, \cdots, \hat{\mathbf{G}}_P$, respectively. Without loss of generality, we can consider the case that $\mathbf{G}_p = \hat{\mathbf{G}}_p$ for $p > 1$. Then the related difference matrices $\Delta\mathbf{X}_p = \mathbf{X}_p - \hat{\mathbf{X}}_p$ are all zero matrices for $2 \leq p \leq P$. So substituting this fact into (5.24), we have $\mathbf{V}\mathbf{P}^b(\mathbf{X} - \hat{\mathbf{X}}) = \bar{\mathbf{V}}_1 \bar{\mathbf{P}}_1^b \Delta\mathbf{X}_1$.

From (5.5), it is easy to get that $m_k = \lfloor k/\Gamma \rfloor + 1$ if $0 \leq k \leq M_t\Gamma - 1$. Thus we have $m_{(m'\Gamma-1)} = m'$ and $m_{m'\Gamma} = m' + 1$ for $1 \leq m' \leq M_t - 1$. If $\varepsilon_{Max} \geq 0.5$, it is possible that $\varepsilon_{m_{m'\Gamma}} - \varepsilon_{m_{(m'\Gamma-1)}} = \varepsilon_{m'+1} - \varepsilon_{m'} = -1$. Therefore condition (5.23) is satisfied corresponding to the case that $l = i + 1$ and $t = 0$. As a consequence, $\mathbf{V}$ is no longer a nonsingular matrix. Actually, according to (5.21), it is easy to get that in this case $\mathbf{v}_{(m'\Gamma-1)}$ is equal to $\mathbf{v}_{m'\Gamma}$. Since $\mathbf{v}_{(m'\Gamma-1)}$ and $\mathbf{v}_{m'\Gamma}$ are also two consecutive columns of $\bar{\mathbf{V}}_1$, $\bar{\mathbf{V}}_1$ is not of full column rank $M_t\Gamma$. Therefore for the considered pair of distinct SF code matrices, we have

$$\begin{aligned} \operatorname{rank}\left(\mathbf{U}^b(\mathbf{X} - \hat{\mathbf{X}})\mathbf{\Lambda}(\mathbf{X} - \hat{\mathbf{X}})^{\mathcal{H}}\mathbf{U}^{b\mathcal{H}}\right) &\leq \operatorname{rank}\left(\mathbf{U}^b(\mathbf{X} - \hat{\mathbf{X}})\right) \\ &= \operatorname{rank}\left(N^{-\frac{1}{2}}\mathbf{F}_N\bar{\mathbf{V}}_1\bar{\mathbf{P}}_1^b\Delta\mathbf{X}_1\right) \\ &\leq \operatorname{rank}\left(\bar{\mathbf{V}}_1\right) \\ &< M_t\Gamma. \end{aligned} \tag{5.25}$$

This implies that diversity order $M_t\Gamma$ cannot be achieved.

5.3.3 Diversity Analysis with the ZF-ML Detection Method

In the above analysis, by treating the ICI terms due to CFOs as a part of an SF code matrix, we find that the achieved diversity order of the SF codes is not decreased by CFOs under the condition that the absolute values of normalized CFOs are less than 0.5. This property is based on the ML decoding which decodes the new (virtual) code after absorbing the CFOs/ICI into the original SF code and jointly considers all the N subcarriers. Its computational complexity will be high when N is not small even for efficient ML detection methods such as the sphere decoding method. We next consider the SF coded system after we equalize the ICI caused by the CFOs using the ZF method, i.e., the two-stage ZF aided ML detection method (ZF-ML). After the ZF equalization, the ML decoding of the SF coded system is similar to the original SF coded system without the CFOs. The ZF-ML detection method is described as follows.

Let us recall the signal model (5.18), which is given by

$$\mathbf{z}^b = \sqrt{\frac{\rho}{M_t}}\mathbf{U}^b\mathbf{X}\mathbf{h} + \mathbf{w}. \tag{5.26}$$

As we have analyzed previously that if $\varepsilon_{Max} < 0.5$, the ICI matrix $\mathbf{U}^b$ is nonsingular. Under this condition we can equalize the ICI matrix $\mathbf{U}^b$ by the ZF method. Thus, after multiplying $\mathbf{z}^b$ by $\mathbf{U}^{b^{-1}}$, we get the ICI free signal model

$$\tilde{\mathbf{z}}^b = \mathbf{U}^{b^{-1}}\mathbf{z}^b = \sqrt{\frac{\rho}{M_t}}\mathbf{X}\mathbf{h} + \tilde{\mathbf{w}}, \tag{5.27}$$

where $\tilde{\mathbf{w}} = \mathbf{U}^{b^{-1}}\mathbf{w}$. From (5.20), $\mathbf{U}^{b^{-1}}$ can be calculated as

$$\mathbf{U}^{b^{-1}} = \left(N^{-\frac{1}{2}}\mathbf{F}_N\mathbf{V}\mathbf{P}^b\right)^{-1} = N^{\frac{1}{2}}\mathbf{P}^{b^{\mathcal{H}}}\mathbf{V}^{-1}\mathbf{F}_N^{\mathcal{H}}. \tag{5.28}$$

Then define the $(p-1)$th $(1 \le p \le P)$ $M_t\Gamma \times 1$ subvector of $\tilde{\mathbf{z}}^b$ as $\tilde{\mathbf{z}}_p^b$ and each $\tilde{\mathbf{z}}_p^b$ is given by

$$\tilde{\mathbf{z}}_p^b = \sqrt{\frac{\rho}{M_t}}\mathbf{X}_p\mathbf{h} + \tilde{\mathbf{w}}_p, \tag{5.29}$$

where $\mathbf{X}_p$ is the $(p-1)$th $M_t\Gamma \times M_tL$ submatrix of $\mathbf{X}$, i.e, the ith $(0 \le i \le M_t\Gamma - 1)$ row of $\mathbf{X}_p$ is the $((p-1)M_t\Gamma + i)$th row of $\mathbf{X}$, and $\tilde{\mathbf{w}}_p = \hat{\mathbf{U}}_p^b\mathbf{w}$ is the $(p-1)$th $M_t\Gamma \times 1$ subvector of $\tilde{\mathbf{w}}$ and $\hat{\mathbf{U}}_p^b$ is the $(p-1)$th $M_t\Gamma \times N$ submatrix of $\mathbf{U}^{b^{-1}}$.

Since $\mathbf{X}_p$ is constructed only from $\mathbf{G}_p$ and $\mathbf{G}_p$ is mapped only from $\mathbf{s}^p$, based on the signal model (5.29) we decode each SF submatrix $\mathbf{G}_p$ ($1 \leq p \leq P$) by the ML criterion, i.e.,

$$\mathbf{s}^{\star p} = \arg\min_{\mathbf{s}^p} \left[(\tilde{\mathbf{z}}_p^b - \sqrt{\frac{\rho}{M_t}}\mathbf{X}_p\mathbf{h})^{\mathcal{H}} \mathbf{T}_{b,p}^{-1} (\tilde{\mathbf{z}}_p^b - \sqrt{\frac{\rho}{M_t}}\mathbf{X}_p\mathbf{h}) \right], \tag{5.30}$$

where the minimization is performed over all admissible $M_t\Gamma \times 1$ information symbol vector $\mathbf{s}^p$. $\mathbf{T}_{b,p}$ is the $M_t\Gamma \times M_t\Gamma$ covariance matrix of the colored noise vector $\tilde{\mathbf{w}}_p$ and is given by

$$\mathbf{T}_{b,p} = \mathrm{E}\left[\tilde{\mathbf{w}}_p \tilde{\mathbf{w}}_p^{\mathcal{H}}\right] = \hat{\mathbf{U}}_p^b \left(\hat{\mathbf{U}}_p^b\right)^{\mathcal{H}}. \tag{5.31}$$

Now, we are in a position to state the following theorem.

Theorem 4 *For the SF code described in Section 5.2, if the absolute values of normalized CFOs ε_m, $1 \leq m \leq M_t$, are all less than 0.5, then the ZF-ML detection method can still achieve the same diversity order as that of the case without CFOs.*

Proof 4 *Proof of Theorem 4 can be found in Appendix 5.7.*

Actually, by using some reasonable approximations, the MMSE-F detection method, which is proposed in Chapter 4 based on the approach of maximizing SINR, is just equivalent to the ZF-ML detection method. This point is the fundamental reason behind the effectiveness of the proposed detection methods in last chapter. The detailed relationship between these two methods can be found in Appendix 5.8.

5.4 Preserving Full Diversity by Permutations

In the previous section, we have seen that if the absolute values of normalized CFOs ε_m, $1 \leq m \leq M_t$, are all less than 0.5, the diversity order of the SF codes, which is described in Section 5.2, is the same as the case without CFOs. On the other hand, if $\varepsilon_{Max} \geq 0.5$, the achieved diversity order of the SF codes may be decreased by multiple CFOs, when the ICI matrix $\mathbf{U}^b$ is singular. By observing (5.19), we can see that the condition that $\mathbf{U}^b$ is singular is not sufficient to lead to the inequality in (5.19). As a consequence, to show a counterexample for Theorem 3, we need to utilize the structures of $\mathbf{C}$ and $\mathbf{V}$. This implies that we may enhance the full

diversity property of the SF code by designing their structure so that full diversity can be still achieved even when $\mathbf{U}^b$ is singular. We explore this possibility in this section and propose a permutation (interleaving) method to enhance the robustness of the SF codes to multiple CFOs. The developed permutation method is described as follows. Throughout this section, the superscript $(\cdot)'$ of a matrix/vector means that the matrix/vector is defined for the permutated SF code $\mathbf{C}'$ similar to them defined for $\mathbf{C}'$.

5.4.1 Proposed Permutation Method

At the transmitter, we re-arrange the SF code $\mathbf{C}$ in (5.2)-(5.3) by some row permutations and denote this row-wisely permuted SF code by $\mathbf{C}'$, which is given by

$$\mathbf{C}' = \sqrt{M_t}\begin{bmatrix} \mathbf{x}_1^1 & \mathbf{0}_\Gamma & \cdots & \mathbf{0}_\Gamma \\ \vdots & \vdots & \ddots & \vdots \\ \mathbf{x}_1^P & \mathbf{0}_\Gamma & \cdots & \mathbf{0}_\Gamma \\ \mathbf{0}_\Gamma & \mathbf{x}_2^1 & \cdots & \mathbf{0}_\Gamma \\ \vdots & \vdots & \ddots & \vdots \\ \mathbf{0}_\Gamma & \mathbf{x}_2^P & \cdots & \mathbf{0}_\Gamma \\ \vdots & \vdots & \ddots & \vdots \\ \mathbf{0}_\Gamma & \mathbf{0}_\Gamma & \cdots & \mathbf{x}_{M_t}^1 \\ \vdots & \vdots & \ddots & \vdots \\ \mathbf{0}_\Gamma & \mathbf{0}_\Gamma & \cdots & \mathbf{x}_{M_t}^P \end{bmatrix}, \tag{5.32}$$

where $\mathbf{x}_m^p$ is defined in (5.3). From the above expression of $\mathbf{C}'$ we can see that after row permutations, the nonzero entries of the mth column of $\mathbf{C}$ are grouped. Note that the subcarriers from $P\Gamma(m-1)$ to $P\Gamma m-1$ are used by the mth transmit antenna. We call these subcarriers the mth group.

Assume that the $((m-1)\Gamma+i)$th row $(0 \le i \le \Gamma-1)$ of $\mathbf{G}_p$ is located at the $n^p_{(m-1)\Gamma+i}$th row, $0 \le n^p_{(m-1)\Gamma+i} \le N-1$, of $\mathbf{C}'$, i.e., $x_{(m-1)\Gamma+i+1}$ of $\mathbf{G}_p$ will be transmitted at the $n^p_{(m-1)\Gamma+i}$th subcarrier by the mth transmit antenna. Then, for (5.32) we have $n^p_{(m-1)\Gamma+i} = (m-1)\Gamma P + (p-1)\Gamma + i$ and $\mathbf{C}' = \mathbf{K}\mathbf{C}$, where $\mathbf{K}$ is a permutation matrix whose entry in $\left(n^p_{(m-1)\Gamma+i}\right)$th row and $((p-1)M_t\Gamma + (m-1)\Gamma + i)$th row is equal to 1.

In [39], it has been shown that the diversity order and coding advantage of this family of SF codes only depend on the relative positions of the permuted rows corresponding to the entries of $\mathbf{x}_m^p$ with respect to the position $n_{(m-1)\Gamma}^p$. Since we do not change the relative positions for the entries of $\mathbf{x}_m^p$, i.e., $n_{(m-1)\Gamma+i}^p - n_{(m-1)\Gamma}^p = i$, for each pair of m and p, $\mathbf{C}'$ should have the same diversity order and coding advantage as that of $\mathbf{C}$.

5.4.2 Receive Signal Model with Permutation

When applying $\mathbf{C}'$ to the cooperative protocol described in Section 5.1.1, similar to the derivation of (5.18), we can get the following SF coded receive signal model:

$$\mathbf{z}'^b = \sqrt{\frac{\rho}{M_t}}\mathbf{U}'^b\mathbf{X}'\mathbf{h} + \mathbf{w}, \tag{5.33}$$

where $\mathbf{X}' = [\mathbf{J}_0 \odot \mathbf{C}', \mathbf{J}_1 \odot \mathbf{C}', \cdots, \mathbf{J}_{L-1} \odot \mathbf{C}']$, $\mathbf{U}'^b = \sum_{m=1}^{M_t} e^{j\theta_{\varepsilon_m}^b}\mathbf{U}_{\varepsilon_m}\mathbf{P}'_m$ and the $N \times N$ matrix $\mathbf{P}'_m$ is defined as

$$\mathbf{P}'_m(l,l') = \begin{cases} 1, & \text{if } l = l' \text{ and } (m-1)P\Gamma \le l \le mP\Gamma - 1 \\ 0, & \text{else} \end{cases}, \tag{5.34}$$

for $0 \le l, l' \le N-1$. Then $\mathbf{U}'^b$ can be further rewritten as

$$\mathbf{U}'^b = N^{-\frac{1}{2}}\mathbf{F}_N\mathbf{V}'\mathbf{P}'^b, \tag{5.35}$$

where $\mathbf{V}' = N^{\frac{1}{2}}\sum_{m=1}^{M_t}\mathbf{\Omega}_{\varepsilon_m}\mathbf{F}_N^{\mathcal{H}}\mathbf{P}'_m$ and the diagonal unitary matrix $\mathbf{P}'^b = \sum_{m=1}^{M_t} e^{j\theta_{\varepsilon_m}^b}\mathbf{P}'_m$. Considering the expressions of $\mathbf{\Omega}_{\varepsilon_m}$ and $\mathbf{P}'_m$, we can derive that the kth $(0 \le k \le N-1)$ column of $\mathbf{V}'$ (denoted by $\mathbf{v}'_k$) is the kth column of $N^{\frac{1}{2}}\mathbf{\Omega}_{\varepsilon_{m_k}}\mathbf{F}_N^{\mathcal{H}}$ and has the same expression as that of $\mathbf{v}_k$ by

$$\mathbf{v}'_k = [1, e^{j2\pi(\varepsilon_{m_k}+k)/N}, e^{j2\pi(\varepsilon_{m_k}+k)2/N}, \cdots, e^{j2\pi(\varepsilon_{m_k}+k)(N-1)/N}]^{\mathcal{T}}. \tag{5.36}$$

Here m_k still denotes that kth subcarrier is used by m_kth transmit antenna for $1 \le m_k \le M_t$. For $\mathbf{C}'$, m_k is given by

$$m_k = \left\lceil \frac{k+1}{P\Gamma} \right\rceil \text{ for } 0 \le k \le N-1, \tag{5.37}$$

which is different from that for $\mathbf{C}$. Following the way from (5.21) to (5.22), we can see that $\mathbf{V}'$ is also a Vandermonde matrix. Then the sufficient and necessary condition for $\mathbf{V}'$ to be singular is given by

$$\det(\mathbf{V}') = 0 \Leftrightarrow \exists\, i, l, k \text{ that } \varepsilon_{m_l} - \varepsilon_{m_i} = tN + i - l \Leftrightarrow \mathbf{v}'_i = \mathbf{v}'_l, \tag{5.38}$$

for $0 \leq i < l \leq N-1$ and t, l and i are all integers. Here $\mathbf{v}'_n$ denotes the nth column of $\mathbf{V}'$.

5.4.3 Diversity Analysis of SF Codes with Permutation in the Presence of Multiple CFOs

Motivation

Observing the expression of $\mathbf{V}/\mathbf{V}'$ (5.20)/(5.35), we can see that $\mathbf{V}/\mathbf{V}'$ is a concatenation of $M_t\Gamma$ columns of $N^{\frac{1}{2}}\mathbf{\Omega}_{\varepsilon_m}\mathbf{F}_N^{\mathcal{H}}$ for $1 \leq m \leq M_t$, since right multiplying $N^{\frac{1}{2}}\mathbf{\Omega}_{\varepsilon_m}\mathbf{F}_N^{\mathcal{H}}$ by $\mathbf{P}_m/\mathbf{P}'_m$ only preserving its N/M_t columns corresponding to the nonzero diagonal entries of $\mathbf{P}_m/\mathbf{P}'_m$. Therefore, due to the difference between $\mathbf{P}_m$ and $\mathbf{P}'_m$, the kth $(0 \leq k \leq N-1)$ columns of $\mathbf{V}$ and $\mathbf{V}'$ may be preserved from kth column of different matrices $N^{\frac{1}{2}}\mathbf{\Omega}_{\varepsilon_m}\mathbf{F}_N^{\mathcal{H}}$.

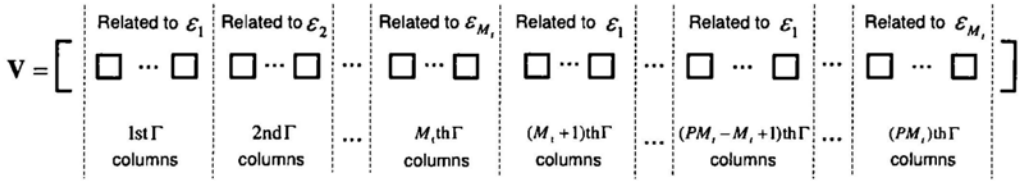

Figure 5.1: Structure of $\mathbf{V}$.

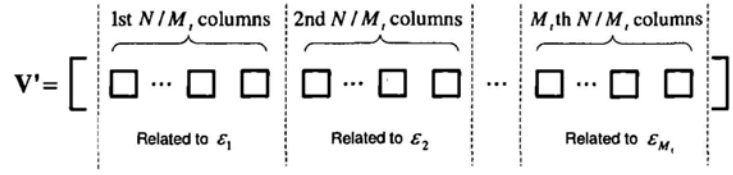

Figure 5.2: Structure of $\mathbf{V}'$.

Fig.5.1 shows the structure of $\mathbf{V}$, where each square stands for one column of $\mathbf{V}$. Due to the structure of $\mathbf{P}_m$ (5.5), the columns of $\mathbf{V}$ are divided into PM_t groups, where each group contains Γ consecutive columns and all the columns in nth ($1 \leq n \leq PM_t$) group are equal to those columns of $N^{\frac{1}{2}}\mathbf{\Omega}_{\varepsilon_{(n)_{M_t}}}\mathbf{F}_N^{\mathcal{H}}$. Therefore, the columns of the same group are related to the same CFO. Fig.5.2 shows the structure of $\mathbf{V}'$. Due to the proposed permutation, the columns of $\mathbf{V}'$ preserved from each $N^{\frac{1}{2}}\mathbf{\Omega}_{\varepsilon_m}\mathbf{F}_N^{\mathcal{H}}$ are grouped. Therefore, the columns of $\mathbf{V}'$ are divided into M_t groups and all the N/M_t ($N/M_t = P\Gamma$) columns of mth ($1 \leq m \leq M_t$) group are related to ε_m.

Similar to the definition of $\mathbf{X}_p$, $\bar{\mathbf{V}}_p$ and $\bar{\mathbf{P}}_p^b$ (5.24), for the permutated SF code $\mathbf{C}'$, we also define $\mathbf{X}'_p$, $\bar{\mathbf{V}}'_p$ and $\bar{\mathbf{P}}'^b_p$ for $1 \leq p \leq P$. $\mathbf{X}'_p$ is an $M_t\Gamma \times M_tL$ submatrix of $\mathbf{X}'$ and contains all the columns of $\mathbf{X}'$ related to $\mathbf{G}_p$. $\bar{\mathbf{V}}'_p$ contains $M_t\Gamma$ columns of $\mathbf{V}'$ whose column indexes are equal to the row indexes of the rows of $\mathbf{X}'$ contained by $\mathbf{X}'_p$. $\bar{\mathbf{P}}_p^b$ is a $M_t\Gamma \times M_t\Gamma$ diagonal matrix which contains $M_t\Gamma$ diagonal entries of $\mathbf{P}^{b'}$ corresponding to the rows of $\mathbf{X}'$ contained by $\mathbf{X}'_p$. Therefor, we have

$$\mathbf{V}'\mathbf{P}^{b'}\mathbf{X}' = \sum_{p=1}^{P} \bar{\mathbf{V}}'_p \bar{\mathbf{P}}'^b_p \mathbf{X}'_p. \tag{5.39}$$

Let us recall the counterexample for Theorem 3, where we consider the case of $\mathbf{G}_p = \hat{\mathbf{G}}_p$ for $2 \leq l \leq P$. As analyzed in that counterexample, the achieved diversity order of SF codes is upper bounded by the rank of $\bar{\mathbf{V}}_1$, which is the first $N \times M_t\Gamma$ submatrix of $\mathbf{V}$. Then if there exists $\varepsilon_{m'+1} - \varepsilon_{m'} = -1$ ($1 \leq m' \leq M_t - 1$), according to (5.21) the last column of m' group of $\mathbf{V}$ would be equal to the first column of its $(m'+1)$th group, which leads to $\text{rank}(\bar{\mathbf{V}}_1) = M_t\Gamma - 1$. Fig.5.3 shows the structure of $\bar{\mathbf{V}}_1$ in this case, where two equal columns are connected by a line. Therefore, we can conclude that for the considered case the achieved diversity order of $\mathbf{C}$ is smaller than $M_t\Gamma$.

Similarly, for the same case of $\mathbf{G}_p = \hat{\mathbf{G}}_p$ for $2 \leq l \leq P$, we can obtain that the achieved diversity of permutated SF code $\mathbf{C}'$ is upper bounded by the rank of $\bar{\mathbf{V}}'_1$. However, due to permutations, $\bar{\mathbf{V}}'_1$ does not contains $M_t\Gamma$ consecutive columns of $\mathbf{V}'$. Instead, as shown by Fig.5.4, $\bar{\mathbf{V}}'_1$ contains the first Γ columns of each group of $\mathbf{V}'$, where each group contains $P\Gamma$ ($P\Gamma = N/M_t$) consecutive columns of $\mathbf{V}'$ and are related to the same CFO.

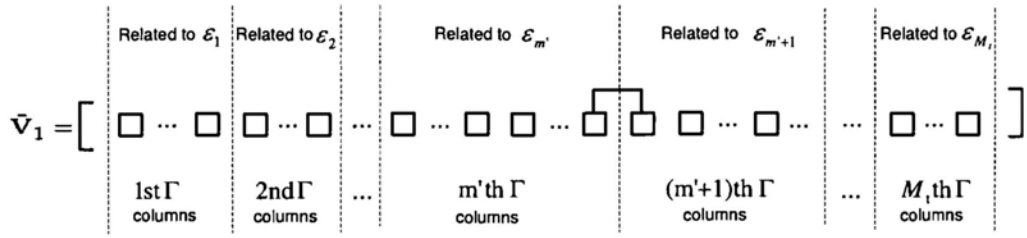

Figure 5.3: Structure of $\bar{\mathbf{V}}_1$.

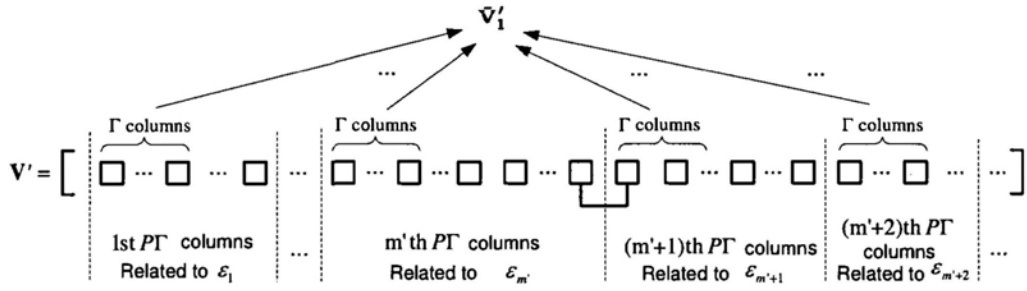

Figure 5.4: Structure of $\bar{\mathbf{V}}_1'$.

Then under the same condition, i.e., $\varepsilon_{m'+1} - \varepsilon_{m'} = -1$ $(1 \leq m' \leq M_t - 1)$, according to (5.38), in $\mathbf{V}'$ the last column of m'th group would be equal to the first column of $(m'+1)$th group. As shown by Fig.5.4, these two equal columns are connected by a line. However, different from $\bar{\mathbf{V}}_1$, due to the proposed permutation method, $\bar{\mathbf{V}}_1'$ does not contain the last column of m'th group. Thus $\bar{\mathbf{V}}_1'$ still has full column rank $M_t\Gamma$, although $\mathbf{V}'$ is singular. This means that by considering the case of $\mathbf{G}_p = \hat{\mathbf{G}}_p$ for $2 \leq l \leq P$, we cannot get the same conclusion on $\mathbf{C}'$ as on $\mathbf{C}$, i.e., the achieved diversity order may be decreased by multiple CFOs.

But apart from the case of $\mathbf{G}_p = \hat{\mathbf{G}}_p$ for $2 \leq p \leq P$, to show that the proposed permutation method can preserve the full diversity property of SF codes in the presence of multiple CFOs, we need to take all the cases of $\mathbf{C}' \neq \hat{\mathbf{C}}'$ into consideration. Fortunately, by utilizing the properties of $\mathbf{V}'$, we can get a sufficient condition under which the permutated SF codes can achieve the same diversity order as the case without multiple CFOs, even when $\mathbf{U}'^b$ is singular. This sufficient condition is given by the following theorem:

Theorem 5 *Let ε_m is the normalized CFO. If $|\varepsilon_m|$ for $1 \leq m \leq M_t$ are all less than*

$\frac{(P-1)\Gamma+1}{2}$ *and* P *is larger than* 1 *, the permuted SF codes described in (5.32) can always achieve a full diversity order of* $\sum_{m=1}^{M_t} L_m$ *given* $\Gamma \geq \max_m(L_m)$*, where* M_t *is the number of relay nodes incorporated in cooperation.*

Before proving Theorem 5, let us first see some properties of $\mathbf{V}'$ in the condition that $|\varepsilon_m| < \frac{(P-1)\Gamma+1}{2}$ and $P \geq 2$, which will be utilized in the remainder of this section.

Properties of $\mathbf{V}'$ when $|\varepsilon_m| < \frac{(P-1)\Gamma+1}{2}$ and $P \geq 2$

Before deeper insight, we define some additional notation. Define the $(m-1)$th $(1 \leq m \leq M_t)$ $N \times P\Gamma$ submatrix of $\mathbf{V}'$ as $\mathbf{V}'_m$, i.e., $\mathbf{V}' = [\mathbf{V}'_1, \mathbf{V}'_2, \cdots, \mathbf{V}'_{M_t}]$. The $(p-1)$th $(1 \leq p \leq P)$ $N \times \Gamma$ submatrix of $\mathbf{V}'_m$ is further denoted by $\mathbf{V}'^{p}_{m}$, i.e., $\mathbf{V}'_m = [\mathbf{V}'^{1}_{m}, \mathbf{V}'^{2}_{m}, \cdots, \mathbf{V}'^{P}_{m}]$.

To derive the properties of $\mathbf{V}'$, we need utilize the following proposition.

Proposition 1 *For the matrix* $\mathbf{V}'$ *defined in (5.35), provided* $|\varepsilon_m| < \frac{(P-1)\Gamma+1}{2}$ $(1 \leq m \leq M_t)$ *and* $P > 1$, $\mathbf{V}'$ *is singular if and only if there exist at least a pair of integers* i *and* l *for* $0 \leq i < l \leq N-1$ *and* $m_i \neq m_l$ *that satisfy either one of the following two cases:*

Case 1: $\varepsilon_{m_l} - \varepsilon_{m_i} = i - l$ *for* $\varepsilon_{m_l} - \varepsilon_{m_i} \in \{-(P-1)\Gamma, -(P-1)\Gamma+1, \cdots, -1\}$ *and* $m_l - m_i = 1$.

Case 2: $\varepsilon_{m_l} - \varepsilon_{m_i} = N + i - l$ *for* $\varepsilon_{m_l} - \varepsilon_{m_i} \in \{1, 2, \cdots, (P-1)\Gamma\}$, $m_i = 1$ *and* $m_l = M_t$.

In both of these two cases, $\mathbf{v}'_i = \mathbf{v}'_l$*. Here,* ε_m *is the normalized CFO,* m_k *denotes* k*th* $(0 \leq k \leq N-1)$ *subcarrier is used by* m_k*th* $(1 \leq m_k \leq M_t)$ *transmit antenna and* $\mathbf{v}'_k$ *is the* k*th column of* $\mathbf{V}'$.

Proof 5 *Proof of Proposition 1 can be found in Appendix 5.9.*

From Proposition 1, we can see that if $\mathbf{V}'$ is singular, there should exist m' $(1 \leq m' \leq M_t)$ so that some columns of $\mathbf{V}'_{m'}$ are equal to some columns of $\mathbf{V}'_{(m')_{M_t}+1}$. As an example, a singular matrix $\mathbf{V}'^{*}$ for the case of $\varepsilon_{m'+1} - \varepsilon_{m'} = -1$ $(1 < m' < M_t)$ and

$\varepsilon_{M_t} - \varepsilon_1 = 2$ takes the form

$$\begin{aligned}\mathbf{V}'^{*} = [&\underbrace{\mathbf{v}'_0, \mathbf{v}'_1, \cdots, \mathbf{v}'_{P\Gamma-1}}_{\mathbf{V}'_1}, \cdots, \\ &\underbrace{\mathbf{v}'_{(m'-1)P\Gamma}, \cdots, \mathbf{v}'_{m'P\Gamma-1}}_{\mathbf{V}'_{m'}} \underbrace{\mathbf{v}'_{m'P\Gamma-1}, \mathbf{v}'_{m'P\Gamma+1}, \cdots, \mathbf{v}'_{(m'+1)P\Gamma-1}}_{\mathbf{V}'_{m'+1}}, \cdots, \\ &\underbrace{\mathbf{v}'_{(M_t-1)P\Gamma}, \cdots, \mathbf{v}'_0, \mathbf{v}'_1}_{\mathbf{V}'_{M_t}}].\end{aligned} \tag{5.40}$$

Since $\varepsilon_{m'+1} - \varepsilon_{m'} = -1$ satisfies the case 1 of Proposition 1, the last column of $\mathbf{V}'_{m'}$, i.e., $\mathbf{v}'_{m'P\Gamma-1}$, is equal to the first column of $\mathbf{V}'_{m'+1}$, i.e., $\mathbf{v}'_{m'P\Gamma}$. Similarly, from the case 2 of Proposition 1, we know that the last two columns of $\mathbf{V}'_{M_t}$, i.e., $\mathbf{v}'_{N-2}$ and $\mathbf{v}'_{N-1}$, are equal to the first two columns of $\mathbf{V}'_1$, i.e., $\mathbf{v}'_0$ and $\mathbf{v}'_1$, respectively.

For each $\mathbf{V}'_m$ $(1 \le m \le M_t)$, we define a set $\mathcal{B}_m$ as

$$\mathcal{B}_m = \{t_{m,1}, t_{m,2}, \cdots, t_{m,T_m}\} \text{ for } t_{m,1} < t_{m,2} < \cdots < t_{m,T_m} \text{ and } T_m = |\mathcal{B}_m|, \tag{5.41}$$

which contains all the indices of the columns belonging to $\mathbf{V}'_m$, that are equal to the related columns in $\mathbf{V}'_{(m)_{M_t+1}}$, since multiple CFOs may satisfy Proposition 1.

We then define a function $f_m(t)$ for $t \in \mathcal{B}_m$, which is used to calculate the index of the column belonging to $\mathbf{V}'_{(m)_{M_t+1}}$ so that $\mathbf{v}'_t = \mathbf{v}'_{f_m(t)}$. According to Proposition 1, $f_m(t)$ has the following form

$$f_m(t) = \begin{cases} t - \varepsilon_{m+1} + \varepsilon_m & \text{for } 1 \le m \le M_t - 1 \\ t - N + \varepsilon_{M_t} - \varepsilon_1 & \text{for } m = M_t \end{cases}. \tag{5.42}$$

Similar to the definition of $\mathcal{B}_m$, for $\mathbf{V}'_m$ we also define a set $\bar{\mathcal{B}}_m$ containing all of the indices of the columns belonging to $\mathbf{V}'_m$, which are equal to the related columns in $\mathbf{V}'_{(m-2)_{M_t+1}}$. $\bar{\mathcal{B}}_m$ is given by

$$\bar{\mathcal{B}}_m = \{\bar{t}_{m,1}, \bar{t}_{m,2}, \cdots, \bar{t}_{m,\bar{T}_m}\} \text{ for } \bar{t}_{m,1} < \bar{t}_{m,2} < \cdots < \bar{t}_{m,\bar{T}_m} \text{ and } \bar{T}_m = |\bar{\mathcal{B}}_m|. \tag{5.43}$$

From the definitions of $\mathcal{B}_m$ and $\bar{\mathcal{B}}_m$, we can see that $\bar{\mathcal{B}}_m$ is actually the image of $\mathcal{B}_{(m-2)_{M_t+1}}$ under the injective function $f_{(m-2)_{M_t+1}}$, when $\mathcal{B}_{(m-2)_{M_t+1}}$ is not null.

With the aid of $\mathcal{B}_m$ and $\bar{\mathcal{B}}_m$, from Proposition 1, we can obtain the following properties of $\mathbf{V}'$, when $\mathcal{B}_m$ or $\bar{\mathcal{B}}_m$ is not null. The proofs of these properties can be found in Appendix 5.9.

Property 1: $mP\Gamma - (P-1)\Gamma \leq t_{m,1}$

Property 2: $f_m(t_{m,1}) = (m)_{M_t} P\Gamma$, which means that $\mathbf{v}'_{t_{m,1}}$ is equal to the first column of $\mathbf{V}'_{(m)_{M_t}}$.

Property 3: $\mathcal{B}_m$ has the form $\mathcal{B}_m = \{t_{m,1}, t_{m,1}+1, \cdots, mP\Gamma - 1\}$.

Property 4: $\bar{t}_{m,\bar{T}_m} \leq mP\Gamma - \Gamma - 1$.

Property 5: $\bar{\mathcal{B}}_m$ has the form

$$\begin{aligned} \bar{\mathcal{B}}_m &= \{(m-1)P\Gamma, (m-1)P\Gamma + 1, \cdots, (m-1)P\Gamma + \bar{T}_m - 1\} \\ &= \{f_{m'}(t_{m',1}), f_{m'}(t_{m',2}), \cdots, f_{m'}(t_{m',T_{m'}})\}, \end{aligned} \tag{5.44}$$

where $m' = (m-2)_{M_t} + 1$.

Property 6: If both $\bar{\mathcal{B}}_m$ and $\mathcal{B}_m$ are not null sets, we must have $t_{m,1} - \bar{t}_{m,\bar{T}_m} \geq \Gamma + 1$. From Property 6 of $\mathbf{V}'$, we know that the intersection of $\bar{\mathcal{B}}_m$ and $\mathcal{B}_m$ is always a null set, which implies that in $\mathbf{V}'$, we cannot find more than two equal columns. Otherwise, there must exist m so that $\bar{\mathcal{B}}_m \cap \mathcal{B}_m \neq \phi$, which is contradictory to Property 6 of $\mathbf{V}'$.

Property 7: There must exist m' ($1 \leq m' \leq M_t$) so that $\mathcal{B}_{m'} = \phi$.

Property 8: There must exist m' so that $\bar{\mathcal{B}}_{m'} = \phi$

By using $\mathcal{B}_m$ or $\bar{\mathcal{B}}_m$, we further define two N dimension vector sets $\mathcal{V}$ and $\bar{\mathcal{V}}$ with the forms

$$\begin{aligned} \bar{\mathcal{V}} &= \{\mathbf{v}'_n\} \text{ for } n \in \bar{\mathcal{A}} \text{ and } \bar{\mathcal{A}} = \{\mathcal{B}_1 \cup \mathcal{B}_2 \cup \cdots \mathcal{B}_{M_t}\} \\ \mathcal{V} &= \{\mathbf{v}'_n\} \text{ for } n \in \mathcal{A} \text{ and } \mathcal{A} = \{0, 1, \cdots, N-1\} \setminus \bar{\mathcal{A}}. \end{aligned} \tag{5.45}$$

According to the properties of $\mathbf{V}'$, we can get the following facts of $\mathcal{V}$ and $\bar{\mathcal{V}}$. Firstly, from $\mathcal{A} \cup \bar{\mathcal{A}} = \{0, 1, \cdots, N-1\}$, we know that $\mathcal{V} \cup \bar{\mathcal{V}}$ consists of all the columns of $\mathbf{V}'$. Secondly, the columns in $\mathcal{V}$ are independent from one another, in that we cannot find two elements in $\mathcal{A}$ to satisfy Proposition 1. Finally, each column in $\bar{\mathcal{V}}$ is equal to a certain column in $\mathcal{V}$, which means that $\bar{\mathcal{V}} \subset \mathcal{V}$. From the above facts, we can conclude that actually $\mathcal{V}$ consists of all the distinct columns of $\mathbf{V}'$ and forms a basis of the column space of $\mathbf{V}'$.

Proof of Theorem 5

Based on the properties of $\mathbf{V}'$, we give the proof of Theorem 5 in Appendix 5.10.

Actually, by slightly modifying the proof of Theorem 5, it can be shown that under the conditions provided by Theorem 5, for arbitrary values of L_m ($1 \leq m \leq M_t$) and Γ, the permuted SF codes $\mathbf{C}'$ can achieve diversity order $\sum_{m=1}^{M_t} \min(L_m, \Gamma)$ in the presence of multiple CFOs. The related explanation can be found at the end of Appendix 5.10.

On the other hand, if there is an m so that $|\varepsilon_m| \geq \frac{(P-1)\Gamma+1}{2}$, the maximum achieved diversity order of SF codes may be less than $M_t\Gamma$, although $L_m \geq \Gamma$ for $1 \leq m \leq M_t$. Once more, let us observe the case of $\mathbf{G}_p = \hat{\mathbf{G}}_p$ for $2 \leq p \leq P$. If $|\varepsilon_m| \geq \frac{(P-1)\Gamma+1}{2}$, it is possible that there exists m' ($1 \leq m' \leq M_t - 1$) so that $\varepsilon_{m'+1} - \varepsilon_{m'} = -(P-1)\Gamma - 1$. Therefore, condition (5.38) is satisfied corresponding to the case that $l = i+(P-1)\Gamma+1$ $t = 0$, $m_i = m'$ and $m_l = m' + 1$. As a consequence, the first column of $\mathbf{V}'_{m'+1}$, is equal to the $(\Gamma - 1)$th column of $\mathbf{V}'_{m'}$. Fig.5.5 shows the structure of $\bar{\mathbf{V}}'_1$ in this case, where two equal columns in $\bar{\mathbf{V}}'_1$ are connected by a line. Thus, $\bar{\mathbf{V}}'_1$ has no full column rank $M_t\Gamma$. As the achieved diversity order is upper bounded by the rank of $\bar{\mathbf{V}}'_1$, we can see that in this case the permutated SF codes cannot achieve full diversity order $M_t\Gamma$.

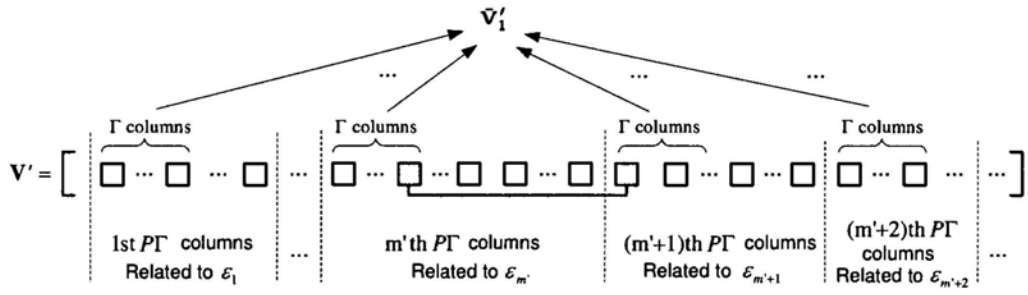

Figure 5.5: Structure of $\bar{\mathbf{V}}'_1$ when $\varepsilon_{m'+1} - \varepsilon_{m'} = -(P-1)\Gamma - 1$.

5.4.4 Signal Detection When U′ is Singular

In the above analysis, we show that by applying the proposed permutation method, the SF codes can still achieve full diversity, even when the ICI matrix $\mathbf{U}'$ is singular. Since this property is still based on the ML decoding and needs to jointly consider all the N subcarriers, its computational complexity will be high if N is not small even for efficient ML detection methods, such as the sphere decoding method. When $\mathbf{U}'$ is

singular, this problem becomes more serious, because the ZF-ML detection method cannot be directly applied to reduce the computational complexity of decoding. In this subsection, to tackle this problem, we propose two suboptimal detection methods suitable to the case that $\mathbf{U}'$ is singular. They are the ZF-ML-Zn and the ZF-ML-PIC detection methods.

ZF-ML-Zn Method

From the Property 3 and Property 5 of $\mathbf{V}'$, we know that if $\mathbf{V}'$ is singular, there must exist m^* so that $\mathbf{v}'_{\bar{t}_{m^*,k}} = \mathbf{v}'_{t_{m',k}}$ for $m' = (m^* - 2)_{M_t} + 1$ and $1 \le k \le \bar{T}_{m^*}$. As $\mathbf{v}'_{\bar{t}_{m^*,k}}$ and $\mathbf{v}'_{t_{m',k}}$ are the left and right boundary columns of $\mathbf{V}'_{m^*}$ and $\mathbf{V}'_{m'}$, respectively, to make the ZF-ML detection method still applicable, we may not use the last n subcarriers of each group at the cost of some efficiency loss. We denote this detection method as the ZF-ML-Zn method, where n is the number of unused subcarriers of each group. So, total $M_t n$ subcarriers are not used. Fig.5.6 shows the structure of $\mathbf{V}'$ for the ZF-ML-Zn method when $\bar{T}_{m^*} = n$, where the equal columns are connected by lines. In the figure, the last n marked squares in each group stands for columns which are related to unused subcarriers. Therefore, if $\bar{T}_{m^*} \le n$, all the $N - M_t n$ active columns of $\mathbf{V}'$, i.e., the columns related to used subcarriers, are still linearly independent. As a consequence, the ZF-ML detection method can be directly used.

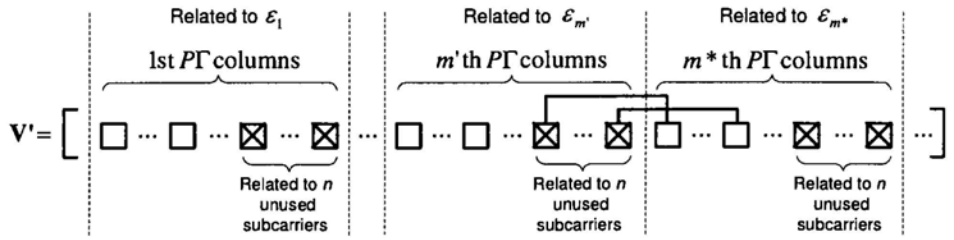

Figure 5.6: Structure of $\mathbf{V}'$ for the ZF-ML-Zn method when $\bar{T}_{m^*} = n$.

Define an $M_t(P\Gamma - n) \times N$ matrix $\mathbf{R}$ whose effect is to extract nonzero rows of $\mathbf{X}'$. Since the last n subcarriers of each group are not used, $\mathbf{R}$ takes the form

$$\mathbf{R}_m(l, l') = \begin{cases} 1, & \text{if } l = l' - \lfloor \frac{l}{P\Gamma - n} \rfloor n \\ 0, & \text{else} \end{cases}, \tag{5.46}$$

for $0 \leq l \leq M_t(P\Gamma - n) - 1$ and $0 \leq l' \leq N - 1$. Then for the ZF-ML-Zn detection method, the received signal model (5.33) can be rewritten as

$$\begin{aligned}
\mathbf{z}'^b &= \sqrt{\frac{\rho}{M_t}}\mathbf{U}'^b\mathbf{R}^{\mathcal{T}}\mathbf{R}\mathbf{X}'\mathbf{h} + \mathbf{w} \\
&= \sqrt{\frac{\rho}{M_t}}N^{-\frac{1}{2}}\mathbf{F}_N\mathbf{V}'\mathbf{P}'^b\mathbf{R}^{\mathcal{T}}\mathbf{R}\mathbf{X}'\mathbf{h} + \mathbf{w} \\
&= \sqrt{\frac{\rho}{M_t}}\left(N^{-\frac{1}{2}}\mathbf{F}_N\mathbf{V}'\mathbf{R}^{\mathcal{T}}\mathbf{R}\mathbf{P}'^b\mathbf{R}^{\mathcal{T}}\right)\mathbf{R}\mathbf{X}'\mathbf{h} + \mathbf{w}, \qquad (5.47)
\end{aligned}$$

where we have used the fact that $\mathbf{U}' = N^{-\frac{1}{2}}\mathbf{V}'\mathbf{P}'^b$ and $\mathbf{P}'^b$ is a diagonal unitary matrix. We now have the following theorem for the ZF-ML-Zn detection method.

Theorem 6 *Let ε_m is the normalized CFO. If $|\varepsilon_m|$, $1 \leq m \leq M_t$, are all less than $\frac{n+1}{2}$, for the permuted SF codes described in (5.32), the ZF-ML-Zn detection method can still achieve the same diversity order as that of the case without CFOs.*

Proof 6 *Similar to the derivation of Property 1 of $\mathbf{V}'$, by simply replacing $(P-1)\Gamma$ by n, provided $|\varepsilon_m| < \frac{n+1}{2}$, we can get that $mP\Gamma - n \leq t_{m,1}$ for $1 \leq m \leq M_t$. Since $t_{m,T_m} = mP\Gamma - 1$ (Property 3 of $\mathbf{V}'$), we immediately get that $T_m \leq n$. From the definition of the set $\mathcal{V}$ (5.45), we know that $\mathcal{V}$ consists of all the first $P\Gamma - T_m$ columns of $\mathbf{V}'_m$ for $1 \leq m \leq M_t$. On the other hand, the $N \times M_t(P\Gamma - n)$ matrix $\mathbf{V}'\mathbf{R}^{\mathcal{T}}$ consists of all the first $P\Gamma - n$ columns of $\mathbf{V}'_m$. Since $T_m \leq n$, the columns of $\mathbf{V}'\mathbf{R}^{\mathcal{T}}$ construct a subset of $\mathcal{V}$ with $M_t(P\Gamma - n)$ elements. Therefore, $\mathbf{V}'\mathbf{R}^{\mathcal{T}}$ has full column rank $M_t(P\Gamma - n)$. Combined with the fact that $\mathbf{F}_N$ and $\mathbf{R}\mathbf{P}'^b\mathbf{R}^{\mathcal{T}}$ are unitary matrices, we can see that the equivalent ICI matrix $\left(N^{-\frac{1}{2}}\mathbf{F}_N\mathbf{V}'\mathbf{R}^{\mathcal{T}}\mathbf{R}\mathbf{P}'^b\mathbf{R}^{\mathcal{T}}\right)$ has full column rank. As a consequence, the ZF-ML detection method can be applied to the signal model (5.47) to achieve the same diversity order as that of the case without CFOs.*

ZF-ML-PIC Method

To describe the ZF-ML-PIC method, by substituting (5.35) and (5.39) into (5.33), we rewrite received signal $\mathbf{z}'^b$ as

$$\begin{aligned}\mathbf{z}'^b &= \sqrt{\frac{\rho}{M_t}}\mathbf{U}'^b\mathbf{X}'\mathbf{h} + \mathbf{w} \\ &= \sqrt{\frac{\rho}{M_t}}N^{-\frac{1}{2}}\mathbf{F}_N\mathbf{V}'\mathbf{P}^{b'}\mathbf{X}'\mathbf{h} + \mathbf{w} \\ &= \sqrt{\frac{\rho}{M_t}}N^{-\frac{1}{2}}\mathbf{F}_N\sum_{p=1}^{P}\bar{\mathbf{V}}'_p\bar{\mathbf{P}}'^b_p\mathbf{X}'_p\mathbf{h} + \mathbf{w}. \end{aligned} \tag{5.48}$$

Then we construct an $N \times |\mathcal{V}|$ matrix $\check{\mathbf{V}}'$, whose $(k-1)$th column is the kth element of $\mathcal{V}$ for $1 \le k \le |\mathcal{V}|$. From the definition of $\mathcal{V}$ (5.45), we know that $\check{\mathbf{V}}'$ consists of all of the distinct columns of $\mathbf{V}'$ which are linearly independent from one another. As $\bar{\mathbf{V}}'_p$ $(1 \le p \le P)$ is a submatrix of $\mathbf{V}'$, $\check{\mathbf{V}}'$ contains all the columns of $\bar{\mathbf{V}}'_p$, as well. Here, we assume that the ith $(0 \le i \le M_t\Gamma - 1)$ column of $\bar{\mathbf{V}}'_p$ is equal to the $n_{p,i}$th column of $\check{\mathbf{V}}'$. We also construct a set $\bar{\mathcal{P}}$ which contains all the indices p $(1 \le p \le P)$ so that the columns of $\bar{\mathbf{V}}'_p$ are unique in $\mathbf{V}'$. $\bar{\mathcal{P}}$ is given by

$$\bar{\mathcal{P}} = \{\bar{p}_1, \bar{p}_2, \cdots, \bar{p}_{\bar{P}}\}, \tag{5.49}$$

for $1 \le \bar{p}_1 < \bar{p}_2 < \cdots < \bar{p}_{\bar{P}}$ and $\bar{P} = |\bar{\mathcal{P}}|$. When $\bar{\mathcal{P}}$ is not null, the ZF-ML-PIC detection method is described as follows:

1. Decode total $\bar{P}$ SF submatrices $\mathbf{G}_p$ for $p \in \bar{\mathcal{P}}$ by the ZF-ML detection method.
2. Jointly decode the rest $P - \bar{P}$ SF submatrices by first canceling all of the power in $\mathbf{z}'$, which comes from decoded $\mathbf{G}_p$ for $p \in \bar{\mathcal{P}}$.

Let $\check{\mathbf{U}} = N^{-\frac{1}{2}}\mathbf{F}_N\check{\mathbf{V}}'$. Since $\check{\mathbf{U}}$ has full column rank as well as $\check{\mathbf{V}}'$, its pseudo-inverse matrix $\check{\mathbf{U}}^\dagger$ can be calculated by

$$\begin{aligned}\check{\mathbf{U}}^\dagger &= \left(\check{\mathbf{U}}^{\mathcal{H}}\check{\mathbf{U}}^b\right)^{-1}\check{\mathbf{U}}^{\mathcal{H}} \\ &= N^{\frac{1}{2}}\left(\check{\mathbf{V}}'^{\mathcal{H}}\check{\mathbf{V}}'\right)^{-1}\check{\mathbf{V}}'^{\mathcal{H}}\mathbf{F}_N^{\mathcal{H}} \\ &= N^{\frac{1}{2}}\check{\mathbf{V}}'^{\dagger}\mathbf{F}_N^{\mathcal{H}}, \end{aligned} \tag{5.50}$$

where $\check{\mathbf{V}}'^{\dagger} = \left(\check{\mathbf{V}}'^{\mathcal{H}}\check{\mathbf{V}}'\right)^{-1}\check{\mathbf{V}}'^{\mathcal{H}}$ is the pseudo-inverse matrix of $\check{\mathbf{V}}'$. Multiplying $\mathbf{z}'^b$ (5.48) by $\check{\mathbf{U}}^{\dagger}$, we obtain

$$\begin{aligned}\check{\mathbf{z}}'^b &= \check{\mathbf{U}}^{\dagger}\mathbf{z}'^b \\ &= \sqrt{\frac{\rho}{M_t}}\sum_{p=1}^{P}\check{\mathbf{V}}'^{\dagger}\bar{\mathbf{V}}'_p\bar{\mathbf{P}}'^b_p\mathbf{X}'_p\mathbf{h} + \check{\mathbf{w}}, \end{aligned} \tag{5.51}$$

where (5.50) has been used and $\check{\mathbf{w}} = \check{\mathbf{U}}^{\dagger}\mathbf{w}$. Because the columns of $\bar{\mathbf{V}}'_p$ for $p \in \bar{\mathcal{P}}$ are unique in $\mathbf{V}'$, it is not hard to show that we can get an ICI free signal model for $\mathbf{G}_{\bar{p}_t}$ ($1 \le t \le \bar{P}$), which is given by

$$\check{\mathbf{z}}'^b_{\bar{p}_t} = \sqrt{\frac{\rho}{M_t}}\bar{\mathbf{P}}'^b_{\bar{p}_t}\mathbf{X}'_{\bar{p}_t}\mathbf{h} + \check{\mathbf{w}}_{\bar{p}_t}, \tag{5.52}$$

where $\check{\mathbf{z}}'^b_{\bar{p}_t} = [\check{\mathbf{z}}'^b(n_{\bar{p}_t,0}), \check{\mathbf{z}}'^b(n_{\bar{p}_t,1}), \cdots, \check{\mathbf{z}}'^b(n_{\bar{p}_t,M_t\Gamma-1})]^{\mathcal{T}}$, $\check{\mathbf{w}}^b_{\bar{p}_t} = [\check{\mathbf{w}}^b(n_{\bar{p}_t,0}), \check{\mathbf{w}}^b(n_{\bar{p}_t,1}), \cdots, \check{\mathbf{w}}^b(n_{\bar{p}_t,M_t\Gamma-1})]^{\mathcal{T}}$ and $n_{p,i}$ denotes that the ith column of $\bar{\mathbf{V}}'_p$ is equal to the $n_{p,i}$th column of $\check{\mathbf{V}}'$ for $0 \le i \le M_t\Gamma - 1$. As $\bar{\mathbf{P}}'^b_{\bar{p}_t}$ is a diagonal unitary matrix, with the similar approach to prove Theorem 4, it can been shown that based on the signal model (5.52) decoding $\mathbf{G}_{\bar{p}_t}$ ($1 \le t \le \bar{P}$) by ML achieves the same diversity order as the case without CFOs. Here we denote the decoded SF submatrix by $\tilde{\mathbf{G}}_{\bar{p}_t}$.

After decoding $\mathbf{G}_{\bar{p}_t}$ for $1 \le t \le \bar{P}$, the rest $P - \bar{P}$ SF submatrices are jointly decoded by first canceling all of the power coming from $\mathbf{G}_{\bar{p}_t}$. In signal model (5.48), for decoding $\mathbf{G}_p$ ($1 \le p \le P$ and $p \notin \bar{\mathcal{P}}$), we regard all of the power coming from $\mathbf{G}_{\bar{p}_t}$ for $1 \le t \le \bar{P}$ as interference. So we reconstruct all the interference by using $\tilde{\mathbf{G}}_{\bar{p}_t}$ and then cancel it from $\mathbf{z}'^b$. Finally, we jointly decode the rest $P - \bar{P}$ SF submatrices $\mathbf{G}_p$ for $p \notin \bar{\mathcal{P}}$.

For example, Fig.5.7 shows the structure of $\mathbf{V}'$ when $M_t = 2$, where each square symbol stands for one column of $\mathbf{V}'$ and two equal columns are connected by a line. From this figure, we can see that the columns of $\bar{\mathbf{V}}'_1$ and $\bar{\mathbf{V}}'_P$ are not unique in the columns of $\mathbf{V}'$. Therefore, for the ZF-ML-PIC detection method, $\mathbf{G}_p$ ($2 \le p \le P-1$) are first decoded. Then after canceling all the power from the decoded $\mathbf{G}_p$ in $\mathbf{z}$, $\mathbf{G}_1$ and $\mathbf{G}_P$ are jointly decoded.

For the ZF-ML-PIC detection method, we have the following theorem.

Theorem 7 *When $\bar{\mathcal{P}}$ is not null, for the permuted SF code $\mathbf{C}'$ described by (5.32),*

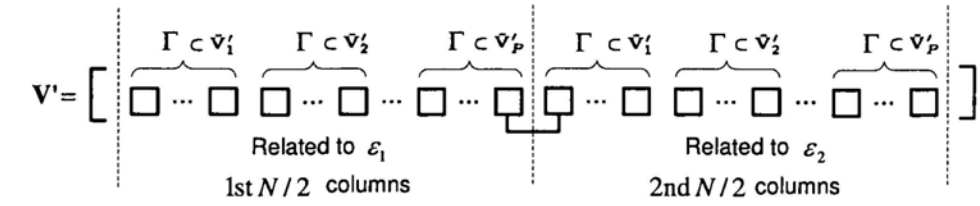

Figure 5.7: Structure of $\mathbf{V}'$ when $\bar{\mathcal{P}} = \{2, 3, \cdots, P-1\}$ and $M_t = 2$.

the ZF-ML-PIC detection method can still achieve the same diversity order as that of the case without CFOs.

Proof 7 *Assume that without CFOs the permuted SF codes* $\mathbf{C}'$ *can achieve diversity order d. Then we can express its SER/BER as* $P_a = \frac{1}{c_1}\mathrm{SNR}^{-d}$, *where* c_1 *is the coding gain of* $\mathbf{C}'$. *Then we define a Bernoulli random variable* I_a *with a probability mass function given by*

$$I_a = \begin{cases} 0, & \textit{if bits/symbols in } \mathbf{G}_{\bar{p}_t}\ (1 \le t \le \bar{P}) \\ & \textit{is not all correctly decoded} \\ 1, & \textit{otherwise} \end{cases}. \tag{5.53}$$

Similarly, we define a Bernoulli random variable I_b *given by*

$$I_b = \begin{cases} 0, & \textit{if bits/symbols in } \mathbf{G}_p\ (p \notin \bar{\mathcal{P}}) \\ & \textit{are not all correctly decoded} \\ 1, & \textit{otherwise} \end{cases}. \tag{5.54}$$

We denote P_b *as the BER/SER for decoding* $\mathbf{G}_p$ $(p \notin \bar{\mathcal{P}})$. *Then* P_b *can be calculated as*

$$P_b = \mathrm{P}\{I_b = 0 | I_a = 1\}\mathrm{P}\{I_a = 1\} + \mathrm{P}\{I_b = 0 | I_a = 0\}\mathrm{P}\{I_a = 0\}. \tag{5.55}$$

In (5.55), $\mathrm{P}\{I_b = 0 | I_a = 1\}$ *is the BER/SER for jointly decoding* $\mathbf{G}_p$ $(p \notin \bar{\mathcal{P}})$ *in the condition that* $\mathbf{G}_{\bar{p}_t}$ *are all correctly decoded for* $1 \le t \le \bar{P}$. *From Theorem 5, we know that for the case of* $\mathbf{G}_p = \tilde{\mathbf{G}}_p$ $(p \in \bar{\mathcal{P}})$, *the achieved diversity order is not decreased by multiple CFOs. Thus we can express* $\mathrm{P}\{I_b = 0 | I_a = 1\}$ *as*

$$\mathrm{P}\{I_b = 0 | I_a = 1\} = \frac{1}{c_2}\mathrm{SNR}^{-d}. \tag{5.56}$$

From the definition of I_a, we can see that

$$\mathrm{P}\{I_a = 0\} = P_a = \frac{1}{c_1}\mathrm{SNR}^{-d}. \tag{5.57}$$

Substituting (5.56) and (5.57) into (5.55), we obtain

$$\begin{aligned} P_b &= \mathrm{P}\{I_b = 0|I_a = 1\}(1 - \mathrm{P}\{I_a = 0\}) + \mathrm{P}\{I_b = 0|I_a = 0\}\mathrm{P}\{I_a = 0\} \\ &= \frac{1}{c_2}\mathrm{SNR}^{-d}(1 - \frac{1}{c_1}\mathrm{SNR}^{-d}) + \mathrm{P}\{I_b = 0|I_a = 0\}\frac{1}{c_1}\mathrm{SNR}^{-d} \\ &= \frac{1}{c_2}\mathrm{SNR}^{-d} - \frac{1}{c_1 c_2}\mathrm{SNR}^{-2d} + \mathrm{P}\{I_b = 0|I_a = 0\}\frac{1}{c_1}\mathrm{SNR}^{-d} \\ &< \frac{1}{c_2}\mathrm{SNR}^{-d} + \mathrm{P}\{I_b = 0|I_a = 0\}\frac{1}{c_1}\mathrm{SNR}^{-d} \\ &< (\frac{1}{c_1} + \frac{1}{c_2})\mathrm{SNR}^{-d} \end{aligned} \tag{5.58}$$

where the last inequality follows from the fact $\mathrm{P}\{I_b = 0|I_a = 0\} \leq 1$. *From (5.58), we immediately see that the ZF-ML-PIC detection method can achieve the same diversity order as that of the case without CFOs for each* $\mathbf{G}_p$ $(1 \leq p \leq P)$.

Examining the ZF-ML-PIC detection method, we can see that when $\mathbf{U}'^b$ is singular, only $(P - |\bar{\mathcal{P}}|)$ SF submatrices need to be jointly decoded. So when $|\bar{\mathcal{P}}|$ is larger, the ZF-ML-PIC detection method has much lower computational complexity than that of jointly considering all the N subcarriers. Actually, from the properties of $\mathbf{V}'$, it is not hard to obtain that

$$|\bar{\mathcal{P}}| = P - 2\left\lceil \frac{\max_{1\leq m\leq M_T}(T_m)}{\Gamma} \right\rceil. \tag{5.59}$$

Moreover, when $\mathcal{B}_m$ is not null, from the Property 3 and Property 5 of $\mathbf{V}'$, we know that $T_m = mP\Gamma - t_{m,1}$ and $f_m(t_{m,1}) = (m)_{M_t}P\Gamma$, respectively. Further considering the definition of $f_m(t)$ (5.42), we can derive that $T_m = |\varepsilon_m - \varepsilon_{(m)_{M_t}+1}|$. Therefore, $|\bar{\mathcal{P}}|$ is lower bounded by $P - 2\left\lceil \frac{\lfloor 2\varepsilon_{Max} \rfloor}{\Gamma} \right\rceil$.

Taken together, for the permuted SF code $\mathbf{C}'$ (5.32), both the ZF-ML-Zn and the ZF-ML-PIC detection methods are suitable to the case that $\mathbf{U}'^b$ is singular. More importantly, they can achieve the same diversity order as the case without CFOs. Especially, when $\max_{1\leq m\leq M_t}(T_m)$ is small, they have much lower computational complexity than that of jointly considering all the N subcarriers. Compared to the ZF-ML-PIC detection method, the ZF-ML-Zn detection method has a lower computational complexity at the cost of some bandwidth efficiency loss.

Furthermore, similar to the MMSE-F method proposed in Chapter 4, it is not hard to show that the matrix inverse for the ZF-ML, ZF-ML-Zn and ZF-ML-PIC methods is independent of the OFDM symbol index for a channel realization, if we consider channel changing caused by CFOs. Therefore, the cost of calculating ZF matrix can be averaged by the number of OFDM symbols in one channel realization. In the case that the coherence time of the channel is short or the number of subcarriers is large, since for the ZF-ML-Zn and ZF-ML-PIC methods the subcarriers used by the same transmit antenna are grouped, the M-FFT aided methods proposed in Chapter 4 can be used to further reduce computational complexity in the expense of a certain performance loss.

5.5 Simulation Results

In this section, we present some simulations to verify our previous analysis on the diversity order achieved by the SF codes $\mathbf{C}$ and the permuted SF codes $\mathbf{C}'$ in the presence of multiple CFOs.

Firstly, an $M_t = 2$ system with 8 OFDM tones, i.e., $N = 8$, is simulated. The bandwidth is 20 MHz and BPSK modulation is employed. The channels from relay nodes to the destination node are frequency-selective with two equal power rays $[\tau_m(0), \tau_m(1)] = [0, 0.05]\mu s$ for $1 \leq m \leq M_t$. We also assume that the destination node has only one receive antenna. For each channel realization, each ε_m is uniformly selected from $[-\varepsilon_{Max}, \varepsilon_{Max}]$. The SF code proposed in [39] is applied. Coding parameter Γ is set as 2. Thus P is equal to 2. Without multiple CFOs, full diversity order 4 can be achieved. At the destination node the sphere decoding method is applied to jointly consider all of the subcarriers if CFOs exist.

Fig.5.8 shows the SER performance of the non-permuted SF codes $\mathbf{C}$ in the presence of multiple CFOs. We can see that when $\varepsilon_{Max} = 0.4$, since diversity order 4 can still be achieved, the performance loss is very small and the slope of SER curve is similar to that of the case without CFOs. However, when $\varepsilon_{Max} = 0.8$, since when $\varepsilon_m > 0.5$ full diversity cannot always be achieved for each realization of CFOs, the slope is no longer parallel with the curve without CFOs at the high SNR range. Fi-

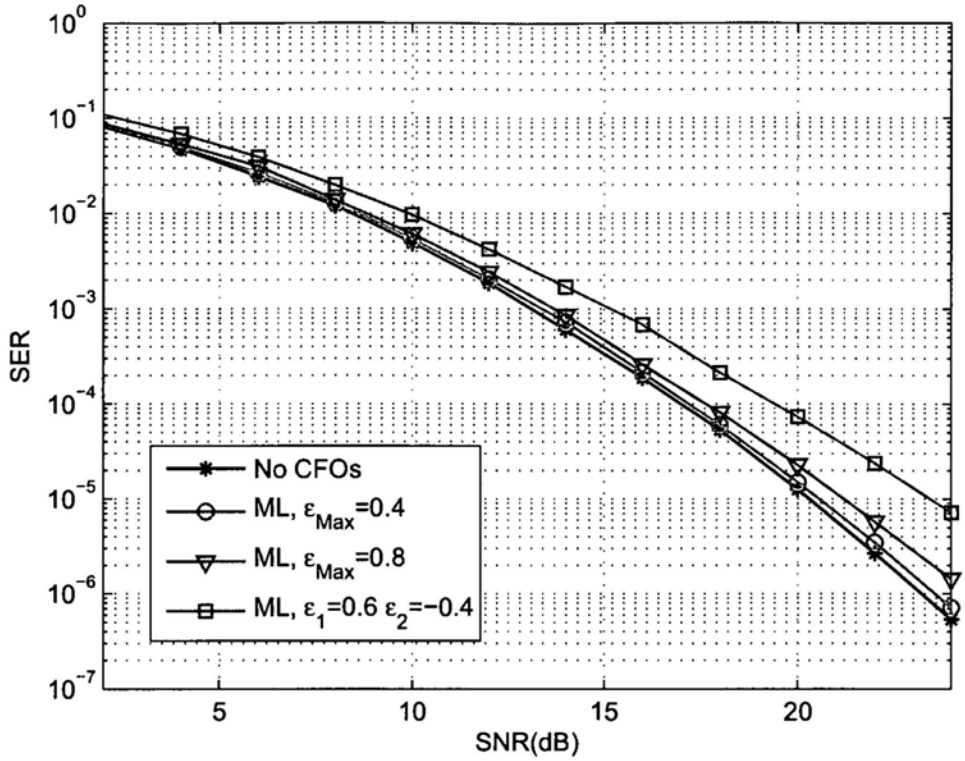

Figure 5.8: Performance of the SF codes $\mathbf{C}$ in the presence of multiple CFOs.

nally, we simulated a special case, i.e., $\varepsilon_1 = 0.6$ and $\varepsilon_2 = -0.4$. From the analysis of the counterexample after Theorem 3, we see that for this special case full diversity cannot be achieved. The simulation result confirms our analysis. In Fig.5.8, the slope of its SER curve is obviously less than that of the SER curve without CFOs.

Fig.5.9 shows the SER performance of the permuted SF codes $\mathbf{C}'$ in the presence of multiple CFOs. Compared with Fig.5.8, we note that without CFOs the proposed permutation operation does not affect the SER performance of the SF codes. According to Theorem 5, we know that for $P = 2$ and $\Gamma = 2$, the achieved diversity order of the permuted SF codes $\mathbf{C}'$ is not decreased when $\varepsilon_{Max} < 1.5$. This is confirmed by the simulation results as the SER curves in the case of $\varepsilon_{Max} = 1.4$ has the same slope of the SER curve as that of the case without CFOs. Even in the special case of $\varepsilon_1 = 0.6$ and $\varepsilon_2 = -0.4$, although the ICI matrix $\mathbf{U}'$ is singular, the permuted SF code $\mathbf{C}'$ still achieves the same slope of SER curve as that in the case of no CFOs. How-

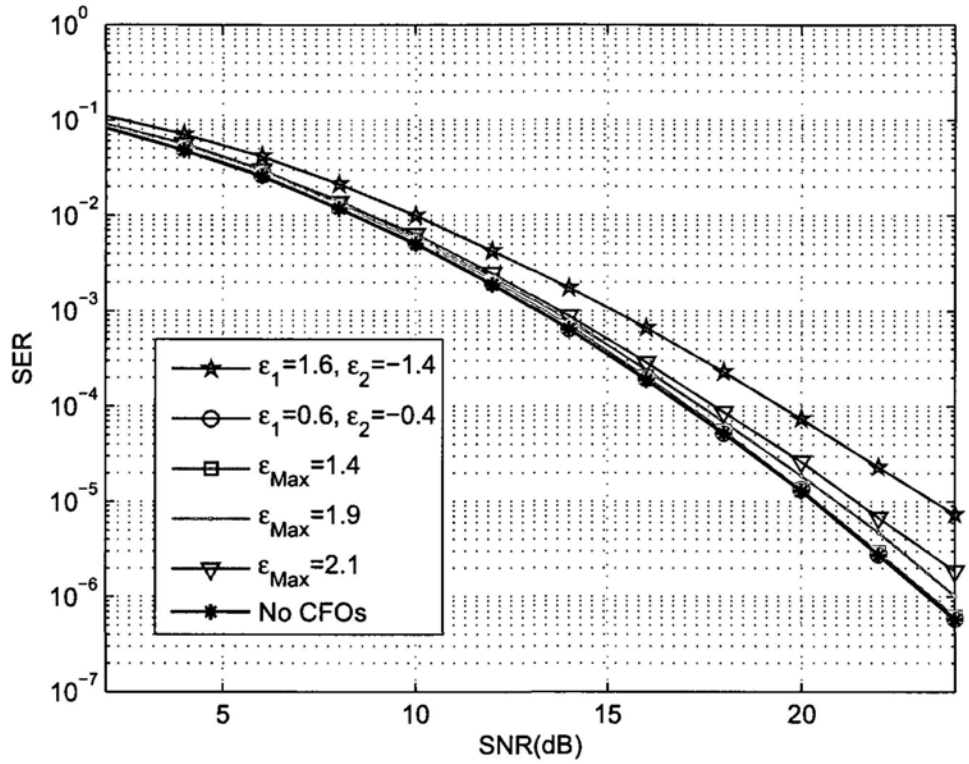

Figure 5.9: Performance of the permuted SF codes $\mathbf{C}'$ in the presence of multiple CFOs.

ever, when $\varepsilon_{Max} = 1.9$ and $\varepsilon_{Max} = 2.1$, the slope is no longer parallel with the curve without CFOs at the high SNR range, since when $\varepsilon_m > 1.5$ full diversity cannot always be achieved for each realization of CFOs. Finally, we simulated a special case, i.e., $\varepsilon_1 = 1.6$ and $\varepsilon_2 = -1.4$. From the analysis the counterexample after Theorem 5, we see that $\mathbf{C}'$ cannot achieve full diversity for this special case. The simulation result confirms our analysis. In Fig.5.9, the slope of its SER curve is obviously less than that of the SER curve without CFOs.

To investigate the SER performance of the two-stage suboptimal detection methods, i.e., the ZF-ML, MMSE-F, ZF-ML-Zn and ZF-ML-PIC detection methods, we also consider an $M_t = 2$ system with 64 OFDM tones ($N = 64$). The channels from relays to the destination node are all frequency-selective fading with two equal power rays and $[\tau_m(0), \tau_m(1)] = [0, 0.5]\mu s$ for $1 \leq m \leq 2$. The data symbol is QPSK modu-

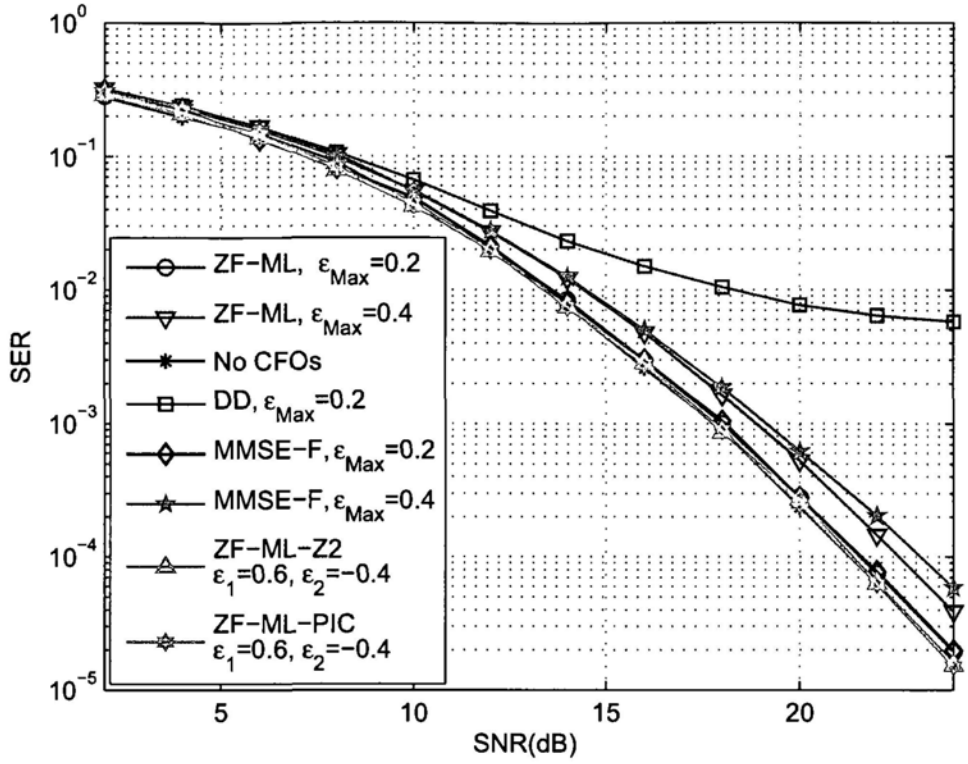

Figure 5.10: Performance of the two-stage suboptimal detection methods.

lated. To achieve full diversity order 4 we set Γ as 2. For the ZF-ML and MMSE-F detection methods, the un-permutated SF code $\mathbf{C}$ is applied. For the ZF-ML-Zn and ZF-ML-PIC detection methods, we use the permuted SF code $\mathbf{C}'$.

Fig.5.10 shows the simulation results. We can see that in the presence of CFOs, the OFDM system will quickly suffer from an error floor with increasing SNR if we directly decode (referred to as DD) the SF code by only ignoring all of the ICI terms due to CFOs. When ε_{Max} = 0.2, for the ZF-ML method, the performance loss is very small and the same slope of SER curve as that of the case without CFOs is observed. As ε_{Max} is increased from 0.2 to 0.4, the performance of the ZF-ML detection method is degraded. Since ε_{Max} is still less than 0.5, from the previous analysis, we see that when ε_{Max} = 0.4 the ZF-ML method can still achieve full diversity. This is confirmed by simulation results. In Fig.5.10, its slope is still parallel with the curve without CFOs at the high SNR range. Note that ML decoding all the

subcarriers should be the optimal method to achieve full diversity. However, when N is 64 and QPSK modulation is applied, a great burden is added to the system even for efficient ML detection methods such as the sphere decoding method. To make a contrast, we also plot two SER curves for the MMSE-F detection method when $\varepsilon_{Max} = 0.2$ and $\varepsilon_{Max} = 0.4$, respectively. We can see that when $\varepsilon_{Max} = 0.2$, the MMSE-F detection method nearly has the same SER performance as that of the ZF-ML detection method. On the other hand, when $\varepsilon_{Max} = 0.4$, the ZF-ML detection method outperforms the MMSE-F detection method from 16dB, because the filtered noise vector may not be well approximated by a white noise vector, when CFO is large.

Finally, we consider the permuted SF code $\mathbf{C}'$ in the case of $\varepsilon_1 = 0.6$ and $\varepsilon_2 = -0.4$, which is possible when $\varepsilon_{Max} \geq 0.5$. Note that as we have analyzed, in this case the un-permuted SF code $\mathbf{C}$ cannot achieve full diversity any longer. Since the ICI matrix $\mathbf{U}'$ is singular in this case, the ZF-ML detection method cannot be directly applied. To still achieve full diversity, we apply the ZF-ML-Z2 and ZF-ML-PIC detection methods. For the ZF-ML-Z2 detection method, the 30th, 31st, 62nd and 63rd subcarriers are not used. According to Theorem 6, full diversity can be achieved as long as both ε_1 and ε_2 are smaller than 1.5. For the ZF-ML-PIC detection method, $\mathbf{G}_1$ and $\mathbf{G}_{16}$ need to be jointly decoded. The simulation results are consistent with our previous analysis. In Fig.5.10, it is apparent that both of these two detection methods achieve nearly the same SER performance as that in the case without CFOs.

5.6 Conclusions

In this chapter, we investigated the effect of multiple CFOs in a cooperative OFDM based system on a family of SF codes proposed in [39]. By treating the CFOs as a part of the SF code matrix, we showed that if all of the absolute values of normalized CFOs are less than 0.5, the full diversity order for the SF codes are not affected by the multiple CFOs in the SF coded OFDM cooperative system. We further prove that this full diversity property is still preserved if the zero forcing (ZF) method is used to equalize the multiple CFOs. In addition, to improve the robustness of the SF codes to

multiple CFOs, we proposed a permutation method to enable the SF codes to achieve full diversity even when $\varepsilon_{max} \geq 0.5$. We further proposed two full diversity achievable detection methods, i.e., the ZF-ML-Zn and ZF-ML-PIC detection methods, which are suitable to the case that ICI matrix is singular. All these imply that the SF codes proposed in [39] for MIMO-OFDM systems are robust to both timing errors and frequency offsets in a cooperative system.

5.7 Appendix: Proof of Theorem 4

Recall that $\mathbf{P}^b$ is a diagonal unitary matrix. Then based on (5.28), $\hat{\mathbf{U}}_p^b$ $(1 \le p \le P)$ can be written as

$$\hat{\mathbf{U}}_p^b = N^{\frac{1}{2}} \mathbf{P}_p^{b\mathcal{H}} \hat{\mathbf{V}}_p \mathbf{F}_N^{\mathcal{H}}, \tag{5.60}$$

where $\mathbf{P}_p^b$ is a diagonal matrix given by

$$\mathbf{P}_p^b(l,l) = \mathbf{P}^b((p-1)M_t\Gamma + l, (p-1)M_t\Gamma + l) \tag{5.61}$$

for $0 \le l \le M_t\Gamma - 1$, and $\hat{\mathbf{V}}_p$ is the $(p-1)$th $M_t\Gamma \times N$ submatrix of $\mathbf{V}^{-1}$. Substituting (5.60) into (5.31), we get

$$\mathbf{T}_{b,p} = N\mathbf{P}_p^{b\mathcal{H}} \hat{\mathbf{V}}_p \hat{\mathbf{V}}_p^{-\mathcal{H}} \mathbf{P}_p^b. \tag{5.62}$$

When $\varepsilon_{max} < 0.5$, $\mathbf{V}$ is nonsingular. Thus we have $\text{rank}\left(\hat{\mathbf{V}}_p\right) = M_t\Gamma$. Consequently, the covariance matrix $\mathbf{T}_{b,p}$ is a nonsingular matrix. Let us now consider the eigendecomposition of the matrix $N\hat{\mathbf{V}}_p\hat{\mathbf{V}}_p^{-\mathcal{H}}$ and then get

$$\mathbf{T}_{b,p} = \mathbf{P}_p^{b\mathcal{H}} \mathbf{A}_p \mathbf{\Lambda}_p \mathbf{A}_p^{\mathcal{H}} \mathbf{P}_p^b = \mathbf{A}_{b,p} \mathbf{\Lambda}_p \mathbf{A}_{b,p}^{\mathcal{H}}, \tag{5.63}$$

where $\mathbf{\Lambda}_p$ is an $M_t\Gamma \times M_t\Gamma$ diagonal matrix with M_t positive eigenvalues of $N\hat{\mathbf{V}}_p\hat{\mathbf{V}}_p^{-\mathcal{H}}$ on its diagonal, $\mathbf{A}_p$ is an $M_t\Gamma \times M_t\Gamma$ unitary matrix and $\mathbf{A}_{b,p} = \mathbf{P}_p^{b\mathcal{H}}\mathbf{A}_p$ which is a unitary matrix as well. Substituting (5.63) into (5.30), we have

$$\begin{aligned}
\mathbf{s}^{*p} &= \arg\min_{\mathbf{s}^p} \left[(\tilde{\mathbf{z}}_p^b - \sqrt{\rho/M_t}\mathbf{X}_p\mathbf{h})^{\mathcal{H}} (\mathbf{A}_{b,p}\mathbf{\Lambda}_p\mathbf{A}_{b,p}^{\mathcal{H}})^{-1} (\tilde{\mathbf{z}}_p^b - \sqrt{\rho/M_t}\mathbf{X}_p\mathbf{h}) \right] \\
&= \arg\min_{\mathbf{s}^p} \left[(\tilde{\mathbf{z}}_p^b - \sqrt{\rho/M_t}\mathbf{X}_p\mathbf{h})^{\mathcal{H}} (\mathbf{A}_{b,p}\mathbf{\Lambda}_p^{-1}\mathbf{A}_{b,p}^{\mathcal{H}}) (\tilde{\mathbf{z}}_p^b - \sqrt{\rho/M_t}\mathbf{X}_p\mathbf{h}) \right] \\
&= \arg\min_{\mathbf{s}^p} \left[\left(\mathbf{\Lambda}_p^{-\frac{1}{2}} \mathbf{A}_{b,p}^{H} (\tilde{\mathbf{z}}_p^b - \sqrt{\rho/M_t}\mathbf{X}_p\mathbf{h}) \right)^{\mathcal{H}} \left(\mathbf{\Lambda}_p^{-\frac{1}{2}} \mathbf{A}_{b,p}^{\mathcal{H}} (\tilde{\mathbf{z}}_p^b - \sqrt{\rho/M_t}\mathbf{X}_p\mathbf{h}) \right) \right].
\end{aligned} \tag{5.64}$$

Observing (5.64), it is easy to see that the ML detection for the signal model (5.29) is equivalent to that for the following signal model:

$$\tilde{\mathbf{z}}_p^b = \mathbf{\Lambda}_p^{-\frac{1}{2}} \mathbf{A}_{b,p}^{\mathcal{H}} \tilde{\mathbf{z}}_p^b = \sqrt{\frac{\rho}{M_t}} \mathbf{\Lambda}_p^{-\frac{1}{2}} \mathbf{A}_{b,p}^{\mathcal{H}} \mathbf{X}_p\mathbf{h} + \mathbf{\Lambda}_p^{-\frac{1}{2}} \mathbf{A}_{b,p}^{\mathcal{H}} \tilde{\mathbf{w}}_p, \tag{5.65}$$

where it can be verified that the covariance matrix of the equivalent noise vector $\mathbf{\Lambda}_p^{-\frac{1}{2}} \mathbf{A}_{b,p}^{\mathcal{H}} \tilde{\mathbf{w}}_p$ is an $M_t\Gamma \times M_t\Gamma$ identity matrix. Based on signal model (5.65), clearly in the presence of multiple CFOs, the achieved diversity order of the ZF-ML method is

equal to the minimum rank of the matrix $\mathbf{\Lambda}_p^{-\frac{1}{2}}\mathbf{A}_{b,p}^{\mathcal{H}}(\mathbf{X}_p - \hat{\mathbf{X}}_p)\mathbf{\Lambda}(\mathbf{X}_p - \hat{\mathbf{X}}_p)^{\mathcal{H}}(\mathbf{\Lambda}_p^{-\frac{1}{2}}\mathbf{A}_{b,p}^{\mathcal{H}})^{\mathcal{H}}$ for any distinct $\mathbf{s}^p$ and $\hat{\mathbf{s}}^p$. Since $\mathbf{\Lambda}_p^{-\frac{1}{2}}\mathbf{A}_{b,p}^{\mathcal{H}}$ is an $M_t\Gamma \times M_t\Gamma$ nonsingular matrix, we have

$$\operatorname{rank}\left(\mathbf{\Lambda}_p^{-\frac{1}{2}}\mathbf{A}_{b,p}^{\mathcal{H}}(\mathbf{X}_p - \hat{\mathbf{X}}_p)\mathbf{\Lambda}(\mathbf{X}_p - \hat{\mathbf{X}}_p)^{\mathcal{H}}(\mathbf{\Lambda}_p^{-\frac{1}{2}}\mathbf{A}_{b,p}^{\mathcal{H}})^{\mathcal{H}}\right) = \operatorname{rank}\left((\mathbf{X}_p - \hat{\mathbf{X}}_p)\mathbf{\Lambda}(\mathbf{X}_p - \hat{\mathbf{X}}_p)^{\mathcal{H}}\right), \tag{5.66}$$

which means that for the ZF-ML detection method, the achieved diversity order is not decreased by multiple CFOs as long as $\varepsilon_{Max} < 0.5$.

5.8 Appendix: Relationship between the ZF-ML Detection Method and the MMSE-F Detection Method

In this appendix, we will show the relationship between the MMMSE-F detection method and the ZF-ML detection method.

As introduced in Chapter 4, according to the signal model (4.22) for the MMSE-F method the $N \times N$ filtering matrix $\mathbf{\Xi}^b$ is calculated by

$$\mathbf{\Xi}^b = \mathbf{\Pi}^b \left(\mathbf{D}^{b\mathcal{H}} \mathbf{D}^b + \frac{1}{\rho} \mathbf{I}_N \right)^{-1} \mathbf{D}^{b\mathcal{H}}, \tag{5.67}$$

where $\mathbf{D}^b = \sum_{m=1}^{M_t} e^{j\theta_{\varepsilon_m}^b} \mathbf{U}_{\varepsilon_m} \mathrm{diag}(\mathrm{H}_m) \mathbf{P}_m$. $\mathbf{\Pi}^b$ is an $N \times N$ real diagonal matrix, whose role is to enable each row of $\mathbf{\Xi}^b$ to have unit Euclidean norm. By following the similar derivation as that of (5.12), we get

$$\begin{aligned} \mathbf{D}^b &= \sum_{m=1}^{M_t} e^{j\theta_{\varepsilon_m}^b} \mathbf{U}_{\varepsilon_m} \mathbf{P}_m \mathrm{diag}(\mathrm{H}_m) \\ &= \sum_{m=1}^{M_t} e^{j\theta_{\varepsilon_m}^b} \mathbf{U}_{\varepsilon_m} \mathbf{P}_m \left(\sum_{m'=1}^{M_t} \mathbf{P}_{m'} \mathrm{diag}(\mathrm{H}_{m'}) \right) \\ &= \mathbf{U}^b \bar{\mathbf{H}}, \end{aligned} \tag{5.68}$$

where $\bar{\mathbf{H}} = \sum_{m=1}^{M_t} \mathbf{P}_m \mathrm{diag}(\mathrm{H}_m)$. According to the properties of $\mathbf{P}_m$ (5.5) and (5.6), clearly $\bar{\mathbf{H}}$ is a diagonal matrix and $\bar{\mathbf{H}}(t\Gamma M_t + (m-1)\Gamma + i, t\Gamma M_t + (m-1)\Gamma + i) = \mathrm{H}_m(t\Gamma M_t + (m-1)\Gamma + i)$ for $0 \le t \le P-1$, $1 \le m \le M_t$ and $0 \le i \le \Gamma - 1$.

Substituting (5.68) into (5.67), we can have

$$\mathbf{\Xi}^b = \mathbf{\Pi}^b \left(\bar{\mathbf{H}}^{\mathcal{H}} \mathbf{U}^{b\mathcal{H}} \mathbf{U}^b \bar{\mathbf{H}} + \frac{1}{\rho} \mathbf{I}_N \right)^{-1} \bar{\mathbf{H}}^{\mathcal{H}} \mathbf{U}^{b\mathcal{H}}. \tag{5.69}$$

Then at high SNR range we just simply ignore the term $\frac{1}{\rho}\mathbf{I}_N$ in (5.69) and approximate $\mathbf{\Xi}^b$ by

$$\begin{aligned} \mathbf{\Xi}^b &\approx \mathbf{\Pi}^b \left(\bar{\mathbf{H}}^{\mathcal{H}} \mathbf{U}^{b\mathcal{H}} \mathbf{U}^b \bar{\mathbf{H}} \right)^{-1} \bar{\mathbf{H}}^{\mathcal{H}} \mathbf{U}^{b\mathcal{H}} \\ &= \mathbf{\Pi}^b \bar{\mathbf{H}}^{-1} \mathbf{U}^{b-1}. \end{aligned} \tag{5.70}$$

Then the normalization matrix $\mathbf{\Pi}^b$ should has the form as

$$\mathbf{\Pi}^b(i,i) = \frac{1}{|\bar{\mathbf{H}}^{-1}(i,i)| \|\hat{\mathbf{u}}_i^b|_F} \tag{5.71}$$

for $0 \leq i \leq N-1$, where $\hat{\mathbf{u}}_i^b$ is the ith row of $\mathbf{U}^{b^{-1}}$. Therefore from (5.18), we get the filtered signal model as

$$\begin{aligned} \Xi^b \mathbf{z}^b &= \mathbf{\Pi}^b \bar{\mathbf{H}}^{-1} \mathbf{U}^{b^{-1}} \mathbf{z}^b \\ &= \mathbf{\Pi}^b \bar{\mathbf{H}}^{-1} \tilde{\mathbf{z}}^b \\ &= \sqrt{\frac{\rho}{M_t}} \mathbf{\Pi}^b \bar{\mathbf{H}}^{-1} \mathbf{X}\mathbf{h} + \Xi^b \mathbf{w}, \end{aligned} \tag{5.72}$$

where owing to the effect of the normalization matrix $\mathbf{\Pi}^b$, the covariance matrix of the filtered noise vector $\Xi^b \mathbf{w}$ has unit diagonal entries.

For the MMSE-F detection method, to simplify decoding we just ignore the off-diagonal terms in the covariance matrix of the filtered noise vector $\Xi^b \mathbf{w}$, i.e., $\Xi^b \Xi^{b^{\mathcal{H}}}$. Then similar to the ZF-ML detection method, decoding the SF submatrix $\mathbf{G}_p$ ($1 \leq p \leq P$) by the ML criterion, we have

$$\mathbf{s}^{*p} = \arg\min_{\mathbf{s}^p} \left[\left| \mathbf{\Pi}_p^b \bar{\mathbf{H}}_p \tilde{\mathbf{z}}_p^b - \sqrt{\frac{\rho}{M_t}} \mathbf{\Pi}_p^b \bar{\mathbf{H}}_p \mathbf{X}_p \mathbf{h} \right|_F^2 \right], \tag{5.73}$$

where the minimization is performed over all admissible $M_t\Gamma \times 1$ information symbol vector $\mathbf{s}^p$. $\mathbf{\Pi}_p^b$ and $\bar{\mathbf{H}}_p$ are the $(p-1)$th $M_t\Gamma \times N$ submatrix of $\mathbf{\Pi}^b$ and $\bar{\mathbf{H}}^{-1}$, respectively. $\tilde{\mathbf{z}}_p^b$ and $\mathbf{X}_p$ have the same definitions as those defined in (5.29). Furthermore, we can rewrite (5.73) as

$$\begin{aligned} \mathbf{s}^{*p} &= \arg\min_{\mathbf{s}^p} \left[\left(\mathbf{\Pi}_p^b \bar{\mathbf{H}}_p \tilde{\mathbf{z}}_p^b - \sqrt{\frac{\rho}{M_t}} \mathbf{\Pi}_p^b \bar{\mathbf{H}}_p \mathbf{X}_p \mathbf{h} \right)^{\mathcal{H}} \left(\mathbf{\Pi}_p^b \bar{\mathbf{H}}_p \tilde{\mathbf{z}}_p^b - \sqrt{\frac{\rho}{M_t}} \mathbf{\Pi}_p^b \bar{\mathbf{H}}_p \mathbf{X}_p \mathbf{h} \right) \right] \\ &= \arg\min_{\mathbf{s}^p} \left[\left(\tilde{\mathbf{z}}_p^b - \sqrt{\frac{\rho}{M_t}} \mathbf{X}_p \mathbf{h} \right)^{\mathcal{H}} \mathbf{\Phi}_p^b \left(\tilde{\mathbf{z}}_p^b - \sqrt{\frac{\rho}{M_t}} \mathbf{X}_p \mathbf{h} \right) \right], \end{aligned} \tag{5.74}$$

where $\mathbf{\Phi}_p^b = \mathbf{\Pi}_p^{b^{\mathcal{H}}} \bar{\mathbf{H}}_p^{\mathcal{H}} \bar{\mathbf{H}}_p \mathbf{\Pi}_p^b$. By using (5.71), we can see that $\mathbf{\Phi}_p^b$ has the form

$$\mathbf{\Phi}_p^b = \mathrm{diag}\left(\frac{1}{|\hat{\mathbf{u}}_{(p-1)M_t\Gamma}^b|_F^2}, \frac{1}{|\hat{\mathbf{u}}_{(p-1)M_t\Gamma+1}^b|_F^2}, \cdots, \frac{1}{|\hat{\mathbf{u}}_{pM_t\Gamma-1}^b|_F^2} \right). \tag{5.75}$$

Now let us look back to the ZF-ML detection method. For the ICI free signal model (5.27), if we also ignore the off-diagonal terms in the covariance matrix of the filtered noise vector $\mathbf{U}^{b^{-1}}\mathbf{w}$, i.e., $\mathbf{U}^{b^{-1}}\mathbf{U}^{b^{-\mathcal{H}}}$ as we have done for the MMSE-F detection method, the inverse of $\mathbf{T}_{b,p}$ defined in (5.31) will be equal to $\mathbf{\Phi}_p^b$. Then by comparing (5.30) with (5.74), we can clearly see that by above two approximations the ZF-ML detection given by (5.30) has just the same form as that of the MMSE-F detection given by (5.74).

5.9 Appendix: Proofs of Proposition 1 and Properties of V′

Proof of Proposition 1

From (5.38), we can see that $\mathbf{V}'$ is singular, if and only if there exist at least three integers t, i and l which satisfy

$$\varepsilon_{m_l} - \varepsilon_{m_i} = tN + i - l, \tag{5.76}$$

for $0 \leq i < l \leq N-1$, which leads to $\mathbf{v}'_i = \mathbf{v}'_l$. Since $0 \leq i < l \leq N-1$, we immediately get $-N+1 \leq i-l \leq -1$. As a consequence, we have

$$tN - N + 1 \leq tN + i - l \leq tN - 1. \tag{5.77}$$

When (5.76) holds, substituting (5.76) into (5.77), we obtain

$$tN - N + 1 \leq \varepsilon_{m_l} - \varepsilon_{m_i} \leq tN - 1. \tag{5.78}$$

On the other hand, provided $|\varepsilon_m| < \frac{(P-1)\Gamma+1}{2}$ and $P > 1$, we have

$$-N < -(P-1)\Gamma - 1 < \varepsilon_{m_l} - \varepsilon_{m_i} < (P-1)\Gamma + 1 < N. \tag{5.79}$$

Now let us examine (5.76) in great detail.

Firstly, if $\varepsilon_{m_l} - \varepsilon_{m_i} = 0$, from (5.76) we have $tN + i - l = 0$ and then $t = \frac{l-i}{N}$. On the other hand, since $-N+1 \leq i-l \leq -1$, we can get $\frac{1}{N} \leq \frac{l-i}{N} \leq 1 - \frac{1}{N}$. Therefore, we obtain $\frac{1}{N} \leq t \leq 1 - \frac{1}{N}$, which is contradictory to the fact that t is an integer. Thus $\varepsilon_{m_l} - \varepsilon_{m_i}$ cannot be equal to zero.

Secondly, if $\varepsilon_{m_l} - \varepsilon_{m_i} < 0$, given (5.79), $\varepsilon_{m_l} - \varepsilon_{m_i}$ should be in the set $\{-(P-1)\Gamma, -(P-1)\Gamma + 1, \cdots, -1\}$, since when (5.76) holds, $\varepsilon_{m_l} - \varepsilon_{m_i}$ should be an integer as well. To let both (5.78) and (5.79) hold, it is required that $tN - N + 1 < 0$ and $tN - 1 > -N$, which lead to $t < 1 - \frac{1}{N}$ and $t > -1 + \frac{1}{N}$, respectively. Considering the fact that t is an integer, we can easily derive that t can only be equal to 0. Thus we have $\varepsilon_{m_l} - \varepsilon_{m_i} = i - l$. From (5.37), we know that all the columns belonging to $\mathbf{V}'_m$ are related to ε_m. So from $i < l$ and $\varepsilon_{m_i} \neq \varepsilon_{m_l}$, we can see that m_i must be smaller than m_j. Then from $1 \leq m_i < m_l \leq M_t$, we obtain that $1 \leq m_i \leq M_t - 1$ and $2 \leq m_l \leq M_t$.

Furthermore, since $\varepsilon_{m_l} - \varepsilon_{m_i}$ is in the set $\{-(P-1)\Gamma, -(P-1)\Gamma+1, \cdots, -1\}$ and $\varepsilon_{m_l} - \varepsilon_{m_i} = i - l$, we can get

$$1 \leq l - i \leq (P-1)\Gamma. \tag{5.80}$$

Then from (5.37), we have

$$\begin{aligned} m_l - m_i &= \left\lceil \frac{l+1}{P\Gamma} \right\rceil - \left\lceil \frac{i+1}{P\Gamma} \right\rceil \\ &\leq \left\lceil \frac{i+(P-1)\Gamma+1}{P\Gamma} \right\rceil - \left\lceil \frac{i+1}{P\Gamma} \right\rceil \\ &= \left\lceil \frac{i+1}{P\Gamma} + \frac{(P-1)\Gamma}{P\Gamma} \right\rceil - \left\lceil \frac{i+1}{P\Gamma} \right\rceil \\ &\leq \left\lceil \frac{i+1}{P\Gamma} \right\rceil + 1 - \left\lceil \frac{i+1}{P\Gamma} \right\rceil \\ &= 1, \end{aligned} \tag{5.81}$$

where the second inequality follows from the fact that $0 < \frac{(P-1)\Gamma}{P\Gamma} < 1$. On the other hand, from $1 \leq m_i < m_l \leq M_t$ we have $m_l - m_i \geq 1$. Therefore, $m_l - m_i$ should be equal to 1. Based on the fact that $\mathbf{v}'_i$ is one column of $\mathbf{V}'_{m_i}$, we can get that $(m_i - 1)P\Gamma \leq i \leq m_i P\Gamma - 1$. As $m_l - m_i = 1$, we then have

$$(m_l - 2)P\Gamma \leq i \leq (m_l - 1)P\Gamma - 1. \tag{5.82}$$

Substituting (5.82) into (5.80), we obtain

$$(m_l - 2)P\Gamma + 1 \leq l \leq m_l P\Gamma - 1 - \Gamma. \tag{5.83}$$

As $\mathbf{v}'_l$ is one column of $\mathbf{V}'_{m_l}$, we immediately have $(m_l - 1)P\Gamma \leq l$. Thus from (5.83) we finally obtain

$$(m_l - 1)P\Gamma \leq l \leq m_l P\Gamma - 1 - \Gamma. \tag{5.84}$$

By a similar approach, from (5.80), (5.82) and (5.84), we can get

$$m_i P\Gamma - (P-1)\Gamma \leq i \leq m_i P\Gamma - 1. \tag{5.85}$$

Thirdly, if $\varepsilon_{m_l} - \varepsilon_{m_i} > 0$, by the similar analysis, it is not hard to obtain that when (5.76) holds, $\varepsilon_{m_l} - \varepsilon_{m_i} \in \{1, 2, \cdots, (P-1)\Gamma\}$, $1 \leq m_i \leq M_t - 1$, $2 \leq m_l \leq M_t$ and t can only be equal to 1. From $t = 1$, we have $\varepsilon_{m_l} - \varepsilon_{m_i} = N + i - l$. Since $\varepsilon_{m_l} - \varepsilon_{m_i}$ is in the set $\{1, 2, \cdots, (P-1)\Gamma\}$, we get

$$1 \leq N + i - l \leq (P-1)\Gamma. \tag{5.86}$$

From $1 \leq m_i \leq M_t - 1$ and (5.37), we also have

$$0 \leq i \leq (M_t - 1)P\Gamma - 1. \tag{5.87}$$

From (5.86), (5.87) and $l \leq N - 1$, it is not hard to get the inequality

$$N - (P - 1)\Gamma \leq l \leq N - 1. \tag{5.88}$$

Considering (5.37), we have $m_l = M_t$. Then adding both sides of (5.88) to that of (5.86), we can obtain

$$0 \leq i \leq (P - 1)\Gamma - 1. \tag{5.89}$$

and $m_i = 1$.

By summarizing results of the above analysis, we can get Proposition 1.

Proofs of Properties of V′

Proof of Property 1

The proof directly comes from the lower bound of i in (5.85) and that of l in (5.88).

Proof of Property 2

Assume $f_m(t_{m,1}) > (m)_{M_t}P\Gamma$. Then it is not hard to show that $t_{m,1}-1$ and $f_m(t_{m,1})-1$ are also a pair of integers that satisfies Proposition 1. So we can have $\mathbf{v}'_{t_{m,1}-1} = \mathbf{v}'_{f_m(t_{m,1})-1}$ and then $(t_{m,1} - 1) \in \mathcal{B}_m$, which is contradictory to the assumption that $t_{m,1}$ is the minimum element of $\mathcal{B}_m$. Therefore, we have $f_m(t_{m,1}) \leq (m)_{M_t}P\Gamma$. Since $f_m(t_{m,1})$ cannot be smaller than $(m)_{M_t}P\Gamma$, we obtain our conclusion.

Proof of Property 3

From the fact that $t_{m,1}$ and $f_m(t_{m,1})$ are a pair of integers that satisfies Proposition 1, it is not hard to get that if $t_{m,1} < mP\Gamma-1$, $t_{m,1}+k$ and $f_m(t_{m,1})+k$ for $1 \leq k \leq mP\Gamma-1-t_{m,1}$ are also a pair of integers that satisfies Proposition 1. Therefore, $\mathcal{B}_m$ has the form $\mathcal{B}_m = \{t_{m,1}, t_{m,1} + 1, \cdots, mP\Gamma - 1\}$.

Proof of Property 4

Directly comes from the upper bound of l in (5.83) and that of i in (5.89).

Proof of Property 5

Directly follows from the Property 2 and Property 3 of $\mathbf{V}'$ and the relationship between $\mathcal{B}_m$ and $\bar{\mathcal{B}}_m$.

Proof of Property 6

In this proof, we consider three different cases of m, i.e., $m = 1$, $2 \leq m \leq M_t - 1$ and $m = M_t$. Here only the derivation for the case of $2 \leq m \leq M_t - 1$ is given. For the other two cases, the same conclusion can be obtained by following the similar strategy.

Since $\bar{\mathcal{B}}_m$ is not null, from Property 5 of $\mathbf{V}'$, we know that $\bar{t}_{m,\bar{T}_m} = (m-1)\Gamma + \bar{T}_m - 1 = f_{m-1}(t_{m-1,T_{m-1}})$. From Property 3 of $\mathbf{V}'$, we have $t_{m-1,T_{m-1}} = (m-1)P\Gamma - 1$. Thus, we get $\bar{t}_{m,\bar{T}_m} = f_{m-1}((m-1)P\Gamma - 1)$. Then by using (5.42), $\bar{t}_{m,\bar{T}_m}$ can be expressed by

$$\bar{t}_{m,\bar{T}_m} = (m-1)P\Gamma - 1 - \varepsilon_m + \varepsilon_{m-1}. \tag{5.90}$$

On the other hand, based on Property 2 of $\mathbf{V}'$, we have $f_m(t_{m,1}) = mP\Gamma$. From (5.42), we get

$$mP\Gamma = t_{m,1} - \varepsilon_{m+1} + \varepsilon_m. \tag{5.91}$$

Adding each side of (5.91) to that of (5.90), we can get

$$\varepsilon_{m+1} - \varepsilon_{m-1} = t_{m,1} - \bar{t}_{m,\bar{T}_m} - P\Gamma - 1. \tag{5.92}$$

Given $|\varepsilon_m| < \frac{(P-1)\Gamma+1}{2}$, we can obtain that $\varepsilon_{m+1} - \varepsilon_{m-1} > -(P-1)\Gamma - 1$. Substituting this inequality into (5.92), we can get

$$t_{m,1} - \bar{t}_{m,\bar{T}_m} > \Gamma. \tag{5.93}$$

Since $t_{m,1} - \bar{t}_{m,\bar{T}_m}$ is an integer, we finally obtain $t_{m,1} - \bar{t}_{m,\bar{T}_m} \geq \Gamma + 1$.

Proof of Property 7

Assume that $\mathcal{B}_m \neq \phi$ for $1 \leq m \leq M_t$. From the case 1 of Proposition 1, we have $-(P-1)\Gamma \leq \varepsilon_m - \varepsilon_{m-1} \leq -1$ for $2 \leq m \leq M_t$. Then we can obtain that $\sum_{m=2}^{M_t} -(P-1)\Gamma \leq \sum_{m=2}^{M_t} \varepsilon_m - \varepsilon_{m-1} \leq \sum_{m=2}^{M_t} -1$, which leads to

$$-(M_t-1)(P-1)\Gamma \leq \varepsilon_{M_t} - \varepsilon_1 \leq -(M_t-1). \tag{5.94}$$

On the other hand, since $\mathcal{B}_{M_t} \neq \phi$, from the case 2 of Proposition 1, we get that $1 \leq \varepsilon_{M_t} - \varepsilon_1 \leq (P-1)\Gamma$, which is contradictory to (5.94). Therefore, there must exist m' so that $\mathcal{B}_{m'} = \phi$.

Proof of Property 8

From Property 7, we know that there must exist n ($1 \leq n \leq M_t$) so that $\mathcal{B}_n = \phi$. From the relationship between $\mathcal{B}_n$ and $\bar{\mathcal{B}}_{(n)_{M_t+1}}$ (Property 5 of $\mathbf{V}'$), we can deduce that $\mathcal{B}_n = \bar{\mathcal{B}}_{(n)_{M_t+1}} = \phi$. Therefore, Property 8 holds.

5.10 Appendix: Proof of Theorem 5

Since multiple CFOs cannot increase achieved diversity order, from the receive signal model(5.33), we can see that to prove Theorem 5 it is sufficient to show that

$$\text{rank}(\mathbf{U}'^{b}\Delta\mathbf{X}'\mathbf{\Lambda}^{\frac{1}{2}}) = \sum_{m=1}^{M_t} L_m, \tag{5.95}$$

over all pairs of distinct SF code matrices $\mathbf{C}'$ and $\hat{\mathbf{C}}'$ given $\varepsilon_{Max} < \frac{(P-1)\Gamma+1}{2}$, where $\Delta\mathbf{X}' = \mathbf{X}' - \hat{\mathbf{X}}'$ and $\varepsilon_{Max} = \max_{1\le m\le M_t}(|\varepsilon_m|)$. Actually, as $\mathbf{\Lambda}$ is an $M_t\Gamma \times M_t\Gamma$ diagonal matrix with $\sum_{m=1}^{M_t} L_m$ nonzero diagonal entries, $\text{rank}(\mathbf{U}'^{b}\Delta\mathbf{X}'\mathbf{\Lambda}^{\frac{1}{2}})$ cannot be larger than $\sum_{m=1}^{M_t} L_m$.

Without loss of generality, here for $\mathbf{J}_l$ $(0 \le l \le L-1)$ defined in (5.15), if $l \ge L_m$, we assign a value to $\tau_m(l)$ for $L_m \le l \le L-1$ so that $\tau_m(L_m - 1) < \tau_m(L_m) < \tau_m(L_m + 1) < \cdots < \tau_m(L-1) \le L_{cp}$. So $\mathbf{X}'$ would has the similar form as that in the case of $L_m = L$ for $1 \le m \le M_t$. Note that due to $\alpha_m(l) = 0$ for $l \ge L_m$, $\mathbf{X}'\mathbf{\Lambda}^{\frac{1}{2}}$ is not changed by this operation. Therefore, following this operation, we only need to prove that $\mathbf{U}'^{b}\Delta\mathbf{X}$ has full column rank M_tL.

Obviously, if $\mathbf{U}'^{b}$ is nonsingular, we immediately get the equality that

$$\text{rank}(\mathbf{U}'^{b}\Delta\mathbf{X}'\mathbf{\Lambda}^{\frac{1}{2}}) = \text{rank}(\Delta\mathbf{X}'\mathbf{\Lambda}^{\frac{1}{2}}) \tag{5.96}$$

Thus in the case that $\mathbf{U}'^{b}$ is nonsingular, Theorem 5 is true, since without CFOs the permuted SF codes $\mathbf{C}'$ can achieve full diversity. Therefore, we only need to consider the case that $\mathbf{U}'^{b}$ is singular.

Property of SF Codes

Besides the properties of $\mathbf{V}'$, in order to realize our goal, we need to utilize some properties of the SF cods as reviewed in the below.

From (5.15), we know that the $(m-1)$th $(1 \le m \le M_t)$ column of $\mathbf{J}_l \odot \mathbf{C}'$ $(0 \le l \le L-1)$ is $\mathbf{f}^{\tau_m(l)} \odot \mathbf{c}'_m$, where $\mathbf{c}'_m$ is the $(m-1)$th column of $\mathbf{C}'$. Define $\mathbf{y}^p_{m,l} = \mathbf{f}^{\tau_m(l)}_{(m-1)P+p-1} \odot \mathbf{x}^p_m$, where $\mathbf{f}^{\tau_m(l)}_k$ $(0 \le k \le M_tP-1)$ denotes kth $\Gamma \times 1$ subvector of

$\mathbf{f}^{\tau_m(l)}$. Then we can express $\mathbf{J}_l \odot \mathbf{C}'$ as

$$\mathbf{J}_l \odot \mathbf{C}' = \begin{bmatrix} \mathbf{y}^{1\mathcal{T}}_{1,l} & \cdots & \mathbf{y}^{P\mathcal{T}}_{1,l} & \mathbf{0}^{\mathcal{T}}_{\Gamma} & \cdots & \mathbf{0}^{\mathcal{T}}_{\Gamma} & \cdots & \mathbf{0}^{\mathcal{T}}_{\Gamma} & \cdots & \mathbf{0}^{\mathcal{T}}_{\Gamma} \\ \mathbf{0}^{\mathcal{T}}_{\Gamma} & \cdots & \mathbf{0}^{\mathcal{T}}_{\Gamma} & \mathbf{y}^{1\mathcal{T}}_{2,l} & \cdots & \mathbf{y}^{P\mathcal{T}}_{2,l} & \cdots & \mathbf{0}^{\mathcal{T}}_{\Gamma} & \cdots & \mathbf{0}^{\mathcal{T}}_{\Gamma} \\ \vdots & \ddots & \vdots & \vdots & \ddots & \vdots & \ddots & \vdots & \ddots & \vdots \\ \mathbf{0}^{\mathcal{T}}_{\Gamma} & \cdots & \mathbf{0}^{\mathcal{T}}_{\Gamma} & \mathbf{0}^{\mathcal{T}}_{\Gamma} & \cdots & \mathbf{0}^{\mathcal{T}}_{\Gamma} & \cdots & \mathbf{y}^{1\mathcal{T}}_{M_t,l} & \cdots & \mathbf{y}^{P\mathcal{T}}_{M_t,l} \end{bmatrix}^{\mathcal{T}}. \quad (5.97)$$

Observing (5.97), we can see that in the $(m-1)$th $(1 \le m \le M_t)$ $P\Gamma \times M_t$ submatrix of $\mathbf{J}_l \odot \mathbf{C}'$, only the $(m-1)$th column has nonzero entries. For each m, by collecting all of these nonzero $P\Gamma \times 1$ columns from $\mathbf{J}_l \odot \mathbf{C}'$ $(0 \le l \le L-1)$, we further define the $P\Gamma \times L$ matrix $\mathbf{Y}_m$ $(1 \le m \le M_t)$ by

$$\mathbf{Y}_m = \begin{bmatrix} \mathbf{y}^1{}_{m,0} & \mathbf{y}^1{}_{m,1} & \cdots & \mathbf{y}^1{}_{m,L-1} \\ \mathbf{y}^2{}_{m,0} & \mathbf{y}^2{}_{m,1} & \cdots & \mathbf{y}^2{}_{m,L-1} \\ \vdots & \vdots & \ddots & \vdots \\ \mathbf{y}^P{}_{m,0} & \mathbf{y}^P{}_{m,1} & \cdots & \mathbf{y}^P{}_{m,L-1} \end{bmatrix}, \quad (5.98)$$

and denote the $(p-1)$th $(1 \le p \le P)$ $\Gamma \times L$ submatrix of $\mathbf{Y}_m$ by $\mathbf{Y}^p_m$, which are all related to $\mathbf{x}^p_m$. Let $\Delta\mathbf{Y}_m$ is the difference matrix between $\mathbf{Y}_m$ and $\hat{\mathbf{Y}}_m$ which are constructed from $\mathbf{C}'$ and $\hat{\mathbf{C}}'$, respectively. Then one property of this SF code [36, 37, 39, 113] can be stated in the following proposition.

Proposition 2 *If* $\mathbf{G}_{p_0} \neq \hat{\mathbf{G}}_{p_0}$ $(1 \le p_0 \le P)$, *the difference matrix* $\Delta\mathbf{Y}^{p_0}_m$ *always has full rank, i.e.,* $\mathrm{rank}(\mathbf{Y}^p_m) = \min(\Gamma, L)$.

Proof 8 *Assume that* $\mathbf{G}_p = \hat{\mathbf{G}}_p$ *for any case of* $p \neq p_0$ $(1 \le p_0 \le P)$ *and* $L_1 = L_2 = \cdots = L_{M_t} = L$. *Then, by carefully observing* $\Delta\mathbf{X}'$, *we can see that* $\mathrm{rank}(\Delta\mathbf{X}') = \sum_{m=1}^{M_t} \mathrm{rank}(\Delta\mathbf{Y}^{p_0}_m)$. *On the other hand, without CFOs we know that the SF codes can achieve diversity order* $M_t \min(\Gamma, L)$ *when* $L_1 = L_2 = \cdots = L_{M_t} = L$. *This implies that for any cases of* $\mathbf{C}' \neq \hat{\mathbf{C}}'$, *we have* $\mathrm{rank}(\Delta\mathbf{X}') = M_t \min(\Gamma, L)$. *Therefore, we obtain* $\sum_{m=1}^{M_t} \mathrm{rank}(\Delta\mathbf{Y}^{p_0}_m) = M_t \min(\Gamma, L)$. *From the fact that* $\mathrm{rank}(\Delta\mathbf{Y}^{p_0}_m) \le \min(\Gamma, L)$, *we directly arrive at Proposition 2.*

Proof of $\mathrm{rank}(\mathbf{U}'\Delta\mathbf{X}') = M_t L$ when $\mathbf{U}'$ is Singular

Because $\mathrm{rank}(\mathbf{U}'\Delta\mathbf{X}') = \mathrm{rank}(\mathbf{V}'\mathbf{P}'^b\Delta\mathbf{X}')$, to achieve our goal, it is equivalent to prove that $\mathrm{rank}(\mathbf{V}'\mathbf{P}'^b\Delta\mathbf{X}') = M_t L$ for any two distinct $\mathbf{C}'$ and $\hat{\mathbf{C}}'$. Note since $\mathbf{P}'^b$ is a diago-

nal matrix with full rank N, if we regard $\mathbf{P}'^{b}\mathbf{X}'$ as $\mathbf{X}'$, we can still get the Proposition 2, which we will utilize in the following proof. So to simplify the notation, we just set $\mathbf{P}'^{b}$ as an identity matrix. Let $\mathbf{a}$ be an $M_t L \times 1$ coefficient vector. Then to prove $\text{rank}(\mathbf{V}'\Delta\mathbf{X}') = M_t L$, we only need to show that $\mathbf{V}'\Delta\mathbf{X}'\mathbf{a} = \mathbf{0}_N$, only if $\mathbf{a} = \mathbf{0}_{M_t L}$.

Define a $L \times 1$ coefficient vector $\mathbf{a}_m$ $(1 \le m \le M_t)$ by $\mathbf{a}_m = [\mathbf{a}(m-1), \mathbf{a}(m-1+M_t), \mathbf{a}(m-1+2M_t), \cdots, \mathbf{a}(m-1+(L-1)M_t)]^{\mathcal{T}}$, where $\mathbf{a}(k)$ $(0 \le k \le N-1)$ denotes the kth entry of $\mathbf{a}$. Then by carefully observing the structure of $\mathbf{X}'$, we can rewrite $\mathbf{V}'\Delta\mathbf{X}'\mathbf{a}$ as

$$\mathbf{V}'\Delta\mathbf{X}'\mathbf{a} = \sum_{m=1}^{M_t} \mathbf{V}'_m \Delta\mathbf{Y}_m \mathbf{a}_m = \sum_{m=1}^{M_t}\sum_{p=1}^{P} \mathbf{V}'^{p}_{m} \Delta\mathbf{Y}^{p}_{m} \mathbf{a}_m, \tag{5.99}$$

where $\mathbf{V}'_m$ is the $(m-1)$th $(1 \le m \le M_t)$ $N \times P\Gamma$ submatrix of $\mathbf{V}'$, i.e., $\mathbf{V}' = [\mathbf{V}'_1, \mathbf{V}'_2, \cdots, \mathbf{V}'_{M_t}]$, and $\mathbf{V}'^{p}_{m}$ is the $(p-1)$th $(1 \le p \le P)$ $N \times \Gamma$ submatrix of $\mathbf{V}'_m$, i.e., $\mathbf{V}'_m = [\mathbf{V}'^{1}_{m}, \mathbf{V}'^{2}_{m}, \cdots, \mathbf{V}'^{P}_{m}]$.

Proof of $\mathbf{a}_1 = \mathbf{0}_L$

From the Property 8 of $\mathbf{V}'$, we know there exists m' $(1 \le m' \le M_t)$ so that $\bar{\mathcal{B}}_{m'} = \phi$. Without loss of generality, we assume that $m' = 1$. Let p_1^* $(1 \le p_1^* \le P)$ is the maximum number so that no indices of the columns belonging to $\mathbf{V}'^{p}_{1}$ are in the set $\mathcal{B}_1$ for $1 \le p \le p_1^*$. From Property 1 of $\mathbf{V}'$, we know that $t_{1,1} \ge \Gamma$. Therefore, p_1^* is at least equal to 1. Then we rewrite (5.99) as

$$\begin{aligned}\mathbf{V}'\Delta\mathbf{X}'\mathbf{a} \;=\; & \sum_{p=1}^{p_1^*} \mathbf{V}'^{p}_{1} \Delta\mathbf{Y}^{p}_{1} \mathbf{a}_1 + \sum_{p=p_1^*+1}^{P} \mathbf{V}'^{p}_{1} \Delta\mathbf{Y}^{p}_{1} \mathbf{a}_1 + \sum_{p=1}^{P} \mathbf{V}'^{p}_{2} \Delta\mathbf{Y}^{p}_{2} \mathbf{a}_2 \\ & + \sum_{m=3}^{M_t}\sum_{p=1}^{P} \mathbf{V}'^{p}_{m} \Delta\mathbf{Y}^{p}_{m} \mathbf{a}_m,\end{aligned} \tag{5.100}$$

and regard $\mathbf{V}'\Delta\mathbf{X}'\mathbf{a}$ as a linear combination of the columns of $\mathbf{V}'$ with the $N \times 1$ coefficient vector $\Delta\mathbf{X}'\mathbf{a}$.

Firstly, let us look at the first term in the right-hand side of (5.100). Since $\bar{\mathcal{B}}_1 = \phi$, there are no columns in $\mathbf{V}'_{M_t}$ which are equal to that in $\mathbf{V}'_1$. On the other hand, since k $(0 \le k \le p_1^*\Gamma - 1)$ is not in the set $\mathcal{B}_1$, no columns in $\mathbf{V}'^{p}_{1}$ for $1 \le p \le p_1^*$ are equal to the columns belonging to $\mathbf{V}'_2$. Therefore, the columns in $[\mathbf{V}'^{1}_{1}, \mathbf{V}'^{2}_{1}, \cdots, \mathbf{V}'^{p_1^*}_{1}]$ only appear in this term, i.e., $\sum_{p=1}^{p_1^*} \mathbf{V}'^{p}_{1} \Delta\mathbf{Y}^{p}_{1} \mathbf{a}_1$. Further considering the fact that all the

distinct columns of $\mathbf{V}'$ form a basis of the column space of $\mathbf{V}'$, to let $\mathbf{V}'\Delta\mathbf{X}'\mathbf{a} = \mathbf{0}_N$, we must have

$$\Delta\mathbf{Y}_1^p\mathbf{a}_1 = \mathbf{0}_\Gamma \text{ for } 1 \le p \le p_1^*, \tag{5.101}$$

since $\Delta\mathbf{Y}_1^p\mathbf{a}_1$ is the coefficient vector to $\mathbf{V}'_p$ in $\mathbf{V}'\Delta\mathbf{X}'\mathbf{a}$. Assume that there exists p_0 for $1 \le p_0 \le p_1^*$ so that $\mathbf{G}_{p_0} \neq \hat{\mathbf{G}}_{p_0}$ Then from (5.101), we have

$$\Delta\mathbf{Y}_1^{p_0}\mathbf{a}_1 = \mathbf{0}_\Gamma. \tag{5.102}$$

By Proposition 2, we know that given $\Gamma \ge L$, $\Delta\mathbf{Y}_1^{p_0}$ has full column rank L. This implies that the homogeneous system described in (5.102) only has the trivial solution, i.e., $\mathbf{a}_1 = \mathbf{0}_L$. So in the case that there exists p_0 ($1 \le p_0 \le p_1^*$) so that $\mathbf{G}_{p_0} \neq \hat{\mathbf{G}}_{p_0}$, $\mathbf{V}'\Delta\mathbf{X}' = \mathbf{0}_N$, only if $\mathbf{a}_1 = \mathbf{0}_L$.

Secondly, let us turn to the case of $\mathbf{G}_p = \hat{\mathbf{G}}_p$ for $1 \le p \le p_1^*$. In this case, substituting $\Delta\mathbf{Y}_m^p = \mathbf{0}_{\Gamma\times L}$ for $1 \le p \le p_1^*$ and $1 \le m \le M_t$ into (5.100), we have

$$\begin{aligned}\mathbf{V}'\Delta\mathbf{X}'\mathbf{a} &= \mathbf{V}'^{p_1^*+1}_1\Delta\mathbf{Y}_1^{p_1^*+1}\mathbf{a}_1 + \sum_{p=p_1^*+2}^{P}\mathbf{V}'^p_1\Delta\mathbf{Y}_1^p\mathbf{a}_1 + \sum_{p=p_1^*+1}^{P}\mathbf{V}'^p_2\Delta\mathbf{Y}_2^p\mathbf{a}_2 \\ &\quad + \sum_{m=3}^{M_t}\sum_{p=p_1^*+1}^{P}\mathbf{V}'^p_m\Delta\mathbf{Y}_m^p\mathbf{a}_m.\end{aligned} \tag{5.103}$$

Since $t_{1,1} \le (p_1^*+1)\Gamma - 1$, from the Property 3 and property 5 of $\mathbf{V}'$, the last $(p_1^*+1)\Gamma - t_{1,1}$ columns of $\mathbf{V}'^{p_1^*+1}_1$ are equal to the first $(p_1^*+1)\Gamma - t_{1,1}$ columns of $\mathbf{V}'^1_2$. However, due to $\Delta\mathbf{Y}_2^1 = \mathbf{0}_{\Gamma\times L}$, the term $\mathbf{V}'^1_2\Delta\mathbf{Y}_2^1\mathbf{a}_2$ does not exist any longer in the right-hand side of (5.103). Note that from Property 6 of $\mathbf{V}'$, we know in $\mathbf{V}'$ there are no more than 2 equal columns. Therefore, in (5.103) only the term $\mathbf{V}'^{p_1^*+1}_1\Delta\mathbf{Y}_1^{p_1^*+1}\mathbf{a}_1$ is related to the columns of $\mathbf{V}'^{p_1^*+1}_1$. Since all the distinct columns of $\mathbf{V}'$ form a basis of the column space of $\mathbf{V}'$, to let $\mathbf{V}'\Delta\mathbf{X}'\mathbf{a} = \mathbf{0}_N$, we must have $\Delta\mathbf{Y}_1^{p_1^*+1}\mathbf{a}_1 = \mathbf{0}_L$. Furthermore, if $\mathbf{G}_{p_1^*+1} \neq \hat{\mathbf{G}}_{p_1^*+1}$, from Proposition 2 we know that $\Delta\mathbf{Y}_1^{p_1^*+1}$ has full column rank L. Therefore, in the case of $\mathbf{G}_{p_1^*+1} \neq \hat{\mathbf{G}}_{p_1^*+1}$, $\Delta\mathbf{Y}_1^{p_1^*+1}\mathbf{a}_1 = \mathbf{0}_L$, only if $\mathbf{a}_1 = \mathbf{0}_L$. Combined with previous analysis results, we can see that in the case that there exists p_0 for $1 \le p_0 \le p_1^* + 1$ so that $\mathbf{G}_{p_0} \neq \hat{\mathbf{G}}_{p_0}$, $\mathbf{V}'\Delta\mathbf{X}' = \mathbf{0}_N$, only if $\mathbf{a}_1 = \mathbf{0}_L$.

Then in order to show that given $\mathbf{X}' \neq \hat{\mathbf{X}}'$, $\mathbf{V}'\Delta\mathbf{X}'\mathbf{a} = \mathbf{0}_N$, only if $\mathbf{a}_1 = \mathbf{0}_L$, we need to consider the case of $\mathbf{G}_p = \hat{\mathbf{G}}_p$ for $1 \le p \le p_1^* + 2$. In this case by substituting $\Delta\mathbf{Y}_m^p = \mathbf{0}_{\Gamma\times L}$ for $1 \le p \le p_1^* + 1$ and $1 \le m \le M_t$ into (5.100), we

get a similar condition to we do in the previous case of $\mathbf{G}_p = \hat{\mathbf{G}}_p$ $(1 \leq p \leq p_1^*)$. Owing to the fact that $\Delta\mathbf{Y}_2^p = \mathbf{0}_{\Gamma\times L}$ for $1 \leq p \leq p_1^* + 1$, only the term $\mathbf{V}'^{p_1^*+2}_1 \Delta\mathbf{Y}_1^{p_1^*+2}\mathbf{a}_1$ is related to the columns of $\mathbf{V}'^{p_1^*+2}_1$ in the linear combination of the columns of $\mathbf{V}'$. As a consequence, we can get that once there exists p_0 for $1 \leq p_0 \leq p_1^* + 2$ so that $\mathbf{G}_{p_0} \neq \hat{\mathbf{G}}_{p_0}$, $\mathbf{V}'\Delta\mathbf{X}' = \mathbf{0}_N$, only if $\mathbf{a}_1 = \mathbf{0}_L$. By repeating this analysis step for additional $P - p_1^* - 2$ times, we can finally get as expected, i.e., in the case that there exists p_0 $(1 \leq p_0 \leq P)$ so that $\mathbf{G}_{p_0} \neq \hat{\mathbf{G}}_{p_0}$, $\mathbf{V}'\Delta\mathbf{X}' = \mathbf{0}_N$, only if $\mathbf{a}_1 = \mathbf{0}_L$.

Proof of $\mathbf{a}_m = \mathbf{0}_L$ for $2 \leq m \leq M_t$

Similarly, let p_2^* $(1 \leq p_2^* \leq P)$ is the maximum number so that no indices of the columns belonging to $\mathbf{V}'^p_2$ are in the set $\mathcal{B}_2$ for $1 \leq p \leq p_2^*$. Substituting $\mathbf{a}_1 = \mathbf{0}_L$ into (5.99), we can obtain

$$\begin{aligned}\mathbf{V}'\Delta\mathbf{X}'\mathbf{a} &= \sum_{p=1}^{p_2^*} \mathbf{V}'^p_2 \Delta\mathbf{Y}_2^p \mathbf{a}_2 + \sum_{p=p_2^*+1}^{P} \mathbf{V}'^p_2 \Delta\mathbf{Y}_2^p \mathbf{a}_2 + \sum_{p=1}^{P} \mathbf{V}'^p_3 \Delta\mathbf{Y}_3^p \mathbf{a}_3 \\ &\quad + \sum_{m=4}^{M_t} \sum_{p=1}^{P} \mathbf{V}'^p_m \Delta\mathbf{Y}_m^p \mathbf{a}_m. \end{aligned} \tag{5.104}$$

Comparing (5.104) with (5.100), obviously, we get the similar situation to we do in the proof of $\mathbf{a}_1 = \mathbf{0}_L$. Therefore, with the same analyzing strategy, we can get that given $\mathbf{C}' \neq \hat{\mathbf{C}}'$, $\mathbf{V}'\Delta\mathbf{X}'\mathbf{a} = \mathbf{0}_N$, only if $\mathbf{a}_2 = \mathbf{0}_L$. Actually, for each m $(2 \leq m \leq M_t)$ by substituting $\mathbf{a}_{m'} = \mathbf{0}_L$ for $1 \leq m' \leq m - 1$ into (5.99), we can get a similar situation. Thus by repeating this analysis strategy for additional $M_t - 2$ times, we can get that given $\mathbf{C}' \neq \hat{\mathbf{C}}'$, $\mathbf{V}'\Delta\mathbf{X}'\mathbf{a} = \mathbf{0}_N$, only if $\mathbf{a}_m = \mathbf{0}_L$ for $3 \leq m \leq M_t$ in turn. As a consequence, we can see that provided $\mathbf{C}' \neq \hat{\mathbf{C}}'$, $(\mathbf{V}'\Delta\mathbf{X}')\mathbf{a} = \mathbf{0}_N$, only if $\mathbf{a}_m = \mathbf{0}_L$ for $1 \leq m \leq M_t$. It implies that under the conditions provided in Theorem 5, the SF codes can still achieve full diversity in the presence of multiple CFOs, even if the ICI matrix $\mathbf{U}'$ is singular.

Discussion for Arbitrary Values of L_m and Γ

In the above analysis, we have proved that provided $\Gamma \geq L_m$ for $1 \leq m \leq M_t$, the permuted SF codes $\mathbf{C}'$ can achieve full diversity order $\sum_{m=1}^{M_t} L_m$, even when the ICI matrix $\mathbf{U}'$ is singular. Actually, similar to the case without CFOs, by slightly

modifying the above analysis, we can show that under the conditions provided in Theorem 5, the permuted SF codes $\mathbf{C}'$ can achieve diversity order $\sum_{m=1}^{M_t} \min(L_m, \Gamma)$ for arbitrary values of L_m and Γ. The key idea of this proof is to construct an $N \times \sum_{m=1}^{M_t} \min(L_m, \Gamma)$ submatrix of $\mathbf{V}'\mathbf{X}'\mathbf{\Lambda}^{\frac{1}{2}}$ by extracting the first $\min(\Gamma, L_m)$ $(1 \leq m \leq M_t)$ columns of $\mathbf{Y}_m$.

Let $\bar{\mathbf{Y}}_m$ $(1 \leq m \leq M_t)$ be a $P\Gamma \times \min(\Gamma, L_m)$ submatrix of $\mathbf{Y}_m$, which consists of the first $\min(\Gamma, L_m)$ columns of $\mathbf{Y}_m$. Note that due to the structure of $\mathbf{X}'$ and $\mathbf{\Lambda}$, the lth $(0 \leq l \leq \min(\Gamma, L_m) - 1)$ column of $\mathbf{V}_m'\mathbf{Y}_m$ is just the $(lM_t + m - 1)$th column of $\mathbf{V}'\mathbf{X}'$ and corresponds a nonzero diagonal entry of $\mathbf{\Lambda}^{\frac{1}{2}}$. Furthermore, from the property of SF codes, it is not hard to see that provided $\mathbf{G}_p \neq \hat{\mathbf{G}}_p$, the $(p-1)$th $(1 \leq p \leq P)$ $\Gamma \times \min(\Gamma, L_m)$ submatrix of $\Delta\bar{\mathbf{Y}}_m$ has full column rank $\min(\Gamma, L_m)$. Based on this fact, following the similar way as proving Theorem 5, we can finally obtain that the $N \times \sum_{m=1}^{M_t} \min(L_m, \Gamma)$ submatrix of $\mathbf{V}'\Delta\mathbf{X}'$, which consists of all the columns of $\mathbf{V}_m'\Delta\bar{\mathbf{Y}}_m$ for $1 \leq m \leq M_t$, has full column rank. Therefore, we obtain the expected result.

□ End of chapter.

Chapter 6

Conclusions and Future Works

6.1 Conclusions

Cooperative communications is a novel way of enabling a single-antenna transmitter to achieve spatial diversity. By using appropriate cooperative protocols, most diversity achieving space-time (ST) and space-frequency (SF) codes can be directly applied to cooperative communication systems to achieve spatial diversity when all the intermediate nodes are synchronized. Unfortunately, a major challenge for cooperative communications is the synchronization in that the multiple transmissions in cooperative systems may not be well synchronized in either time or frequency. With synchronization errors, most ST codes may not work well. Since OFDM is not sensitive to timing errors, SF coded OFDM cooperative systems have been proposed to achieve both full cooperative and full multipath diversities without the time synchronization requirement. However, these systems still need to face the problem of multiple carrier frequency offsets (CFOs). Since the columns of an ST or SF code matrix are transmitted from different relay nodes with their own oscillators, they may have multiple CFOs that cannot be compensated simultaneously. For SF coded OFDM cooperative systems, this problem becomes greatly stringent because CFO can lead to inter-carrier interference (ICI) in OFDM systems.

This thesis focuses on the multiple CFO problem in ST and SF coded cooperative communication systems. We have investigated the effect of multiple CFOs on delay diversity, the Alamouti code, and a family of SF codes from the view of diversity

analysis. Especially by utilizing the SF codes structure, we have proposed effective and efficient signal detection methods for combatting multiple CFOs for the SF coded cooperative system. Both our theoretical analysis and simulation results imply that the SF coded OFDM system is robust to both timing errors and CFOs in a cooperative communication system.

Above all, we have investigated the effect of multiple CFOs on delay diversity and the Alamouti code. For delay diversity, we found that both of its achieved diversity order and diversity product are not affected by multiple CFOs. For the Alamouti code, when $\frac{1}{3} < (\Delta\varepsilon)_1 < \frac{2}{3}$, the diversity product is decreased by multiple CFOs. Here $\Delta\varepsilon = \varepsilon_2 - \varepsilon_1$ and ε_m $(1 \leq m \leq 2)$ is the normalized CFO for the link from the mth relay node to the destination node. For the worst case of $(\Delta\varepsilon)_1 = 0.5$, full diversity order 2 cannot be achieved. Finally, extensive simulations have been presented to demonstrate our main conclusions.

The major contribution of the thesis lies in the systematic study of the signal detection problem in an SF coded cooperative communication system with multiple CFOs, where the applied SF codes not only can achieve both full spatial and full multipath diversity orders, but also always have full data rate 1 regardless of the number of transmit antennas.

We began with the traditional way of ICI mitigation. To preserve the performance of the SF code, we suggest increasing the SINR of each subcarrier but not to equalizing the SF precoding matrix. Due to the structure of the SF code, increasing each subcarrier's SINR of an MISO-OFDM system is equivalent to that of an SISO-OFDM system. Thus, a classical MMSE filter can be used to maximize the SINR of each subcarrier. Furthermore, we found that due to the structure of the SF codes, the MMSE filter coefficients were easy to update for each realization of channel, where the matrix inverse is independent of the OFDM symbol index. The Q-T method is a popular approximate method for computing the MMSE filter coefficient in the OFDM system, and can be directly applied to solve the problem. To improve performance, we considered a simple two-stage FS-Q-T method where a frequency shift (FS) operation was done before the Q-T method. By exploiting the structure of the SF codes again, we proposed an M-FFT method. For this method, we only

needed to re-arrange the SF codes at the transmitter in a simple way without performance loss. Then, at the destination node, the SINR was effectively increased by multiple FS and FFT operations. Based on its properties, the M-FFT method can be easily combined with the other methods to further improve its performance, e.g., M-FFT-Q-T, M-FFT-Zn and M-FFT with SIC methods. Our simulation results have been presented to illustrate the effectiveness of the methods and show that, for the same SER level, the M-FFT based methods require the least operations.

To gain further insight into this problem, we then studied this problem by conducting diversity analysis. By treating the CFOs as part of the SF codeword matrix, we were able to show that if all the absolute values of normalized CFOs are less than 0.5, the full diversity order for the SF codes are not affected by the multiple CFOs in the SF coded OFDM cooperative system. Moreover, we have proven that this full diversity property can still be preserved if the zero forcing (ZF) method is used to equalize the multiple CFOs. Actually, by some reasonable approximations, this method was equivalent to the MMSE-F detection method. In addition, to improve the robustness of the SF codes to multiple CFOs, we also proposed a permutation (interleaving) method. The permutated SF codes can still achieve full diversity, even if the absolute values of normalized CFOs are equal to or greater than 0.5. To reduce computational complexity, we finally proposed two full diversity achievable detection methods, i.e., the ZF-ML-Zn and ZF-ML-PIC detection methods, which are suitable to the case when the ICI matrix is singular.

6.2 Perspectives of Future Work

Although our study has shown the robustness of the SF coded OFDM system to synchronization errors in cooperative communication systems, what this paper has achieved is just a beginning in the direction of building practical cooperative communication systems. The following are some potential research directions in the future.

When the channels from relay nodes to the destination node are frequency flat fading, it may not be necessary to apply OFDM modulation such that the complexity

of the transmitter and the receiver can be reduced. Recently, in [119] a new family of distributed linear convolutive space-time codes (DLC-STCs) were proposed. Not only are DLC-STCs tolerant to time delay, it has been found that these codes can also be decoded by linear receivers, such as ZF, MMSE and MMSE-DFE receivers, with full diversity. Moreover, for DLC-STCs compensating multiple CFOs during decoding procedure does not increase the computational complexity much. Thus, DLC-STCs are very attractive for asynchronous cooperative communications. However, how multiple CFOs affect DLC-STC has not yet been answered. Therefore, the design of DLC-STCs tolerant to multiple CFOs is worthwhile for further exploration.

In recent years, it has been demonstrated that for wireless networks, better system performance (e.g., power efficiency, system throughput and fulfilling quality of service (QOS) requirements) can be obtained by cross-layer design, where information is exchanged across different layers. Therefore, it is of interest to thoroughly investigate how ST/SF coding can be combined with some high layer cooperative/synchronization protocols to achieve full diversity with synchronization errors.

□ End of chapter.

Bibliography

[1] A. Bria, F. Gessler, O. Queseth, R. Stridh, M. Unbehaun, J. Wu, and J. Zander, "4th-generation wireless infrastructures: Scenarios and research challenges," *IEEE Pers. Commun.*, pp. 25–31, Dec. 2001.

[2] R. Berezdivin, R. Breinig, R. Topp, and R. T. Raytheon, "Next-generation wireless communications concepts and technologies," *IEEE Commun. Mag.*, vol. 40, pp. 108–116, Mar. 2002.

[3] T. S. Rappaport, *Wireless Communications Principles and Practice*. Prentice Hall, 1996.

[4] G. Stüber, *Principles of Mobile Communications*. Kluwer Academic Publishers, 2001.

[5] *Digital Communications*, 4th ed. New York, NY: McGraw Hill, Inc., 2001.

[6] M. Pätzold, *Mobile fading channels*. John Wiley & Sons, Ltd., 2002.

[7] D. Tse and P. Viswanath, *Fundamentals of Wireless Communication*. Cambridge University Press, 2005.

[8] H. Sampath, S. Talwar, J. Tellado, and A. Paulraj, "A fourth-generation MIMO-OFDM broadband wireless system: Design, performance, and field trial results," *IEEE Commun. Mag.*, vol. 40, pp. 143–149, Sept. 2002.

[9] H. W. Yang, "A road to future broadbamd wireless access: MIMO-OFDM-Based air interface," *IEEE Commun. Mag.*, vol. 43, pp. 53–60, Jan. 2005.

[10] L. J. Cimini, "Analysis and simulation of a digital mobile channel using orthogonal frequency division multiplexing," *IEEE Trans. Commun.*, vol. COM-33, pp. 665–675, July 1985.

[11] ETSI, "Radio broadcast systems: Digital audio broadcasting (DAB) to mobile, portable and fixed receivers," ETSI EN 300 401 V1.3.3, May 2001.

[12] Digital Video Broadcasting: Framing Structure, Channel coding, and Modulation for Digital Terrestrial Television, Geneva, Switzerland, Jan. 1999, Draft EN300 744 V1.2.1.

[13] Wireless LAN Medium Access Control (MAC) and Physical Layer (PHY) Specifications: High-Speed Physical Layer in the 5GHz Band, Piscataway, NJ: IEEE Std. 802.11a, Sept. 1999.

[14] Wireless LAM Medium Access Control (MAC) and Physical Layer (PHY) Specifications: Future Higher Data Rate Extension in the 2.4 GHz Band, Piscataway, NJ: IEEE Std. 802.11g, June 2003.

[15] Wireless MAN Working Group http://WirelesMAN.org/.

[16] S. B. Weinstein and P. M. Ebert, "Data transmission by frequency-division multiplexing using the discrete Fourier transform," *IEEE Trans. Commun. Technol.*, vol. COM-19, pp. 628–634, Oct. 1971.

[17] P. S. Chow, J. C. Tu, and J. M. Cioffi, "Performance evaluation of a multichannel transceiver system for ADSL and VHDSL services," *IEEE J. Sel. Areas Commun.*, vol. 9, pp. 909–919, Aug. 1991.

[18] W. Y. Zou and Y. Wu, "COFDM: A review," *IEEE Trans. Broadcast.*, vol. 41, pp. 1–8, Mar. 1995.

[19] A. R. S. Bahai, B. R. Saltzberg, and M. Ergen, *Multi-Carrier Digital Communicatioins: Theory and Application of OFDM*. Springer New York, 2004.

[20] T. Pollet, M. V. Bladel, and Moeneclaey, "BER sensitivity of OFDM systems to carrier frequency offset and Wiener phase noise," *IEEE Trans. Commun.*, vol. 43, pp. 191–193, July 1995.

[21] W. Hwang, H. Kang, and K. Kim, "Sensitivity of SNR degradation of OFDM to carrier frequency offset in shadowed two-path channels," *IEICE Trans. Commun.*, vol. E86-B, pp. 3630–3633, Dec. 2003.

[22] A. J. Paulraj and C. B. Papadias, "Space-time processing for wireless communications," *IEEE Signal Process. Mag.*, vol. 14, pp. 49–83, Nov. 1997.

[23] C. Shannon, "A mathematical theory of communication," *Bell Labs Tech. J.*, vol. 27, pp. 623–656, July and Oct. 1948.

[24] E. Telatar, "Capacity of multi-antenna gaussian channnels," AT&T Bell Lab., Tech. Rep., June 1995.

[25] ——, "Capacity of multi-antenna gaussian channnels," *Europ. Trans. Telecommun.*, vol. 10, pp. 585–595, Nov. 1999.

[26] G. J. Foschini and M. Gans, "On the limits of wireless communication in a fading enviroment when using multiple antennas," *Wireless Personal Commun.*, vol. 6, no. 3, pp. 311–335, Mar. 1998.

[27] T. Marzetta and B. Hochwald, "Capacity of a mobile multiple-antenna communication link in Rayleigh flat fading," *IEEE Trans. Inf. Theory*, vol. 45, pp. 139–157, Jan. 1999.

[28] A. Paulraj, R. Nabar, and D. Gore, *Introduction to Space-Time Wireless Communications*. UK: Cambridge University Press, 2003.

[29] E. G. Larsson and P. Stoica, *Space-Time Block Coding for Wireless Communications*. UK: Cambridge University Press, 2003.

[30] A. Wittneben, "Base station modulation diversity for digital simulcast," in *Proc. of IEEE Vehicular Technology Conference (VTC)*, 1991, pp. 848–853.

[31] V. Tarokh, N. Seshadri, and A. R. Calderbank, "Space-time codes for high data rate wireless communication: Performance criterion and code construction," *IEEE Trans. Inf. Theory*, vol. 44, no. 2, pp. 744–765, Mar. 1998.

[32] V. Tarokh, H. Jafarkhani, and A. R. Calderbank, "Space-time block codes from orthogonal designs," *IEEE Trans. Inf. Theory*, vol. 45, no. 5, pp. 1456–1467, July 1999.

[33] S. M. Alamouti, "A simple transmit diversity technique for wireless communications," *IEEE J. Sel. Areas Commun.*, vol. 16, pp. 1451–1458, Oct. 1998.

[34] H. Bölcskei and A. J. Paulraj, "Space-frequency coded broadband OFDM systems," in *Proc. IEEE Wireless Communications and Networking Conf. (WCNC)*, Chicago, IL, Sept. 23-28 2000, pp. 1–6.

[35] S. Zhou and G. B. Giannakis, "Space-time coding with maximum diversity gains over frequency-selective fading channels," *IEEE Signal Process. Lett.*, vol. 8, no. 10, pp. 269–272, Oct. 2001.

[36] L. Shao, S. Roy, and S. Sandhu, "Rate-one space-frequency block codes with maximum diversity gain for MIMO-OFDM," in *Proc. IEEE Global Telecommun. Conf. (Globecom)*, Dec. 1-5 2003, pp. 809–813.

[37] L. Shao and S. Roy, "Rate-one space-frequency block codes with maximum diversity gain for MIMO-OFDM," *IEEE Trans. Wireless Commun.*, vol. 4, no. 4, pp. 1674–1687, July 2005.

[38] W. Su, Z. Safar, and K. J. R. Liu, "Systematic design of space-frequency codes with full rate and full diversity," in *Proc. IEEE Wireless Communications and Networking Conf. (WCNC)*, vol. 3, Mar. 21-25 2004, pp. 1436–1441.

[39] ——, "Full-rate full-diversity space-frequency codes with optimum coding advantage," *IEEE Trans. Inf. Theory*, vol. 51, no. 1, pp. 229–249, Jan. 2005.

[40] Z. Liu, Y. Xin, and G. B. Giannakis, "Space-time-frequency coded OFDM over frequency-selective fading channels," *IEEE Trans. Signal Process.*, vol. 50, pp. 2465–2476, Oct 2002.

[41] Y. Gong and K. B. Letaief, "Space-frequency-time coded OFDM for broadband wireless communications," in *Proc. IEEE Global Telecommun. Conf. (Globecom)*, San Antonio, USA, Nov. 2001, pp. 519–523.

[42] A. F. Molisch, M. Z. Win, and J. H. Winters, "Space-time-frequency (STF) coding for MIMO-OFDM systems," *IEEE Commun. Lett.*, vol. 6, pp. 370–372, Sept. 2002.

[43] D. R. V. J. Rao, V. Shashidhar, Z. A. Khan, and B. S. Rajan, "Low-complexity, full-diversity space-time-frequency block codes for MIMO-OFDM," in *Proc. IEEE Global Telecommun. Conf. (Globecom)*, Dallas, Texas, USA, Nov. 29 - Dec. 3, 2004, pp. 204–208.

[44] V. Stankovic, A. Host-Madsen, and Z. Xiong, "Cooperative diversity for wireless ad hoc networks," *IEEE Signal Process. Mag.*, vol. 23, pp. 37–49, Sept. 2006.

[45] A. Sendonaris, E. Erkip, and B. Aazhang, "User cooperation diversity-part I: system description," *IEEE Trans. Commun.*, vol. 51, pp. 1927–1938, Nov. 2003.

[46] ——, "User cooperation diversity-part II: implementation aspects and performance analysis," *IEEE Trans. Commun.*, vol. 51, pp. 1939–1948, Nov. 2003.

[47] J. N. Laneman and G. W. Wornell, "Distributed space-time coded protocols for exploiting cooperative diversity in wireless networks," *IEEE Trans. Inf. Theory*, vol. 49, no. 10, pp. 2415–2425, Oct. 2003.

[48] J. N. Laneman, D. N. C. Tse, and G. W. Wornell, "Cooperative diversity in wireless networks: Efficient protocols and outage behavior," *IEEE Trans. Inf. Theory*, vol. 50, no. 12, pp. 3062–3080, December 2004.

[49] R. U. Nabar, H. Bolcskei, and F. W. Kneubuhler, "Fading relay channels: Performance limits and space-time signal design," *IEEE J. Sel. Areas Commun.*, vol. 22, no. 6, pp. 1099–1109, August 2004.

[50] Y. Jing and B. Hassibi, "Distributed space-time coding in wireless relay networks," *IEEE Trans. Wireless Commun.*, vol. 5, pp. 3524–3536, Dec. 2006.

[51] J. N. Laneman, G. W. Wornell, and D. N. C. Tse, "An efficient protocol for realizing cooperative diversity in wireless networks," in *Proc. IEEE International Symposium on Information Theory (ISIT)*, Washington, DC, June 2001.

[52] P. A. Anghel and Kaveh, "On the performance of distributed space-time coding systems with one and two non-regenerative relays," *IEEE Trans. Wireless Commun.*, vol. 5, no. 3, pp. 682–692, March 2006.

[53] Y. W. Hong, W. J. Huang, F. H. Chiu, and C. C. J. Kuo, "Cooperative communications in resource-constrained wireless networks," *IEEE Signal Process. Mag.*, vol. 24, no. 3, pp. 47–57, May 2007.

[54] F.-C. Zheng and A. G. Burr, "Signal detection for orthogonal space-time block coding over time-selective fading channels: the $\mathcal{H}_i$ systems," *IEEE Trans. Wireless Commun.*, vol. 5, no. 1, pp. 40–46, Jan. 2006.

[55] ——, "Signal detection for orthogonal space-time block coding over time-selective fading channels: A PIC approach for the $\mathcal{G}_i$ systems," *IEEE Trans. Commun.*, vol. 53, no. 6, pp. 969–972, Jun. 2005.

[56] Y. Jing and H. Jafarkhani, "Using orthogonal and quasi-orthogonal designs in wireless relay networks," in *Proc. IEEE Global Telecommun. Conf. (Globecom)*, San Francisco, CA, Nov. 2006.

[57] T. Kiran and B. S. Rajan, "Distributed space-time codes with reduced decoding complexity," in *Proc. IEEE International Symposium on Information Theory (ISIT)*, Seattle, WA, July 2006, pp. 542–546.

[58] ——, "Partially-coherent distributed space-time codes iwth differential encoder and decoder," *IEEE J. Sel. Areas Commun.*, vol. 25, no. 2, pp. 426–433, Feb. 2007.

[59] S. Yang and J.-C. Belfiore, "Optimal space-time codes for the MIMO amplify-and-forward cooperative channel," *IEEE Trans. Inf. Theory*, vol. 25, no. 2, pp. 647–663, Feb. 2007.

[60] X. Li, "Space-time coded multi-transmission among distributed transmitter without perfect synchronization," *IEEE Signal Process. Lett.*, vol. 11, no. 2, pp. 948–951, Dec. 2004.

[61] S. Wei, D. Goeckel, and M. Valenti, "Asynchronous cooperative diversity," in *Proc. Conf. Inform. Sci. and Sys.*, Princeton University, Mar. 2004.

[62] Y. Mei, Y. Hua, A. Swami, and B. Daneshrad, "Combating synchronization errors in cooperative relay," in *Proc. of International Conference on Acoustics, Speech and Signal Processing (ICASSP)*, Philadelphia, PA, Mar. 2005, pp. 369–372.

[63] M. O. Damen and A. R. Hammons, "A new class of asynchronous distributed space-time codes," in *Proc. IEEE International Symposium on Information Theory (ISIT)*, Nice, France, June 2007.

[64] Y. Li and X.-G. Xia, "A family of distributed space-time trellis codes with asynchronous cooperative diversity," *IEEE Trans. Commun.*, vol. 55, pp. 790–800, Apr. 2007.

[65] Y. Shang and X.-G. Xia, "Shift-full-rank matrices and applications in space-time trellis codes for relay networks with asynchronous cooperative diversity," *IEEE Trans. Inf. Theory*, vol. 52, no. 7, pp. 3153–3167, July 2006.

[66] Y. Li, W. Zhang, and X.-G. Xia, "Distributive high-rate full-diversity space-frequency codes for asynchronous cooperative communications," in *Proc. IEEE International Symposium on Information Theory (ISIT)*, Seattle, USA, July 9-14, 2006, pp. 2612–2616.

[67] E. Lindskog and A. Paulraj, "A transmit diversity scheme for schannels with intersymbol interference," in *Proc. IEEE International Conference on Communications (ICC)*, New Orleans, LA. USA, June 2000, pp. 307–311.

[68] D. Flore and E. Lindskog, "Time-reversal space-time block coding vs. transmit delay diversity - A comparison based on a gsm-like system," in *Proc. of the Digital Signal Processing Workshop*, Hunt, Texas, 2000.

[69] E. G. Larsson, P. Stoica, and J. Li, "Space-time block coding for frequency-selective channels," in *Proc. of International Conference on Acoustics, Speech and Signal Processing (ICASSP)*, Orlando, FL, 2002, pp. 2405–2408.

[70] M. Morelli and U. Mengali, "Frequency estimation for the downlink of the UMTS-TDD component," *IEEE Trans. Wireless Commun.*, vol. 1, pp. 554–557, October 2002.

[71] Z. Li and X.-G. Xia, "A simple Alamouti space-time transmission scheme for asynchronous cooperative systems," *IEEE Signal Process. Lett.*, vol. 14, no. 11, pp. 804–807, Nov. 2007.

[72] T. A. Tran and A. B. Sesay, "A generalized linear quasi-ML decoder of OST-BCs for wireless communications over time-selective fading channels," *IEEE Trans. Wireless Commun.*, vol. 3, no. 3, pp. 855–864, May 2004.

[73] F.-C. Zheng and A. G. Burr, "Receiver design for orthogonal space-time block coding for four transmit antennas over time-selective fading channels," in *Proc. IEEE Global Telecommun. Conf. (Globecom)*, vol. 1, San Francisco, CA, Dec. 1-5 2003, pp. 128–132.

[74] Z. Li, D. Qu, and G. Zhu, "An equalization technique for distributed STBC-OFDM system with multiple carrier frequency offsets," in *Proc. IEEE Wireless Communications and Networking Conf. (WCNC)*, vol. 5, Las Vegas, USA, Apr. 2006, pp. 2130–2134.

[75] D. Veronesi and D. L. Goeckel, "Multiple frequency offset compensation in cooperative wireless systems," in *Proc. IEEE Global Telecommun. Conf. (Globecom)*, San Francisco, California, USA, Nov. 2006.

[76] G. Scutari and S. Barbarossa, "Distributed space-time coding for regenerative relay networks," *IEEE Trans. Wireless Commun.*, vol. 4, no. 5, pp. 2387–2399, Sept. 2005.

[77] K. G. Seddic and K. J. R. Liu, "Distributed space-frequency coding over broadband relay channels," to appear in *IEEE Trans. Wireless Commun.*

[78] O. Besson and P. Stoica, "On parameter estimation of MIMO flat-fading channels with frequency offsets," *IEEE Trans. Signal Process*, vol. 51, no. 3, pp. 602–613, Mar. 2003.

[79] D. Qu, G. Zhu, and T. Tao, "Training sequence design and parameter estimation of MIMO channels with carrier frequency offsets," *IEEE Trans. Wireless Commun.*, vol. 5, no. 12, pp. 3662–3666, Dec. 2006.

[80] F. Tian, X.-G. Xia, and P. C. Ching, "Signal detection for space-frequency coded cooperative communication system with multiple carrier frequency offsets," in *Proc. IEEE Wireless Communications and Networking Conf. (WCNC)*, Hong Kong, Mar. 2007, pp. 1221–1225.

[81] ——, "Equalization in space-frequency coded cooperative communication system with multiple frequency offsets," in *Proc. IEEE International Symposium on Signals, Circuits and Systems (ISSCS)*, Iasi, Romania, July 12-13 2007, pp. 577–580.

[82] ——, "A simple ICI mitigation method for a sapce-frequency coded cooperative communication system with multiple CFOs," in *Proc. IEEE International Conference on Acoustics, Speech, and Signal Processing (ICASSP)*, Las Vegas, Nevada, March 30 - April 4, 2008.

[83] ——, "Signal detection in a cooperative communication system with multiple CFOs by exploiting the properties of space-frequency codes," in *Proc. IEEE International Conference on Communications (ICC)*, Beijing, P. R. China, May 19 - 23, 2008.

[84] F. Tian, X.-G. Xia, W.-K. Ma, and P. C. Ching, "Full diversity under multiple carrier frequency offsets of a family of space-frequency codes," in *Proc. IEEE International Conference on Acoustics, Speech, and Signal Processing (ICASSP)*, Taipei, Taiwan, April 19-24 2009.

[85] F. Tian, X.-G. Xia, P. C. Ching, and W. K. Ma, "Signal detection in a space-frequency coded cooperative communication system with multiple carrier frequency offsets by exploiting specific properties of the code structure," *IEEE Trans. Veh. Technol.*, Jan. 2009, accepted for future publication.

[86] A. Papoulis and S. U. Pillai, *Probability, Random Variables and Stochastic Processes*, 4th ed. The McGraw-Hill Companies, Inc., 2002.

[87] M. Mouly and M.-B. Pautet, *The GSM System for Mobile Communications*. Telecom Publishing, 1992.

[88] N. Seshadri and J. Winters, "Two signaling schemes for improving the error performance of frequency-division-duplex (fdd) transmission systems using transmitter antenna diversity," in *Int. J. Wireless Information Networks*, vol. 1, Jan. 1994, pp. 49–60.

[89] M. B. J. Guey, M. Fitz and W. Kuo, "Signal design for transmitter diversity wireles communication systems over Rayleigh fading channels," in *Proc. IEEE Vehicular Technology Conference (VTC)*, vol. 1, Atlanta, GA, 1996, pp. 136–140.

[90] J. C. Guey, M. P. Fitz, M. R. Bell, and W. Y. Kuo, "Signal design for transmitter diversity wireless communication systems over Rayleigh fading channels," *IEEE Trans. Commun.*, vol. 47, no. 4, pp. 527–537, April 1999.

[91] Y. Shang and X.-G. Xia, "A criterion and design for space-time block codes achieving full diversity with linear receivers," in *Proc. IEEE International Symposium on Information Theory (ISIT)*, Nice, France, June 2007, pp. 2906–2910.

[92] J.-K. Zhang, J. Liu, and K. M. Wong, "Trace-orthogonal full diversity triangular cyclotomic space-time codes minimizing worst case pair-wise error probability," in *Proc. IEEE International Symposium on Information Theory (ISIT)*, Adelaide, Australia, Sept. 2005, pp. 1942–1946.

[93] W. Su and X.-G. Xia, "Two generalized complex orthogonal space-time block codes for rate 7/11 and 3/5 for 5 and 6 transmit antennas," *IEEE Trans. Inf. Theory*, vol. 49, pp. 313–316, Jan. 2003.

[94] X.-B. Liang, "A high-rate orthogonal space-time block code," *IEEE Commun. Lett.*, vol. 7, pp. 222–223, May 2003.

[95] H. Wang and X.-G. Xia, "Upper bounds of rates of complex orthogonal space-time block codes," *IEEE Trans. Inf. Theory*, vol. 49, pp. 2788–2796, Oct. 2003.

[96] W. Su, X.-G. Xia, and K. J. R. Liu, "A systematic design of high-rate complex orthogonal space-time block codes," *IEEE Commun. Lett.*, vol. 8, pp. 380–382, Jun. 2004.

[97] X.-B. Liang, "A complex orthogonal space-time block codes for high number of transmit antennas," *IEEE Commun. Lett.*, vol. 9, pp. 115–117, Feb. 2005.

[98] W. Zhang, X.-G. Xia, and P. C. Ching, "High-rate full-diversity space-time-frequency codes for broadband MIMO block-fading channels," *IEEE Trans. Commun.*, vol. 55, no. 1, pp. 25–34, Jan. 2007.

[99] W. Su, Z. Safar, M. Olfat, and K. J. R. Liu, "Obtaining full-diversity space-frequency codes from space-time codes via mapping," *IEEE Trans. Signal Process*, vol. 51, pp. 2905–2916, Nov. 2003.

[100] M. P. Fitz, J. H. Grimm, and S. Siwamogsatham, "A new view of performance analysis techniques in correlated Rayleigh fading," in *Proc. IEEE Wireless Communications and Networking Conf. (WCNC)*, New Orleans, LA, USA, 1999, pp. 139–134.

[101] S. Siwamogsatham, M. P. Fitz, and J. H. Grimm, "A new view of performance analysis techniques in correlated Rayleigh fading," *IEEE Trans. Inf. Theory*, vol. 48, no. 4, pp. 952–956, Apr. 2002.

[102] R. Horn and C. Johnson, *Topics in Matrix Analysis*. UK: Cambridge university Press, 1989.

[103] U. Fincke and M. Pohst, "Improved methods for calculating vectors fo short length in a lattice, including a complexity analysis," *Math. Computation*, vol. 44, pp. 463–471, Apr. 1985.

[104] E. Viterbo and J. Boutros, "A universal lattice code decode for fading channels," *IEEE Trans. Inf. Theory*, vol. 45, no. 5, pp. 1639–1642, 1999.

[105] A. C. O. Damen and N.-C. Belfiore, "Lattice code decoder for space-time codes," *IEEE Commun. Lett.*, vol. 4, no. 5, pp. 161–163, 2000.

[106] K. Boullé and J.-C. Belfiore, "Modulation schemes designed for the rayleigh fading channel," in *Proc. CISS'92*, Mar. 1992.

[107] M. O. Damen, K. A. Meraim, and J. C. Belfiore, "Diagonal algebraic space-time block codes," *IEEE Trans. Inf. Theory*, vol. 48, pp. 628–636, March 2002.

[108] X. Giraud, E. Boutillon, and J. C. Belfiore, "Algebratic tools to build modulation schemes for fading channels," *IEEE Trans. Inf. Theory*, vol. 43, no. 3, pp. 938–952, May 1997.

[109] T. Cover and A. E. Gammal, "Capacity theorems for the relay channel," *IEEE Trans. Inf. Theory*, vol. IT-25, pp. 572–584, Sept. 1979.

[110] A. Chakraharti, E. Erkip, A. Sabharwal, and A. Behnaam, "Code designs for cooperative communication," *IEEE Signal Process. Mag.*, vol. 24, pp. 16–26, Sept. 2007.

[111] J. Boyer, D. D. Falconer, and H. Yanikomeroglu, "Multihop diversity in wireless relaying channels," *IEEE Trans. Commun.*, vol. 52, no. 10, pp. 1820–1830, Oct. 2004.

[112] A. K. Sadek, W. Su, and K. J. R. Liu, "Multinode cooperative communications in wireless networks," *IEEE Trans. Signal Process.*, accepted for furture publication.

[113] Y. Li, W. Zhang, and X.-G. Xia, "Distributive high-rate full diversity space-frequency codes achieving full cooperative and multipath diversities for asynchronous cooperative communications," *IEEE Trans. Veh. Technol.*, accepted for future publication.

[114] W. Zhang, Y. Li, X.-G. Xia, and K. B. Letaief, "Distributed space-frequency coding for cooperative diversity in broadband wireless ad hoc networks," *IEEE Trans. Wireless Commun.*, vol. 7, no. 3, pp. 995–1003, March 2008.

[115] B. Hassibi and B. Hochwald, "High-rate codes that are linear in space and time," *IEEE Trans. Inf. Theory*, vol. 48, pp. 1804–1824, July 2002.

[116] S. Jagannathan, H. Aghajan, and A. Goldsmith, "The effect of time synchronization errors on the performance of cooperative miso systems," in *IEEE Globecom Workshops*, 29 Nov.-3 Dec. 2004, pp. 102–107.

[117] Y. Mei, Y. Hua, A. Swami, and B. Daneshrad, "Combating synchronization errors in cooperative relay," in *IEEE International Conference on Acoustics, Speech, and Signal Processing (ICASSP)*, Philadelphia, PA, USA, Mar. 18-23 2005, pp. 369–372.

[118] S. Wei, D. Goeckel, and M. Valenti, "Asynchronous cooperative diversity," *IEEE Trans. Wireless Commun.*, vol. 5, no. 6, pp. 1547–1557, 2006.

[119] X. Guo and X.-G. Xia, "A distributed space-time coding in asynchronous wireless relay networks," *IEEE Trans. Wireless Commun.*, vol. 7, no. 5, pp. 1812–1816, May 2008.

[120] P. Schniter, "Low-complexity equalization of OFDM in doubly selective channels," *IEEE Trans. Signal Process.*, vol. 52, pp. 1002–1011, April 2004.

[121] H.-M. Wang, X. Chen, S. D. Zhou, and Y. Yao, "A low-complexity ICI cancellation scheme in frequency domain for OFDM in time-varying multipath

channels," in *Proc. IEEE 16th International Symposium on Personal, Indoor and Mobile Radio Communications*, Berlin, Germany, Sept. 2005, pp. 1234–1237.

[122] D. N. Dao and C. Tellambura, "Intercarrier interference self-cancellation space-frequency codes for MIMO-OFDM," *IEEE Trans. Veh. Technol.*, vol. 54, pp. 1729–1738, Sep. 2005.

[123] G. H. Golub and C. F. V. Loan, *Matrix computations*. Baltimore, MD: John Hopkins Univ. Press, 1983.

[124] A. Stamoulis, S. N. Diggavi, and N. Al-Dhahir, "Intercarrier interference in MIMO OFDM," *IEEE Trans. Signal Process.*, vol. 50, pp. 1234–1237, Oct 2002.

[125] A. L. Swindlehurst and G. Leus, "Blind and semi-blind equalization for generalized space-time block codes," *IEEE Trans. Inf. Theory*, vol. 50, no. 10, pp. 2489–2498, Oct. 2002.

[126] Z. Ding, D. B. Ward, and W. H. Chin, "General scheme for equalization of space-time block-coded systems with unknown CSI," *IEEE Trans. Signal Process.*, vol. 54, no. 7, pp. 2737–2746, July 2006.

[127] L. Rugini, P. Banelli, and G. Leus, "Simple equalization of time-varying channels for OFDM," *IEEE Communications Letters*, vol. 9, no. 7, pp. 619–621, July 2005.

[128] H. V. Sorensen, C. S. Burrus, and D. L. Jones, "A new efficient algorithm for computing a few DFT points," in *Proc. IEEE Int. Symp. Circuits and Systems*, vol. 2, 1988, pp. 1915–1918.

[129] H. V. Sorensen and C. S. Burrus, "Efficient computation of the DFT with only a subset of input or output points," *IEEE Trans. Signal Process.*, vol. 41, no. 3, pp. 1184–1200, Mar. 1993.

[130] J. Benesty, Y. A. Huang, and J. Chen, "A fast recursive algorithm for optimum sequential signal detection in a BLAST system," *IEEE Trans. Signal Process.*, vol. 51, pp. 1722–1730, July 2003.

[131] C. Lomont, "Fast inverse square root," *http://www.lomont.org/Math/Papers/2003/InvSqrt.pdf*, 2003.

[132] A. V. Oppenheim, R. W. Schafer, and J. R. Buck, *Discrete-Time Signal Processing*, 2nd ed. Prentice-Hall, 1999.